

ISSN 2663-0419 (Online)
ISSN 2218-8754 (Print)

AZERBAIJAN NATIONAL ACADEMY OF SCIENCES

ANAS TRANSACTIONS

EARTH SCIENCES



www.journalesgia.com

2025
№ 1

We are
Crossref

Member



ELSEVIER
Scopus

Crossref
This journal is included
and indexed in the
GeoRef database

REDAKSİYA HEYƏTİ

Əlizadə Ak.A. – baş redaktor (Azerbaycan), Qədirov F.Ə. – baş redaktorun müavini (Azerbaycan), Quliyev I.S. – baş redaktorun müavini (Azerbaycan), Süleymanov B.Ə. – baş redaktorun müavini (Azerbaycan), Babayev Q.R. – baş redaktorun müavini (Azerbaycan), Süleymanov B.Ə. – baş redaktorun müavini (Azerbaycan), Babazadə V.M. (Azerbaycan), Calalov Q.İ. (Azerbaycan), Abbasov O.R. (Azerbaycan), Əfəndiyev Q.M. (Azerbaycan), Hüseynov D.A. (Azerbaycan), Feyzulayev Ə.Ə. (Azerbaycan), Kəngerli T.N. (Azerbaycan), Rəsulov M.Ə. (Azerbaycan), Yetirmişli Q.C. (Azerbaycan), Qardaşov R.H. (Azerbaycan), Səfərov S.H. (Azerbaycan), Səfərov R.T. (Azerbaycan).

İsmail-zade Ə.T. (Almaniya), Eppelbaum L.V. (İsrail), Sobiseviç A.L. (Rusiya), Boqoyavlenski V. (Rusiya), Şuanqgen C. (Çin), Vernant F. (Fransa), Telesca L. (İtalya), Ali A. (Türkiyə), Maden N. (Türkiyə), Karslı H. (Türkiyə), Çelidze T.L. (Gürcüstan), Kərimov V.Y. (Rusiya), Gliko A.O. (Rusiya), Lavruşin V.Y. (Rusiya), Çifci G. (Türkiyə), Kostyanoy A. (Rusiya), Reyllinger R. (ABŞ), Saqiyə T. (Yaponiya), Tibaldi Alessandro (İtalya), Zavyalov A.D. (Rusiya), Gupta S.P. (Hindistan), Nilfurushan F. (İsvəç), Ergintav S. (Türkiyə).

EDITORIAL BOARD

Alizadeh Ak.A. – Editor-in-Chief (Azerbaijan), Kadirov F.A. – Deputy Editor-in-Chief (Azerbaijan), Suleimanov B.A. – Deputy Editor-in-Chief (Azerbaijan), Guliyev I.S. – Deputy Editor-in-Chief (Azerbaijan), Babayev G.R. – Deputy Editor-in-Chief (Azerbaijan), Suleimanov B.A. – Deputy Editor-in-Chief (Azerbaijan), Babazade V.M. (Azerbaijan), Jalalov G.I. (Azerbaijan), Abbasov O.R. (Azerbaijan), Afandiyev G.M. (Azerbaijan), Hüseynov D.A. (Azerbaijan), Feyzullayev A.A. (Azerbaijan), Jalalov G.I. (Azerbaijan), Kangerli T.N. (Azerbaijan), Rasulov M.A. (Azerbaijan), Yetirmishli G.J. (Azerbaijan), Gardashov R.H. (Azerbaijan), Safarov S.H. (Azerbaijan), Safarov R.T. (Azerbaijan).

Ismail-zadeh A.T. (Germany), Eppelbaum L.V. (Israel), Sobisevich A.L. (Russia), Bogoyavlenski V. (Russia), Shuanggen J. (China), Vernant Ph. (France), Telesca L. (Italy), Ali A. (Turkey), Maden N. (Turkey), Karslı H. (Turkey), Ghelidze T.L. (Georgia), Kerimov V.Y. (Russia), Gliko A.O. (Russia), Lavrushin V.Y. (Russia), Çifci G. (Turkey), Kostyanoy A. (Russia), Reyllinger R. (USA), Sagiyə T. (Japan), Tibaldi A. (Italy), Zavyalov A.D. (Russia), Gupta S.P. (India), Nilfouroushan F. (Sweden), Ergintav S. (Turkey).

РЕДАКЦИОННАЯ КОЛЛЕГИЯ

Ализаде Ак.А. – главный редактор (Азербайджан), Кадиров Ф.А. – зам.главного редактора (Азербайджан), Гулиев И.С. – зам.главного редактора (Азербайджан), Бабаев Т.Р. – зам.главного редактора (Азербайджан), Сулейманов Б.А. – зам.главного редактора (Азербайджан), Бабазаде В.М. (Азербайджан), Джалалов Г.И. (Азербайджан), Аббасов О.Р. (Азербайджан), Эфендиев Г.М. (Азербайджан), Гусейнов Д.А. (Азербайджан), Фейзуллаев А.А. (Азербайджан), Кенгерли Т.Н. (Азербайджан), Расулов М.А. (Азербайджан), Етиришили Г.Дж. (Азербайджан), Гардашов Р.Г. (Азербайджан), Сафаров С.Г. (Азербайджан), Сафаров Р.Т. (Азербайджан).

Исмаил-заде А.Т. (Германия), Эппельбаум Л.В. (Израиль), Собисевич А.Л. (Россия), Богоявленский В.И. (Россия), Шуангген Ж. (Китай), Вернант Ф. (Франция), Телеска Л. (Италия), Айдын Али (Турция), Маден Н. (Турция), Карслы Х. (Турция), Челидзе Т.Л. (Грузия), Керимов В.Ю. (Россия), Глико А.О. (Россия), Лаврушин В.Ю. (Россия), Чифджи Г. (Турция), Костяной А.Г. (Россия), Рейлингер Р. (США), Сагия Т. (Япония), Завялов А.Д. (Россия), Гупта С.П. (Индия), Нилфурушан Ф. (Швеция), Ергинтав С. (Турция).

Buraxılışına məsul: **Qabil Abiyev**

Dizayn/Qrafika: **Kərim Nəbiyev**
Xəlil Nəbiyev

Veb-redaktor: **Tofiq Rəşidov**

Jurnal Geologiya və Geofizika İstututunda
yiğilmiş və səhifələnmişdir

* * *

Responsible for the issue: **Gabil Abiyev**

Design/Graphcs: **Karim Nabiyev**
Khalil Nabiyev

Web-editor: **Tofiq Rashidov**

The journal has been compiled and paginated
at the Geology and Geophysics Institute

* * *

Ответственный за выпуск: **Габил Абиев**

Дизайн/графика: **Керим Набиев**
Халил Набиев

Веб-редактор: **Тофиг Рашидов**

Журнал набран и сверстан в Институте
геологии и геофизики

* * *

Ünvan: AZ1001, Bakı şəhəri, İstiqlaliyyət küçəsi 30,
“ANAS Transactions, Earth Sciences”

Address: “ANAS Transactions, Earth Sciences”
30, İstiqlaliyyat str., Baku, Azerbaijan, AZ1001

Адрес: AZ1001, г. Баку, Истиглалият, 30.
Редакция “ANAS Transactions, Earth Sciences”

* * *

İcraçı redaktorlar: **A.A.İsrafilova, C.S.Qurbanova**

Executive Editors: **A.A.İsrafilova, J.S.Gurbanova**

Исполнительные редакторы: **А.А.Исрафилова**

Дж.С.Курбанова



Formatı: 60x84^{1/8}. Həcmi: 20 ç.v.

Tirajı: 300 nüsxə

© “Elm” nəşriyyatı, 2025

ANALYSIS OF METHODS FOR EVALUATING THE EFFECTIVENESS OF GEOLOGICAL AND TECHNICAL MEASURES AND DECISION-MAKING FOR THEIR SELECTION: CONCEPTUAL REVIEW

Moldabayeva G.Zh.¹, Abbasova S.V.², Zakenov S.T.³, Kirisenko O.G.⁴,

Iklasova J.U.⁵, Zhanturin Zh.K.⁵, Tuzelbayeva Sh.R.¹, Wang J.²

¹KazNRTU named after K.I. Satpayev, Kazakhstan

22, Satbaev str., Almaty, 050013

²Azerbaijan State Oil and Industry University, Azerbaijan

34, Azadliq ave. Baku, AZ1010

³Yessenov University, Aktau, Kazakhstan

microdistrict 32, Main building Index 130000, Aktau

⁴Ministry of Science and Education of the Republic of Azerbaijan,

Oil and Gas Institute, Azerbaijan

F.Amirov str., 9, Baku, AZ1000

⁵Atyrau University of Oil and Gas, Kazakhstan

45A, Baimukhanov St., Privokzalny microdistrict, Atyrau

Keywords: oil field,
geological and technical
measures, fuzzy cluster
analysis, forecasting,
decision-making

Summary. The paper examines modern approaches to the selection and evaluation of the effectiveness of geological and technical measures (GTM) aimed at enhancing oil recovery and developing hard-to-recover reserves. The primary objective is to identify optimal methods that ensure high technical and economic efficiency under complex geological and operational conditions.

The study analyzes traditional and modern methods for assessing GTM effectiveness, including extrapolation of basic production characteristics, analysis of oil production decline curves, and forecasting using probabilistic-statistical models. The paper emphasizes the insufficient reliability of traditional approaches due to data uncertainties, multi-criteria considerations, and the non-linear interaction of factors. A review of literature highlights the potential use of fuzzy logic, "least concessions" methods, cluster analysis, and expert systems, which allow accounting parameter boundary uncertainties and making more accurate decisions in the context of incomplete data.

Examples of applying modern methods to various oil fields are provided. The possibility of developing integrated information systems on decision support, incorporating mathematical algorithms, databases, and predictive models, is discussed. Particular attention is given to selection of parameters to evaluate the effectiveness of measures, such as physical and geological characteristics, water cut, oil production rates, and economic indicators.

The paper substantiates the necessity for further improvement of approaches to GTM evaluation and planning. It proposes the integration of modern methods for data analysis, modeling, and forecasting to enhance the reliability and accuracy of decisions, thereby contributing to the successful optimization of oil field development and risk reduction.

© 2025 Earth Science Division, Azerbaijan National Academy of Sciences. All rights reserved.

1. Introduction

At present, oil field development is increasingly focused on enhancing efficiency through the implementation of new technologies and geological and technical measures (GTM). The task of selecting the most effective methods, capable of ensuring high technical and economic efficiency under specific

conditions is highlighted. Despite the progress made, more than half of geological oil reserves remain untapped. The primary efforts are directed towards developing extraction methods suitable for various geological conditions.

The successful development of hard-to-recover reserves requires the integration of modern mathe-

matical methods, technological solutions, and available data. Consequently, improving systems for data collection, analysis, and decision-making in selecting GTMs remains a pressing challenge.

2. Current State of Research on the Analysis and Evaluation of GTM Efficiency

Currently, there is a wide range of analytical methods available to evaluate the effectiveness of various measures. GTMs are classified into categories such as technical, maintenance, hydrocarbon production intensification, enhanced oil recovery (EOR) methods, and wellbore treatment (WBT). For instance, the EOR-Office software package, (Фахреддинов и др., 2001; Хасанов и др., 2001), automates processes and assists specialists in making well-founded decisions.

The most effective method to evaluate GTM efficiency is the «extrapolation method», which allows actual results to be compared with forecasts based on production history. However, even minor calculation errors can lead to incorrect conclusions while selecting and planning effective measures (Казаков, 2003).

The practical evaluation of GTM effectiveness is generally based on methods related to the characteristics of oil displacement by water. Simply put, the overall efficiency of GTMs can be divided into the effect caused by the specifics of the displacement process and the effect associated with fluid production intensification (Казаков, 1999).

GTM efficiency is determined analyzing oil production decline curves. There are numerous types of displacement characteristics (Казаков, 1999; Шахвердиев и др., 2014), and the main challenge lies in selecting the most suitable one. This choice should correspond to the field's development history and ensure accurate extrapolation for forecasting (Сыртланов, 2002).

In the study carried out by Glukhikh et al. (Глухих и др., 2002), the most accurate methods of evaluation are examined, along with dependencies demonstrating the technological effect achieved through increased oil production rates. The author notes that the forecast of the expected GTM effect, based on the extrapolation of oil production curves (actual and basic), is not always reliable. This indicates that the duration of GTM effects, such as hydraulic fracturing (HF), ranges from 5 to 7 years. Furthermore, the use of water cut curves for long-term forecasting is effective only when the water cut level is 50-70%. At lower water cut levels, forecast accuracy decreases, especially in the early stages of development when the forecast duration is limited to 3-6 months. In such cases, GTMs are typically carried out in wells with water-free production or low water cut levels.

In the study presented by Shpurov et al. (Шпурров и др., 2000), the forecast objects include well clusters, their groupings, formations, oil and gas production areas and other targets, with forecast intervals ranging from one month to one year. It is important to note that the structure and sequence of upcoming measures require numerous calculations, considering various scenarios. This necessitates the use of modern and highly efficient mathematical methods.

Pyankov, Filev (Пьянков, Филев, 2000) outline methods to calculate basic scenarios and provide a classification of indicators reflecting the technological efficiency of various measures in their work. An example is the Ershovsky oil field, where the effectiveness of different geological and technical measures is evaluated.

The authors emphasize that the use of this software significantly improves the accuracy and effectiveness of evaluations as well as the forecasting of qualitative characteristics for the examined oil field. The core principle of the methodology lies in calculating displacement process parameters that best approximate the actual production data obtained during previous stages of field development. Users can independently set the approximation interval based on production history. The method of the least squares is applied to assess approximation errors, enabling comparisons between predicted results and actual production figures obtained during operational activities (Пьянков, Филев, 2000).

In the paper of Sarvaretdinov et al. (Сарваретдинов и др., 2001) the authors employing the «method of fuzzy sets» explore the aspects of forming a database for GTM applications in wells recommended for production. A fuzzy set refers to an object the degree of membership of which is defined not by an absolute value but with a certain degree of confidence. The primary principle of this method is classifying wells based on their suitability for production, i.e., as "recommended for production." However, the multi-criteria nature of the task presents significant challenges in decision-making.

The paper focuses on the application of this method in the decision-making process and highlights the effectiveness of the «least concessions» approach, which facilitates the calculation of predicted GTM efficiency values (Strekov et al., 2013). Methods such as combining criteria into a single generalized measure, the "least concessions" method, and the principles of L. Zadeh's fuzzy set theory are successfully applied under conditions of uncertainty. The classification of uncertainties helps in selection the appropriate decision-making method. To assess the type of uncertainty, the distribution of data criteria and their correspondence to standard distribution laws are analyzed.

The «least concessions» method reduces a multi-criteria decision-making task to the sequential optimization of individual criteria while considering acceptable concessions. The criteria are prioritized by importance, and a concession value is assigned to each, starting with the most significant. This process is repeated on all criteria until optimal strategies are achieved.

The study carried by Strekov et al. (2013) presents the results and approaches for decision-making in selecting the optimal GTM based on variant calculations and a comparative analysis of the effectiveness of different methods under varying conditions. Five criteria were used to determine the best GTM:

1. Duration of the effect;
2. Additional oil production;
3. Increase in oil flow rate;
4. Oil flow rate after GTM implementation;
5. Water cut level after GTM.

The proposed approach enables forecasting efficiency indicators for various targets based on the chosen GTM.

The possibility of calculating GTM qualitative characteristics based on data on technological parameters, physical and geological features, and operational factors is emphasized (Абасов и др., 2003). This data forms a comprehensive data base that serves as a foundation to assess different targets, select optimal technologies for implementing measures, and analyze the degree of their impact on the final outcome. This approach enhances the validity of decision-making and improves the predictability of GTM effectiveness.

The paper by Ilyushin et al. (Илюшин и др., 2015) analyzes a range of fields grouped by geographical location. It highlights that modern GTM methods play a critical role in ensuring stable oil and gas production and in reducing potential risks associated with geological and engineering factors. However, natural systems are highly complex, data is multidimensional, and influence of individual factors remains uncertain. These characteristics limit the accuracy of traditional methods to assess GTM effectiveness. The development of mathematical models and modern information technologies opens new possibilities for analysis and problem-solving, even under conditions of the limited initial data.

Based on the above mentioned, it can be concluded that there is a pressing need to develop and implement new approaches that enable a more adequate and comprehensive techno-economic evaluation not only of individual geological and technical measures (GTM) but also of their collective efficiency. Such approaches would allow optimizing the selection and application of measures for both individual wells and

entire reservoirs, ensuring a holistic approach to managing hydrocarbon production processes.

One promising direction in addressing this challenge is the use of the integrated methods that combine probabilistic-statistical approaches with elements of fuzzy logic. This approach allows more precise evaluation of the effectiveness of measures under high uncertainty conditions particularly (Strekov et al., 2013; Zadeh, 1978; Золотухин и др., 1991). In recent years, technologies such as expert information systems (Wiseman, Gradjan, 2011; Кравченко, Махно, 2009; Выбор геологотехнических мероприятий ..., 2004; Well Flo, electronic resources) and methods of cluster analysis (Савченко, 2010; Эфендиев и др., 2018, 2016; Akhmetov et al., 2018) have been actively implemented.

The paper by Glukhikh et al. (Глухих и др., 2002) presents key issues regarding the selection of the most accurate methods for evaluating GTM efficiency. The authors present dependencies that illustrate different options for differentiating the technological effects of methods aimed at improving the oil recovery factor. In their opinion, forecasting the GTM effect (i.e., calculating the expected impact) based on the extrapolation of actual and basic oil production curves using characteristic methods may be unreliable due to several factors. In particular, this is related to the duration of the effect from certain types of GTMs, such as hydraulic fracturing (HF). As it is noted the use of water cut curves for long-term forecasting is effective only at high water cut levels exceeding 50-70% due to HF effect lasting 5-7 years. It is advisable to limit the forecasting period to 3-6 months at earlier stages of development, with low water cut levels. However, a significant proportion of GTMs are carried out in water-free or low-water-cut wells, making such forecasts less accurate.

Nevertheless, reliable extrapolation of displacement characteristics becomes possible with sufficient data on the dynamics of oil production after GTM implementation (at least 4-6 observation points). In such cases, forecasting methods based on oil production decline coefficients can be effective. If post-GTM oil production data is limited, the authors recommend using decline coefficients calculated on similar wells with a longer operating period after the measures.

Thus, the improvement of methods for selecting and evaluating the effectiveness of GTMs remains a relevant challenge. The development of new tools and analytical technologies that account for the specifics of various wells and reservoirs is essential for enhancing hydrocarbon production efficiency and ensuring sustainable management of oil and gas projects.

Several studies emphasize the necessity of the development of data, mathematical, and software tools aimed at improving the GTM design process. For instance the primary issue in GTM design is identified as the lack of a unified methodology for assessing their effectiveness in Zhanturin's papers (Жантурин, 2007, 2008, 2009). The proposed solution involves the creation of the integrated software to evaluate both actual and forecasted GTM performance, which would significantly enhance the accuracy and validity of decision-making.

From the perspective of monitoring data on the current state of field development, an important aspect is the planning of GTMs, which is examined in studies by Sarvaretdinov et al. (Сарваретдинов и др., 2001), Strekov et al. (2013), Ilyushin et al. (Илюшин и др., 2015), Zadeh (1978), Zolotukhin et al. (Золотухин и др., 1991). One of the major stages in the development of GTM selection algorithms and methods has been the implementation of expert information system technologies, as discussed in papers by Wiseman, Gradijan (2011), Kravchenko, Makhno (Кравченко, Махно, 2009) and Well Flo electronic resources. However, despite progress in creating new models and information systems for planning and forecasting GTM effectiveness, the issue of comprehensive support for all stages of the planning process remains unresolved. The existed approaches and software tools typically cover only specific fragments of the GTM planning lifecycle, limiting their applicability significantly.

Taking into account the complexity of tasks, multi-criteria and multi-factorial analysis, as well as the inaccuracy and limited nature of initial data, the development of decision-making systems for GTM design remains a pressing challenge. These systems should be based on modern probabilistic-statistical methods and fuzzy logic methods. For example, dependencies were constructed for the efficiency of one type of GTM – water inflow restriction – based on geological and technological factors in the paper by Moldabayeva et al. (2023). The calculations and error analysis confirmed the accuracy of the developed models, which allowed determining the impact of each factor within specified intervals of its variation. The models helped estimate key indicators such as the duration of isolation effects, the volume of additional oil extracted, and the amount of water restricted.

Significant factors in the model were identified and selected, simplifying the model by retaining only the variables that significantly influenced the results. Decision-making on the selection of technological solutions was carried out using mathematical statistics methods and fuzzy logic theory. First, predictive calculations of the effectiveness of water isolation measures were performed, then selection of

optimal technological solutions was carried out according to geological conditions. During the analysis, the fuzzy set theory developed by L.Zadeh was applied. This approach allowed considering multiple conflicting criteria and selecting solutions that provided a balanced compromise among them. Thus, the development of methodological foundations for GTM design continues to be a priority requiring the implementation of new integrated methods and technologies.

Summing up the literary analysis, the following conclusions can be drawn. It has been determined that the traditional methods of evaluating the effectiveness of geological and technical measures (GTM) and decision-making, applied until a certain time, do not sufficiently cover the study of the influence of numerous factors, which negatively affects the quality of decisions made. Nevertheless, in recent years, significant progress has been observed in this field due to the introduction of modern mathematical methods for data processing, information analysis, and decision-making. However, there is still no unified methodology or computational framework that could take into account the uncertainty of modeling conditions and decision-making processes.

It is particularly worth noting that traditional approaches rely on models with clearly defined parameters and their boundaries. However, in real-world conditions, parameters and their values often have blurred boundaries, making the decision-making process more complex. To ensure a more accurate assessment of GTM effectiveness, it is essential to consider the following aspects of uncertainty:

- multi-criteria and multi-factorial data: GTM effectiveness depends on numerous factors, each influencing the outcome to varying degrees;
- data inaccuracy: Many parameters are difficult to measure with high precision, which complicates the development of reliable forecasts;
- non-linear interactions: In many cases, factors influence each other in a non-linear manner, reducing the accuracy of traditional analytical methods.

Modern approaches can provide more reliable and adaptable solutions to evaluate GTM effectiveness under uncertain and dynamic conditions solving these challenges.

3. Research Methods

In recent years, data processing and information analysis have increasingly relied on methods that combine mathematical statistics with fuzzy set theory. This approach allows considering uncertainty and data ambiguity, which are characteristic of GTM planning tasks. One of the key approaches applied in this area is fuzzy cluster analysis.

Fuzzy cluster analysis is a method that enables the grouping of objects or parameters while considering their uncertainty. Unlike traditional methods, where an object belongs to only one cluster, this approach allows an object belonging to several clusters simultaneously, with varying degrees of probability. This is particularly important to solve problems where data is heterogeneous and has blurred boundaries. The use of fuzzy clusters makes it possible to account for multiple aspects of uncertainty, thereby increasing the accuracy of evaluations and decision-making processes (Wiseman, Gradijan, 2011).

Thus, further development of methods for evaluating GTM effectiveness requires a comprehensive approach, combining traditional methods with the latest data analysis and processing technologies. This integration will enable the making of more substantiated and accurate decisions, even under conditions of high uncertainty and data ambiguity.

While addressing tasks related to the comparative assessment of GTM effectiveness and selecting optimal solutions, researchers focus on the following critical aspects:

1. Determining Parameters for Analysis.

The effectiveness of GTMs depends on a variety of parameters, each reflecting geological and technological conditions. Key parameters identified by researchers include:

- Total reservoir thickness;
- Oil-saturated thickness;
- Sandiness coefficient;
- Porosity and permeability;
- Oil viscosity and density;
- Gas content and reservoir temperature;
- Oil and fluid production rates before GTM;
- Water cut prior to GTM;
- Economic indicators (e.g., cost of measures, implementation timelines).

These parameters are used for analysis as they have the greatest impact on the selection and effectiveness of the measures undertaken.

2. Data Set Formation.

For each of the listed parameters, value ranges are defined and described using fuzzy sets. For example, parameter efficiency levels can be categorized as “low”, “medium” or “high”. This approach allows taking into account data uncertainty and blurred boundaries, which is particularly important in conditions of the limited data.

3. Application of Fuzzy Clustering Algorithms.

To process and group data, fuzzy clustering algorithms, such as Fuzzy C-Means (FCM) are applied. This algorithm distributes data into clusters based on object characteristics and the degree of their membership in each cluster.

4. Assessing Object Membership in Clusters.

In fuzzy clustering, each parameter of an object is assigned a degree of membership to a specific cluster. This approach accounts for the possibility of a single object belonging to multiple clusters with varying degrees of probability. Such a method provides a more accurate representation of the data and its impact on the final outcome.

In the context of evaluating GTM effectiveness, fuzzy cluster analysis helps grouping various factor combinations into clusters, determining their closest alignment with specific development conditions or scenarios. This method is particularly valuable in situations where:

- Initial data is incomplete or contains significant inaccuracies;
- Geological conditions are highly variable;
- Engineering outcomes are conflicting or ambiguous.

Key Stages of Applying the Method.

1. Defining Fundamental Parameters, such as the duration of the effect, oil production rate increase, reduction in water cut, and the economic feasibility of the measures are identified as primary criteria.

2. Creating an Input Data Matrix, where each parameter is described using fuzzy values (e.g., "low," "medium," "high").

3. Analysis and Clustering of Results which help determining the group of effectiveness each measure belongs to. This process also helps identify potential risks and weaknesses in the proposed solutions.

Thus, fuzzy cluster analysis allows obtaining a more complete and accurate picture of the efficiency of GTM by integrating uncertain and variable data into the decision-making process.

4. Comparative Evaluation of GTM Effectiveness Using Probabilistic-Statistical Methods and Fuzzy Logic

Several studies (Moldabayeva et al., 2023), propose a decision-making framework for selecting optimal measures to restrict water inflows. The key elements of the framework include:

- multi-criteria analysis: decisions are made considering various factors that influence effectiveness, such as geological and physical conditions and past GTM performance;
- model development: mathematical models are created for each indicator, incorporating comprehensive statistical assessments and uncertainty;
- optimization of decisions: algorithms are developed to select the best technological solutions based on the significance of factors, models, and their evaluations.

The paper by Efendiayev et al. (Эфендиев и др., 2025) analyses factors influencing GTM efficiency metrics including:

- duration of the effect;
- average increase in oil production;
- reduction of water inflows;
- profitability of measures.

To address the multi-criteria analysis problem, the following steps are highlighted:

1. Aggregation of Efficiency Indicators: combining various efficiency metrics into a single comprehensive assessment.

2. Data Clustering: dividing data into three homogeneous groups (clusters) using a fuzzy clustering algorithm.

3. Assignment of Linguistic Values such as "high," "low," "medium" to each cluster and their correspondence to the aggregated indicators.

4. Fuzzy Rule Construction: developing rules based on the "if..., then..." principle to forecast GTM effectiveness under different conditions.

The effectiveness of measures is categorized into several levels:

- high;
- good;
- average;
- satisfactory.

This framework, combining probabilistic-statistical methods and fuzzy logic, enables a more comprehensive and adaptable evaluation of GTM performance, especially in conditions with uncertainty and variability. It helps optimizing decisions by integrating key performance indicators and aligning measures with specific field conditions.

The calculation methodology allows determining which GTMs are most effective under specific conditions. Membership functions are used to predict the effectiveness of measures for each oil field.

Forecasting based on fuzzy models helps determining the correspondence between reservoirs and GTMs with high effectiveness. For instance, Fig.1 demonstrates the alignment between reservoirs and GTM types characterized by «high effectiveness». As there, the most effective GTMs were «optimization», «perforation», and «hydraulic fracturing + perforation».

Zhanturin (2008) notes that the best results for specific reservoirs are achieved when combinations such as «hydraulic fracturing + perforation» are applied. Similar figures have been constructed for other clusters, each representing a corresponding level of effectiveness (Fig.1).

This visual representation highlights the practical applications of the fuzzy model, ensuring that GTM selection corresponds to specific geological

and operational conditions ultimately improving the accuracy and reliability of decision-making.

Reservoir (symbols)	GTM types		
	Optimization	Perforation	HF+perform.
1	⊕	⊕	
2	⊕		
3	⊕		
4	⊕		
5	⊕		
6			⊕
7	⊕		
8	⊕		
9			⊕
10	⊕		
11	⊕		
12			⊕
13	⊕		
14	⊕		

Fig. 1. Correlation between reservoirs and GTM types characterized as «High effectiveness»

The results based on GTM technology data provide the ability to:

- select the most suitable measures for specific geological conditions;
- take into account the information gaps;
- make well-grounded decisions.

Similar conclusions were drawn for the conditions analyzed in (Жантурин, 2008). These conclusions, based on actual GTM application data, serve as a guideline to select measures for specific reservoirs, especially in situations with the limited data.

The use of fuzzy modeling and forecasting enables an assessment of the interaction between GTM effectiveness and geological objects, facilitating the optimal selection of measures for various operational conditions.

Thus, modeling and forecasting are crucial tools for addressing data ambiguity and uncertainty, which enhances the accuracy of GTM selection and their effectiveness under operational conditions. The application of modern mathematical methods plays a significant role in achieving these improvements.

5. Conclusions

The problems discussed in this paper are examined from both specific and systemic perspectives incorporating research methods such as probabilistic-statistical approaches and fuzzy logic-based methods. Using these methods, the authors developed models for various GTM efficiency indicators and outlined decision-making pathways under conditions of uncertainty.

The analysis shows that, despite the significant number of results accumulated to date, the improvement of GTM selection methods remains a pressing task. The necessity of integrating mathematical, informational, and software solutions is evident to enhance the accuracy of effectiveness evaluations.

The introduction of comprehensive analytical systems based on modern methods, such as cluster

analysis and fuzzy logic, will optimize the decision-making process and adapt it to complex geological conditions. This approach ensures more reliable, accurate, and context-sensitive GTM planning and implementation.

Acknowledgements. This paper was carried out with the financial support of the Science Committee of the Ministry of Science and Higher Education of the Republic of Kazakhstan (No. AR19674847).

REFERENCES

- Abasov M.T., Efendiayev G.M., Strekov A.S. et al. Comparative evaluation of GTM effectiveness based on comprehensive information. Oil Industry, No. 10, 2003, pp. 70-73 (in Russian).
- Akhmetov D.A., Efendiayev G.M., Karazhanova M.K., Koylibaev B.N. Classification of hard-to-recover hydrocarbon reserves in Kazakhstan using fuzzy cluster analysis. 13th International Conference on Application of Fuzzy Systems and Soft Computing, ICAFS 2018. Warsaw, Poland, August 27-28, 2018, pp. 865-872.
- Efendiayev G.M., Mammadov P.Z., Piriverdiyev I.A., Mammadov V.N. Clustering of geological objects using the FCM algorithm and evaluation of the rate of lost circulation. Procedia Computer Science, Vol. 102, 2016, pp. 159-162, DOI:10.1016/S1877-0509(16)32664-3.
- Efendiayev G.M., Mammadov P.Z., Piriverdiyev I.A., Mammadov V.N. Estimation of lost circulation rate using fuzzy clustering of geological objects by petrophysical properties. Visnyk Taras Shevchenko National University of Kyiv, Geology, Vol. 2 (81), 2018, pp. 28-33, DOI:10.17721/1728-2713.81.04.
- Efendiayev G.M., Moldabayeva G.Z., Abbasova S.V., Tuzelbayeva Sh.R. Models and methods of analysis and decision-making in controlling technological processes of oil and gas production under conditions of uncertainty. SOCAR Proceedings, No. 1, 2025.
- Fakhretdinov R.N., Kaledin Yu.A., Zhitkova M.V. The potential of modern information technologies in assessing the effectiveness of enhanced oil recovery methods. Oil Industry, No. 3, 2001, pp. 54-55 (in Russian).
- Glukhikh I.N., Pyankov V.N., Zabolotnov A.R. Situational models in corporate knowledge bases for geological and technical measures. Oil Industry, No. 6, 2002, pp. 45-48 (in Russian).
- Ilyushin P.Yu., Rakimyanov R.M., Solovyev D.Yu., Kolychev I.Yu. Analysis of well intervention aimed at oil production enhancement in the Perm krai's fields. Bulletin of the Perm National Research Polytechnic University. Geology, Oil, Gas and Mining. Perm, No. 15, 2015, pp. 81-89, DOI:10.15593/2224-9923/2015.15.9 (in Russian).
- Kazakov A.A. Methodological support for unified approaches to assessing the effectiveness of EOR methods. Technologies of Fuel and Energy Complex, Supplement to Oil and Capital journal, No. 2, 2003, pp. 47-53 (in Russian).
- Kazakov A.A. Methodology for assessing the effectiveness of GTM based on oil production decline curves. Oil Industry, No. 12, 1999, pp. 31-34 (in Russian).
- Khasanov M.M., Mukhamedshin R.K., Khatmullin I.F. Computer technologies for solving multi-criteria tasks of oil field development monitoring. Vestnik inzhiniringovogo tsentra YUKOS (Bulletin of the YUKOS Engineering Center), No. 2, 2001, pp. 26-29 (in Russian).
- Kravchenko Yu.A., Makhno D.A. Principles for building decision-support systems to assess the functional state of decision-
- analysis and fuzzy logic, will optimize the decision-making process and adapt it to complex geological conditions. This approach ensures more reliable, accurate, and context-sensitive GTM planning and implementation.
- Acknowledgements.** This paper was carried out with the financial support of the Science Committee of the Ministry of Science and Higher Education of the Republic of Kazakhstan (No. AR19674847).
- ## ЛИТЕРАТУРА
- Akhmetov D.A., Efendiayev G.M., Karazhanova M.K., Koylibaev B.N. Classification of hard-to-recover hydrocarbon reserves in Kazakhstan using fuzzy cluster analysis. 13th International Conference on Application of Fuzzy Systems and Soft Computing, ICAFS 2018. Warsaw, Poland, August 27-28, 2018, pp. 865-872.
- Efendiayev G.M., Mammadov P.Z., Piriverdiyev I.A., Mammadov V.N. Clustering of geological objects using the FCM algorithm and evaluation of the rate of lost circulation. Procedia Computer Science, Vol. 102, 2016, pp. 159-162, DOI:10.1016/S1877-0509(16)32664-3.
- Efendiayev G.M., Mammadov P.Z., Piriverdiyev I.A., Mammadov V.N. Estimation of lost circulation rate using fuzzy clustering of geological objects by petrophysical properties. Visnyk Taras Shevchenko National University of Kyiv, Geology, Vol. 2 (81), 2018, pp. 28-33, DOI:10.17721/1728-2713.81.04.
- Efendiayev G.M., Moldabayeva G.Z., Abbasova S.V., Tuzelbayeva Sh.R. Models and methods of analysis and decision-making in controlling technological processes of oil and gas production under conditions of uncertainty. SOCAR Proceedings, No. 1, 2025.
- Moldabayeva G.Z., Efendiayev G.M., Kozlovskiy A.L., Buktukov N.S., Abbasova S.V. Modeling and adoption of technological solutions in order to enhance the effectiveness of measures to limit water inflows into oil wells under conditions of uncertainty. ChemEngineering, Vol. 7, No. 5, 89, 2023, <https://doi.org/10.3390/chemengineering7050089>.
- Strekov A.S., Mamedov P.Z., Koysheva A.I. Decisions-making on the choice of geological and technical measures under uncertainty. Seventh International Conference on Soft Computing, Computing with Words and Perceptions in System Analysis, Decision and Control, Izmir, Turkey, September 2-3, 2013, pp. 381-384.
- Well Flo – Well modeling and design. (Electronic resource), <http://www.weatherford.com/Products/Production/ProductOptimizer/Software/WellFloSoftware/index.htm>.
- Wiseman H., Gradian F. Regulation of shale gas development, including hydraulic fracturing. Energy Institute, University of Texas at Austin; University of Tulsa Legal Studies, Research Paper No. 2011-11, October 31, 2011, 130 p.
- Zadeh L.A. Fuzzy sets as a basis for a theory of possibility. Fuzzy Sets and Systems, 1978, No. 1, pp. 3-28, [https://doi.org/10.1016/S0165-0114\(99\)80004-9](https://doi.org/10.1016/S0165-0114(99)80004-9).
- Абасов М.Т., Эфендиев Г.М., Стреков А.С. и др. Оценка сравнительной эффективности геолого-технических мероприятий по комплексной информации. Нефтяное Хозяйство, No. 10, 2003, с.70-73.
- Выбор геолого-технических мероприятий при воздействии на призабойную зону скважины. 2004. (электронный ресурс), <https://www.oil-info.ru/content/view/31/51/>.
- Глухих И.Н., Пьянков В.Н., Заболотнов А.Р. Ситуационные модели в корпоративных базах знаний геолого-технологических мероприятий. Нефтяное хозяйство, No. 6, 2002, с.45-48.

- makers. 2009. (Electronic resource). <http://www.cawater-info.net/pdf/kravchenko-mahno.pdf> (in Russian).
- Moldabayeva G.Z., Efendihev G.M., Kozlovskiy A.L., Buktukov N.S., Abbasova S.V. Modeling and adoption of technological solutions to enhance the effectiveness of measures to limit water inflows into oil wells under conditions of uncertainty. *ChemEngineering*, Vol. 7 (5), No. 89, 2023, <https://doi.org/10.3390/chemengineering7050089>.
- Pyankov V.N., Filev A.I. Integral software complex "Baspro-Analyst". *Oil Industry*, No. 9, 2000, pp. 109-114 (in Russian).
- Sarvaretdinov R.G., Gilmanova R.Kh., Khisamov R.S. et al. Formation of a database for GTM optimization in oil production. *Oil Industry*, No. 8, 2001, pp. 32-35 (in Russian).
- Savchenko T.N. Application of cluster analysis methods for processing psychological research data. *Experimental Psychology*, Vol. 3, No. 2, 2010, pp. 67-86 (in Russian).
- Selection of geological and technical measures for influencing the well's near-wellbore zone. 2004. (Electronic resource). <https://www.oil-info.ru/content/view/31/51/> (in Russian).
- Shakhverdiev A.Kh., Panakhov G.M., Abbasov E.M., Rasulova S.R. On the possibility of regulating viscosity anomalies in heterogeneous mixtures. *Bulletin of the Russian Academy of Natural Sciences*, No. 1, 2014, pp. 28-33 (in Russian).
- Shpurov A.V., Pyankov V.N., Klochkov A.A., Brilliant L.S. Planning GTM effectiveness when forecasting oil production. *Oil Industry*, 2000, No. 9, pp. 105-108 (in Russian).
- Strekov A.S., Mamedov P.Z., Koyskina A.I. Decision-making on the choice of geological and technical measures under uncertainty. The Seventh international conference on soft computing, computing with words and perceptions in system analysis, decision and control. Turkey, Izmir, September 2-3, 2013, pp. 381-384.
- Syrtlanov V.R., Kadochnikova L.M., Trushnikova O.M. Methods for evaluating the effectiveness of GTM based on three-dimensional hydrodynamic modeling. *Oil Industry*, No. 6, 2002, pp. 38-40 (in Russian).
- Well Flo – Well modeling and design. (Electronic resource), <http://www.weatherford.com/Products/Production/ProductOptimizer/Software/WellFloSoftware/index.htm>.
- Wiseman H., Gradijan F. Regulation of shale gas development, including hydraulic fracturing. Energy Institute, University of Texas at Austin; University of Tulsa Legal Studies, Research Paper No. 2011-11, October 31, 2011, 130 p.
- Zadeh L.A. Fuzzy sets as a basis for a theory of possibility. *Fuzzy Sets and Systems*, 1978, No. 1, pp. 3-28, [https://doi.org/10.1016/S0165-0114\(99\)80004-9](https://doi.org/10.1016/S0165-0114(99)80004-9).
- Zhanturin Zh.K. Approximate assessment of GTM effectiveness indicators with limited information. *Bulletin of the Atyrau Institute of oil and gas*, No. 12, 2007, pp. 63-65 (in Russian).
- Zhanturin Zh.K. Development of oil production intensification measures for implementation under various geological and physical conditions in Kazakhstan. PhD dissertation in technical sciences. Atyrau, 2009, 115 pp. (in Russian).
- Zhanturin Zh.K. On forecasting GTM effectiveness based on comprehensive information. *Oil and Gas*, No. 4, 2008, pp. 45-49 (in Russian).
- Zolotukhin A.B., Eremin N.A., Nazarova L.N., Ponomarenko E.M. Fuzzy set theory in the selection of methods for influencing oil reservoirs. *Oil Industry*, 1991, No. 3, pp. 21-23 (in Russian).
- Жантурин Ж.К. О прогнозировании эффективности геолого-технических мероприятий по комплексной информации. *Нефть и газ*, No. 4, 2008, с. 45-49.
- Жантурин Ж.К. Ориентировочная оценка показателей эффективности геолого-технических мероприятий при недостаточной информации. *Вестник АИНИГ (Атырауский институт нефти и газа)*, No. 12, 2007, с. 63-65.
- Жантурин Ж.К. Разработка мероприятий по интенсификации добычи нефти с целью их проведения в различных геолого-физических условиях Казахстана. Диссертация канд. технических наук. Атырау, 2009, 115 с.
- Золотухин А.Б., Еремин Н.А., Назарова Л.Н., Пономаренко Е.М. Теория нечетких множеств в выборе методов воздействия на нефтяные пласти. *Нефтяное хозяйство*, No. 3, 1991, с. 21-23.
- Илюшин П.Ю., Рахимзянов Р.М., Соловьев Д.Ю., Колычев И.Ю. Анализ проведения геолого-технических мероприятий по увеличению продуктивности добывающих скважин на нефтяных месторождениях Пермского края. *Вестник Пермского национального исследовательского политехнического университета. Геология, нефтегазовое и горное дело*, Пермь, No. 15, 2015, с. 81-89.
- Казаков А.А. Методика оценки эффективности GTM по кривым падения дебита нефти. *Нефтяное Хозяйство*, No. 12, 1999, с. 31-34.
- Казаков А.А. Методическое обеспечение единых подходов оценки эффективности методов ПНП. *Технологии ТЭК (топливно-энергетического комплекса)*, Приложение к журналу «Нефть и капитал», No. 2, 2003, с. 47-53.
- Кравченко Ю.А., Махно Д.А. Принципы построения систем поддержки принятия решений для оценки функционального состояния лица принимающего решения. 2009, (Электронный ресурс). <http://www.cawater-info.net/pdf/kravchenko-mahno.pdf>.
- Пьянков В.Н., Филев А.И. Интегральный программный комплекс "Баспро-аналитик". *Нефтяное Хозяйство*, No. 9, 2000, с.109-114.
- Савченко Т.Н. Применение методов кластерного анализа для обработки данных психологических исследований. *Экспериментальная психология*, Том 3, No. 2, 2010, с. 67-86.
- Сарвареддинов Р.Г., Гильманова Р.Х., Хисамов Р.С. и др. Формирование базы данных для разработки GTM оптимизации добычи нефти. *Нефтяное Хозяйство*, No. 8, 2001, с. 32-35.
- Сыртланов В.Р., Кадочникова Л.М., Трушникова О.М. Методики оценки эффективности GTM на основе трехмерного гидродинамического моделирования. *Нефтяное Хозяйство*, No. 6, 2002, с. 38-40.
- Фахретдинов Р.Н., Каледин Ю.А., Житкова М.В. Потенциал современных информационных технологий при оценке эффективности методов увеличения нефтеотдачи. *Нефтяное хозяйство*, No. 3, 2001, с. 54-55.
- Хасанов М.М., Мухамедшин Р.К., Хатмуллин И.Ф. Компьютерные технологии решения многокритериальных задач мониторинга разработки нефтяных месторождений. *Вестник инженирингового центра ЮКОС*, No. 2, 2001, с. 26-29.
- Шахвердиеv A.X., Panahov G.M., Abbasov E.M., Rasulova C.R. О возможности регулирования вязкостной аномалии в гетерогенных смесях. *Вестник РАЕН (Российская академия естественных наук)*, No. 1, 2014, с. 28-33.
- Шпуроv A.V., Пьянков В.Н., Клочкиv A.A., Бриллиант Л.С. Планирование эффективности GTM при прогнозировании добычи нефти. *Нефтяное хозяйство*, No. 9, 2000, с.105-108.

АНАЛИЗ МЕТОДОВ ОЦЕНКИ ЭФФЕКТИВНОСТИ ГЕОЛОГО-ТЕХНИЧЕСКИХ МЕРОПРИЯТИЙ И ПРИНЯТИЯ РЕШЕНИЙ ПО ИХ ВЫБОРУ: КОНЦЕПТУАЛЬНЫЙ ОБЗОР

Молдабаева Г.Ж.¹, Аббасова С.В.², Закенов С.Т.³, Кирисенко О.Г.⁴,
Икласова Ж.У.⁵, Жантурин Ж.К.⁵, Тузельбаева Ш.Р.¹, Ванг Дж.²

¹КазНИИТУ им. К.И.Сатпаева, Казахстан
050013, Алматы, ул. Сатпаева, 22

²Азербайджанский государственный университет нефти и промышленности, Азербайджан,
AZ1010, Баку просп. Азадлыг, 34

³Каспийский государственный университет технологий и инженеринга имени Ш. Есенова, Казахстан
130000, Актау, 32 мкр.

⁴Министерство науки и образования Республики Азербайджан, Институт нефти и газа, Азербайджан,
AZ1000, Баку, ул. Ф.Амирова, 9

⁵Атырауский университет нефти и газа, Казахстан
г. Атырау, мкр. Привокзальный, ул. Баймуханова, 45А

Резюме. В статье рассматриваются современные подходы к выбору и оценке эффективности геолого-технических мероприятий (ГТМ), направленных на повышение нефтеотдачи и разработку трудноизвлекаемых запасов. Основной задачей является определение оптимальных методов, обеспечивающих высокую технико-экономическую эффективность в условиях сложных геологических, а также эксплуатационных параметров.

Анализируются традиционные и современные методы оценки эффективности ГТМ, включая экстраполяцию базовых характеристик добычи, методы анализа кривых падения дебита нефти и прогнозирования с использованием вероятностно-статистических моделей. Подчёркивается недостаточная надёжность традиционных подходов из-за неопределенности данных, многокритериальности и нелинейности взаимодействия факторов. В процессе анализа литературных источников рассмотрена возможность использования нечёткой логики, методов «наименьших уступок», кластерного анализа и экспертных систем, которые позволяют учитывать размытость границ параметров и принимать более точные решения в условиях неполноты информации.

В статье приведены примеры применения современных методов на различных месторождениях. Обсуждается возможность создания комплексных информационных систем для поддержки принятия решений, включающих математические алгоритмы, базу данных и прогнозные модели. Особое внимание уделяется выбору параметров для оценки эффективности мероприятий, таких как физико-геологические характеристики, обводнённость, дебиты нефти, а также экономические показатели.

В указанной работе обосновывается необходимость дальнейшего совершенствования подходов к оценке и планированию ГТМ. В ней предлагается интеграция современных методов анализа данных, моделирования и прогнозирования для повышения надёжности и точности решений, что способствует успешному решению задач оптимизации разработки нефтяных месторождений и снижению рисков.

Ключевые слова: месторождение, нечёткий кластер-анализ, геолого-технические мероприятия, прогноз, принятие решений

GEOLOJİ-TEXNİKİ TƏDBİRLƏRİN EFFEKTİLİYİNİN QİYMƏTLƏNDİRİLMƏSİ ÜSULLARININ TƏHLİLİ VƏ ONLARIN SEÇİLMƏSİ ÜZRƏ QƏRARLARIN QƏBUL EDİLMƏSİ: KONSEPTUAL İCMAL

Moldabayeva G.J.¹, Abbasova S.V.², Zakenov S.T.³, Kirisenko O.G.⁴,
İklasova J.U.⁵, Janturin J.K.⁵, Tuzelbayeva Ş.R.¹, Vanq J.²

¹Qazaxistan Respublikası K.I.Satpayev adına Universitet, Qazaxistan
050013, Almatı, Satpayev küç. 22

²Azərbaycan Dövlət Neft və Sənaye Universiteti, Azərbaycan
AZ 1010, Baki şəhəri, Azadlıq pr. 34

³Yesenov adına Xəzər Dövlət Texnologiya və Mühəndislik Universiteti, Qazaxistan
130000, Aktau şəhəri, 32 mkr.

⁴Azərbaycan Respublikası Elm və Təhsil Nazirliyi, Neft və Qaz İnstitutu, Azərbaycan
AZ 1000, Baki şəhəri, F.Əmirov küç., 9

⁵Atrau Neft və Qaz İnstitutu, Qazaxistan
Atrau şəhəri, mkr. Privokzalny, Baymuxanov küç. 45A

Xülasə. Məqalədə müasir yanaşmaların seçimi və qiymətləndirilməsi, geoloji-texniki tədbirlərin (GTT) effektivliyi, neft hasilatının artırılması və çətinliklə hasil olunan ehtiyatlar müzakirə olunur. Burada əsas məsələlərdən biri optimal qərarların qəbul edilməsi bunu üçün aparılan əvvəlki mərhələlərdə müxtəlif geoloji-texniki qərarların modelləşdirilməsi gündəlikdə duran əsas məsələlərdən biridir. Onu da qeyd etmək lazımdır ki, bütün bu məsələlərin həlli hal-hazırkı vaxta qədər çətinliklə çıxarılan ehtiyatların ümumi təsnifatının olmaması səbəbindən nəzərə çarpacaq dərəcədə çətinləşir. Qeyd olunmuş istiqamətdə dərc olunmuş elmi tədqiqat işləri belə bir sistemin metodologiyasının yaranmasının və bunun çərçivəsində çətinliklə çıxarılan ehtiyatların təsnifatı müxtəlif geoloji-fiziki şəraitdə aparılan geoloji-texniki tədbirlər haqqında məlumatın toplanması və təhlili həmin prossesin modelləşdirilməsi və qərarların qəbul edilməsi məsələlərini ümumilikdə aktual bir problem kimi gündəliyə çıxarıb. Bütün bunlar irəli sürülen layihədə nəzərə alınmışdır. Layihədə ilk növbədə işin məqsədi, baxılacaq məsələlər və gözlənilən yeniliklər öz əksini tapmışdır.

Açar sözlər: yataq, qeyri-səlis məntiq, klaster-analiz, geoloji-texniki tədbirlər, neft hasilati, qərarın qəbul edilməsi

ASSESSMENT OF RADIOECOLOGICAL RISKS AND THE SUITABILITY OF WATER QUALITY FOR DRINKING AND AGRICULTURAL USE IN GUBADLI DISTRICT OF THE REPUBLIC OF AZERBAIJAN

Humbatov F.^{1,2}, Ibrahimov G.¹, Aslanova G.¹, Nejati Solut H.¹,
Balayev V.¹, Karimova N.¹, Karimbeyli I.¹

¹ Ministry of Science and Education of the Republic of Azerbaijan,
Institute of radiation problems, Azerbaijan

9, B.Vahabzade str., Baku, AZ 1143: hfamil@mail.ru

²Azerbaijan University of Architecture and Construction, Azerbaijan
5, Ayna Sultanova St., Baku, AZ1073

Keywords: Gubadli district of Azerbaijan, radioecology, water quality management, Residual Sodium Carbonate (RSC), Sodium Absorption Ratio (SAR), Soluble Sodium Percent (SSP)

Summary. In the last 30 years, monitoring and research works have not been carried out in the territory of Karabakh and the Eastern Zangezur economic regions, which include Gubadli region. The paper aims to assess the radioecological risk and ecological safety of the demined area in the Gubadli region of Azerbaijan. Radiation background levels were measured at 64 locations within the area and average radiation background was determined to be 7.5 $\mu\text{R/h}$, which provided comprehensive understanding of radiation levels in the region.

In addition to radiation background analysis, hydrochemical analysis and assessment of water quality in the area, suitable for domestic consumption, agriculture and industrial purposes, and to assist in water management were also carried out. Total 7 water samples were taken from various sources in the area including rivers and other water bodies. These samples were subjected to the detailed analysis to determine their suitability for domestic, livestock consumption, and irrigation purposes. Physicochemical processes in river systems are affected by various parameters of water quality, which makes continuous monitoring essential for environmental and scientific purposes.

The research results revealed that the mineral content in two water samples was higher than others but did not exceed the limits set by World Health Organization (WHO) standards. In addition, high concentrations of iron (Fe) were detected in three samples, and high concentrations of manganese (Mn) in one sample. These results indicate that these water sources are hazardous for drinking, livestock and irrigation, and highlight the need for additional monitoring and restoration efforts in the region.

© 2025 Earth Science Division, Azerbaijan National Academy of Sciences. All rights reserved.

Introduction

Gubadli district is one of 66 districts of Azerbaijan. It is located in the southwest of the country and is included in the Eastern Zangezur Economic Region. The district borders Lachin, Khojavand, Jabrayil and Zangilan districts and Syunik province of Armenia. The region is surrounded by the Karabakh range in the southwest, the Bergushad range in the east, and the Karabakh plateau in the southeast. It is here, in the southeast stream between the winding Bazarchay and the Hekari River, that is the continuation of the Karabakh Plateau which slowly descends up to 450 meters lies the Yaziduzu plain.

The Bargushad, Hekari and their tributaries (the Aga river, Kichic Hekari, Meydandersi, etc.) flow

through the territory of the district. The water of these rivers was mainly used for irrigation purposes.

The length of the Bargushad river (also called the Bazarchay in some sources) is 178 kilometers. The river mainly takes its source from the Zangezur mountains, the Zalkha lake at an altitude of 3040 meters on the Karabakh plateau, and the Arikli mountains. It is called Bazarchay up to the Urud village. 93 kilometers of the river is in the territory of Armenia. The Bargushad river merges with the Hekari river near the Garalar village of Gubadli district and flows into the Araz. The area of the basin is 2711 square km. After joining the Hekari river, it flows through a relatively flat area and divides into a number of tributaries. The annual flow is under-

ground (55%), snow (35%) and rain waters (10%). Snow waters flood the river in spring and summer.

Average annual water consumption is 19.0 cubic m/sec. 45% of it occurs in spring, 25% in summer, 18% in autumn, and 12% in winter.

The length of the Hekari river is 113 km, the area of its basin is 2570 km². It is the second largest river of the Lesser Caucasus after the Tartarchay (together with the Bazarchay) within Azerbaijan. It begins at an altitude of 2580 m, 3.5 km east of the peak of Shishtepe on the southern slope of the Mikhтокен ridge. It is formed by the confluence of Shelvachay and Hojazsuchay rivers (950 m), and connects with the Bargushad river near the Garalar village of Gubadli district (Hindverd Cape). The largest tributary in the Gubadli region is the Lesser Hakari river. Runoff comes from snow (23%), rain (1-5%) and groundwater (62%). Snow waters flood the river in spring and summer. 60-70% of its annual flow passes during the flood period (April-June). The least water consumption in the river is observed in winter.

The water of these rivers is widely used in irrigation and energy. At the same time, these water sources are also evaluated as potential sources of drinking water.

Currently, surface water resources in the territory of Azerbaijan are 27 cubic kilometers, and this figure decreases to 20-21 cubic kilometers in dry years. 70-72 percent of fresh water resources of the country are formed outside the borders of the country (Suleymanov et al., 2008; Ahmadov et al., 2017).

The water resources of rivers in the territory of the Karabakh economic region are 831.7 million cubic meters. The river water reserve formed in the territory of the East-Zangazur economic region is equal to 1622.6 million cubic meters in total. On the territory of Karabakh and East Zangezur economic districts, freed from occupation, the river water reserve is 2508.4 million cubic meters in total. This is equal to 22 percent of the river water reserve formed in the territory of Azerbaijan.

In the last 30 years, monitoring and research works have not been carried out in the territory of Karabakh and the Eastern Zangezur economic regions, which include Gubadli region. During this period, deliberate change of topography of the region, merciless looting of natural resources, and the use of heavy military equipment and various types of explosives polluted the area, disturbed the ecological balance and caused pollution of existing water sources.

For this reason, it is of particular importance to measure the radiation background in the area and to determine the physical-chemical and biological

characteristics of the river in order to control the water quality.

Hydro-chemical analysis and subsequent water quality evaluation often reveals quality of water that is suitable for domestic consumption, agriculture and industrial purposes, as well as aiding in the management of the water resource. Furthermore, it is possible to understand the change in water quality due to either rock water interaction or anthropogenic influence. Water often consists of seven major chemical ions which include cations Ca^{2+} , Mg^{2+} , Na^+ , K^+ and anions Cl^- , HCO_3^- , SO_4^{2-} . Other parameters include pH, Colour, Turbidity, Free Carbon Dioxide and Total Dissolved Solid. These chemical parameters play a significant role in classifying and assessing water quality. In this paper, we present the results of our studies on the radiation measurement and water quality in the territory of Gubadli district of Azerbaijan Republic. The water samples were collected from different water sources of the Gubadli district, were analyzed and compared with water quality standards for domestic, industrial, livestock and irrigation usage.

Materials and methods

It is known that natural background radiation is the main source of exposure for most people. Background radiation is a measure of the level of ionizing radiation present in the environment at a given location that is not due to the intentional application of radiation sources. Background radiation comes from a variety of sources, both natural and man-made. In order to assess the radioecological risk during the research, the radiation background was measured in 64 locations cleared of mines in the territory of Gubadli region (Fig. 1). Gamma radiation exposure dose rates were measured using the IndetIFINDER-2 dosimeter-spectrometer according to the recommendations of the International Atomic Energy Agency (UNSCEAR 1988; UNSCEAR 1993; UNSCEAR 2000a; UNSCEAR 2000b).

Measurements were made according to standard operating procedures, and the average radiation background was determined to be 7.5 $\mu\text{R/h}$, with the natural radiation background observed for these locations varying in the range of 2.5-14.5 $\mu\text{R/h}$. The dose rate of radiation at the measurement points is presented in Fig. 2.

As it can be seen, only one point has a relatively high result. Relatively high radiation levels were observed in the point 22-Davudlu area, which necessitates continuous monitoring. In general, the observed results for radiation background measurements indicate that there are no risks in terms of radiation safety in the study area.

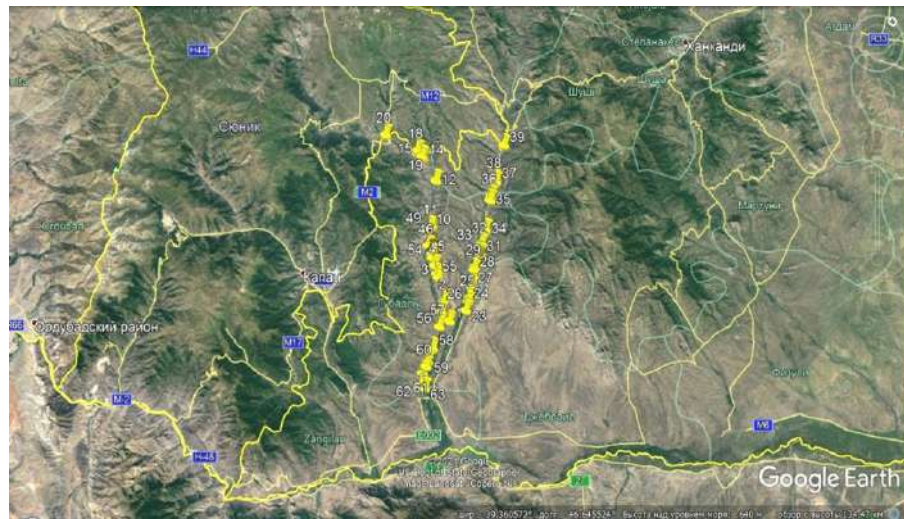


Fig. 1. The measurement of radiation background was carried out in the areas of Gubadli district

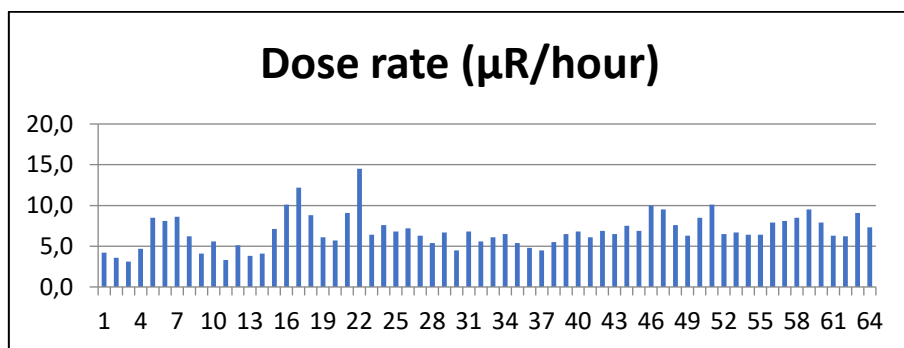


Fig. 2. The dose rate of radiation at the measurement points in the Gubadli district

Water samples were taken from 7 different points of Gubadli area. Water samples were collected using a standard polyethylene water sampler, which was rinsed several times with river water from the sampling point before obtaining representative samples from 30 cm below the water surface. A 200 ml water sample was filtered through a 0.45 µm membrane filter using a manual plastic filtration assembly. A few drops of high-purity nitric acid (HNO_3) were added to the filtrate to adjust the pH. The sample was then securely stored at 4°C during transport to the laboratory. Water sampler was rinsed with deionized water between each sampling event. All plastic ware including sample bottles, pipette tips, filtration units, and flasks were soaked in 10% v/v HNO_3 for 24 hours and rinsed with deionized water before use.

When water samples are brought in sterile containers and cannot be measured immediately, they are stored in a refrigerator. The samples are transferred from the containers to the measuring beakers for immediate measurements.

The pH meter is calibrated first and then used to take measurements. The pH meter electrodes are

rinsed with distilled water to prevent cross-contamination between different samples.

If immediate measurement is not possible, water samples are usually carefully stored in sterile containers in the refrigerator to preserve their integrity. Once ready for analysis, these samples are transferred to measuring containers. This meticulous process helps maintain the integrity and accuracy of pH measurements.

To assess total dissolved solids (TDS), conductivity (Cond), and salinity, a conductivity meter is utilized with its electrodes rinsed using distilled water following each sample measurement. The conductivity meter provides crucial insights into water conductivity levels. The dedicated DO meter is employed for measuring dissolved oxygen (DO) after being cleaned with distilled water offering rapid results within seconds allowing swift analysis of oxygen levels in the samples. Measurements are iterated multiple times ensuring reliable data collection to enhance precision. The results obtained from the water samples are tabulated (Table 1) providing a comprehensive overview of their respective characteristics. This approach guarantees accurate assessment of water composition and quality.

Table 1
Water parameters of samples taken from Gubadli district

	Parameters	Source Coordinates		pH	COND	TDS	DO
N	Sampling points	longitude	latitude		mksm/cm	mg/L	mg/L
1	Mahmudlu v. Bargushad river	39°26'207"	046°33'591"	8.3	250	173	7.29
2	Aliguluushagi-Davudlu, Bargushad river	39°48'53.12"	046°28'149"	8.1	256	187	7.71
3	Spring - Drinking water source	39°26'297"	046°27'286"	8.1	544	339	7.36
4	Armenian border, Bargushad River	39°25'50.0"	046°23'21.4"	8.2	239	164	7.71
5	Lachin border, Gulabird v., Hekari river	39°28'368"	046°37'054"	8.2	292	186	7.64
6	Armenian border, Eyyazlı-Shahverdiler v. (Technical water)	39°25'50.0"	046°23'21.4"	8.5	213	146	6.88
7	Davudlu river	39°26'240"	046°25'342"	8.2	453	301	6.24
	WHO (World Health Organization)			6.5-8.5	500-1000	500	-

Water samples collected for the assessment of metal pollution is a complex process need to ensure accurate analysis. Initially, the collected samples are filtered. These prepared samples are separated as filter and then total sample stored in containers suitable for heavy metal analysis. The water samples were collected after 30 minutes of pumping to avoid stagnant and contaminated water. White plastic containers were rinsed out 3-4 times with sample water. Then the containers were filled up to capacity and were immediately sealed to avoid exposure to air. After collecting the samples, the containers were labelled for identification and brought to the laboratory.

Water samples were tested for pH, TDS, sodium (Na^+), potassium (K^+), calcium (Ca^{2+}), magnesium (Mg^{2+}), sulfate (SO_4^{2-}), chloride (Cl^-), bicarbonate

(HCO_3^-) and metal concentrations were analyzed for Cu, Fe, Mn, Mo, Ni, Zn. Na^+ , K^+ , Ca^{2+} , and Mg^{2+} were determined among the analysed parameters using a flame atomic absorption spectrometer.

After some stages, element concentrations in each sample are measured utilizing an Agilent 7700x ICP-MS (Inductively Coupled Plasma Mass Spectrometry) system operating in helium mode (Mamadzada et al., 2021; Ahmadov et al., 2016). Before analytical measurements, the instrument is allowed thermally equilibrating minimum of 30 minutes. Prior to analysis, mass calibration and resolution checks are performed in the specified mass regions of interest to ensure the accuracy and reliability of the measurements. Metal concentration of samples are given below (Table 2).

Table 2
Comparison of metal concentration with WHO recommended limit values

No	Sampling Point	Cu, $\mu\text{g}/\text{L}$	Fe, $\mu\text{g}/\text{L}$	Mn, $\mu\text{g}/\text{L}$	Mo, $\mu\text{g}/\text{L}$	Ni, $\mu\text{g}/\text{L}$	Zn, $\mu\text{g}/\text{L}$
1	Mahmudlu v. Bargushad river	3.41	425	170	<MDL	7.04	55.4
2	Aliquluushagi-Davudlu,Bargushad river	8.22	314	40.5	6.86	8.6	100
3	Spring - drinking water source	6.16	209	31.2	<MDL	1.54	10.9
4	Armenian border, Bargushad River	5.9	251	32.7	<MDL	7.7	10.2
5	Lachinborder, Gulabird v., Hakari river	4.61	214	42.8	1.06	<MDL	6.3
6	Armenian border, Eyyazlı-Shahverdiler v. (Technical water)	9.93	134	20.4	25.4	1.36	2.3
7	Davudlu river	5.1	325	48.4	<MDL	2.83	2.74
	WHO (World Health Organization)	2000	300	100	70	70	5000

Results and discussion

As shown in Table 1, the electrical conductivity measured for the samples taken from the Davudlu River and the spring (sample number: 3.7) has a higher value than other sources but does not exceed the recommended limit according to the guidelines of the World Health Organization (WHO) and can be recommended as drinking water sources. The relatively high electrical conductivity of the mentioned water sources indicates the high mineralization of these sources. In all the water samples analyzed, the levels of Cu, Mo, Ni and Zn are notably below the thresholds set by the WHO (Table 2). However, at the first sampling point, concentrations of Fe and Mn exceed the recommended limits, while at the second and seventh points, only Fe surpasses the guidelines. Although the average iron concentration in rivers is typically around 0.7 mg/L, post-treatment, Fe levels are usually maintained below 0.3 mg/L for safe drinking water.

Hence, it's not advisable to utilize the mentioned water sources (sampling points 1, 2, and 7) directly for drinking purposes.

Comparing the received conductivity results with the standards showed that all samples complied with the requested standards and may be used in livestock drinking purposes and irrigation. Anions and cations analysis results in samples demonstrate that HCO_3^- , Cl^- , SO_4^{2-} , Na^+ , K^+ , Mg^{2+} , and Ca^{2+} ions dominate in the studied areas.

Comparison of the cation concentrations of the studied water samples showed that water samples 1 and 5 have 1) $\text{Ca}>\text{Mg}>\text{Na}>\text{K}$ sequence, water samples 2,3,4,7 have 2) $\text{Ca}>\text{Na}>\text{Mg}>\text{K}$ sequence, and water sample 6 have 3) $\text{Na}>\text{Ca}>\text{Mg}>\text{K}$ sequence of cations. This means that Na ions prevail over K ions and Ca ions prevail over Mg ions for all sequences of cations. It is known that, observation of the existence of Ca and Mg in water samples is the result of the weathering of crystalline dolomitic limestones and Ca-Mg silicates (amphiboles, pyroxenes, olivine, biotite and others (Zakir et al., 2013; Singh et al., 2009). The origin of Na and K in water may be atmospheric deposition, evaporate dissolution, and silicate as albite, anorthite, orthoclase and microcline weather (Zakir et al., 2013; Ghosh et al., 1983, Singh et al., 2007; Ayers and Westcot, 1985; Singh et al., 2010). As it is noted in (Zakir et al., 2013), if Na concentration in water is less than 50mg/L, it is not dangerous for human drinking and if it is less than 920 mg/L it is not dangerous for irrigation. The concentration of sodium changes in the range of 5.6-38 mg/L and has an average of 15.87 mg/L on the studied water samples. As shown in Table 3, all water samples are suitable for irrigation and for human drinking. K concentration obtained for water samples changes from 2.3mg/L to 6.4mg/L and has the average of 3.5mg/L.

Comparison of potassium concentration in the studied water samples with standards (Table 4) shows that K concentration is less than 100mg/L for all samples and this water is suitable for drinking but the studied water sources are problematic for irrigation. The concentration of Ca for the measured samples changes from 15mg/L to 48 mg/L and has average of 32.7mg/L. If the concentration of Ca in water is less than 800 mg/L, it has no danger for irrigation. Therefore, all measured water samples can be implemented for irrigation and using water of this standard for irrigation is not problematic for soil (Zakir et al., 2013). We can note that all water samples are suitable for human drinking according to Ca results considering the opinion of authors (Zakir et al., 2013; Ghosh et al., 1983, Singh et al., 2007). The concentration of Mg on the studied samples changes in the range of 6.2mg/L – 12.2mg/L, and has the average of 8.67mg/L. As shown in Table 4, if the concentration of Mg in water is less than 120 mg/L, this source has no danger for irrigation. The maximum acceptable concentration of Mg is 30 mg/L for human drinking water (Ghosh et al., 1983). Therefore, all measured samples, may be used as human drinking water. HCO_3^- anion concentration on the studied river waters changes in the range of 61 mg/L –105 mg/L and has average of 78mg/L. Only samples 3 and 7 have more than 92mg/L HCO_3^- anion concentration and these samples are not suitable for irrigation according to the HCO_3^- anion concentration rate. The HCO_3^- anion concentration of the studied samples complies the requested standards (Ghosh et al., 1983) and they are suitable for being used as drinking water.

The concentration of SO_4^{2-} ions in the measured water samples varies from 31 mg/L to 116 mg/L with average of 66.85 mg/L. Water for agriculture usage purposes has a permissible level equal to 20 mg/L for SO_4^{2-} ions according to Tables 3 and 4. Therefore, not all water samples from the investigation areas can be used for irrigation. The recommended levels are 200 mg/L and <250 mg/L for human and livestock drinking water according to (Zakir et al., 2013; NAS 1983). Therefore, all the studied water samples are suitable for usage. The suitability of water for irrigation purposes depends on its mineral constituents. Several criteria for judging its suitability have been proposed in (Wilcox, 1955; Eaton, 1950). Irrigation water containing large amounts of sodium is of special concern due to sodium effects on the soil and its potential to pose sodium hazard. The high concentration of sodium in irrigation water may negatively affect soil structure and decrease soil hydraulic conductivity in fine-textured soil. The degree to which sodium will be absorbed by soil is a function of the amount of sodium to divalent cations (Ca and Mg) and is regularly stated by sodium adsorption ratio (SAR) (Bouwer and Idelovitch, 1987).

Table 3
Data for investigated water parameters

No	pH	Conduc-tivity	TDS	Chlo-ride (Cl ⁻)	Sul-phate (SO ₄ ²⁻)	Bicar-bonate	Sodium (Na)	Potassium (K)	Calcium (Ca)	Magnesium (Mg)
		mkSm/cm	mg/L	mg/L	mg/L	mg/L	mg/L	mg/L	mg/L	mg/L
1	8.3	250	173	5.3	52	76	8.3	2.3	28	8.6
2	8.1	256	187	7.8	54	78	9.4	2.8	29	9.3
3	8.1	544	339	26	116	105	38	6.4	48	8.9
4	8.2	239	164	9.9	48	62	7.8	3.2	26	6.2
5	8.2	292	186	11.4	66	61	5.6	2.3	33.2	8.7
6	8.5	213	146	14	31	62	16	4.4	15	6.8
7	8.2	453	301	24	101	102	26	3.1	46	12.2
min	8.1	213	146	5.3	31	61	5.6	2.3	15	6.2
max	8.5	544	339	26	116	105	38	6.4	48	12.2
mean	8.23	321	213.7	14.05	66.85	78	15.87	3.5	32.17	8.67

Table 4
Geochemical parameters in the water samples compared to desirable standard values for drinking, livestock and irrigation use

Parameters	Range	Mean	Max. desirable value for drinking water	Max. desirable value for livestock drinking water	Max. desirable value for irrigation
pH	8.1-8.5	8.23	6.5-8.5	6.8-7.5	6.0-8.4
EC(μS/cm)	213-544	321	750	-	-
TDS(mg/L)	146-339	213.7	500	<500	-
HCO ₃ ⁻ (mg/L)	61-105	78	200	<400	92
SO ₄ ²⁻ (mg/L)	31-116	66.85	200	<250	20
Cl ⁻ (mg/L)	5.3-26	14.05	250	-	142
Ca ²⁺ (mg/L)	15-48	32.17	75	-	800
Mg ²⁺ (mg/L)	6.2-12.2	8.67	30	-	120
Na ⁺ (mg/L)	5.6-38	15.87	50	-	920
K ⁺ (mg/L)	2.3-6.4	3.5	100	-	2.0

The Sodium Absorption Ratio (SAR) can be calculated from the ratio of sodium to calcium and magnesium (Asadollahfardi G. and Asadollahfardi R., 2011).

The equation is expressed as follows:

$$\text{SAR} = \frac{\text{Na}^+}{\sqrt{(\text{Ca}^{2+} + \text{Mg}^{2+})/2}}$$

where, all the ions are expressed in meq/L.

Variation from 0.2230 to 1.3182 average value of 0.6244 (Table 5). Sodium Absorption Ratios for all water samples are less than 10. The potential for sodium hazard increases in waters with higher sodium adsorption ratios (SAR) values. The sodium absorption ratio (SAR) content in the study area has shown and indicates excellent quality for irrigation. The samples fall in the excellent (S1) category (Table 6).

Soluble Sodium Percent (SSP) is also used to evaluate sodium hazard. SSP is defined as the ratio of sodium to the total cations (Asadollahfardi G. and Asadollahfardi R., 2011; Todd and Mays, 2005):

$$\text{SSP} = \frac{\text{Soluble}(\text{Na}^+ + \text{K}^+) * 100}{\text{Total cations concentration}}$$

where, all the ionic concentrations are expressed in meq/L.

Soluble Sodium Percent (SSP) values less than 50 or equal to 50 indicate good quality water and those more than 50 indicate water quality unsuitable for irrigation. The values of Soluble Sodium Percent (SSP) range from 11.3 to 38.0 and average 23.7. 100% Soluble Sodium Percent (SSP) for water in test areas is less than 50 and indicates good quality water for irrigation purposes (Table 6).

KR: Sodium measured against Ca²⁺ and Mg²⁺ is used to calculate Kelley's ratio. The formula used in the estimation of Kelley's Ratio (Wilcox, 1955; Who 2008):

$$\text{KR} = \text{Na}^+ / (\text{Ca}^{2+} + \text{Mg}^{2+}).$$

Kelley's Ratio (KR) of more than one indicates an excess level of sodium in water. Hence, water with Kelley's Ratio less than one are suitable for

irrigation, while those with a ratio of more than one are unsuitable for irrigation. The values of Kelley's Ratio (KR) range from 0.10 to 0.53 and average 0.29. 100% of Kelley's Ratio values for the water of the test area are less than 1 and indicate good quality water for irrigation purpose (Table 6).

Residual sodium carbonate (RSC): The Residual Sodium Carbonate (RSC) was also calculated and used for irrigation water quality assessment. This parameter is used for the assessment of effect of carbonate and bicarbonate on quality of water for agricultural purposes. RSC is calculated as follows:

$$\text{RSC} = (\text{CO}_3^{2-} + \text{HCO}_3^-) - (\text{Ca}^{2+} + \text{Mg}^{2+})$$

where, all the ions are expressed in meq/L.

The potential for sodium hazard increases as RSC increases, and much of the calcium and the

magnesium are precipitated out of solution when water is applied to the soil. Salts become concentrated when soil dries out, as less soluble ions (as Ca^{2+} and Mg^{2+}) tend to precipitate out of solution (Omotoso and OJO, 2012; Zafar and Ahmad, 2018; Howladar et al., 2017). The values of RSC ranges from -1.64 to -0.30 meq/L with average value of -1.05 (Table 5). In the test area, the RSC is negative showing that Na^+ build-up is unlikely, with practically no Na^+ hazard and therefore classified as suitable for irrigation. Water having less than or equal to 1.25 epm of RSC is safe for irrigation purposes. The water having a RSC from 1.25 to 2.5 epm is marginally suitable for irrigation purposes, whereas water having more than 2.5 epm of RSC is not suitable for irrigation purposes. Based on RSC values, all the samples of the test area have values less than 1.25 epm and are safe for irrigation (Table 6).

Table 5

The results of the geochemical analysis of water samples collected from Gubadli district of Azerbaijan

Nº	Na, meq/L	K, meq/L	Ca, meq/L	Mg, meq/L	Cl ⁻ , meq/L	SO ₄ , meq/L	Bicarbonate meq/L	SAR	% Sodium	RSC	KR
1	0.36	0.06	1.4	0.72	0.15	1.08	1.25	0.3508	16.6	-0.87	0.17
2	0.41	0.07	1.45	0.78	0.22	1.13	1.28	0.3875	17.8	-0.95	0.18
3	1.65	0.16	2.4	0.74	0.73	2.42	1.72	1.3182	36.6	-1.42	0.53
4	0.34	0.08	1.3	0.52	0.28	1.00	1.02	0.3558	18.8	-0.80	0.19
5	0.24	0.06	1.66	0.73	0.32	1.38	1.00	0.2230	11.3	-1.39	0.10
6	0.70	0.11	0.75	0.57	0.39	0.65	1.02	0.8574	38.0	-0.30	0.53
7	1.13	0.08	2.3	1.02	0.68	2.10	1.67	0.8778	26.7	-1.64	0.34
min								0.2230	11.3	-1.64	0.10
max								1.3182	38.0	-0.30	0.53
mean								0.6244	23.7	-1.05	0.29

Table 6

Classification of water based on SAR, KR, SSP and RSC

Parameter	Range	Water Class	Samples	% age
SAR	<10 10-18 18-26 >26	Excellent (S1) Good (S2) Doubtful (S3) Unsuitable (S4)	7	100
SSP	<50/>50	Good/Bad	7/0	100/0
KR	<1/>1	Good/Unsuitable	7/0	100/0
RSC	<1.25 1.25-2.5 >2.5	Good Doubtful Unsuitable	7	100

Conclusion

In order to assess the radioecological risk during the research, the radiation background was measured in 64 locations cleared of mines in the territory of Gubadli region, and the average radiation background was determined to be $7.5\mu\text{R/h}$. For estimation water quality water samples were collected and analyzed for their hydrochemical characteristics and an evaluation of water quality for drinking and irrigation purposes was made. Water samples were tested for pH, TDS, sodium (Na^+), potassium (K^+), calcium (Ca^{2+}), magnesium (Mg^{2+}), sulfate (SO_4^{2-}), chloride (Cl^-), bicarbonate (HCO_3^-) and metal concentrations were analyzed for Cu, Fe, Mn, Mo, Ni, Zn.

In all the water samples analyzed, the levels of Cu, Mo, Ni, and Zn are notably below the thresholds set by the WHO. However, at the first sampling point, concentrations of Fe and Mn exceed the recommended limits, while at the second and seventh points, only Fe surpasses the guidelines. The high concentration observed for Fe and Mn elements can be explained by the leaching of minerals in mountain rivers.

Comparison of the cation concentrations of the studied water samples showed that water samples 1 and 5 have the 1) $\text{Ca}>\text{Mg}>\text{Na}>\text{K}$ sequence, water samples 2,3,4,7 have 2) $\text{Ca}>\text{Na}>\text{Mg}>\text{K}$ sequence, and water sample 6 have 3) $\text{Na}>\text{Ca}>\text{Mg}>\text{K}$ sequence of cations. This means that Na ions prevail over K ions and Ca ions prevail over Mg ions for all sequences of cations. SAR values and sodium percent-

age (Na %) in test locations indicate that all water samples are suitable for use in irrigation.

Hydrochemical analysis demonstrates that samples are typical of shallow fresh waters. The EC values in the studied samples range from 213 to $544\mu\text{S/cm}$. Similarly, pH value of all the collected samples range from 8.1 to 8.5 compared to the recommended WHO guideline range of 6.5-8.5 for drinking water. The anion chemistry of the analyzed water samples show HCO_3^- , Cl^- , and SO_4^{2-} to be the dominant anions at the test area. With respect to HCO_3^- and SO_4^{2-} content, all water samples were found suitable for drinking and livestock usage. The concentration of SO_4^{2-} ions in the measured water samples varies from 31 mg/L to 116 mg/L with average of 66.85 mg/L. Water for agriculture usage purposes has a permissible level equal to 20 mg/L for SO_4^{2-} ions, according to Tables 3 and 4. Therefore, not all water samples from the studied areas can be used for irrigation. With regards to Cl^- , all water samples under the studied area were found suitable for drinking and livestock purposes. Based on RSC values, all samples of the test area have values less than 1.25 epm and are safe for irrigation.

The study underscores the necessity for continuous monitoring and comprehensive analysis of water quality in the Gubadlı district. Given the observed high levels of certain metals, further efforts are needed to ensure the safe use of these water sources, especially for drinking purposes.

REFERENCES

- Ahmədov M.M., Həmbatov F.Y., Balayev V.S., Mikayılova A.J. Estimation of river waters quality in Azerbaijan. Journal of Radiation Researches, Vol. 4 (1), 2017, pp. 24-31.
- Ahmədov M.M., Həmbatov F.Y., Balayev V.S., Suleymanov B.A. Uranium and thorium determination in water samples taken along river Kura. Journal of Materials Science and Engineering, Vol. B6 (3-4), 2016, pp. 80-84, DOI:10.17265/2161-6221/2016.3-4.004.
- Asadollahfardi G. and Asadollahfardi R. The usage of the polluted water for agriculture: wastewater reuse, health aspect, guidelines and standards, methods of treatment for irrigation, Lambert Academic Publishing, Germany, 2011, 72 p.
- Ayers R.S. and Westcot D.W. Water quality for agriculture. FAO Irrigation and Drainage, Paper 29, Food and agriculture organization of the United Nations, Rome, Italy, 1985, pp. 1-117.
- Bouwer H. and Idelovitch E. Quality requirement for irrigation with sewer water. Journal of Irrigation and Drainage Engineering, Vol. 113(4), 1987, pp. 516-535, [https://doi.org/10.1061/\(ASCE\)0733-9437\(1987\)113:4\(516\)](https://doi.org/10.1061/(ASCE)0733-9437(1987)113:4(516)).
- Eaton F.M. Significance of carbonates in irrigation waters. Soil Science, Vol. 69 (2), 1950, pp. 123-134.
- Ghosh A.B., Bajaj J.C., Hasan R., Singh D. Soil and water testing methods, A laboratory manual. Division of soil science and agricultural chemistry, IARI, New Delhi, India, International Mine Water Conference, Pretoria, South Africa, October 19-23, 1983, pp. 31-36.
- Howladar M.F., Al Numanbakhth Md.A. and Faruque M.O. An application of water quality index (WQI) and multivariate

ЛИТЕРАТУРА

- Ahmədov M.M., Həmbatov F.Y., Balayev V.S., Mikayılova A.J. Estimation of river waters quality in Azerbaijan. Journal of Radiation Researches, Vol. 4 (1), 2017, pp. 24-31.
- Ahmədov M.M., Həmbatov F.Y., Balayev V.S., Suleymanov B.A. Uranium and thorium determination in water samples taken along river Kura. Journal of Materials Science and Engineering, Vol. B6 (3-4), 2016, pp. 80-84, DOI:10.17265/2161-6221/2016.3-4.004.
- Asadollahfardi G. and Asadollahfardi R. The usage of the polluted water for agriculture: wastewater reuse, health aspect, guidelines and standards, methods of treatment for irrigation, Lambert Academic Publishing, Germany. 2011, 72 p.
- Ayers R.S. and Westcot D.W. Water quality for agriculture. FAO Irrigation and Drainage, Paper 29, Food and agriculture organization of the United Nations, Rome, Italy, 1985, pp. 1-117.
- Bouwer H. and Idelovitch E. Quality requirement for irrigation with sewer water. Journal of Irrigation and Drainage Engineering, Vol. 113(4), 1987, pp. 516-535, [https://doi.org/10.1061/\(ASCE\)0733-9437\(1987\)113:4\(516\)](https://doi.org/10.1061/(ASCE)0733-9437(1987)113:4(516)).
- Eaton F.M. Significance of carbonates in irrigation waters. Soil Science, Vol. 69 (2), 1950, pp. 123-134.
- Ghosh A.B., Bajaj J.C., Hasan R., Singh D. Soil and water testing methods, A laboratory manual. Division of soil science and agricultural chemistry, IARI, New Delhi, India, International Mine Water Conference, Pretoria, South Africa, October 19-23, 1983, pp. 31-36.
- Howladar M.F., Al Numanbakhth Md.A. and Faruque M.O. An application of water quality index (WQI) and multivariate

- statistics to evaluate the water quality around Maddhapara Granite Mining Industrial Area, Dinajpur, Bangladesh. Environ. Syst. Res., Vol. 6(1), paper 13, 2017, <https://doi.org/10.1186/s40068-017-0090-9>.
- Mammadzada S.Sh., Humbatov F.Y., Mustafayev I.I. Assessment of metal pollution in water and surface sediments of Goranchay River. Chemical Problems, No. 2(19), 2021, pp. 84-93, DOI: 10.32737/2221-8688-2021-2-84-93.
- NAS 1983. Drinking water and health. National Academy of Science, Washington, DC. Vol. 5, 1983, pp. 147-157.
- Omotoso O.A. and Ojo O J. Assessment of quality of river Niger floodplain water at Jebba, central Nigeria: implications for irrigation. Water Utility Journal, Vol. 4, 2012, pp. 13-24.
- Singh A.K., Mahato M.K., Neogi B., Singh K.K. Quality assessment of mine water in the Raniganj coalfield area, India. Mine Water and the Environment, Vol. 29, 2010, pp. 248-262, DOI:10.1007/s10230-010-0108-2.
- Singh A.K., Mondal G.C., Kumar S., Singh T.B., Tewary B.K., Sinha A. Major ion chemistry, weathering processes and water quality assessment in upper catchment of Damodar river basin, India. Environmental Geology, Vol. 54, 22 June 2007, pp. 745-758.
- Singh A.K., Mondal G.C., Tewary B.K., Sinha A. Major ion chemistry, solute acquisition processes and quality assessment of mine water in Damodar Valley Coalfields. Abstracts of the International Mine Water conference, 19–23 October 2009, Pretoria, South Africa, 2009, pp. 267-276
- Suleymanov B., Ahmedov M., Humbatov F., Ibadov N. Hazardous pollutant database for Kura-Araks water quality management. In: Transboundary water resources: A foundation for regional stability in Central Asia (Moerlins J.E. et. al., eds.). Springer. 2008, pp. 171-182, https://doi.org/10.1007/978-1-4020-6736-5_12.
- Todd D.K. and Mays L.W. Groundwater hydrology. 3rd Edition, John Wiley and Sons, Inc. Hoboken, 2005, pp. 329-358.
- UNSCEAR 1988, Sources, effects and risks of ionizing radiation. United Nations Scientific Committee on the Effects of Atomic Radiation 1988 Report to the General Assembly, with annexes. 1988, 647 p. Available at [access date: 07.12.2021]: https://www.unscear.org/docs/publications/1988/UNSCEAR_1988_Report.pdf.
- UNSCEAR 1993, Sources and effects of ionizing radiation. United Nations Scientific Committee on the Effects of Atomic Radiation UNSCEAR 1993 Report to the General Assembly, with Scientific Annexes. 1993, 922 p. Available at [access date: 07.12.2021]: https://www.unscear.org/docs/publications/1993/UNSCEAR_1993_Report.pdf.
- UNSCEAR 2000a. Sources and effects of ionizing radiation. United Nations Scientific Committee on the effects of atomic radiation UNSCEAR 2000 Report to the General Assembly, with Scientific Annexes. Vol. I: Sources. 654 p. Available at [access date: 07.12.2021]: https://www.unscear.org/docs/publications/2000/UNSCEAR_2000_Report_Vol.I.pdf.
- UNSCEAR 2000b. Sources and effects of ionizing radiation. United Nations Scientific Committee on the effects of atomic radiation UNSCEAR 2000 Report to the general assembly, with scientific annexes. Vol. II: Effects. 566 p. Available at [access date: 07.12.2021]: https://www.unscear.org/docs/publications/2000/UNSCEAR_2000_Report_Vol.II.pdf.
- WHO 2008 Guidelines for drinking-water quality. Third edition incorporating the first and second addenda, Vol. 1, Recommendations, Geneva, 2008.
- Wilcox L.V. Classification and Use of Irrigation Waters. U.S. Department of Agriculture, Circular No. 969, Washington DC, U.S.A, 1955.
- Zafar M.U. and Ahmad W. Water quality assessment and apportionment of northern Pakistan using multivariate statistical techniques – a case study. International Journal of Hydrology, statistics to evaluate the water quality around Maddhapara Granite Mining Industrial Area, Dinajpur, Bangladesh. Environ. Syst. Res., Vol. 6(1), paper 13, 2017, <https://doi.org/10.1186/s40068-017-0090-9>.
- Mammadzada S.Sh., Humbatov F.Y., Mustafayev I.I. Assessment of metal pollution in water and surface sediments of Goranchay River. Chemical Problems, No. 2(19), 2021, pp. 84-93, DOI: 10.32737/2221-8688-2021-2-84-93.
- NAS 1983. Drinking water and health. National Academy of Science, Washington, DC. Vol. 5, 1983, pp. 147-157.
- Omotoso O.A. and Ojo O J. Assessment of quality of river Niger floodplain water at Jebba, central Nigeria: implications for irrigation. Water Utility Journal, Vol. 4, 2012, pp. 13-24.
- Singh A.K., Mahato M.K., Neogi B., Singh K.K. Quality assessment of mine water in the Raniganj coalfield area, India. Mine Water and the Environment, Vol. 29, 2010, pp. 248-262, DOI:10.1007/s10230-010-0108-2.
- Singh A.K., Mondal G.C., Kumar S., Singh T.B., Tewary B.K., Sinha A. Major ion chemistry, weathering processes and water quality assessment in upper catchment of Damodar river basin, India. Environmental Geology, Vol. 54, 22 June 2007, pp. 745-758.
- Singh A.K., Mondal G.C., Tewary B.K., Sinha A. Major ion chemistry, solute acquisition processes and quality assessment of mine water in Damodar Valley Coalfields. Abstracts of the International Mine Water conference, 19–23 October 2009, Pretoria, South Africa, 2009, pp. 267-276.
- Suleymanov B., Ahmedov M., Humbatov F., Ibadov N. Hazardous pollutant database for Kura-Araks water quality management. In: Transboundary water resources: A foundation for regional stability in Central Asia (Moerlins J.E. et. al., eds.). Springer. 2008, pp. 171-182, https://doi.org/10.1007/978-1-4020-6736-5_12.
- Todd D.K. and Mays L.W. Groundwater hydrology. 3rd Edition, John Wiley and Sons, Inc. Hoboken, 2005, pp. 329-358.
- UNSCEAR 1988, Sources, effects and risks of ionizing radiation. United Nations Scientific Committee on the Effects of Atomic Radiation 1988 Report to the General Assembly, with annexes. 1988, 647 p. Available at [access date: 07.12.2021]: https://www.unscear.org/docs/publications/1988/UNSCEAR_1988_Report.pdf.
- UNSCEAR 1993, Sources and effects of ionizing radiation. United Nations Scientific Committee on the Effects of Atomic Radiation UNSCEAR 1993 Report to the General Assembly, with Scientific Annexes. 1993, 922 p. Available at [access date: 07.12.2021]: https://www.unscear.org/docs/publications/1993/UNSCEAR_1993_Report.pdf.
- UNSCEAR 2000a. Sources and effects of ionizing radiation. United Nations Scientific Committee on the effects of atomic radiation UNSCEAR 2000 Report to the General Assembly, with Scientific Annexes. Vol. I: Sources. 654 p. Available at [access date: 07.12.2021]: https://www.unscear.org/docs/publications/2000/UNSCEAR_2000_Report_Vol.I.pdf.
- UNSCEAR 2000b. Sources and effects of ionizing radiation. United Nations Scientific Committee on the effects of atomic radiation UNSCEAR 2000 Report to the general assembly, with scientific annexes. Vol. II: Effects. 566 p. Available at [access date: 07.12.2021]: https://www.unscear.org/docs/publications/2000/UNSCEAR_2000_Report_Vol.II.pdf.
- WHO 2008 Guidelines for drinking-water quality. Third edition incorporating the first and second addenda, Vol. 1, Recommendations, Geneva, 2008.
- Wilcox L.V. Classification and Use of Irrigation Waters. U.S. Department of Agriculture, Circular No. 969, Washington DC, U.S.A, 1955.
- Zafar M.U. and Ahmad W. Water quality assessment and apportionment of northern Pakistan using multivariate statistical techniques – a case study. International Journal of Hydrology,

Vol. 2(1), 2018, pp. 1-7, DOI: 10.15406/ijh.2018.02.00040.
Zakir H.M., Islam M.M., Arafat M.Y., Sharmin S. Hydrogeochemistry and quality assessment of waters of an open coal mine area in a developing country: A Case study from Barapukuria, Bangladesh. International Journal of geosciences research, Vol. 1, No. 1, 2013, pp. 20-44.

Vol. 2(1), 2018, pp. 1-7, DOI: 10.15406/ijh.2018.02.00040.
Zakir H.M., Islam M.M., Arafat M.Y., Sharmin S. Hydrogeochemistry and quality assessment of waters of an open coal mine area in a developing country: A Case study from Barapukuria, Bangladesh. International Journal of geosciences research, Vol. 1, No. 1, 2013, pp. 20-44.

ОЦЕНКА РАДИОЭКОЛОГИЧЕСКИХ РИСКОВ И ПРИГОДНОСТИ КАЧЕСТВА ВОДЫ ДЛЯ ПИТЬЕВОГО И СЕЛЬСКОХОЗЯЙСТВЕННОГО ИСПОЛЬЗОВАНИЯ В ГУБАДЛИНСКОМ РАЙОНЕ РЕСПУБЛИКИ АЗЕРБАЙДЖАН

Гумбатов Ф.^{1,2}, Ибрагимов Г.¹, Асланова Г.¹, Неджати Солут Х.¹,
Балаев В.¹, Каримова Н.¹, Каримбейли И.¹

¹Министерство науки и образования Республики Азербайджан, Институт радиационных проблем, Азербайджан
AZ 11439, Баку, ул. Б.Вахабзаде, 9: hfamil@mail.ru

²Азербайджанский Университет архитектуры и строительства, Азербайджан
AZ1073, Баку, ул. Айна Султанова, 5

Резюме. За последние 30 лет на территории Карабаха и Восточно-Зангезурского экономических районов, куда входит Губадлы, мониторинг и исследовательские работы не проводились. В статье приводятся результаты работ по оценке радиоэкологического риска и экологической безопасности разминированной территории в Губадлинском районе Азербайджана. Уровень радиационного фона был измерен в 64 точках данной территории, и средний радиационный фон составил 7.5 мкР/час, что дало полное представление об уровне радиации в регионе.

Кроме анализа радиационного фона, также были проведены гидрохимический анализ и оценка в этом районе качества воды, пригодного для бытового потребления, сельского хозяйства и промышленных целей. Всего было взято 7 образцов воды из различных источников, включая реки и другие водоемы. Эти образцы подверглись детальному анализу с целью определения их пригодности для бытового использования, потребления скотом и орошения. Физико-химические процессы в речных системах зависят от различных параметров качества воды, что делает постоянный мониторинг необходимым для экологических и научных исследований.

Результаты исследования показали, что содержание минералов в двух образцах воды было выше, чем в других, но не превышало пределов, установленных стандартами ВОЗ. Кроме того, в трех образцах были обнаружены высокие концентрации железа (Fe), а в одном образце – высокая концентрация марганца (Mn). Эти результаты свидетельствуют о том, что данные источники воды непригодны для питья, использования для скота и орошения, что подчеркивает необходимость дальнейшего мониторинга и устранения загрязнений в этом регионе.

Ключевые слова: Губадлинский район Азербайджана, радиоэкология, управление качеством воды, остаточный карбонат натрия (OKN), коэффициент поглощения натрия (КПН), процент растворимого натрия (ПРН)

AZƏRBAYCAN RESPUBLİKASININ QUBADLI RAYONUNDA RADİOEKOLOJI RİSKLƏRİN VƏ SU KEYFİYYƏTİNİN İÇMƏLİ VƏ KƏND TƏSƏRRÜFATI ÜÇÜN YARARLILIĞININ QİYMƏTLƏNDİRİLMƏSİ

Hümbətov F.^{1,2}, İbrahimov G.¹, Aslanova G.¹, Necati Solut H.¹,
Balayev V.¹, Karimova N.¹, Karimbəyli I.¹

¹Azərbaycan Respublikası Elm və Təhsil Nazirliyi, Radasiya Problemləri İnstitutu, Azərbaycan
AZ 11439, Bakı, B. Vahabzadə küç. 9: hfamil@mail.ru

²Azərbaycan Memarlıq və İnşaat Universiteti, Azərbaycan
AZ1073, Bakı, Ayna Sultanova küç., 5

Xülasə. Son 30 ildə Qarabağ və Şərqi Zəngəzur iqtisadi rayonlarında, o cümlədən Qubadlıda monitorinq və tədqiqat işləri aparılmayıb. Tədqiqatın əsas məqsədi Azərbaycanın Qubadlı rayonunda yerləşən minadan təmizlənmiş ərazilərdə radioekoloji riskin qiymətləndirilməsi və ekoloji təhlükəsizliyin öyrənilməsidir. Ərazinin 64 nöqtəsində radasiya fonu ölçülülmüş və orta radasiya fonu $7.5 \mu\text{R/saat}$ olaraq müəyyən edilmişdir ki, bu da həmin ərazilərdə radasiya səviyyəsi haqqında geniş məlumat əldə etməyə imkan verir.

Radasiya fonunun təhlili ilə yanaşı, əraziləki suyun məişət istehləki, kənd təsərrüfatı və sənaye məqsədləri, həmçinin su ehtiyatlarının idarə edilməsində kömək üçün uyğun olan hidrokimyəvi təhlil və qiymətləndirmə aparılmışdır. Müxtəlif su mənbələrindən, o cümlədən çaylardan və digər su hövzələrindən 7 su nümunəsi götürülmüşdür. Bu nümunələr məişət, heyvandarlıq və kənd təsərrüfatı üçün yararlığını müəyyən etmək üçün analiz edilmişdir. Çay hövzələrində başverən fiziki-kimyəvi proseslər suyun keyfiyyət parametrlərinə asılıdır və bu parametrlərin davamlı monitorinqi elmi tədqiqatlar və ekoloji nəzarət üçün vacibdir.

Tədqiqatın nəticələri iki su nümunəsindəki mineral tərkibin digərlərinə nisbətən daha yüksək olduğunu, lakin ÜST standartları ilə müəyyən edilmiş həddləri keçmədiyini göstərmişdir. Bundan əlavə, üç nümunədə dəmirin (Fe) başqa bir nümunədə isə manqanın (Mn) yüksək konsentrasiyası aşkar edilmişdir. Bu nəticələr göstərir ki, həmin su mənbələri içməli su, heyvandarlıq və suvarma üçün yararsızdır, bu isə bölgədə əlavə monitorinq və təmizləmə işlərinin vacibliyini vurgulayır.

Açar sözlər: Azərbaycanın Qubadlı rayonu, radioekologiya, suyun keyfiyyətinin idarə edilməsi, natrium karbonat qalığı (NKQ), natrium udulma əmsali (NUƏ), həll olunan natrium faizi (HNF)

PALEOSEISMOLOGICAL STUDIES IN THE PLEISTOSEISMIC AREA OF THE 1668 AND 1902 SHAMAKHI EARTHQUAKES

Pierce I.¹, Gulyev I.S.², Yetirmishli G.J.³, Kazimova S.E.³, Walker R.¹,
Kazimov I.E.³, Abdullayev N.R.², Johnson B.¹, Marshall N.¹,

¹*University of Oxford, United Kingdom*
3 S Parks Road, Oxford

²*Presidium of the Azerbaijan National Academy of Sciences, Azerbaijan*
30, Istiglaliyyat str., Baku, AZ1001

³*Republican Seismic Survey Center of Azerbaijan National Academy of Science, Baku, Azerbaijan*
123, Huseyn Javid ave., Baku, AZ1141

Keywords: paleoseismic trenches, Shamakhi earthquakes 1902, Kur fold-thrust belt, satellite imagery, drone modeling, OxCal sequence model, surface rupture

Summary. The Caucasus region located at the junction of the Eurasian and Arabian tectonic plates is a key area for understanding continental collision processes and their impact on seismic activity. The aim of this work is to analyze the region's tectonic processes, seismic history, and the risks associated with potential large earthquakes. The study employs modern methods including satellite imagery, GNSS data, drone-based modeling, and paleoseismic trenching. In April–May 2022, a team of scientists from the University of Oxford, in collaboration with early-career researchers from the RSSC, carried out the first geological fieldwork in Azerbaijan focused on paleoseismology and active tectonic processes. Two trenches were analyzed. One of the key findings was the identification of active faults, such as the Aghsu fault, and evidence of surface ruptures associated with historical earthquakes. Two surface rupture events (1713–1895 and 1872–2003) were identified likely linked to the surface displacements caused by the 1668 and 1902 earthquakes, which inflicted significant damage on the city of Shamakhi. Our reassessment of the 1902 earthquake suggests its magnitude may have reached Mw 7.4, whereas earlier estimates placed it at M 6.9. Additionally, evidence of a surface-rupturing earthquake dated between 334 and 118 BCE was found in a second trench located 60 km west of Aghsu near Goychay along with signs of another possible event within the past 2000 years. This work highlights the importance of continued field investigations to better constrain fault lengths, assess historical earthquake magnitudes, and improve regional seismic hazard maps.

© 2025 Earth Science Division, Azerbaijan National Academy of Sciences. All rights reserved.

1. Introduction

The Caucasus mountain system located at the junction of the Eurasian and Arabian plates represents a key site for understanding the complex geo-dynamic processes of continental collisions and their influence on seismic activity. Despite the fact that much of the structural paragenesis of orogenic zones has been thoroughly studied, the morphological features of mountain systems such as the Greater Caucasus still require further exploration. These mountain forms not only reflect the history of tectonic forces but also serve as indicators of underlying geodynamic processes offering valuable insights, especially when direct geological data is limited.

The seismicity of the Greater Caucasus has historically been significant with numerous destructive earthquakes recorded over the centuries. These events, such as the earthquakes of 1139, 1668, and

the series from 1828 to 1902 have left an indelible mark on the history of the region. However, the lack of instrumental earthquake data for much of the region complicates our understanding of the full seismic potential of the area. Turning to historical earthquake records and modern geophysical data reveals that the fault systems of the region are active with the possibility of significant seismic events still looming. The goal of this study is to explore the geo-dynamic conditions of the Greater Caucasus focusing on historical seismicity and the active faults responsible for shaping the region's seismic landscape.

The research in this article presents a comprehensive analysis of the region's tectonic processes, seismic history, and current risks associated with potential future earthquakes based on modern technologies such as satellite imagery, drone modeling, GNSS technologies, as well as paleoseismic trenching.

On April – May, 2022, a team of five scientists from Oxford University Department of Earth Sciences led by Professor Richard Walker collaborated with young scientists from RSSC to conduct the first field geological studies focused on paleoseismology, earthquake geology, and active tectonics in Azerbaijan. The aim of this research was to understand the potential locations and frequency of strong destructive earthquakes (M7+) that occurred before the development of modern seismic networks.

At the conclusion of this research, a comprehensive article titled "**Surface Rupturing Earthquakes of the Greater Caucasus Frontal Thrusts, Azerbaijan**" was published. Our article is a summary of that study, which was published in 2024. It provides a concise overview of the research helping a broader audience quickly understand the key findings.

1.1. The Mountain System of the Greater Caucasus

To date, the structural paragenesis of orogenic zones has been thoroughly studied but the morphological features of the orogens themselves remain incompletely understood. These differences reflect geodynamic processes and can serve as indicators of these processes, particularly in cases where direct geological data are absent or insufficient. Structurally, orographic forms of orogens retain data on the geodynamic conditions of their formation (Makarova et al., 2000; Коркуганова, 2000). In recent decades, numerous studies in the fields of geology, geodynamics, geodesy, and geophysics have been conducted to investigate the evolution of the Caucasus and its surrounding areas, as well as to refine our understanding of current tectonic processes, lithospheric deformations, seismicity, and the associated seismic risks and hazards. The results of these studies are reflected in a number of papers published in international journals, as well as in those published in the former Soviet Union, Armenia, Azerbaijan, Georgia, and Russia. Furthermore, recent geological, geophysical, and geochemical studies have provided additional clarification on the tectonic framework of the region. The question of the age of continental collision remains unresolved with various studies suggesting a range from the Late Cretaceous to the Pliocene (Ismail-Zadeh et al., 2022).

The Caucasus region is known to be part of the ongoing continental collision between the Arabian and Eurasian plates. For over 100 million years, the lithosphere of the Neo-Tethyan Ocean has been subducted beneath Eurasia (Хайн, 1975; Adamia et al., 1985). This process has led to inversion and the formation of fold-and-thrust belts in the Greater and Lesser Caucasus (Mosar et al., 2010).

The diagram showing the tectonic structure of the Eastern Black Sea region is presented in Figure 1. The following key tectonic units can be identified within this region (Муратов, 1969; Letouzey et al., 1977; Starostenko et al., 2004; Saintot et al., 2006; Афанасенко и др., 2007; Rolland et al., 2011; Nkishin et al., 2012): (1) the South Crimea Orogen, (2) the Greater Caucasus Orogen, (3) the system of terranes of the Central and Eastern Pontides with Mesozoic volcanic belts (Middle Jurassic and Cretaceous), and (4) the Eastern Black Sea Basin with oceanic crust and strongly stretched continental crust due to rifting.

The Greater Caucasus mountain system, which stretches approximately 900 km between the Black and Caspian Seas, is considered to have formed as a result of tectonic inversion of a former back-arc basin that developed on continental crust and opened in the early Mesozoic above the northern subduction zone of Neo-Tethyan Ocean (Adamia, 1985; Mosar et al., 2010). Thermochronological studies have shown that the formation of the topography of the western Greater Caucasus began as early as the Oligocene (Vincent et al., 2018a,b). Estimates of total shortening across the Greater Caucasus remain uncertain ranging from 150 to 400 km with shortening increasing from west to east (Ismail-Zadeh et al., 2022). Continued convergence has generated compressive stress, which activated deformation and uplift of the Greater Caucasus during the Pliocene. According to McQuarrie and Van Hinsbergen (2013), the closure of the Neo-Tethyan Ocean to the north of the Arabian Plate occurred about 27 million years ago, although subduction continues along the Hellenic and Cyprian trenches. Cowgill et al. (2016) link the changes in the Arabian-Eurasian collision zone to the closure of the rift basin on the southern slope of the Greater Caucasus. However, Vincent et al. (2018a) argue that, sedimentological and seismological data suggest an earlier closure of the basin around the early Oligocene at least for the western part of the Greater Caucasus. Cowgill et al. (2018) propose that basin closure began around 35 million years ago and was completed around 5 million years ago when the Lesser Caucasus collided with the Scythian Platform forming the Greater Caucasus. The final collision of the Arabian and Eurasian plates and the formation of the modern intracontinental mountain structure of the Caucasus occurred during the Neogene-Quaternary period (Ismail-Zadeh et al., 2022).

The paper (Sengor et al., 2023) proposes a revision of traditional models highlighting the Pacific-type margin and the dynamic motion of the continent. The Cimmerian Continent was a complex tectonic structure that not only rifted from Gondwana but also underwent internal extension forming oceanic basins such as the Neo-Tethys (Fig. 2).

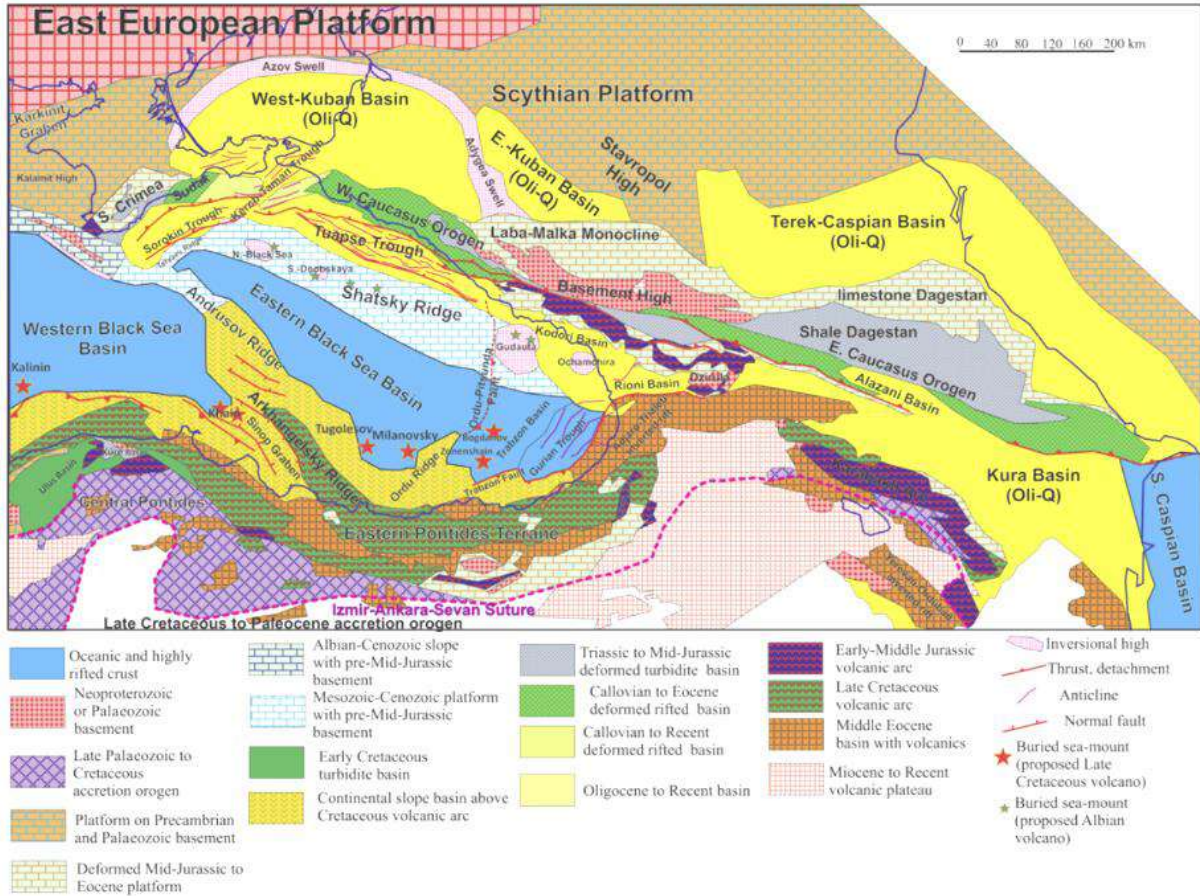


Fig. 1. Tectonic scheme of the Caucasus– Eastern Black Sea region. The scheme has been compiled in collaboration with A. Okay, O.Tüysüz and A. Demirer for the Black Sea region. Oli-Q, Oligocene–Quaternary (Nikishin et al., 2015)

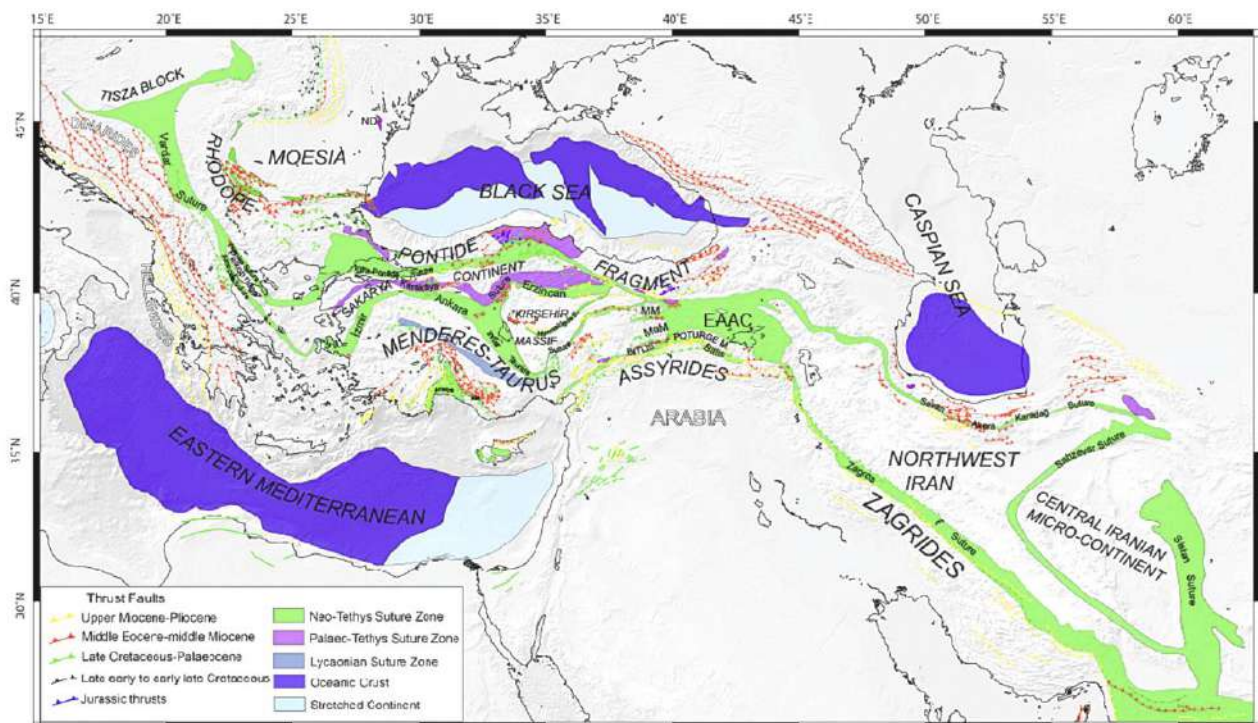


Fig. 2. Distribution of suture zones in and around Turkey afterwards (Sengor et al., 2023).

Its evolution is tied to the subduction of the Palaeo-Tethys and its subsequent closure as well as the opening of new basins and eventual collision with Laurasia. The northern margin of the Cimmerian Continent was of Pacific-type not Atlantic-type as claimed by some authors implying active subduction processes and back-arc basin formation.

The continent traversed the Tethyan realm in a "serpentine motion" making it impossible to reconstruct synthetic isochrons to precisely track its northward migration (except for simplified visualizations of its journey). Oceanic basins including the Neo-Tethys opened as back-arc basins behind the subducting slab.

The movement of the Cimmerian continent across the Tethyan region occurred between the Late Triassic and Late Jurassic and in some places possibly even in the Early Cretaceous, when the Cimmerian continent collided with the Laurasian margin. Due to the complex nature of this movement, the authors note that it is impossible to construct synthetic isochrons to accurately track the northward migration of the Cimmerian continent except for a simplified visualization of its path across the Tethyan region.

Many outstanding scientists have studied the tectonics, geodynamics, and seismicity of the Greater Caucasus and Azerbaijan including G.V.Abich, R.A.Agamirzoyev, Sh.A.Adamia, A.A.Alizade, F.S.Akhmedbeyli, B.K.Balavadze, G.Sh.Shengelia, G.I.Baranov, R.M.Gadzhiev, I.S.Guliyev, F.A.Kadirov, T.N.Kengerli, M.L.Kopp, V.V.Korobanov, E.E.Milanovsky, V.E.Khain, and others (Abich, 1862, 1873; Агамирзоев, 1987; Adamia, 1985; Ализаде и др., 1968; 1982; Ахмедбейли, 1991, 2001; Balavadze et al., 1975, 1966; Баранов и Греков, 1982; Гаджиев, 1965; Guliev et al. 2002; Kengerli, 1997; Копп, 1997; Korobanov, 1990; Милановский и др., 1963; Хайн, 1984; Хайн и др., 2005).

1.2. Paleoseismogeological studies and historical tectonic activity of the Greater Caucasus.

The first paleoseismogeological studies in the Greater Caucasus region began in the late 1960s based on the hypothesis that large earthquakes that occurred in the distant past leave traces on the Earth's surface in the form of paleoseismodislocations (Florensov, 1960). Evidence of such events was recorded in various parts of the Caucasus: on the southern slopes of the Northwestern Caucasus in the central Western Caucasus (Хромовских и др., 1979) near Mount Elbrus (Nikonov, 1991) in the vicinity of the Caucasian Mineral Waters (Белоусов и др., 2000) in North Ossetia (Никитин и др., 1993) in North Caucasus and in mountainous Dagestan, and on the coast of the Caspian Sea (Бунин, 1985; Korzhenkov et al., 2019; Овсяченко и др., 2014; Rogozhin et al., 2015; Gmyrya et al., 2019). These studies revealed that the seismic ac-

tivity of the region might be significantly higher than previously believed on the basis of traditional seismicity statistics. Most of the identified ancient seismogenic structures were linked to gravitational processes. However, in most cases, researchers could not precisely determine the locations, magnitudes, and ages of ancient earthquake sources. One exception was the work led by V.P.Solonenko (Хромовских и др., 1979), where the first estimates of earthquake magnitudes and focal zones were obtained. In the late 1980s and early 1990s, several significant earthquakes occurred in the Caucasus region affecting both the Lesser and Greater Caucasus. These included the 1986 Paravan earthquake with a magnitude of 6.5, the 1988 Spitak earthquake with a magnitude of 6.9, the 1991 Racha earthquake (magnitude 7.0), the 1991 Java earthquake with a magnitude of 6.5, and the 1992 Barisakh earthquake with a magnitude of 6.2 (Рогожин и др., 2014).

The primary tectonic structure associated with this process is the Main Caucasus Thrust characterized by northward dip. Around 1.5 million years ago, deformation began to spread to the Kur foreland fold-thrust belt, which experiences shortening at a rate of 6.7–13.6 mm/yr as determined from reconstructed balanced cross-sections (Forte et al., 2015; Kangarli et al., 2018), and through GNSS measurements, which show a rate of around 10 mm/yr in the Kur Basin (Reilinger et al., 2006; Yetirmishli et al., 2022).

The Kur fold-thrust belt stretches from west to east for about 275 km, from the vicinity of Tbilisi in Georgia to the Shamakhi area in Azerbaijan. Its structure consists of a series of overlapping thrusts, the number of which varies from one to four depending on the section of the belt. Despite the fact that no earthquake with $M > 7.0$ has been recorded in the southeastern part of the Greater Caucasus during the instrumental period, the region has experienced numerous destructive earthquakes in the pre-instrumental period. The region is known for its historical earthquakes, the most destructive of which were the events of 1139, 1668, and a series of earthquakes between 1828 and 1902 (Ismail-Zadeh et al., 2022; Pierce et al., 2024). The widely felt earthquakes of 1668 and 1902 devastated the medieval capital of Shamakhi (Fig. 3b), while moderate ($M \sim 6$) events in 1828, 1859, 1869, and 1872 caused serious damage to the city. The 1859 event claimed 100 lives and destroyed 741 buildings prompting the capital to move from Shamakhi to Baku. The 1872 event claimed 118 lives and destroyed all but 20 buildings (Шебалин, 1982). The 1902 event claimed 2,000 lives and destroyed 4,000 homes. In Fig. 3a, we have transformed the isoseists for the Shamakhi earthquakes of 1828–1902, initially recorded on the intensity scale developed by Weber. Weber (1903) constructed isoseists for the 1902 earthquake using observations from 120 villages throughout the region (Pierce et al., 2024).

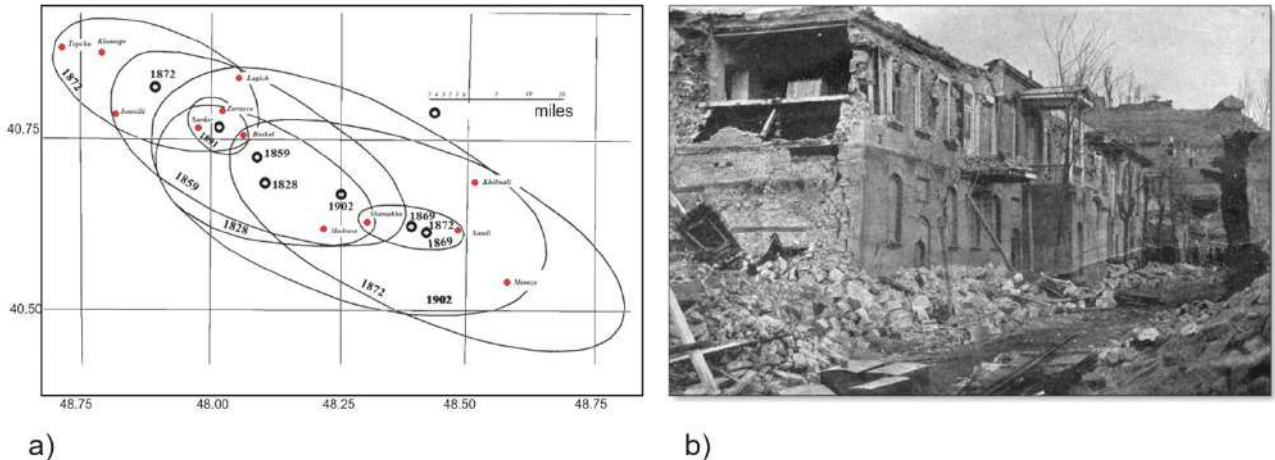


Fig. 3. MMI scale isoseismals of the 1828–1902 yy. Shamakhi earthquakes adapted from the original intensity scale (a) and destruction after the Shamakhi earthquake of 1902 developed by Weber (1903)

These isoseismal maps suggest that the epicenter was located near Shamakhi and that the rupture that occurred follows the general trend of the Kur thrust. Our paleoseismic trenching results from Aghsu indicate two surface-rupturing events since the early 18th century (1713–1895 and 1872–2003). The more recent of these rupturing events could be the surface rupture of the 1902 Shamakhi earthquake, while the penultimate event may correspond to the 1668 earthquake if we disregard two radiocarbon dates. Modern Shamakhi located just 18 km northeast on the hanging wall of the Aghsu basin would have experienced intense ground shaking if the northeast fault rupture occurred, so the destruction recorded during these events aligns with our paleoseismic results (Pierce et al., 2024).

According to the research by Jackson and Ambroseys (1997), historical seismicity data over the last 400 years account for only about 25% of the total crustal shortening in the Caucasus region. This presents significant challenges in estimating the seismic potential of the region, as it remains unclear whether the lack of major earthquakes west of Shamakhi is due to insufficient historical records, aseismic processes such as fault creep, or the buildup of unresolved tectonic stresses within the fold and thrust system.

2. Methodology

The study employed advanced technologies, including satellite imagery, drone modeling, GNSS technologies, seismic positioning, and paleoseismic trenching. Faults were remotely mapped using Google Earth and elevation models derived from Sentinel satellite stereo images (Smith, Johnson, 2022) before fieldwork conducted from 2020 to 2022. Field surveys included vehicle and on-foot

exploration of fault sections as shown in Fig. 4. Key sections were carefully examined using photogrammetry, where images were captured with a Teokit-equipped DJI Phantom 4 Pro v2 drone (Pierce, Koehler, 2023). Teokit is a differential GPS system (dGPS) used for accurately geolocating the images, which were corrected then using the Post-Processing Kinematic (PPK) method via the Emlid Reach RS2 dGPS base station (Zhang et al., 2019).

The captured photographs were processed using Agisoft Metashape software to generate digital elevation models (DEMs) and orthomosaic images with a resolution of 6–10 cm/pixel and 3–5 cm/pixel, respectively. Two paleoseismic trenches were excavated across mapped faults, which were then cleaned, gridded, and documented (Fig. 4) (Pierce et al., 2022, 2023). Documentation was based on 3D models created using Structure-from-Motion (SfM) from photographs taken with Samsung Galaxy S20 Ultra (2022) and Pixel 7 Pro (2023) smartphones. These models were precisely adjusted, oriented, and scaled using reference points from LiDAR scans of the trench walls performed with an iPad. Before generating and exporting 2D orthomosaic images, this process yielded 2D images of the trench walls with centimeter-level geometric accuracy (Pierce et al., 2024).

Layers and faults were then drawn on these 2D images using an iPad. The units and faults were separated and described following standard paleoseismic methods (McCalpin, 2009), including sedimentary facies, cross-cutting relationships, and soil development. Samples of charcoal, plant material, bones, and soil were documented in trench logs, collected, processed, and then analyzed at the Beta Analytic laboratory in Miami, Florida. They were calibrated using OxCal v4.4 (Bronk, Ramsey, 1995) with the IntCal20 calibration curve.

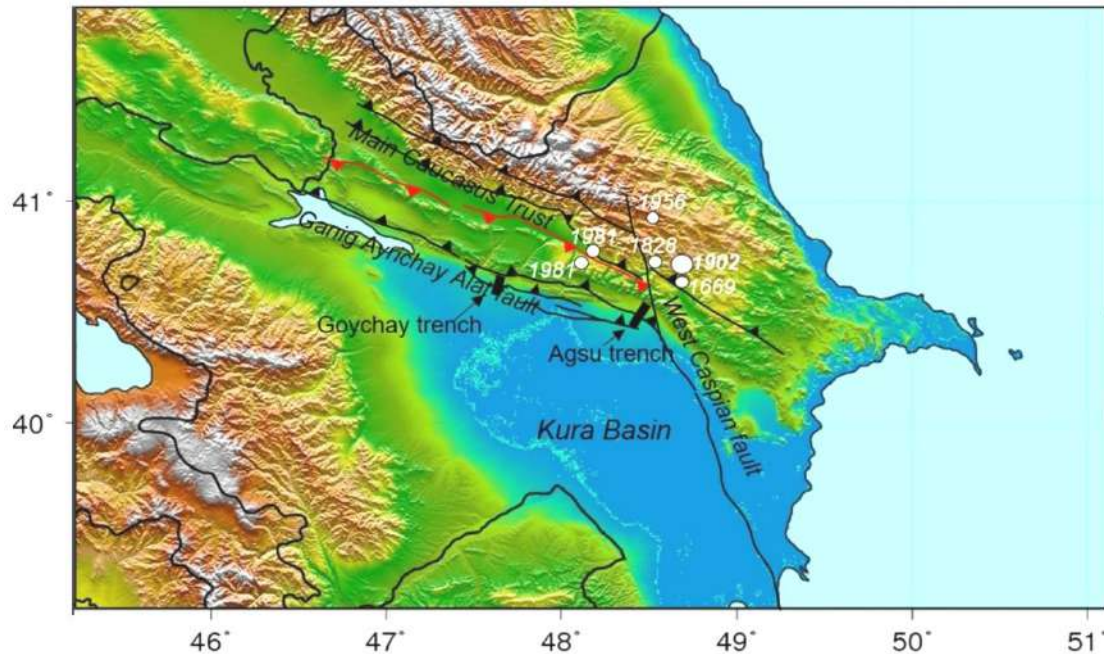


Fig. 4. Tectonic map of the southeastern part of the Greater Caucasus, paleoseismic trenches in the Aghsu and Goychay areas, and epicenters of major ($M > 5.0$) historical earthquakes occurring between 1669 and 1956

2.1. Formation of covers in the Shamakhi-Gobustan trough

The study used advanced technologies including satellite imagery, drone modeling, GNSS technologies, seismic positioning and paleoseismic excavations. Horizontal movements at a rate of 10 mm/yr between the Arabian and Eurasian plates are mainly provided by the Main Caucasus fold-and-thrust belt, which extends between central Azerbaijan and Georgia along the southern front of the Greater Caucasus (45–48°E) (Pierce et al., 2022, 2023). In the southern foothills of the Greater Caucasus most fold-and-thrust faults arose under compressional condi-

tions resulting in southerly and, occasionally, southwesterly displacements of the massifs. These faults are clearly visible on the seismic tomographic profile constructed from earthquake traveltimes data for the period 2017–2023. The construction method is described (Gunnels et al., 2021; Kazimova, 2020) (Fig. 5). The modern structure of these dislocations consists of local folds, which are complicated by faults. In the Shamakhi-Gobustan trough, a large Perikyushkul-Baskal nappe stands out, which continues west almost to the Geychay River valley. Here, the displacement amplitude of the allochthonous part of the nappe is 20–25 km.

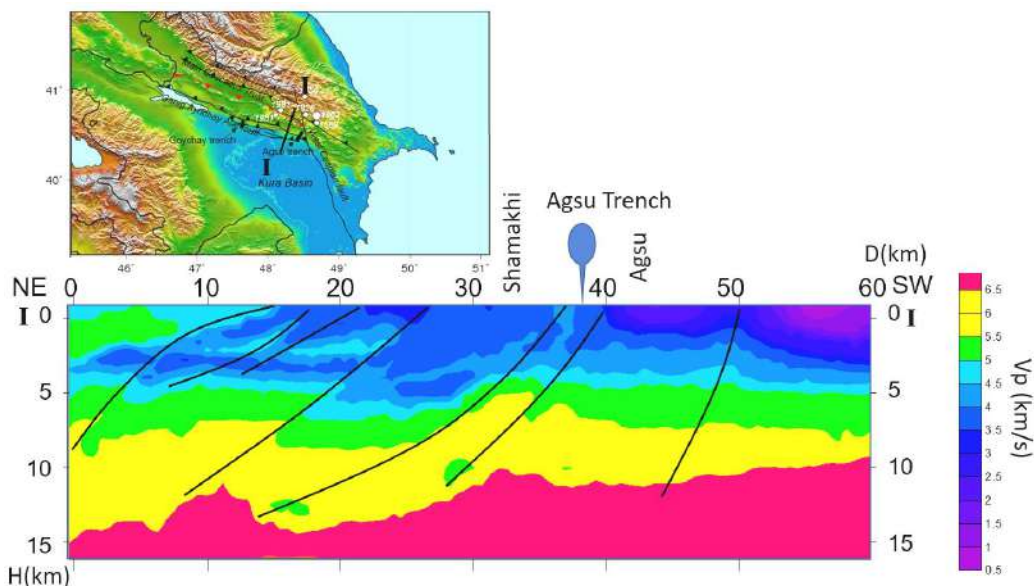


Fig. 5. Seismic tomographic section along profile 1-1 across the strike of the thrust structure in the NE-SW direction

In some places, the thrust plate overlaps the Miocene layers indicating active compressive stresses in the neotectonic period. Clayey rocks in the Upper Miocene were subjected to intense deformation and have many cracks. Similar stresses are observed in other local structures of Central Gobustan.

Thus, compression in the mountainous region of the Greater Caucasus is the main cause of horizontal movements in the above-mentioned structural elements: Gobustan, Ajinour and the Kur interfluve. It is also important to note the significant influence of the Ganykh-Ayrichay-Alat deep fault, which showed high activity in late orogenic tectonic processes. There is a high probability that the geodynamic impact of this fault contributed to the formation of rupture and fold dislocations in the Ajinour and Gobustan zones. If the current geological processes continue, it can be assumed that the young folded zones of the Kur-Ajinohur interfluve, as well as the Shamakhi-Gobustan trough are at the initial stage of the formation of the future orogen. Currently, the foothills of the southern slope of the Greater Caucasus are rising at a rate of 2-3 mm per year. Based on these observations, it can be concluded that the foothill zone is already beginning to form as an extended pile, which indicates the further development of late-orogen processes.

2.2. Space geodesy data (GNSS)

Based on the GNSS space geodesy data of the RSSC and seismological data, the current geodynamic conditions in the territory of Azerbaijan for 2014-2024 were analyzed. The data were taken from Yetirmishli et al. works (2022; 2023; 2024). One of the most noticeable features of the horizontal movement velocity field is the decrease in the velocity values perpendicular to the direction of the Greater Caucasus strike from south to north. The velocity field

clearly illustrates the movement of the Earth's surface in the N-NE direction. (Fig. 6) This phenomenon reflects the process of successive accumulation of elastic deformations in the zone of subduction interaction of the structures of the northern side of the South Caucasian microplate with the accretionary prism of the Greater Caucasus. In addition, within the Middle Kur Depression and the Lesser Caucasus, a tendency toward horizontal displacement is observed, which is expressed in an increase in the velocity of movement from west to east along the continuation of the ridge. It has been established that on the Absheron Peninsula the Earth's crust is contracting at a rate of ~5 mm/yr. Earthquakes that occurred during this period are localized in the zones of the transition gradient from maximum to minimum velocities. These are mainly the Ismailly, Shamakhi, Aghdam and Shamkir regions. In this zone, a change in the magnitude of the GNSS velocity vectors is observed, which can be explained by the main reason for the accumulation of stress.

The maximum values of horizontal velocities were recorded at the stations of Aghdam, Lerik, Lankaran, Jalilabad, Fizuli, and Saatly with an average speed across the republic of 7.3 mm/yr. In 2021, the average speed across the entire territory of the republic was 7.6 mm/yr. The highest speeds were noted at the stations of Yardimli (12.2 mm/yr), Lankaran (13.1 mm/yr), and Saatly (12.3 mm/yr).

Along the Kur Depression (from the Middle Kur Depression to the Lower Kur Depression, i.e., from NW to SE), there is a gradual increase in horizontal movement speed from 7.3 to 11.3 mm/yr, which characterizes a state of compression. The average speed of the mega-zone on the southern slope of the Greater Caucasus ranges from 4.2 to 5.4 mm/yr. The Middle Kur mega-zone is characterized by speed of 8.85 mm/yr.

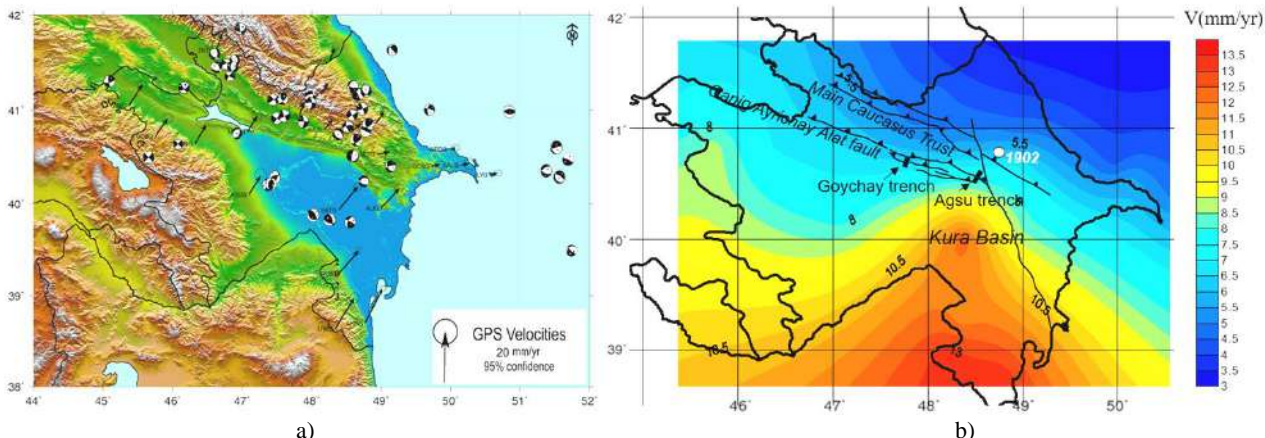


Fig. 6. Overview map of (a) Azerbaijan showing GNSS velocities relative to stable Eurasia (Kadirov et al., 2024), faults from the Active Faults of Eurasia Database, and focal mechanisms of earthquakes from the database of RSSC (Compiled by Kazimova), b) map of horizontal movement velocity distribution based on GNSS station data from the RSSC (Compiled by Kazimov)

3. Paleoseismic Trenches in Aghsu

The Kur thrust located immediately next to Aghsu runs along the front of the Greater Caucasus range. In this area, the active fault has created an uplifted bench approximately 50 meters high tilting back towards the northeast with a distinct fold at its crest. About 2.5 km east of Aghsu, a small alluvial valley cuts through this bench, where a stream has incised perpendicularly to the fault trace. Within this valley, two low terraces have formed T1, the lower terrace, and T2, which is elevated by about 1 meter. These terraces have smooth, flat surfaces and can be continuously traced upstream for approximately 300 meters from the valley mouth (Fig. 7).

At the entrance to the valley, both terraces exhibit vertical displacement marked by fault scarps approximately 2 meters in height. Along the western edge of the valley, a minor stream has deeply eroded the T1 terrace. A hillshade image obtained from drone data reveals signs of human alteration on the scarp of the T2 terrace; however, the T1 terrace shows no such modifications on either side of the fault allowing for clear correlation. A paleoseismic trench was dug across the 2-meter-high scarp intersecting the T1 terrace within this alluvial valley.

3.1. Stratigraphic and Structural Analysis of the Aghsu Trench Exposure

The length of the trench that was excavated in the Aghsu region was 22 meters, and the depth was 5 meters (Fig. 8). The eastern trench wall was meticulously documented through detailed logging and photography. The excavation exposed a sequence of clay, alluvial, and colluvial deposits that have been disrupted by a low-angle fault (F0), which branches into multiple splays (F1-F4) as it extends upward.

The lowest stratigraphic layer, U1, consists of a colluvial deposit with a mixture of rounded cobbles and gravel embedded in a silty-sandy matrix.

Overlying U1 is U2, a fluvial deposit that thickens southward, comprising well-sorted, grain-supported sands, gravels, and rounded cobbles. The contact zone where U2 overlaps U1, marked in gray consists of fine-grained sediments potentially representing a paleosol. At the top of U2, a distinct ~40 cm thick, light-colored paleosol is visible extending across the southern part of the trench. In the hanging wall, U3 is a 1.5-meter-thick, laminated clay layer that fractures into prismatic blocks and shows significant shearing near the fault zone. Above this, U4 consists of finely laminated clays, silts, and sands. Units U4 and U5 are exclusive to the hanging wall with U5 containing laminated silts, sands, a thin cobble layer, and traces of modern plastic debris in its upper 20–30 cm.

Above U2 lies W1, a colluvial deposit composed of a poorly sorted mixture of small boulders, cobbles, and gravels within a fine-grained matrix. A ~20 cm thick light-colored paleosol caps W1, which is thickest near the fault scarp and gradually thins southward. Overlying W1 is W2, another colluvial deposit made up of angular clay blocks within a fine-grained matrix with sparse pebble inclusions. A nearly horizontal fault (F0) cuts across the trench branching into four distinct faults (F1–F4) in the hanging wall. F4 forms a shear zone within U3, while F3 and F2 enclose a shear band composed of U1 material, indicated by aligned cobbles and pebbles. F1 displaces the paleosol at the top of U2. The hanging wall units (U1–U4) show clear folding, whereas U2 in the footwall remains largely undisturbed.



Fig. 7. Paleoseismological investigations of a trench excavated in 2022 in the Aghsu area

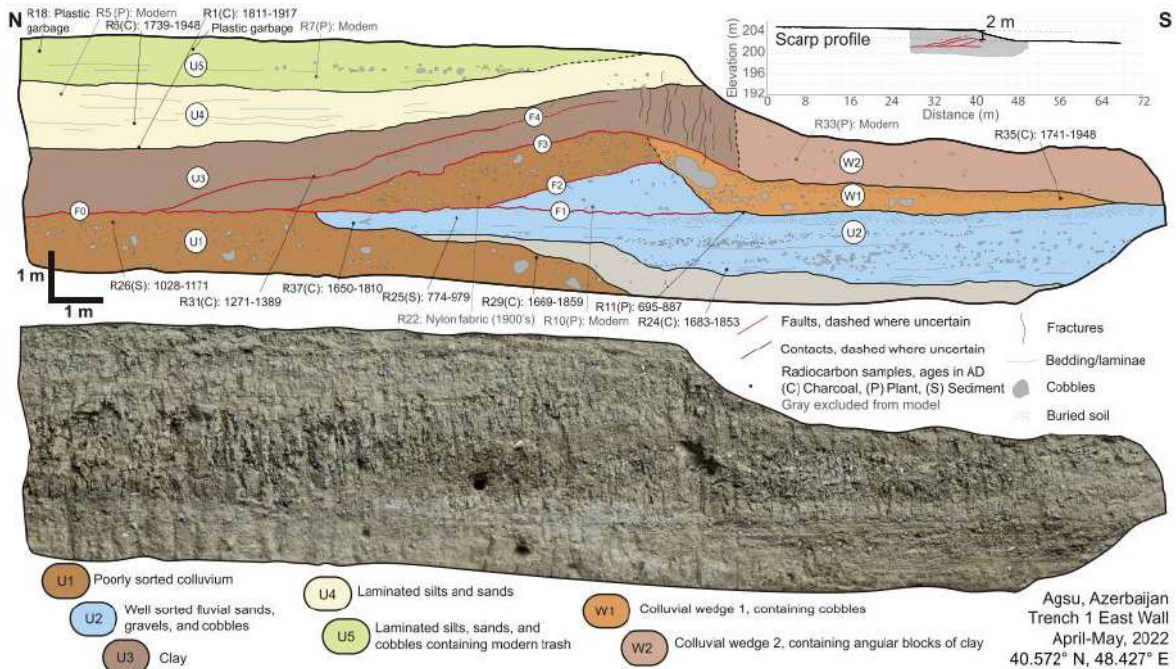


Fig. 8. Geological section of the Aghsu trench. The ages provided are modeled as outlined in the text. Evidence of two events is mainly inferred from the colluvial wedge stratigraphy on the footwall (W1 and W2) (Pierce et al., 2024)

The stratigraphy observed in the southern section of the trench reveals evidence of two distinct faulting events indicated by the presence of two colluvial wedges (W1 and W2) overlying the undisturbed fluvial deposits of unit U2 (Fig. 4). A reconstruction model of fault displacement is illustrated in Fig. 9. The earlier of these events (E1) led to the formation of the W1 colluvial wedge, which consists of an unsorted mixture of cobbles and gravels covering the paleosol that had developed atop the U2 fluvial sediments. Over time, a thin layer of fine-grained soil accumulated on the surface of W1. The more recent seismic event (E2) resulted in the deposition of the W2 colluvial wedge, primarily composed of angular clay blocks derived from U3. This wedge subsequently buried the thin soil layer that had formed on top of W1.

The contrast between the two colluvial wedges is highly pronounced. During the penultimate E1 event, the F0, F1, and F2 faults ruptured through the U1 colluvial layer and the upper portion of the U2 alluvial deposit at the base of the northern section of the trench following a sub-horizontal fault plane (Fig. 9). As F0 branched into F1 and F2, it caused a sharp fold in segments of U2 and the U1 colluvium, which subsequently collapsed, giving rise to the E1 wedge. The thick clay layer, U3 was deposited before the E1 event and may have accumulated behind a fold in U1, possibly formed by an earlier rupture along a different fault strand. However, as this strand is not visible in the trench exposure, this interpretation remains uncertain. In this scenario, U3

would have initially covered and laterally bordered U1 before the E1 rupture occurred.

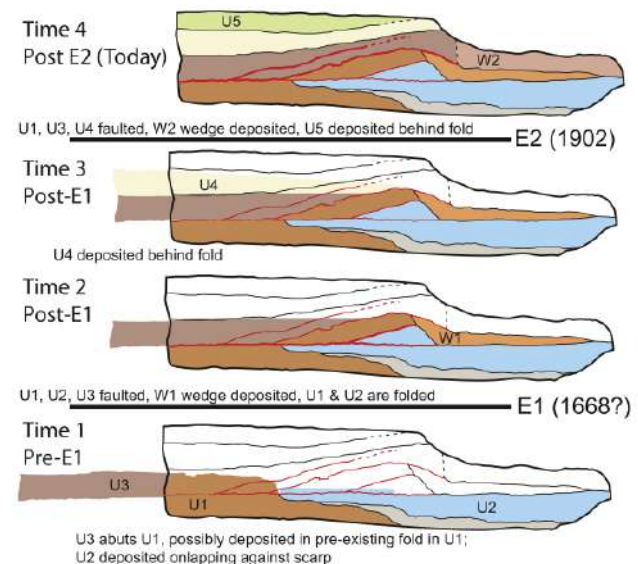


Fig. 9. Reverse-slip reconstruction of the Aghsu trench. The colors and symbols correspond to those used in Fig. 4. The most distinct evidence of seismic events is found in the colluvial wedge stratigraphy (W1 & W2) within the footwall (Pierce et al., 2024)

During the E1 rupture, the U1 unit was displaced into the near-surface fault zone along the nearly horizontal F0 fault. It is possible that the extreme flatness of F0 in this exposure is partly due to the trench's oblique orientation relative to the fault. Additionally, the U3 clay unit, being significantly more rigid than the U1 colluvial deposit may have

influenced fault propagation, as the fault exploited this contrast in material strength. Initially, U3, which both capped and laterally bordered U1 remained unaffected by the surface rupture. It was only after further slip accumulation during the subsequent E2 event that U3 was incorporated into the fault zone.

Following the E1 rupture, fine-grained sediments of U4 were deposited atop U3 within the hanging wall accumulating behind the fold generated by the E1 event. By restoring the displacement of U1 along faults F1 and F2, a minimum of 6.6 meters of slip is estimated for the E1 rupture. During the more recent E2 event, fault F0 was reactivated, and fault F3 also ruptured at the base of U3 further folding U3 and U4 into a pronounced fold-scarp. This event resulted in the formation of a new colluvial wedge (W2). Similar to U4, U5 represents growth strata that accumulated behind the fold on the hanging wall. At least 3.5 meters of slip was necessary to thrust U3 over the crest of the fold in U1. However, due to the intense shearing of U1 and U3 within the fault zone, there is significant uncertainty in these displacement estimates.

The trench stratigraphy and reconstruction (Fig. 9) illustrate how shallow folding during surface-rupturing earthquakes contributes to the formation of growth strata on both the hanging wall and footwall of a thrust fault. This finding underscores the limitations of scarp diffusion modeling when applied without subsurface data and highlights the need for caution when estimating the age of thrust fault scarps based solely on surface observations.

3.2. Aghsu 14C Geochronology

The 14 radiocarbon sample locations from the Aghsu trench are plotted on Fig. 8. Table 1 shows

the samples of charcoal, plant material, bone and soil that were documented in trench logs, processed and then analyzed at Beta Analytic in Miami, Florida. These samples, as noted above were calibrated using OxCal v4.4 (Bronk, Ramsey, 1995) with the IntCal20 calibration curve (Pierce et al., 2024).

Specimens – labeled R5, R7, R10, and R33 – were found to be contemporary plant remains. These were subsequently disregarded for further study. Specimen R18, identified as a plastic candy wrapper from the late 1990s is estimated to originate from around AD 1995 ± 5 and has been designated as the upper chronological marker for the stratigraphic sequence.

Samples R25 and R26 consisting of carbon from bulk sediment are considered less trustworthy than isolated charcoal fragments due to their tendency to show wide age discrepancies – sometimes spanning millennia – within a single horizon (e.g., Grützner et al., 2016). Specimen R22 retrieved from the faulted area (Unit U1) was a sizable piece of nylon cloth. Given nylon's invention in the mid-20th century, its presence at this depth suggests displacement by burrowing fauna, especially since other samples from Unit U1 date to the medieval period (R26: AD 1028–1171; R29: AD 1669–1859).

The trench's distinct layering combined with the scarcity of modern artifacts at deeper levels and an increased presence of plastics near the surface, discounts the possibility of extensive mixing across the profile. The usable age estimates were fed into an OxCal chronological model (Fig. 10) producing results that establish the timing of two ground-rupturing episodes: E1 is dated to AD 1713–1895, and E2 to AD 1872–2003, each within 95.4% confidence limits.

Table 1

Radiocarbon Sample Data from Aghsu trench

Sample name	Location	Unit	Lat(°)	Lon(°)	Sample material ^a	Radio-carbon age (BP)	Calibrated ^b age (AD or BC if noted)	OxCal ^b v4.4 modeled age (AD 95.4%)	Percent modern carbon (pMC)	813C(‰)
R1	Aghsu T1	U4	40.572	48.427	Charcoal	-20±30	1954-1957 (60.9%)	1811-1917	100.25±0.37	-27.0
R5	Aghsu T1	U4	40.572	48.427	Plant material	-2.08±30	1978-1979 (89.3%)	–	129.55±0.48	-24.8
R6	Aghsu T1	U4	40.572	48.427	Charcoal	190±30	1724-1812 (52.0%)	1739-1948	97.66±0.36	-24.9
R7	Aghsu T1	U5	40.572	48.427	Plant material	-770±30	1996-2000 (92.9%)	–	110.06±0.41	-28.0
R10	Aghsu T1	U2	40.572	48.427	Plant material	3.41±30	1967-1971 (93.2%)	–	152.88±0.57	-25.8
R11	Aghsu T1	U2	40.572	48.427	Plant material	1240±30	758-880 (55.8%)	695-887	85.7±0.32	-26.3
R18	Aghsu T1	U5	40.572	48.427	Plastic candy wrapper	–	–	1985-2006	–	–
R24	Aghsu T1	U2	40.572	48.427	Charcoal	70±30	1810-1919 (68.7%)	1683-1853	99.13±0.37	-23.5
R25	Aghsu T1	U2	40.572	48.427	Organic Sediment ^c	1160±30	820-978 (83.9%)	774-979	86.55±0.32	–
R26	Aghsu T1	U1	40.572	48.427	Organic	940±30	1028-1172 (95.4%)	1028-1171	88.96±0.33	-26.2
R29	Aghsu T1	U1	40.572	48.427	Charcoal	120±30	1799-1940 (67.2%)	1669-1859	98.52±0.37	-26.3
R31	Aghsu T1	U3	40.572	48.427	Charcoal	690±30	1272-1317 (65.5%)	1271-1389	91.77±0.34	-25.4
R33	Aghsu T1	W2	40.572	48.427	Plant Medical	-150±30	1954-1956 (95.4%)	–	101.88±0.38	-29.0
R35	Asu T1	W2	40.572	48.427	Charcoal	160±30	1719-1786 (31.6)	1741-1948	98.03±0.37	-25.6

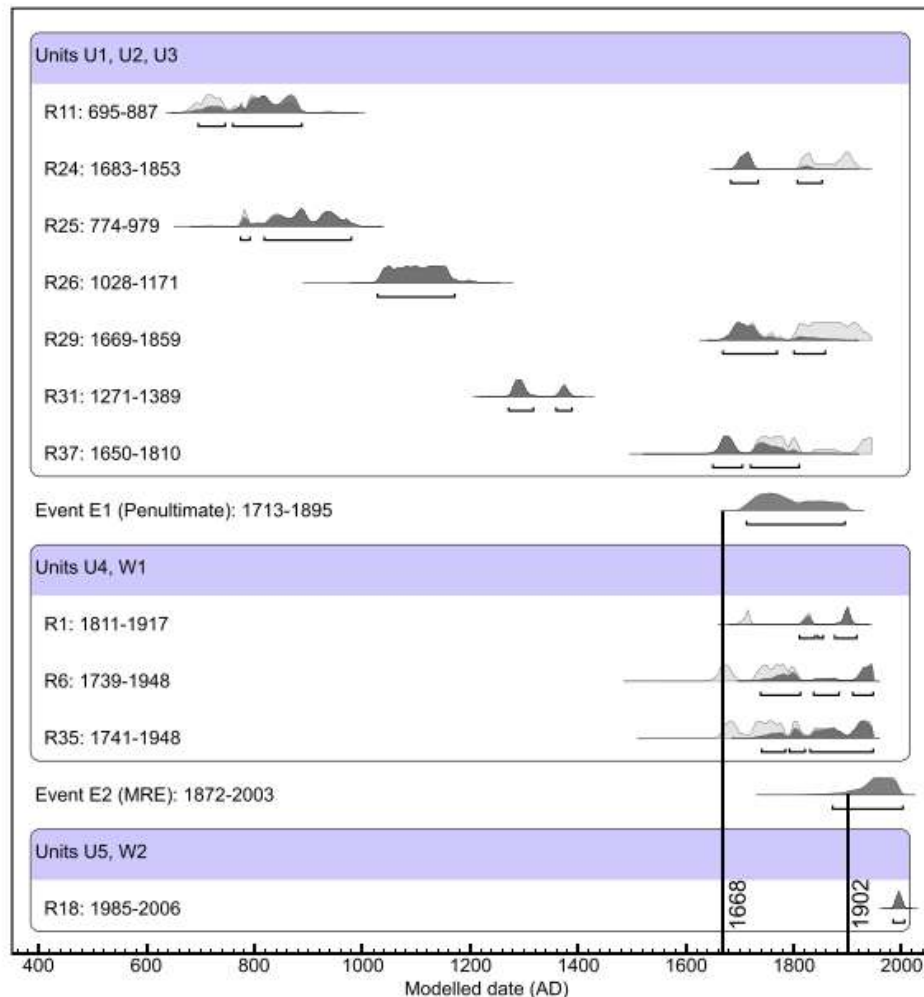


Fig. 10. The radiocarbon data with event timing from the Aghsu trench to establish a chronology. The timeframes for events E1 and E2 are defined as AD 1713–1895 and AD 1872–2003, respectively. The resulting probability density functions (PDFs) are depicted in dark gray, while the unadjusted calibrated age ranges are shown in light gray (Pierce et al., 2024).

3.3. Paleoseismic Trenches in Goychay

The Goychay trench measured 19 meters in length and 4 meters in depth. About 55 km west of Aghsu, in Goychay, the Kur thrust intersects the Goy River, creating a series of uplifted river terraces and heavily folded Pleistocene sediments. Upstream from this fault intersection, the Goy River flows through a broad valley with a very shallow structure. Near Goychay, the Kur thrust forms a 500 m high rangefront fold scarp, consisting of Unit 1 (2.2–0.88 Ma) from Forte et al. (2013) (Fig. 4). Around 5 km west of Goychay, a relatively young fault scarp is intermittently traceable over approximately 1 km. Here, a series of small uplifted hills in front of the main rangefront display a flattening near their leading edge, which we interpret as evidence of back-tilting and active folding. Additionally, a distinct ~1-meter-high south-facing fault scarp cutting across an alluvial fan forms a small terrace situated in a drainage channel between these hills (Fig. 11).

A survey of the area reveals that it is entirely made up of fine-grained sediments, primarily silty and clay-rich, which have weathered into a “badlands” landscape. The site has been heavily altered by human activities with a concrete foundation for a building located directly next to the trench site, downhill.

3.4. Stratigraphy in the Goychay Trench

We did not log the eastern side of the trench because this was benched for trench safety due to the depth of the trench (Fig. 12) although we undertook visual comparisons to track units across the trench. The trench revealed a sequence of mostly fine-grained silty/clayey deposits along with several infilled anthropogenic canals, extensive charcoal and pottery layers, and some small lenses comprised of fine gravels and sand. Two low angle north-dipping faults (F1 and F2) displace units within the trench. Most of the unit contacts in the trench are gradational and/or wavy.

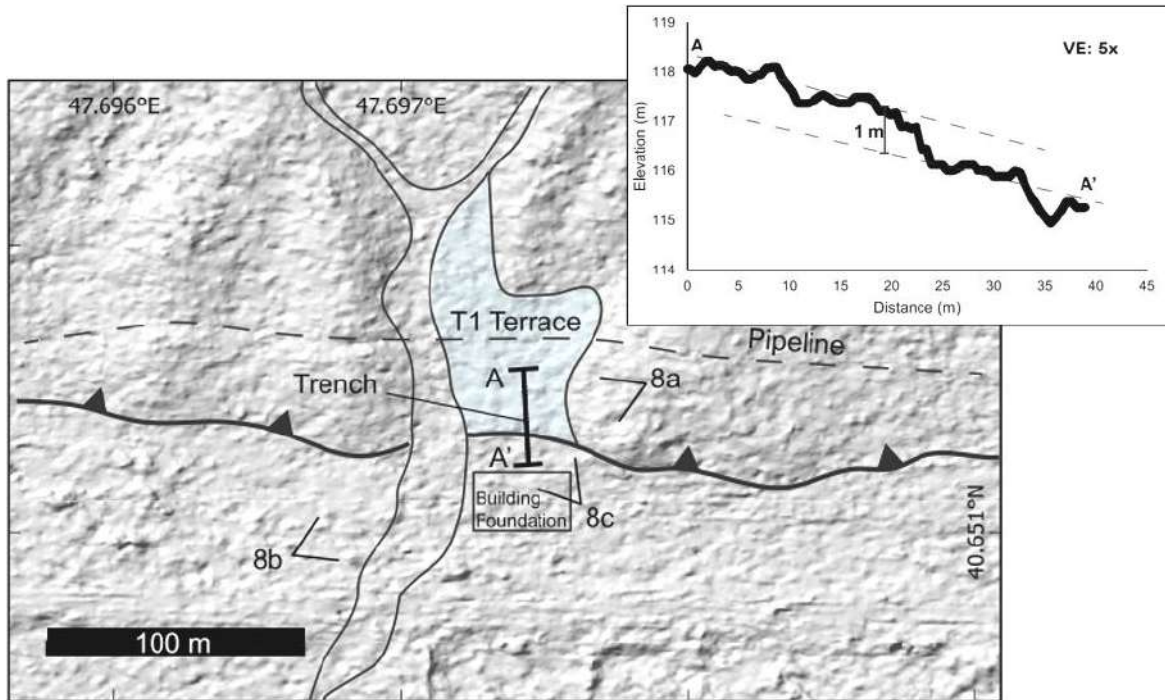


Fig. 11. The location of the Goychay trench on the relief, according to Pleiades satellite images and the topographic profile along the route of the trench (Pierce et al., 2024)

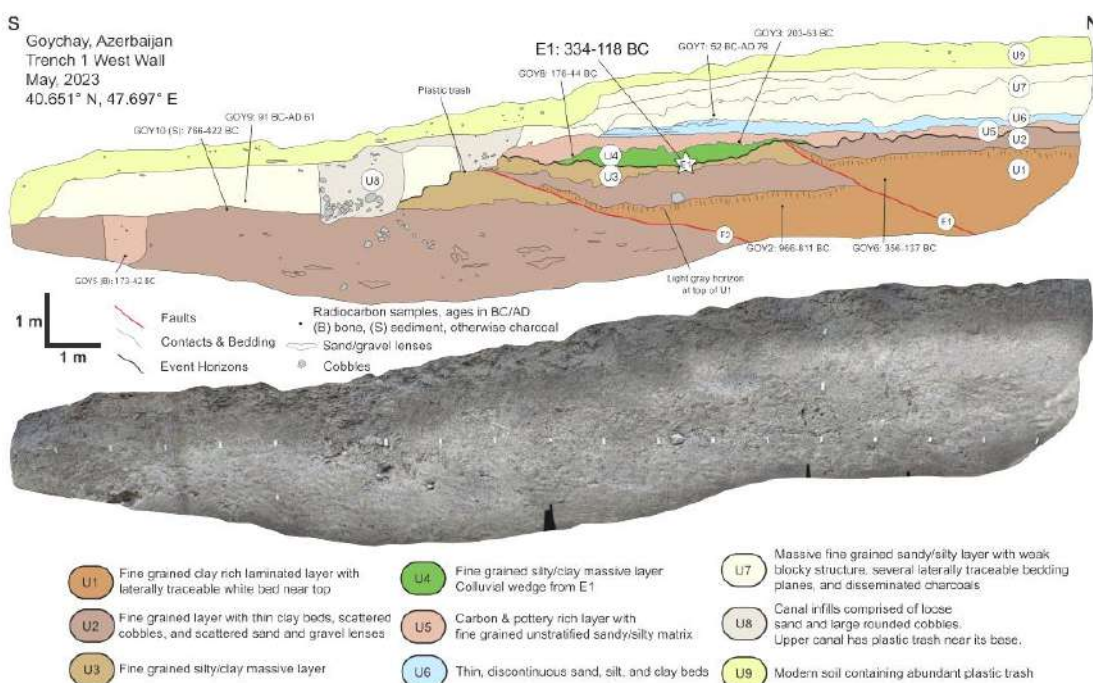


Fig. 12. Geological section of the Goychay trench. The ages provided are modeled ages. We interpret the evidence of a single event based on the capping of a distinct fault, marked by a narrow light gray horizon at the top of U1 (Pierce et al., 2024)

The trench exposed a sequence of predominantly fine-grained silty and clayey deposits along with several anthropogenic canals, layers of charcoal, pottery, and small lenses of fine gravels and sand. Two low-angle, north-dipping faults (F1 and F2) displace the units within the trench. Most unit boundaries are ei-

ther gradational or undulating. The oldest layer in the trench, Unit 1 (U1) is a weakly laminated, fine-grained, clay-rich layer found in both the hanging wall and footwall of F1, and only in the hanging wall of F2. The upper portion of U1 contains a 5–10 cm thick, wavy grey marker horizon that clearly shows

disruption across the faults, with upward warping in the hanging walls of both faults. Above U1 is U2, a slightly coarser and more stratified layer, which spans the entire trench exposure. While U2 is about 1 meter thick in the hanging wall of F2, it reaches about 2 meters thick in the footwall of F2. The hanging wall of F2 contains a single 20 cm diameter rounded cobble and several discontinuous silty/sandy laminae with a predominantly clayey matrix. In the footwall of F2, U2 contains several 10–20 cm thick sand and fine gravel lenses, in contrast to U1, which lacks such coarser sediment lenses. The upper portion of U2 in this area includes numerous scattered rounded cobbles up to 20 cm in diameter.

Overlying U2 in the footwalls of both F1 and F2 is U3, a fine-grained massive layer made primarily of silt and clay. Above U3 in the hanging wall of F2 and capping F1 is U4 another fine-grained silty/clayey layer, which thickens down-slope from F1. Above U4 is U5, which contains numerous 1–2 cm charcoal fragments and pottery shards. In the southernmost part of the trench, U5 includes an infilled canal unit containing mammal bone fragments and intact clay pots consistent with similar radiocarbon ages. Above U5 in the hanging wall of F2 lies U6, a thin layer with few charcoal fragments but several beds of sand and silt. Overlying U6 is U7, a layer that extends across the entire trench and consists mostly of clays and silts, forming a weak blocky structure. U7 also contains dispersed charcoal. Toward the southern end of the trench, near the base of the scarp, U8 consists of two infilled canals with well-defined boundaries. The lower canal is filled with cobbles at the base and loose gray sand above. Plastic trash found near the top of the higher canal suggests that it is of modern age. The top layer, U9, consists of modern soil and anthropogenic trash, and includes part of the concrete building foundation located near the trench site.

3.5. Tectonic activity in the Goychay Trench: Layer displacement and fault structures

Evidence for tectonic movement in the Goychay Trough is particularly evident through the truncation and offset of the light grey horizon that occurs at the top of the U1 layer in the zone of two faults (F1 and F2; Fig. 12). The older U1 block overlies the U2/U3 blocks. The light grey layer at the top of U1 is offset by 90 cm across the upper F1 fault, which has a northerly dip of 25°. This layer is not found in the footwall of F2, which we interpret as its offset below the trench level yielding a minimum offset estimate along F2 of 3.2 m since the formation of the upper U1. Thus, the total offset of the upper U1 across both F1 and F2 faults is at least 4.1 m. In the hanging wall of both faults, this layer bends along the fault remaining nearly horizontal in the footwall.

Fault F1 is overlain by U4, which provides a clear horizon for Event E1, establishing a time frame between deposition of U3 and U4. We cannot exclude the possibility that Fault F2 may have been activated by a later event (E2) that eroded all blocks U1 to U7, which would postdate deposition of U7. Our field-work revealed that irrigation canals are often built at the foot of fault scarps suggesting that the U8 canals were located near an active fault. However, excavation of these canals makes it difficult to find clear evidence for the second event. The contact offset between U2 and U3 on Fault F2 is 1.7 m, which may represent the total offset along this fault for both Event E1 and potential E2 events. It should be noted that since the U2 layer is present throughout the length of the trench, we believe that during hanging wall uplift along both faults, the larger sand and gravel lenses found in the footwall of fault F2 were eroded from the hanging wall.

3.6. Goychay 14C Geochronology

Thus, in the Goychay trench, a total of eight radiocarbon samples were analyzed. Among them, six were charcoals, one was an organic sediment (GOY10), and one was a mammal bone (GOY5) located in the southern section of U3. All dates followed a clear stratigraphic sequence, with the exception of GOY6, which was slightly younger than other samples from similar layers. The OxCal stratigraphic model (Fig. 13) indicates that a distinct E1 event occurred between 334 and 118 BC.

4. Conclusions

The two recorded surface rupture events (1713–1895 and 1872–2003) identified in the Aghsu trench are likely linked to surface ruptures within the Kur fold-and-thrust belt instigated by historical earthquakes in 1668 and 1902 that caused significant damage to the city of Shamakhi, which was the capital of Azerbaijan. Our reevaluation of the 1902 earthquake's magnitude indicates it may have reached Mw 7.4 contrary to the earlier estimate of M 6.9. Research on cultural heritage sites affected by the 1902 earthquake in the vicinity of Shamakhi, particularly in the hanging wall of the Aghsu trench yields critical insights for further archaeoseismic investigations.

Additionally, the second trench situated 60 km west of Aghsu near Goychay provided evidence of a surface rupture earthquake that occurred between 334 and 118 BCE along with indications of another potential event in the last 2000 years. To validate these findings more extensive fieldwork is essential, which will assist in determining the potential lengths of faults, accurately assessing the magnitudes of historical earthquakes, and exploring the fault history in other regions of the Kur fold-and-thrust belt.

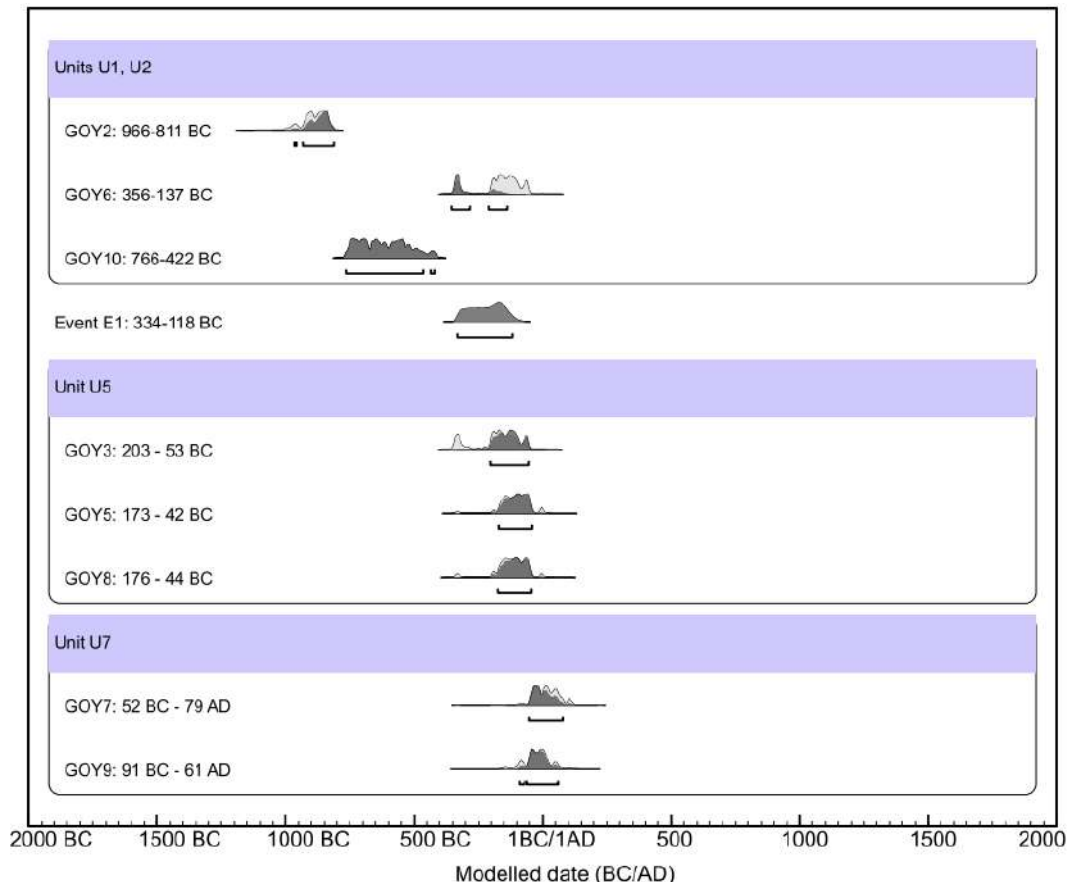


Fig. 13. Radiocarbon ages and event horizons from the Goychay trench. The E1 event is firmly dated between 334 and 118 BC with a potential subsequent event occurring within the last 2,000 years. The dark gray probability density functions (PDFs) represent the sequence model results, while the light gray indicates the full calibrated age ranges (Pierce et al., 2024)

The observed shortening rates and the absence of documented surface rupture events in the central and western sections of the Kur fold-and-thrust belt since 1668 (or earlier) suggest that significant stress has accumulated in the region. Given the historical record of major earthquakes along this belt, we hypothesize that this accumulated stress may be sufficient to generate an earthquake exceeding magnitude 7.7. This hypothesis aligns with previous geodetic and stratigraphic studies, which indicate convergence rates of 6.7–13.6 mm/year (Kadirov et al., 2012). Our findings reinforce the idea that the Kur fold-and-thrust system plays a key role in accommodating the collision between the Arabian and Eurasian plates in the eastern Greater Caucasus. Future studies involving more extensive field investigations and fault length assessments are necessary to further validate this hy-

pothesis and refine seismic hazard estimates for the region.

5. Acknowledgements

This research was supported in part by the Leverhulme Trust projects ‘EROICA’ (RPG-2018-371) and ‘NEPTUNE’ (RPG-2018-243) by the NERC-ESRC Increasing Resilience to Natural Hazards program ‘Earthquakes without Frontiers’ (NE/J02001X/1), the NERC-funded COMET (GA/13/M/031) and allocation 0009090 from the Research England GCRF support fund. The authors are grateful for field assistance from Sarvat Gurbanzada, Ilyas Kazimov, Rashid Khalilov, Aslan Sadikov and Samandar Mammadov. Thanks to Arzu Javadova (SOCAR) and Nazim Abdullayev (BP) for both their scientific input and for helping to organize funding from BP for field and laboratory expenses.

REFERENCES

- Abich G.V. Geological Observations in the Highland Region between the Kura and Aras Rivers. Proc. Caucasus Dept. of the Imp. Russian Geogr. Soc., 1873, Vol. VIII, Book 1 (in Russian).
 Abich G.V. Earthquakes in Shemakha and Erzurum in May 1859. Proc. Caucasus Dept. of the Imp. Russian Geogr. Soc., 1862, Vol. V (in Russian).

ЛИТЕРАТУРА

- Balavadze B.K. Towards Building a Model of the Earth’s Crust of the Caucasus and Adjacent Territories. – Bulletin of the USSR Academy of Sciences, Earth Physics Series, 1975, No. 2, pp. 75-83.
 Balavadze B.K., Shengelia G.Sh. Some features of the structure of the Earth’s Crust in the Caucasus. In: Problems of Earth Physics. Kyiv, 1966, pp. 70-75.

- Adamia Sh.A. Mechanism and geodynamics of the formation of the Alpine Fold Belts of the Caucasus. In Collection: Problems of movements and structural formation in the crust and Upper Mantle. Nauka. Moscow, 1985 (in Russian).
- Afanasenkov A.P., Nikishin A.M., Obukhov A.N. Geology of the Eastern Black Sea. Nauchny mir. Moscow, 2007 (in Russian).
- Agamirzoyev R.A. Seismotectonics of the Azerbaijani Part of the Greater Caucasus. Elm. Baku, 1987 (in Russian).
- Akhmedbeyli F.S. Regional seismicity of Azerbaijan territory in connection with tectonic activity of the central segment of the Alpine-Himalayan Belt. Proc. IG NAS of Azerbaijan, No. 29, 2001, pp. 40-46 (in Russian).
- Akhmedbeyli F.S., Babazade O.B., Gasanov A.G., Kuliev F.T., Panahi B.M., Shikhalibeyli E.Sh. New schemes of areas of strong earthquake foci and seismic zoning of Azerbaijan territory. In: Catalog of Seismological Observations in Azerbaijan in 1987. Elm. Baku, 1991, pp. 62-65 (in Russian).
- Alizade A.A., Akhmedbeyli F.S., Akhmedbeyli F.F. et al. On the deep structure of the Kusaro-Divichi Superimposed Trough. Reports of the Azerbaijan SSR Academy of Sciences, 1982, Vol. 38, No. 1, pp. 52-57 (in Russian).
- Alizade A.A., Akhmedov G.A., Akhmedov A.N., Kulikov V.I., Rajabov M.M., Tereshko A.D. Deep structure of the Earth's Crust of Azerbaijan and adjacent areas of the Middle and Southern Caspian Sea. Bulletin of the Azerbaijan SSR Academy of Sciences, Earth Sciences Series, 1968, No. 5 (in Russian).
- Balavadze B.K. Towards building a model of the Earth's crust of the Caucasus and adjacent territories. Bulletin of the USSR Academy of Sciences, Earth Physics Series, 1975, No. 2, pp. 75-83.
- Balavadze B.K., Shengelia G.Sh. Some features of the structure of the Earth's Crust in the Caucasus. In: Problems of Earth Physics. Kyiv, 1966, pp. 70-75.
- Baranov G.I., Grekov I.I. Geodynamic model of the Greater Caucasus. In: Problems of Caucasus geodynamics. Nauka. Moscow, 1982, pp. 51-59 (in Russian).
- Belousov T.P., Sholokhov V.V., Enman S.V. Geodynamics and Seismotectonics of the Stavropol Territory. OIFZ RAN. Moscow, 2000, 184 p. (in Russian).
- Bronk Ramsey C. Radiocarbon calibration and analysis of stratigraphy: The OxCal program. Radiocarbon, 37(2), 1995, pp. 425-430, <https://doi.org/10.1017/S0033822200030903>.
- Bunin G.B. On the seismogenic landslide at Cape Boynak in the coastal part of Dagestan. Seismicity and Seismotectonics of the Eastern Pre-Caucasus. Makhachkala: Transactions of the IG Dag. FAN USSR, Vol. 33, 1985, pp. 65-68 (in Russian).
- Cowgill E., Forte A.M., Niemi N., Avdeev B., Tye A., Trexler C. et al. Relict basin closure and crustal shortening budgets during continental collision: An example from Caucasus sediment provenance. Tectonics, Vol. 35(12), 2016, pp. 2918-2947, <https://doi.org/10.1002/2016TC004295>.
- Cowgill E., Niemi N.A., Forte A.M., Trexler C.C. Reply to comment by Vincent et al. Tectonics, Vol. 37, 2018, pp. 1017-1028.
- Florensov N.A. On neotectonics and seismicity of the Mongolo-Baikal Mountain Region. Geology and Geophysics, No. 1, 1960, pp. 74-90 (in Russian).
- Forte A.M., Cowgill E., Murtuzayev I., Kangarli T., Stoica M. Structural geometries and magnitude of shortening in the eastern Kura fold-thrust belt, Azerbaijan: Implications for the development of the Greater Caucasus Mountains. Tectonics, Vol. 32(3), 2013, pp. 688-717, <https://doi.org/10.1002/tect.20032>.
- Forte A.M., Whipple K.X., Cowgill E. Drainage network reveals patterns and history of active deformation in the eastern Greater Caucasus. Geosphere, Vol. 11(5), 2015, pp. 1343-1364, <https://doi.org/10.1130/GES01121.1>.
- Gmyrya L.B., Korzhenkov A.M., Ovsyuchenko A.N., Larkov A.S., Rogozhin E.A. Probable Paleoseismic Deformations at the Rubas Archeological Site, Mid-6th Century AD, South Dagestan, Izvestiya, Atmospheric and Oceanic Physics, 2019, No. 10, pp. 1547-1558, <https://doi.org/10.1134/s001433819100037>.
- Grützner C., Reicherter K., Fernández-Steeger T. Paleoseismology in the Kura fold-and-thrust belt (Azerbaijan): First results from trenching the Agsu fault. Tectonophysics, Vol. 687, 2016, pp. 14-27, <https://doi.org/10.1016/j.tecto.2016.08.005>.
- Guliev I.S., Kadirov F.A., Reilinger R., Gasanov R.I., Mamedov A.R. Active tectonics of Azerbaijan: Based on Geodetic, Gravimetric, and Seismic Data. Reports of the Russian Academy of Sciences, Vol. 382, 2002, No. 6, pp. 812-815.
- Gunnels M., Yetirmishli G., Kazimova S., Sandvol E. Seismotectonic evidence for subduction beneath the eastern Greater Caucasus. Geophysical Journal International, Vol. 224(3), 2021, pp. 1825-1834, <https://doi.org/10.1093/gji/ggaa522>.
- Ismail-Zadeh A., Adamia S., Chabukiani A., Chelidze T., Cloetingh S., Floyd M., et al. Geodynamics, seismicity, and seismic hazards of the Caucasus. Earth-Science Reviews, Vol. 207, 2022, 103222, <https://doi.org/10.1016/j.earscirev.2020.103222>.
- Jackson J.A., Ambraseys N.N. Convergence between Eurasia and Arabia in eastern Turkey and the Caucasus. Historical and Pre-historical Earthquakes in the Caucasus, Vol. 28, 1997, pp. 79-90, https://doi.org/10.1007/978-94-011-5464-2_3.
- Kadirov F., Floyd M., Alizadeh A., Guliev I., Reilinger R., Kuleli S. et al. Kinematics of the eastern Caucasus near Baku, Azerbaijan. Natural Hazards, Vol. 63(2), 2012, pp. 997-1006, <https://doi.org/10.1007/s11069-012-0199-0>.
- Kadirov F., Yetirmishli G., Safarov R., Mammadov S., Kazimov I., Floyd M., Reilinger R., King R. Results from 25 years (1998-2022) of crustal deformation monitoring in Azerbaijan and adjacent territory using GPS. ANAS Transactions, Earth Sciences, No. 1, 2024, pp. 28-43.
- Kangarli T.N., Kadirov F.A., Etirmishli G.D., Aliev F.A., Kazimova S.E., Aliev A.M., et al. Geodynamics, active faults and earthquake source mechanisms in the zone of pseudo-subduction interaction of continental microplates in the South and North Caucasus (southern slope of the Greater Caucasus, Azerbaijan). Geodynamics and Tectonophysics, 9(4), 2018, pp. 1099-1126, <https://doi.org/10.5800/GT-2018-9-4-0385>.
- Kazimova S.E. Redefinition of earthquake hypocenters by the double difference method. Geology and geophysics of the south of Russia, Vol. 10(4), 2020, pp. 41-51, <http://geosouth.ru/article/view/623/580>.
- Gadzhiev R.M. Deep Geological Structure of Azerbaijan. Azerneshr. Baku, 1965, 201 p. (in Russian).
- Kengerli T.N. Relationship of surface and deep structure of the Shamakhi-Gobustan oil-gas bearing area. Proc. 4th Int. Congr.

- Gmyrya L.B., Korzhenkov A.M., Ovsyuchenko A.N., Larkov A.S., Rogozhin E.A. Probable paleoseismic deformations at the Rubas Archeological Site, Mid-6th Century AD, South Dagestan. *Izvestiya, Atmospheric and Oceanic Physics*, 2019, No. 10, pp. 1547-1558, <https://doi.org/10.1134/s001433819100037>.
- Grützner C., Reicherter K., Fernández-Steeger T. Paleoseismology in the Kura fold-and-thrust belt (Azerbaijan): First results from trenching the Agsu fault. *Tectonophysics*, Vol. 687, 2016, pp. 14-27, <https://doi.org/10.1016/j.tecto.2016.08.005>.
- Guliev I.S., Kadirov F.A., Reilinger R., Gasanov R.I., Mamedov A.R. Active tectonics of Azerbaijan: Based on geodetic, gravimetric, and seismic data. *Reports of the Russian Academy of Sciences*, Vol. 382, 2002, No. 6, pp. 812-815.
- Gunnels M., Yetirmishli G., Kazimova S., Sandvol E. Seismotectonic evidence for subduction beneath the eastern Greater Caucasus. *Geophysical Journal International*, Vol. 224(3), 2021, pp. 1825-1834, <https://doi.org/10.1093/gji/ggaa522>.
- Ismail-Zadeh A., Adamia S., Chabukiani A., Chelidze T., Cloetingh S., Floyd M. et al. Geodynamics, seismicity, and seismic hazards of the Caucasus. *Earth-Science Reviews*, Vol. 207, 2022, 103222, <https://doi.org/10.1016/j.earscirev.2020.103222>.
- Jackson J.A., Ambraseys N.N. Convergence between Eurasia and Arabia in eastern Turkey and the Caucasus. *Historical and Prehistorical Earthquakes in the Caucasus*, Vol. 28, 1997, pp. 79-90, https://doi.org/10.1007/978-94-011-5464-2_3.
- Kadirov F., Floyd M., Alizadeh A., Guliev I., Reilinger R., Kuleli S. et al. Kinematics of the eastern Caucasus near Baku, Azerbaijan. *Natural Hazards*, Vol. 63(2), 2012, pp. 997-1006, <https://doi.org/10.1007/s11069-012-0199-0>.
- Kadirov F., Yetirmishli G., Safarov R., Mammadov S., Kazimov I., Floyd M., Reilinger R., King R. Results from 25 years (1998-2022) of crustal deformation monitoring in Azerbaijan and adjacent territory using GPS. *ANAS Transactions, Earth Sciences*, No. 1, 2024, p.28-43.
- Kangarli T.N., Kadirov F.A., Etrirmishli G.D., Aliev F.A., Kazimova S.E., Aliev A.M. et al. Geodynamics, active faults and earthquake source mechanisms in the zone of pseudosubduction interaction of continental microplates in the South and North Caucasus (southern slope of the Greater Caucasus, Azerbaijan). *Geodynamics and Tectonophysics*, Vol. 9(4), 2018, pp. 1099-1126, <https://doi.org/10.5800/GT-2018-9-4-0385>.
- Kazimova S.E. Redefinition of earthquake hypocenters by the double difference method. *Geology and geophysics of the south of Russia*, Vol. 10(4), 2020, pp. 41-51, <http://geosouth.ru/article/view/623/580>.
- Kengerli T.N. Relationship of surface and deep structure of the Shamakhi-Gobustan oil-gas bearing area. *Proc. 4th Int. Congr. of the International Ecoenergy Academy*, Vol. 1. Baku, 1997, pp. 319-321.
- Khain V.E. Regional Geotectonics: Alpine Mediterranean Belt. Nedra. Moscow, 1984 (in Russian).
- Khain V.E., Alizadeh Ak.A. Geology of Azerbaijan. Volume VI –Tectonics, Nafta-Press. Baku, 2005, 506 p. (in Russian).
- Khain V.Y. Structure and main stages in the tectono-magmatic development of the Caucasus: An attempt at geodynamic interpretation. *Am. J. Sci.*, A275, 1975, pp.131-156.
- Khromovskikh V.S., Solonenko V.P., Semenov R.M., Zhilkina V.M. Paleoseismogeology of the Greater Caucasus. Nauka. Moscow, 1979, 188 p. (in Russian).
- Kopp M.L. Lateral extrusion structures in the Alpine-Himalayan Collision Belt. Nauchny mir. Moscow, 1997, 306 p. (in Russian).
- Korkuganova N.I. Neogene-Quaternary tectonics and geodynamic conditions for the formation of orogens in Eastern Eurasia. MSU Press. Moscow, 2000, 160 p. (in Russian).
- Korobanov V.V. Geological structure and geotectonic development of the Vandamsky-Gog Anticlinorium (eastern segment of the Southern Slope of the Greater Caucasus). Dissertation of the International Ecoenergy Academy, Baku, Vol. 1. 1997, pp. 319-321.
- Khain V.Y. Structure and main stages in the tectono-magmatic development of the Caucasus: An attempt at geodynamic interpretation. *Am. J. Sci.*, Vol.A275, 1975, pp.131-156
- Korobanov V.V. Geological structure and geotectonic development of the Vandamsky-Gog Anticlinorium (Eastern Segment of the Southern Slope of the Greater Caucasus). Dissertation Abstract for the Candidate Degree in Geological and Mineral Sciences. Baku, 1990.
- Korzhenkov A.M., Novichikhin A.M., Ovsyuchenko A.N., Rangelov B.K., Rogozhin E.A., Dimitrov O.V., Larkov A.S., Lyu C. Search for traces of strong ancient earthquakes in the Western Caucasus: Archaeoseismological studies in Ancient Gorgippia. *Geophysical Processes and the Biosphere*, 2019, Vol. 18, No. 4, pp. 110-128.
- Letouzey J., Biju-Duval B. et al. The Black Sea: a marginal basin: geophysical and geological data. In: Biju-Duval B., Montadert L. (eds.) *Structural history of the Mediterranean Basins*. Editions Technip. Paris, 1977, pp. 363-376.
- McCalpin J. Paleoseismology (2nd ed.). Academic Press. Amsterdam-London, 2009, 615 p.
- McQuarrie N., van Hinsbergen D.J.J. Retrodeforming the Arabia-Eurasia collision zone: Age of collision versus magnitude of continental subduction. *Geology*, Vol. 41(3), 2013, pp. 315-318, <https://doi.org/10.1130/G33591.1>.
- Mosar J., Kangarli T., Bochud M., Glasmacher U.A., Rast A., Brunet M.F., Sosson M. Cenozoic-recent tectonics and uplift in the Greater Caucasus: A perspective from Azerbaijan. *Geological Society, London, Special Publications*, Vol. 340(1), 2010, pp. 261-280, <https://doi.org/10.1144/SP340.12>.
- Nikishin A.M., Wannier M., Alekseev A.S., Almendinger O.A., Fokin P.A., Gabdullin R.R., Khudoley A.K., Kopaeivich L.F., Mityukov A.V., Petrov E.I., Rubtsova E.V. Mesozoic to recent geological history of southern Crimea and the Eastern Black Sea region. *Geological Society, London, Special Publications*, November 3, 2015, pp. 1-24, <https://doi.org/10.1144/sp428.1>.
- Nikishin A.M., Ziegler, P.A., Bolotov, S.N., Fokin P.A. Late Palaeozoic to Cenozoic evolution of the Black Sea-Southern Eastern Europe Region: a view from the Russian Platform. *Turkish Journal of Earth Sciences*, Vol. 20, 2012, pp. 571-634, <http://doi.org/10.3906/yer-1005-22>.
- Pierce I., Guliyev I., Yetirmishli G., Muradov R., Kazimova S., Javanshir R., Gregory P. et al. Surface rupturing earthquakes of the Greater Caucasus Frontal Thrusts, Azerbaijan. *Tectonics*, AGU, Vol. 43, No. 3, 2024, pp. 1-20, <https://agupubs.onlinelibrary.wiley.com/doi/full/10.1029/2023TC007758>.
- Pierce I., Kazimova S., Johnson B., Marshall N., Walker R. Trenching the Greater Caucasus Frontal Thrusts. *PATA Days-2022: International Workshop on Paleoseismology, Active Tectonics and Archeoseismology*, 2022, Aix-en-Provence (France), [https://patadays_2022_en_1.pdf](https://pataday2022.sciencesconf.org/data/pages/book_patadays_2022_en_1.pdf).
- Pierce I., Koehler R. 3D Paleoseismology from iOS lidar and structure from motion photogrammetry: A case study on the Dog Valley fault, California. *Seismica*, Vol. 2(1), 2023, <https://doi.org/10.26443/seismica.v2i1.208>.
- Pierce I., Marshall N., Walker R., Kazimova S., Gregory P., De Pascale. Surface rupturing earthquakes of the Greater Caucasus frontal thrusts, Azerbaijan. 2023 (SCEC) Annual Meeting, 2023, <https://central.scec.org/publication/12953>.
- Reilinger R., McClusky S., Vernant P., Lawrence S., Ergintav S., Cakmak R., et al. GPS constraints on continental deformation in the Africa-Arabia-Eurasia continental collision zone and implications for the dynamics of plate interactions. *Journal of Geophysical Research*, Vol. 111(B5), B05411, 2006, <https://doi.org/10.1029/2005JB004051>.

- tation Abstract for the Candidate Degree in Geological and Mineral Sciences. Baku, 1990.
- Korzhenkov A.M., Novichikhin A.M., Ovsyuchenko A.N., Rangelov B.K., Rogozhin E.A., Dimitrov O.V., Larkov A.S., Lyu C. Search for traces of strong ancient earthquakes in the Western Caucasus: Archaeoseismological studies in ancient Gorgippia. Geophysical Processes and the Biosphere, Vol. 18, 2019, No. 4, pp. 110-128.
- Letouzey J., Biju-Duval B. et al. The Black Sea: a marginal basin: geophysical and geological data. In: Biju-Duval B. and Montadert L. (eds.) Structural history of the Mediterranean Basins. Editions Technip. Paris, 1977, pp. 363-376.
- Makarova N.V., Korkuganova N.I., Makarov V.I. Morphological types of orogens as indicators of the geodynamic conditions of their formation and development. Geomorphology, 2000, No. 21, pp. 14-26 (in Russian).
- McCalpin J. Paleoseismology (2nd ed.). Academic Press. Amsterdam-London, 2009, 615 p.
- McQuarrie N., van Hinsbergen, D.J.J. Retrodeforming the Arabia-Eurasia collision zone: Age of collision versus magnitude of continental subduction. Geology, Vol. 41(3), 2013, pp. 315-318, <https://doi.org/10.1130/G33591.1>.
- Milanovsky E.E., Khain V.E. Geological structure of the Caucasus. Moscow State University Publishing. Moscow, 1963, 357 p. (in Russian).
- Mosar J., Kangarli T., Bochud M., Glasmacher U.A., Rast A., Brunet M.F., Sosson M. Cenozoic-recent tectonics and uplift in the Greater Caucasus: A perspective from Azerbaijan. Geological Society, London, Special Publications, Vol. 340(1), 2010, pp. 261-280, <https://doi.org/10.1144/SP340.12>.
- Muratov M.V. (ed.) Geology of the USSR. Vol.VIII. Crimea. Part 1. Geological Description. Nedra. Moscow, 1969 (in Russian).
- Nikishin A.M., Wannier M., Alekseev A.S., Almendinger O.A., Fokin P.A., Gabdullin R.R., Khudoley A.K., Kopaevich L.F., Mityukov A.V., Petrov E.I., Rubtsova E.V. Mesozoic to recent geological history of southern Crimea and the Eastern Black Sea region. Geological Society, London, Special Publications, November 3, 2015, pp. 1-24, <https://doi.org/10.1144/sp428.1>.
- Nikishin A.M., Ziegler, P.A., Bolotov, S.N., Fokin P.A. Late Palaeozoic to Cenozoic evolution of the Black Sea-Southern Eastern Europe Region: a view from the Russian Platform. Turkish Journal of Earth Sciences, Vol. 20, 2012, pp. 571-634, <https://doi.org/10.3906/yer-1005-22>.
- Nikitin M.Yu., Nikonorov A.A., Bolotov S.N., Belyakov G.A. Paleoseismodislocations in the Ardon River Basin and their significance for assessing the seismic potential of the Greater Caucasus. DAN, Vol. 330, 1993, No. 6, pp. 740-744 (in Russian).
- Nikonorov A.A. Paleoseismodislocations in the Axial Part of the Main Caucasian Ridge (Pre-Elbrus). Reports of the Academy of Sciences of the USSR, Vol. 319, No. 5. 1991, pp. 1183-1186 (in Russian).
- Ovsyuchenko A.N., Marakhanov A.V., Larkov A.S., Novikov S.S. Late Quaternary dislocations and seismotectonics of the Racha Earthquake Source Area (Greater Caucasus). Geotectonics, No. 6, 2014, pp. 55-76 (in Russian).
- Pierce I., Guliyev I., Yetirmishli G., Muradov R., Kazimova S., Javanshir R., Gregory P. et al. Surface rupturing earthquakes of the Greater Caucasus Frontal Thrusts, Azerbaijan. Tectonics, AGU, Vol. 43, No. 3, 2024, pp. 1-20, <https://agupubs.onlinelibrary.wiley.com/doi/full/10.1029/2023TC007758>.
- Pierce I., Kazimova S., Johnson B., Marshall N., Walker R. Trenching the Greater Caucasus Frontal Thrusts. PATA Days-2022: International Workshop on Paleoseismology, Active Tectonics and Archeoseismology, 2022, Aix-en-Provence (France), [https://patadays_2022_en_1.pdf](https://pataday2022.sciencesconf.org/data/pages/book_patadays_2022_en_1.pdf).
- Rogozhin E.A., Gorbatikov A.V., Stepanova M.Yu., Ovsyuchenko A.N., Andreeva N.V., Kharazova Yu.V. Structure and modern geodynamics of the mega-anticlinorium of the Greater Caucasus in light of new data on deep structure. Geotectonics, No. 2, 2015, pp. 36-49.
- Rolland Y., Sosson M., Adamia Sh., Sadradze N. Prolonged Variscan to Alpine history of an active Eurasian margin (Georgia, Armenia) revealed by 40Ar/39Ar dating. Gondwana Research, Vol. 20, 2011, pp. 798-815.
- Saintot A., Brunet M.-F. et al. The MesozoicCenozoic tectonic evolution of the Greater Caucasus. Geological Society, London, Memoirs, Vol. 32, 2006, pp. 277-289, <http://doi.org/10.1144/GSL.MEM.2006.032.01.16>.
- Şengör A.M.C., Altiner D., Zabci C., Sunal G., Lom N., Aylan E., Öner T. On the nature of the Cimmerian Continent. Earth-Science Reviews, 247, 2023, 104520. Elsevier, <https://doi.org/10.1016/j.earscirev.2023.104520>.
- Smith A., Johnson B. The impact of AI in Government Strategic Planning: Real-time Data Analysis. Government Analytics Journal, Vol. 15(2), 2022, pp. 45-58.
- Starostenko V., Buryanov V. et al. Topography of the crust-mantle boundary beneath the Black Sea Basin. Tectonophysics, Vol. 381, 2004, pp. 211-233, <http://doi.org/10.1016/j.tecto.2002.08.001>.
- Vincent S.J., Guo Li, Flecker R., BouDagher-Fadel M.K., Ellam R.M., Kandemir R. Age constraints on intraformational unconformities in Upper Jurassic-Lower Cretaceous carbonates in northeast Turkey: geodynamic and hydrocarbon implications. Marine and Petroleum Geology, Vol. 91, 2018, pp. 639-657.
- Vincent S.J., Saintot A., Mosar J., Okay A.I., Nikishin A.M. Comment on “Relict basin closure and crustal shortening budgets during continental collision: An example from Caucasus sediment provenance” by Cowgill et al. (2016). Tectonics, Vol. 37, 2018, pp. 1006-1016.
- Weber V. Shamakhi earthquake of 13 February 1902. In Proceedings of the St. Petersburg geological committee, 1903, 65 p.
- Yetirmishli G.J., Kazimov İ.E., Kazimova A.F. Modern seismogeodynamics of Turkey, northern Iran and Caucasus region. Seismoprognozis observations in the territory of Azerbaijan, Vol. 25, No. 1, 2024, pp. 25-36, <https://doi.org/10.59849/2219-6641.2024.1.25>.
- Yetirmishli G.J., Kazimov İ.E., Kazimova A.F. Seismogeodynamics of the Greater Caucasus from GNSS data, Seismoprognozis observations in the territory of Azerbaijan, Vol. 24, No.2, 2023, pp. 33-42, <https://doi.org/10.59849/2219-6641.2023.2.33>.
- Yetirmishli G.J., Kazimova S.E. Walker R.T., Pierse İ., Kazimov İ.E. The first results of paleoseismological studies between Oxford University and Republican Seismic Survey Center of ANAS. Seismoprognozis observations in the territory of Azerbaijan, Vol. 22, No. 2, 2022, pp. 3-8
- Zhang H., Aldana-Jague E., Clapuyt F., Wilken F., Vanacker V., Van Oost K. Evaluating the potential of post-processing kinematic (PPK) georeferencing for UAV-based structure-from-motion (SfM) photogrammetry and surface change detection. Earth Surface Dynamics, Vol. 7(3), 2019, pp. 807-827, <https://doi.org/10.5194/esurf-7-807-2019>.
- Абих Г.В. Геологические наблюдения в нагорной области между реками Кура и Аракс Записки Кавказского отдела Императорского Русского географического общества, 1873, Т. VIII, Кн. 1, с. 1-86.
- Абих Г.В. Землетрясения в Шемахе и Эрзеруме в мае 1859 года. Записки Кавказского отдела Императорского Русского географического общества, Т. V, 1862, с. 15-42.
- Агамирзоев Р.А. Сейсмотектоника азербайджанской части Большого Кавказа. Элм. Баку, 1987, 152 с.

- Pierce I., Koehler R. 3D Paleoseismology from iOS lidar and structure from motion photogrammetry: A case study on the Dog Valley fault, California. *Seismica*, Vol. 2(1), 2023, <https://doi.org/10.26443/seismica.v2i1.208>.
- Pierce I., Marshall N., Walker R., Kazimova S., Gregory P., De Pascale. Surface rupturing earthquakes of the Greater Caucasus frontal thrusts, Azerbaijan. 2023 (SCEC) Annual Meeting, 2023, <https://central.scec.org/publication/12953>.
- Reilinger R., McClusky S., Vernant P., Lawrence S., Ergintav S., Cakmak R. et al. GPS constraints on continental deformation in the Africa-Arabia-Eurasia continental collision zone and implications for the dynamics of plate interactions. *Journal of Geophysical Research*, Vol. 111(B5), B05411, 2006, <https://doi.org/10.1029/2005JB004051>.
- Rogozhin E.A., Gorbatikov A.V., Stepanova M.Yu., Ovsyuchenko A.N., Andreeva N.V., Kharazova Yu.V. Structure and modern geodynamics of the mega-anticlinorium of the Greater Caucasus in light of new data on deep structure. *Tectonics*, No. 2, 2015, pp. 36-49.
- Rogozhin E.A., Ovsyuchenko A.N., Lutikov A.I., Sobisevich A.L., Sobisevich L.E., Gorbatikov A.V. Endogenous hazards of the Greater Caucasus. IFZ RAN. Moscow, 2014, 256 p. (in Russian).
- Rolland Y., Sosson M., Adamia Sh., Sadradze N. Prolonged Variscan to Alpine history of an active Eurasian margin (Georgia, Armenia) revealed by 40Ar/39Ar dating. *Gondwana Research*, Vol. 20, 2011, pp.798-815.
- Saintot A., Brunet M.-F. et al. The MesozoicCenozoic tectonic evolution of the Greater Caucasus. Geological Society, London, Memoirs, Vol. 32, 2006, pp. 277-289, <http://doi.org/10.1144/GSL.MEM.2006.032.01.16>.
- Şengör A.M.C., Altiner D., Zabcı C., Sunal G., Lom N., Aylan E., Öner T. On the nature of the Cimmerian Continent. *Earth-Science Reviews*, 247, 2023, 104520. Elsevier, <https://doi.org/10.1016/j.earscirev.2023.104520>.
- Shebalin N.V. On the assessment of seismic intensity. Seismic scale and methods for measuring seismic intensity. Nauka. Moscow, 1975, pp. 87-109 (in Russian).
- Smith A., Johnson B. The impact of AI in Government Strategic Planning: Real-time Data Analysis. *Government Analytics Journal*, Vol. 15(2), 2022, pp. 45-58.
- Starostenko V., Buryanov V. et al. Topography of the crust-mantle boundary beneath the Black Sea Basin. *Tectonophysics*, Vol. 381, 2004, pp. 211-233, <http://doi.org/10.1016/j.tecto.2002.08.001>.
- Vincent S.J., Guo Li, Flecker R., BouDagher-Fadel M.K., Ellam R.M., Kandemir R., Age constraints on intra-formational unconformities in Upper Jurassic-Lower Cretaceous carbonates in northeast Turkey; geodynamic and hydrocarbon implications. *Marine and Petroleum Geology*, Vol. 91, 2018a, pp. 639-657.
- Vincent S.J., Saintot A., Mosar J., Okay A.I., Nikishin A.M. Comment on "Relict basin closure and crustal shortening budgets during continental collision: An example from Caucasus sediment provenance" by Cowgill et al. (2016). *Tectonics*, Vol. 37, 2018b, pp.1006-1016.
- Weber V. Shamakhi earthquake of 13 February 1902. In Proceedings of the St. Petersburg geological committee, 1903, 65 p.
- Yetirmishli G.J., Kazimov İ.E., Kazimova A.F. Modern seismo-geodynamics of Turkey, northern Iran and Caucasus region. Seismoprognoz observations in the territory of Azerbaijan, V. 25, No.1, 2024, pp. 25-36, <https://doi.org/10.59849/2219-6641.2024.1.25>.
- Yetirmishli G.J., Kazimov İ.E., Kazimova A.F. Seismogeodynamics of the Greater Caucasus from GNSS data. Seismoprognoz observations in the territory of Azerbaijan, Vol. 24, No. 2, 2023, pp. 33-42, <https://doi.org/10.59849/2219-6641.2023.2.33>.
- Адамия Ш.А. Механизм и геодинамика формирования альпийских складчатых поясов Кавказа. Проблемы движений и структурообразования в земной коре и верхней мантии. Наука. Москва, 1985, с. 72-89.
- Ализаде А.А., Ахмедбейли Ф.С., Ахмедбейли Ф.Ф. и др. О глубинном строении Кусаро-Дивичинского наложенного прогиба. Доклады АН Азербайджанской ССР. Т. 38, №. 1, 1982, с. 52-57.
- Ализаде А.А., Ахмедов Г.А., Ахмедов А.Н., Куликов В.И., Раджабов М.М., Терешко А.Д. Глубинное строение земной коры Азербайджана и прилегающих районов Среднего и Южного Каспия. Известия АН Азербайджанской ССР, Серия наук о Земле, №. 5, 1968, с. 14-26.
- Афанасенков А.П., Никишин А.М., Обухов А.Н. Геология восточной части Черного моря. Научный мир. Москва, 2007, 210 с.
- Ахмедбейли Ф.С. Региональная сейсмичность территории Азербайджана в связи с тектонической активностью центрального сегмента Альпийско-Гималайского пояса. Труды ИГ НАН Азербайджана, 2001, №. 29, с. 40-46.
- Ахмедбейли Ф.С., Бабазаде О.Б., Гасанов А.Г., Кулиев Ф.Т., Панахи Б.М., Шихалибейли Э.Ш. Новые схемы районов очагов сильных землетрясений и сейсмического районирования территории Азербайджана. Каталог сейсмологических наблюдений по Азербайджану за 1987 год. Элм. Баку, 1991, с. 62-65.
- Баранов Г.И., Греков И.И. Геодинамическая модель Большого Кавказа. В: Проблемы кавказской геодинамики. Наука. Москва, 1982, стр. 51-59.
- Белоусов Т.П., Шолохов В.В., Энман С.В. Геодинамика и сейсмотектоника Ставропольского края. ОИФЗ РАН. Москва, 2000, 184 с.
- Бунин Г.Б. О сейсмогенном оползне на мысе Бойнак в прибрежной части Дагестана. Сейсмичность и сейсмотектоника Восточного Предкавказья. Труды ИГ Даг. ФАН СССР, Махачкала, Т. 33, 1985, с. 65-68.
- Гаджиев Р.М. Глубинное геологическое строение Азербайджана, Азернецир. Баку, 1965, 200с.
- Копп М.Л. Структуры латерального выжимания в Альпийско-Гималайском коллизионном поясе. Научный мир. Москва, 1997.
- Коркуганова Н.И. Неогеново-четвертичная тектоника и геодинамические условия формирования орогенов в Восточной Евразии. Изд-во МГУ. Москва, 2000, 160 с.
- Макарова Н.В., Коркуганова Н.И., Макаров В.И. Морфологические типы орогенов как индикаторы геодинамических условий их формирования и развития. Геоморфология, №. 21, 2000, с. 14-26.
- Милановский Е.Е., Хайн В.Е. Геологическое строение Кавказа. Издательство МГУ. Москва, 1963, 357 с.
- Муратов М.В. (ред.) Геология СССР. Т. VIII. Крым. Ч. 1. Геологическое описание. Недра. Москва, 1969.
- Никитин М.Ю., Никонов А.А., Болотов С.Н., Беляков Г.А. Палеосейсмодислокации в бассейне реки Ардон и их значение для оценки сейсмического потенциала Большого Кавказа. ДАН, Т. 330, №. 6, 1993, с. 740-744.
- Никонов А.А. Палеосейсмодислокации в осевой части Главного Кавказского хребта (ПрЭльбрусье). Доклады Академии наук СССР, Т. 319, №. 5, 1991, с. 1183-1186.
- Овсяченко А.Н., Мараханов А.В., Ларьков А.С., Новиков С.С. Позднечетвертичные дислокации и сейсмотектоника очага землетрясения Рача (Большой Кавказ). Геотектоника, 2014, №. 6, с. 55-76.
- Рогожин Е.А., Овсяченко А.Н., Лутиков А.И., Собисевич А.Л., Собисевич Л.Е., Горбатиков А.В. Эндогенные опасности Большого Кавказа. ИФЗ РАН. Москва, 2014, 256 с.
- Флоренсов Н.А. О неотектонике и сейсмичности Монголо-Байкальской горной области. Геология и геофизи-

- Yetirmishli G.J., Kazimova S.E. Walker R.T., Pierse İ., Kazimov İ.E. The first results of paleoseismological studies between Oxford University and Republican Seismic Survey Center of ANAS. Seismoprognoz observations in the territory of Azerbaijan, Vol. 22, No. 2, 2022, p. 3-8.
- Zhang H., Aldana-Jague E., Clapuyt F., Wilken F., Vanacker V., Van Oost K. Evaluating the potential of post-processing kinematic (PPK) georeferencing for UAV-based structure-from-motion (SfM) photogrammetry and surface change detection. Earth Surface Dynamics, Vol. 7(3), 2019, pp. 807-827, <https://doi.org/10.5194/esurf-7-807-2019>.
- Хайн В.Е. Региональная геотектоника: Альпийский средиземноморский пояс. Недра. Москва, 1984.
- Хайн В.Е., Ализаде Ак.А. Геология Азербайджана. Том VI. Тектоника, Нафта-Пресс. Баку, 2005, 506 с.
- Хромовских В.С., Солоненко В.П., Семёнов Р.М., Жилкина В.М. Палеосейсмогеология Большого Кавказа. Наука. Москва, 1979, 188 с.
- Шебалин Н.В. Оценка сейсмической интенсивности. Сейсмическая шкала и методы измерения сейсмической интенсивности. Наука. Москва, 1975, с. 87-109.

ПАЛЕОСЕЙСМОЛОГИЧЕСКИЕ ИССЛЕДОВАНИЯ В ПЛЕЙСТОСЕЙСМИЧЕСКОЙ ОБЛАСТИ ШАМАХИНСКИХ ЗЕМЛЕТРЯСЕНИЙ 1668 И 1902 ГГ.

Пирс И.¹, Гулиев И.С.², Етирмишли Г.Дж.³, Казимова С.Э.³, Уолкер Р.¹,
Казимов И.Э.³, Абдуллаев Н.Р.², Джонсон Б.¹, Маршалл Н.¹

¹Оксфордский университет, Великобритания

²3 S Паркс Роуд, Оксфорд
Президиум Национальной академии наук Азербайджана, Азербайджан
Ул. Истиглалият, 30, Баку, AZ1001

³Республиканский центр сейсморазведки Национальной академии наук Азербайджана, Азербайджан
123, просп. Гусейна Джавида, Баку, AZ1141

Резюме. Кавказский регион, расположенный на стыке Евразийской и Аравийской тектонических плит, является важной зоной для понимания процессов континентальных столкновений и их влияния на сейсмическую активность. Целью работы является анализ тектонических процессов региона, сейсмической истории и рисков, связанных с возможными сильными землетрясениями. В исследовании использованы современные методы, включая спутниковую съемку, данные GNSS, моделирование с помощью дронов и палеосейсмическое зондирование. В период с апреля по май 2022 года команда ученых из Оксфордского университета совместно с молодыми исследователями из РЦСС провела первые полевые геологические исследования, направленные на изучение палеосейсмологии и активных тектонических процессов в Азербайджане. Были проанализированы две траншеи. Одним из ключевых результатов исследования стало выявление активных разломов, таких как разлом Агсу, и обнаружение следов поверхностных нарушений, связанных с историческими землетрясениями. Было обнаружено два зарегистрированных события сдвига по поверхности (1713–1895 и 1872–2003), вероятно, связанны с поверхностными смещениями, вызванными историческими землетрясениями 1668 и 1902 годов, которые нанесли значительный ущерб городу Шемаха. По результатам нашей переоценки магнитуда землетрясения 1902 года, его величина могла достигать Mw 7.4, в то время как ранее она оценивалась как M 6.9. Кроме того, во второй траншее, расположенной в 60 км к западу от Агсу, недалеко от города Гёйчай, были получены свидетельства поверхностного сдвига, вызванного землетрясением, произошедшим между 334 и 118 гг. до н.э., а также указания на еще одно возможное событие, произошедшее за последние 2000 лет. Работа подчеркивает важность дальнейших полевых исследований для более точного уточнения длины разломов, оценки магнитуд исторических землетрясений и уточнения карт сейсмических рисков в регионе.

Ключевые слова: палеосейсмические траншеи, землетрясение в Шемахе 1902 года, складчато-надвиговый пояс Куры, спутниковые снимки, моделирование с помощью дронов, модель последовательности OxCal, поверхностные сдвиги

1668-CI VƏ 1902-CI İLLƏRİN ŞAMAXI ZƏLZƏLƏLƏRİNİN PLEİSTOSESİMİK BÖLGƏSİNDE PALEOSEYSMOLOJİ TƏDQİQATLAR

Pirs İ.¹, Quliyev İ.S.², Yetirmişli Q.C.³, Kazimova S.E.³, Uolker R.¹,
Kazimov İ.E.³, Abdullayev N.R.², Conson B.¹, Marşal N.¹

¹Oxford Universiteti, Böyük Britaniya

²3 S Parks Road, Oksford

²Azərbaycan Milli Elmlər Akademiyasının Rəyasət Heyəti, Azərbaycan
İstiqlaliyyət küç, 30, Baki, AZ1001

³Azərbaycan Milli Elmlər Akademiyasının Seysmik Kəşfiyyat Mərkəzi, Azərbaycan
123, Hüseyn Cavid prospekti, Baki, AZ1141

Xülasə. Bu tədqiqat Böyük Qafqaz regionunun geodinamik şəraitinin təhlilinə həsr olunmuşdur. Diqqət tarixi seysmikliyə, aktiv qırımlara və gölçəkədə baş verə biləcək seysmik hadisələrə yönəlmışdır. Avrasiya və Ərəb tektonik plitələrinin qoşlaşğında yerləşən Qafqaz regionu qıtə toqquşmalarının və onların seysmik fəallığa təsirinin öyrənilməsi baxımından mühüm əhəmiyyətə malikdir. Orogen zonaları ilə bağlı geniş tədqiqatlara baxmayaraq, Böyük Qafqaz kimi dağ sistemlərinin morfoloji xüsusiyyətləri əlavə araşdırma tələb edir. Tədqiqatın məqsədi regiondakı tektonik prosesləri, seysmik tarixi və güclü zəlzələlərlə bağlı riskləri təhlil etməkdir. Tədqiqat zamanı peyk görüntüləri, GNSS məlumatları, dron vasitəsilə modelləşdirmə və paleoseysmik tədqiqatlar daxil olmaqla müasir metodlardan istifadə olunmuşdur. 2022-ci ilin aprel-may aylarında Oksford Universitetinin alımları və RSSX-dən olan gənc tədqiqatçılar Azərbaycanda paleoseysmologiya və aktiv tektonik proseslərin öyrənilməsinə yönəlmüş ilk sahə geoloji tədqiqatlarını həyata keçirmişlər. İki qazılmış xəndək analiz olunmuşdur. Əsas nəticələrdən biri Ağsu qırılması kimi aktiv qırılmanın müəyyən olunması və tarixi zəlzələlərlə əlaqəli səthi qırılma izlərinin aşkarlanması olmuşdur. İki səthi qırılma hadisəsi (1713–

1895 və 1872–2003) qeydə alınmışdır və bunlar çox güman ki, 1668 və 1902-ci illərdə baş vermiş, Şamaxı şəhərinə ciddi ziyan vurmuş zəlzələlərlə əlaqəlidir. 1902-ci il zəlzələsinin yenidən qiymətləndirilməsi nəticəsində onun maqnitudasının əvvəlki M=6.9 dəyəri ilə müqayisədə Mw=7.4-ə qədər çata biləcəyi müəyyən edilmişdir. Bundan əlavə, Ağsu şəhərindən 60 km qərbdə, Göyçay yaxınlığında yerləşən ikinci xəndəkdə eramızdan əvvəl 334–118-ci illər arasında baş vermiş səthi qırılma zəlzələsinin sübutları, həmçinin son 2000 il ərzində baş vermiş ola biləcək başqa bir hadisənin əlamətləri müəyyən edilmişdir. Bu tədqiqat regionda fayların uzunluğunu dəqiqləşdirmək, tarixi zəlzələlərin maqnitudasını qiymətləndirmək və seysmik risk xəritələrinin dəqiqləşdirilməsi üçün gələcək sahə tədqiqatlarının vacibliyini vurğulayır.

Açar sözlər: paleoseysmik xəndəklər, 1902 Şamaxı zəlzələsi, Kür üstəgəlmə-sixılma zolağı, peyk görüntüləri, dron modelləşdirilməsi, OxCal ardıcılıq modeli, səthi qırılma

APPLICATION OF MACHINE LEARNING METHODS AND NEURAL NETWORKS IN THE OBJECTIVES OF LITHOFACIES MAPPING AND RESERVOIR PROPERTIES ASSESSMENT: ANALYSIS AND SELECTION OF METHODS

Abetov A.E.¹, Seitzhanov A.K.², Samenov Ye.R.¹

¹Satbayev University, Kazakhstan

22, Satpayev Str., Almaty, 050013

²Kazakh-British Technical University, Kazakhstan
59, Tole Bi Str., Almaty, 050000: ansar.seitzhanov.98@mail.ru

Keywords: artificial intelligence, machine learning, classification of geological problems, linear and polynomial regression, clusterization of lithofacies, reservoir properties

Summary. The paper discusses the application of artificial intelligence (AI) methods to address challenges in lithofacies mapping and the assessment of reservoir properties. The choice of an AI method depends on the nature of the data, objectives of the study (such as classification, regression, clustering, or image segmentation), and requirements on the final interpretation and modeling results. An analysis of various machine learning (ML) algorithms including the support vector machine (SVM), random forest (RF), neural networks, etc. were conducted. Evaluated effectiveness of each method was evaluated on the basis of open-source data and geological datasets. Advantages and disadvantages of these methods were analyzed and factors influencing on the selection of an appropriate AI method were identified. Classification of geological problems and corresponding AI methods, encompassing SVM, RF, linear and polynomial regression, k-means clustering, hierarchical clustering, and convolutional neural networks (CNN) were presented. The article also introduces open-source ML platforms such as TensorFlow, PyTorch, and Keras along with factors influencing on the selection of the optimal AI method for lithofacies analysis and reservoir property assessment. Recommendations to select the most suitable AI methods for specific objectives were provided. The importance of data volume and quality in selection of AI method and prevention of model overfitting was emphasized.

© 2025 Earth Science Division, Azerbaijan National Academy of Sciences. All rights reserved.

1. Introduction

In modern petroleum geology, where data volume increases exponentially, artificial intelligence (AI) becomes an essential tool to solve complex problems. Traditional methods based on the interpretation and modeling of field and well geophysical data, as well as laboratory studies of core, cuttings, and fluid properties are usually labor-intensive, time-consuming, subjective, and limited in their ability to process massive data.

The labor intensity and time consumption are determined by: a) the level of professional expertise of specialists, the availability of equipment, methodological complexes, and software; b) insufficient flexibility of workflows; c) the necessity to write additional scripts for software to optimize the process.

Subjective limitations are determined by: a) overestimated expectations from clients and/or insufficient competence of the performers; b) the need to configure machine learning (ML) based on the results of "expert" training. The system will not cre-

ate something entirely new; it will attempt to replicate the expert's solution. This is relevant while considering the specifics of commercial software.

Limited capabilities to process big data sets addressed as positive ML use cases emerge. The advanced software already incorporates «Python» as one of the programming modules/languages, which has significantly expanded their capabilities.

According to the Technological Research of KPMG (2025), AI in Central Asia and the Caucasus is not yet a priority technology for most companies. Only 17% of organizations actively use AI, while 29% face insufficient management support and investment constraints, which hinders its implementation.

Moreover, only 44% of companies in Central Asia and the Caucasus plan to implement AI for automating routine targets and improving employee productivity. This indicates a growing interest in using AI as a tool for optimizing operational processes and reducing costs. Additionally, 36% of or-

ganizations aim to apply AI for developing new products and services highlighting its role in maintaining competitive advantage and stimulating innovation (KPMG, Caucasus and Central Asia, 2025).

In this context, increasing attention was paid to the application of AI methods, which have the ability to rapidly process big data and identify patterns opening new opportunities for more accurate, efficient, and objective forecasting of oil and gas potential in exploration targets. Of particular relevance is the use of AI to solve objectives related to lithofacies mapping and the assessment of reservoir properties, which play a key role in success of geological exploration in any oil and gas prospective region.

Therefore, the goal of this study was to analyze and determine the capabilities of AI methods for solving lithofacies mapping and reservoir property assessment targets, with a focus on their practical application based on a comprehensive analysis of available archival and published data and requirements for the results.

An important role in this process was played by the analysis and selection of optimal AI methods depending on specific targets and data characteristics. Significant attention was given to the correctness of the initial data, the algorithms of their preparation, and the configuration of models. This is particularly relevant since not all objectives have been fully resolved, especially when it comes to deep convolutional networks. To overcome the identified challenges, it recommended to empirically assembling such networks to address the following objectives:

- Review of existing AI methods applied in petroleum geology for lithofacies mapping and the assessment of reservoir properties.
- Classification of AI methods based on the types of objectives to solve and their functionality.
- Determination of criteria to select the optimal AI method depending on the nature of the data, research objectives, available resources, and requirements for the interpretability of results.
- Analysis of examples of successful applications of AI methods in oil and gas industry.

2. Research methods and data

The modern world of AI in petroleum geology characterized by openness and active exchange of ideas. There are numerous open-source ML platforms to create AI systems, such as TensorFlow, PyTorch, Keras, MxNet, CNTK, Caffe, Paddle, Scikit-learn, and Weka, which significantly simplify and accelerate the process of interpretation and modeling geological, geophysical, and field data (Ng, 2023).

For example, Keras is a software interface or library that allows building deep networks and simplifies working with the core functions of TensorFlow

making them more user-friendly and accessible. It provides high-level abstractions, automates routine processes, and reduces the complexity of writing code while retaining the full power and flexibility of the original framework ([Keras.io/](https://keras.io/)).

Scikit-learn is a library for data processing. It can solve most objectives in conjunction with Pandas. Pandas is a Python software library for data processing and analysis (Scikit-learn official documentation).

In addition to ML, there are nonlinear neural networks that enable inverse-predictive modeling during the integrated interpretation of seismic, drilling, and other data. In such cases, big data allow the use of more complex algorithms, which require a significant number of examples of training.

In these scenarios, it is crucial to consider the issue of model overfitting, a common problem in ML where the model "memorizes" the training data too well, including noise and random deviations, instead of identifying general patterns in the real geological environment. As a result, such a model performs excellently on the training dataset but poorly on new data (Easyoffer.ru/question/5440).

Combating overfitting is a classic step in tuning ML algorithms. Through a Pipeline (an automated data processing workflow that includes collection, cleaning, transformation, model training, and result evaluation), the data samples obtained after the analytical stage are divided into tuning and blind test sets. The tuning dataset were divided for internal cross-validation. This helps prevent overfitting, as only the parameters that yield the best results according to the search metric are selected during the model tuning phase, discarding the overfitting stage.

The problem of model overfitting due to insufficient data (Easyoffer.ru/question/5440) can also be addressed by applying regularization methods, such as ridge regression. Regularization introduces a penalty term into the loss function of the model reducing its tendency to overfit. Essentially, ridge regression implements L2-regularization. This penalty term limits the magnitude of the model's parameters by minimizing their squared values, thereby reducing model complexity and enhancing its generalization ability (Hastie et al., 2009). This approach becomes particularly important in situations with limited data availability, which is typical for many studies where the existing information is often insufficient to build reliable models

In addition to traditional neural networks, a new type of neural network based on the Kolmogorov-Arnold mathematical theorem (Kolmogorov-Arnold network – KAN) for representing multivariate functions gains popularity. According to this theorem, any continuous function of several variables can rep-

resent as a superposition (composition) of continuous functions of one variable followed by an addition operation (Simplified explanation of the new Kolmogorov-Arnold network from MIT, 2024).

Due to the improved approximation and interpretability, KAN can be used for: a) building models that classify lithofacies and reservoir properties based on well logging and seismic data; b) identifying complex relationships between geophysical parameters and lithofacies types.

At the same time, the choice of the optimal AI method or methods for lithofacies analysis and the assessment of reservoir properties determined by a combination of factors related to the nature of the data, research objectives, available resources, and interpretation requirements.

Data presented as numerical arrays (e.g., well logging values, results of core and thin section laboratory analyses, seismic data, electrical, gravity, and magnetic survey data) play a key role in selection of the AI method.

The methodology of the conducted research involves the analysis and selection of AI methods based on the following factors:

- Nature of the data (type, volume, quality).
- Research objectives (classification, regression, clustering, image segmentation).
- Requirements for the interpretability of results.
- Available resources.

This article provides an overview of modern methods to apply AI in lithofacies analysis and the assessment of reservoir properties. Various approaches based on ML, neural networks, and other AI algorithms are discussed.

3. Research results

In the practical assessment of lithofacies and reservoir properties, data from seismic surveys, well logging, and laboratory core studies (petrophysical properties, lithological descriptions), as well as geological data on the study area, are used.

Next, the presented overview of ML methods was applied to solve various geological targets. The methods were classified by their functionality with a brief description of their essence and geological examples.

Various ML algorithms can be used to solve the objectives, such as:

- **Support Vector Machines (SVM):** Effective for classification and regression in complex environments. Classification was performed: a) based on anomalies on geophysical maps; b) at separating rock samples into different types based on geochemical, petrographic, or geophysical data; c) determining the probability of

hydrocarbon presence based on geological, geochemical, and field data.

- **Random Forest (RF):** An ensemble of decision trees that provides high accuracy and resistance to overfitting by using random subsets of features and training data for each case.
- **Neural Networks:** Capable of approximating complex nonlinear relationships using inversion techniques to calculate the contrast volume of geophysical parameters around the target layer improving the correlation of target parameters.

The prediction procedure consists of two stages:

- 1) Training: The stage of training neural networks using paired input data (attributes of potential geophysical fields and sets of map values in sliding windows) with the calculation of optimal neural network coefficients by minimizing the objective function;
- 2) Computation: The stage of calculating the attribute of potential geophysical fields based on a set of the given maps.

The output includes maps of standard deviation P10, P50, and P90 (pessimistic, realistic, and optimistic forecasts). This approach considered valid when dealing with a discrete parameter, such as reservoir/non-reservoir. In this case, the model outputs a probability. Subsequently, the probability distribution can be converted into an array indicating the presence or absence of a reservoir, based on a defined threshold value.

However, if the parameter is continuous, the solution search will rely on the standard approach of minimizing the residual functional of multiple variables.

Artificial Neural Network (ANN): Consists of multiple interconnected "neurons" organized in layers. It is capable of approximating complex nonlinear relationships between input and output data.

- Convolutional Neural Networks (CNN): Well-suited for processing seismic data to identify structures and classify rock types.
- Recurrent Neural Networks (RNN): Used for processing sequential data to identify patterns, such as modeling changes in mineral concentrations.
- Generative Adversarial Networks (GAN): Used for generating new data. GANs can be employed to create realistic three-dimensional models of mineral deposits (Introduction to machine learning, 2019).

When applied to solving practical issues in petroleum geology, the aforementioned ML and neural network methods should consider the specific geological environment in each case. For example, the subsalt carbonate of the Precaspian depression (including its southeastern board) is the primary targets

for hydrocarbon production. These sediments are characterized by high heterogeneity and complex structures including widespread fracturing making them one of the most challenging objectives for traditional analysis methods.

Nevertheless, modern ML algorithms, such as SVM, RF, ANN, CNN, RNN, and GAN enable effective solutions to classification, regression, and modeling targets in complex fractured environments.

For instance, in studies of carbonate reservoirs, ANNs were used to predict the distribution of fracturing based on seismic inversion data. The model improves the correlation between geophysical parameters and actual fracturing data obtained from core samples. Of particular importance is the ability to analyze the orientation, density, and size of fractures, which is crucial to comprehend the filtration properties of reservoirs.

Neural Network Learning

The fundamental element of neural networks is the "mathematical neuron" or perceptron. This is a simplified mathematical model of a biological neuron, which forms the basis of ANN (Neural networks for beginners, 2023).

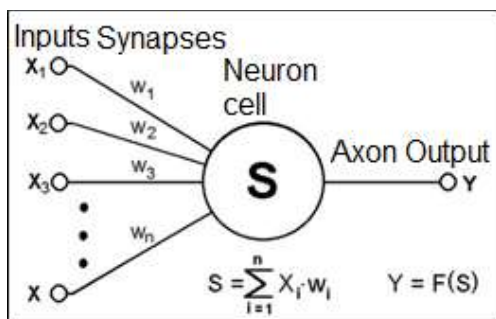


Fig. 1. Artificial neuron (Neural networks for beginners, 2023)

A neuron performs a nonlinear transformation of input signals. First, the values of the input signals

(x_i) multiplied by their corresponding weights (w_i). Then, the resulting products were summed. The result of this summation undergoes a nonlinear transformation using an activation function. The output of this transformation is the neuron's output signal (Neural networks. psy.wikireading, 2023).

In Fig. 2 the algorithm of lithofacies and reservoir properties evaluation were shown using Kolmogorov neural networks (Simplified explanation of the new Kolmogorov-Arnold network from MIT, 2024) based on seismic data with the application of deep networks (convolution and shifting are implemented within tensors). The activation function plays an independent role and was defined separately. Typically, this is a sigmoid function, where the perceptron's response can be determined as yes/no based on cutoff value of the activation function.

At the same time, it is important to consider that modern industry software already incorporates ML algorithms for calculating inversion based on seismic data, which produce an inversion cube as output. The primary focus should be on calibrating seismic and well data to enhance the resolution of seismic impedance.

KAN were used to approximate nonlinear relationships between input data (well logs and seismic attributes) and output parameters (lithology and reservoir properties). Cross-validation allows assessing how well the trained network will perform on new, previously unseen data and helps to prevent overfitting.

Fig. 3 shows a cross-plot comparing the results of calculating parameters such as PIMP (P-wave acoustic impedance), VP/VS (ratio of compressional to shear wave velocities), and porosity obtained using two different methods: the synchronous inversion algorithm (red curve) and ML algorithms (blue curve).

The comparison reveals that the results were obtained by the two methods align, but differences are observed, which attributed to the methodologies of the two approaches.

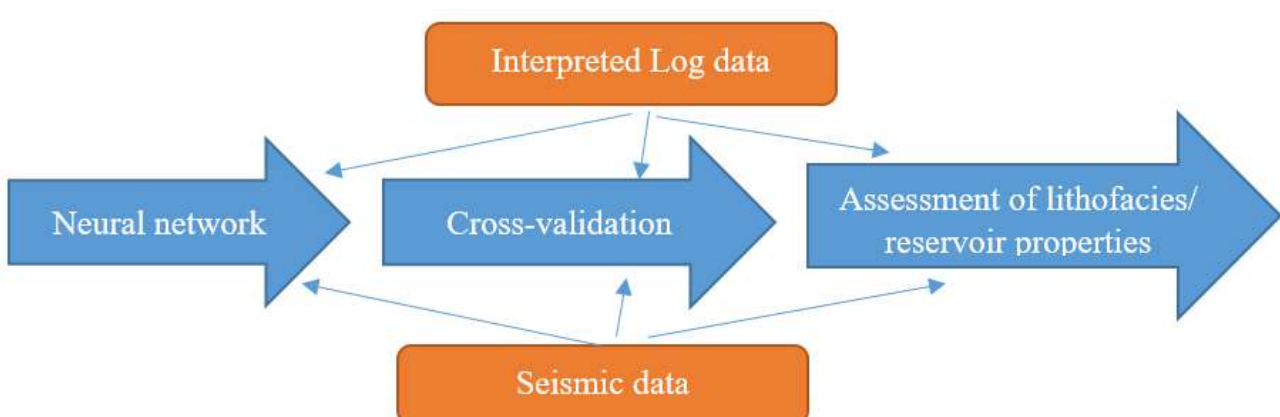


Fig. 2. Evaluation of lithofacies and reservoir properties using KAN (Simplified explanation of the new Kolmogorov-Arnold network from MIT, 2024)

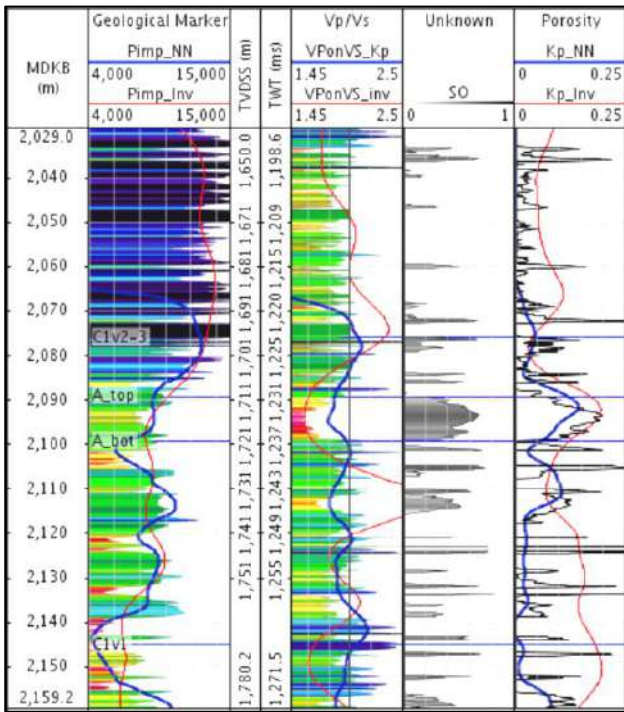


Fig. 3. Comparison of parameters calculated by the synchronous inversion algorithm (red curve) and ML algorithms (blue curve) with the original well logs (based on data from PGSK, 2025)

Synchronous inversion is based on physical models and requires precise knowledge of initial parameters, such as the acoustic properties of rocks and boundary conditions. It can be more sensitive to noise in the data and requires careful calibration.

ML uses data to train models that can identify complex nonlinear relationships not always explicitly described by physical equations. To mitigate these differences, cross-plotting across the entire dataset is necessary.

The article (Приезжев и др., 2023) describes the successful application of neural network prediction (using KAN) for creating geological models of hydrocarbon fields. In particular, upon completion of drilling Well 7, the predicted distribution of the reservoir was confirmed, which allowed refining the 3D model and optimizing drilling, thereby improving the economic efficiency of the project (see Fig. 4) (Приезжев и др., 2023).

A consolidated reservoir (characterized by a high degree of compaction and cementation, leading to the predominance of secondary porosity) identified using neural network prediction (highlighted contour on the upper cross-section), was confirmed by Well 7 (Приезжев и др., 2023).

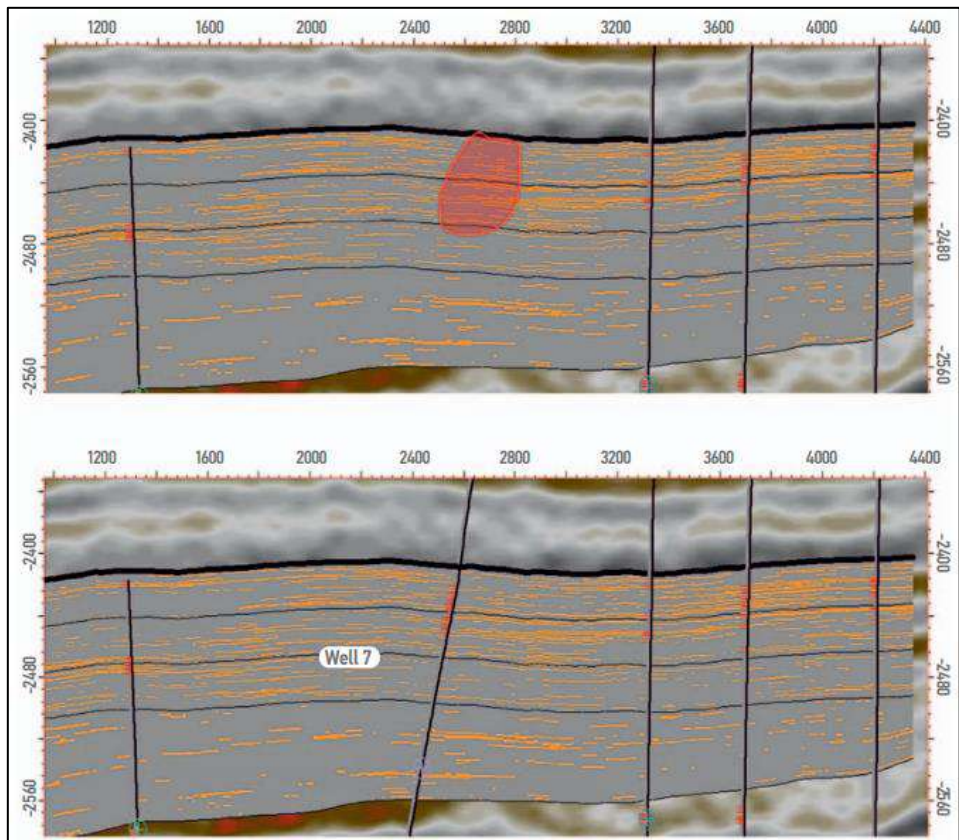


Fig. 4. Cross-section from the three-dimensional reservoir model- extracted using the neural network prediction methodology before drilling Well 7 (top), and the updated model after drilling Well 7 (bottom) (Приезжев и др., 2023)

The possibility of comparing the net pay of the model (H_{eff} model) and the net pay determined from well logging data (H_{eff} logging) exists, but it requires a comprehensive approach.

To compare H_{eff} model and H_{eff} logging, it is necessary to calibrate the model based on well logging data. This involves comparing calculated values with real data and adjusting model parameters such as porosity, permeability, and saturation. An important step is the construction of petrophysical relationships that associate parameters measured in wells with logging data. For example, the relationship between acoustic impedance and porosity allows refining the model and improving its alignment with real data (Добрынин, 2009).

In the study (Priezzhev et al., 2019), a method for analyzing seismic facies was proposed using 3D Kohonen neural networks. This approach enables the establishment of complex, nonlinear relationships between various parameters of seismic traces. Optimization of the classification process was achieved through the application of ML and self-organizing maps (SOM). RGB blending of 1D, 2D, and 3D projections were used to visualize the results, which helps identify relationships between classes and obtain a more accurate geological interpretation based on well data and analogs (Priezzhev et al., 2019).

RGB blending is a data visualization method in which three different parameters or datasets were displayed as color channels (red, green, and blue) to create the integrated image (Браун, 2011).

According to the article (Колбикова, 2021), the tuning of the cluster model was carried out in several stages which allows solving objectives related to lithotype classification and saturation prediction. Initially, a model was created to group limestones based on their ability to hand over oil. Then, a more detailed model to distinguish various rock types was developed using well logging and core data. Accordingly, the statistical algorithm Multi-Resolution Graph-based Clustering (MRGC) was applied, which associates geophysical data to rock type. This method is based on comparing new data with known examples and takes into account various rock characteristics. As a result, five main rock types including two reservoir types were identified (Колбикова, 2021).

In the paper (Merembayev et al., 2021), the assessment of lithofacies was studied using ML algorithms of geological data from Kazakhstan and Norway. ML methods such as k-nearest neighbors (kNN), decision trees, RF, XGBoost, and Light GBM both with and without wavelet transformation of the data were considered. Input data of the ML models include gamma ray, acoustic and neutron logs, etc. (Merembayev et al., 2021).

For the evaluation of lithofacies and reservoir properties in the southeastern board of the Precaspian Basin, it is advisable to use a comprehensive approach combining various AI methods considering the complexity of the region's geological structure.

For lithofacies classification, where high accuracy and resistance to overfitting are required, methods such as RF are most suitable. SVM and neural network learning are recommended to assess reservoir properties, where the ability to approximate nonlinear relationships is important.

However, any ML method is resistant to overfitting, and this is achieved within the basic "workflow." In this case, the key factor is the balance between accuracy and computation time. The calculations can be performed on different models followed by selecting the one that best solves the problem considering limitations on accuracy and time. To enhance the robustness of the calculations, a "voting" model can be applied, incorporating several different models.

For example, as it is noted above, the Upper Paleozoic fractured carbonate reservoirs in the southeastern Precaspian Basin is characterized by high heterogeneity due to the presence of secondary porosity (fractures, vugs, and leaching channels). Analyzing such reservoirs requires a method capable of accounting for spatial variability and identifying lithological and facies features.

The most suitable AI method for solving these targets is CNN, which can effectively process seismic data and well logs, enabling the identification of fracture systems and vuggy intervals that play a key role in the formation of the filtration and storage properties of productive reservoirs.

Based on the analysis of inversion results and neural network learning with actual well data, it was established that neural network learning demonstrates convergence in absolute values and possesses high resolution. This is due to the consideration of nonlinear transformations that neural networks can effectively be modeled. The use of a nonlinear operator based on neural networks and evolutionary algorithms provides the following advantages:

- The model has the ability to establish nonlinear relationships between heterogeneous types of data significantly improving the accuracy of interpretation and prediction of characteristics of set of geological objects, such as fractured carbonate reservoirs, where traditional methods may not account for complex interrelationships between lithological, textural, and structural features of rocks.
- The model automatically adapts to various types of input data and conditions, increasing its efficiency.

Automatic tuning of model parameters contributes to achieving optimal results, i.e., obtaining hyperparameters. The search for these defined by an iterative solution search code based on gradient descent – this is part of the workflow in model tuning.

Gradient descent, or the gradient descent method is a numerical method for finding the local minimum or maximum of a function by moving along the gradient, and it is one of the primary numerical methods in modern optimization (Scikit-learn official documentation)

4. Discussion

For the subsalt reservoirs of the southeastern Precaspian Depression, as it is noted above, the most suitable methods for assessing lithofacies and reservoir properties are SVM and RF.

Both methods exhibit high sensitivity to noise, which is crucial for processing geophysical data that usually contain interference. They also have medium computational complexity (Table 1) making them accessible for processing.

An important factor is that both methods are well-adapted for processing, interpreting, and modeling geological sections including seismic sections, which play a key role in studying the Precaspian Depression.

In addition, RF also exhibits resistance to overfitting, which is a significant advantage while working with limited data. Overall, the choice between SVM and RF depends on the specific task and avail-

able resources. If high classification accuracy is required, RF may be preferable. Another advantage of RF is that it does not require data standardization.

If speed is important, SVM may be more suitable.

The application of neural network learning in the southeastern board of the Precaspian Depression can demonstrate its effectiveness due to its ability to account for nonlinear relationships between seismic fields and parameters measured in wells.

The main factors contributing to the advantages of neural networks include:

- Accounting for nonlinear distortions: Neural networks can model nonlinear dependencies. This is particularly important in geological settings where salt structures, fault zones, and other distorting factors are present.
- Absence of theoretical limitations: Neural networks do not require strict theoretical frameworks to handle nonlinear distortions making them more versatile.

However, neural networks are just one group among many ML methods and do not always yield the best results. In such cases, it is necessary to adopt a comprehensive approach, i.e., seismic data and well measurements to build a high-frequency model, which significantly enhances resolution and prediction accuracy.

The tasks addressed using AI in lithofacies analysis can be divided into several main categories, as presented in Table 2.

Comparison of characteristics of AI methods (Shamaev, 2022)

AI method name	Computational complexity	Amount of data required for training	Sensitivity to noise	Suitability for processing 2D geophysical data
SVM	Medium	Small	High	Medium
Relevance Vector Machines	High	Small	Low	Medium
Decision Tree	Medium	Medium	High	Medium
RF	Medium	Medium	High	Medium
Genetic Algorithms	High	Not Required	Low	Poor
Gaussian Process Regression	Medium	Small	Medium	Poor
kNN	Low	Medium	Low	Poor
Logistic Regression	Medium	Medium	Low	Poor
Ridge Regression	Medium	Medium	Medium	Medium
Jackknife Regression	Medium	Medium	Medium	Medium
ANN (CNN, RNN, GAN)	High	Medium	Low	Good

Table 2
Categories of tasks solving using AI

Task/Function	Objective	Methods
Facies / lithofacies classification	Assigning rocks to specific facies types based on available data (lithological, geophysical, petrophysical).	<ul style="list-style-type: none"> SVM – effective for classifying complex data, handles nonlinear class boundaries well. RF – ensemble of decision trees, resistant to overfitting and noise, provides good classification accuracy. Naive Bayes Classifier – simple and fast method, works well on data with independent features.
Regression for reservoir property estimation	Estimating quantitative reservoir properties (porosity, permeability, oil saturation) based on available data.	<ul style="list-style-type: none"> Linear Regression – method used to establish a linear relationship between variables. Polynomial Regression - An extension of linear regression, allowing modeling of nonlinear relationships.
Clustering	Dividing a dataset into groups (clusters) based on similarity of their characteristics.	<ul style="list-style-type: none"> k-means – simple and popular method that divides data into k clusters by minimizing intra-cluster distance. Hierarchical Clustering – Builds a hierarchy of clusters, allowing analysis of data structure at different levels.
Image segmentation	Identifying regions in images corresponding to different minerals, pores, fractures, and other elements.	<ul style="list-style-type: none"> CNN: Architectures like U-Net, SggNet, and others – Show high effectiveness in image segmentation tasks.

Thus, the application of AI methods for lithofacies analysis and reservoir property assessment in the southeastern Precaspian Basin opens new opportunities for more accurate and efficient interpretation of geological, geophysical, and field data. However, the choice of a specific AI method requires careful analysis and consideration of several factors (accuracy, data completeness, and desired results).

6. Conclusions

The article analyzes the application of AI methods in solving objectives related to lithofacies mapping and reservoir property assessment of play zones, which is a highly promising direction capable of significantly improving the efficiency and accuracy of geological exploration. This facilitated by the diversity of AI methods, such as ML, neural networks, and genetic algorithms, which provide a wide range of tools for solving various objectives related to the analysis of geological, geophysical, and field data.

For facies and lithofacies classification, methods such as SVM, RF, and the Naive Bayes classifier are recommended. Regression methods, including linear and polynomial regression can be applied for reservoir property assessment.

A key aspect for ML methods is understanding the parameters to be worked with – whether they are continuous or discrete – and whether the applied algorithms have versions for both regression and classification.

Clustering, particularly k-means and hierarchical clustering also finds applications in geology.

For image segmentation, CNN are used, although the option of using other tools is not excluded.

Practical examples show that CNNs are effective for identifying fractures in rock masses due to their ability to process 2D geophysical data (Шамаев, 2022). For lithofacies classification goals based on well logging data, KAN can be useful due to their improved approximation and interpretability (Simplified explanation of the new KAN from MIT, 2024).

At the same time, it is necessary to check the sensitivity of models to their inputs and evaluate the importance of each variable in the optimized model. This verification was conducted using a separate library, which enhances the interpretability of most models.

For seismic facies analysis, effective methods such as 3D Kohonen neural networks were proposed, which allow establishing complex, nonlinear relationships between various parameters of seismic traces. Optimization of the classification process was achieved through the application of ML and SOM. Visualization of results using RGB blending of 1D, 2D, and 3D projections helps to identify relationships between classes and obtain a more accurate geological interpretation based on well data and analogs.

In summary, the most effective methods were recognized as SVM, RF, and neural networks for the southeastern board of Precaspian Basin.

- RF exhibits high resistance to overfitting and can handle high-dimensional data, making it useful for classification and prediction.

- Neural networks demonstrate high accuracy and resolution due to their ability to account for nonlinear distortions in seismic signals and dependencies between geophysical parameters.
- SVM have proven effective in lithofacies classification goals, especially in conditions of limited data volume and the presence of noise.

At the same time, it is important to note the integration of several AI methods, which enhances the accuracy of predicting reservoir properties and lithofacies.

Despite the obvious successes achieved, the application of AI in geology and geophysics remains a

relevant and promising direction with many issues requiring further study, understanding, and handling. The problems related to the interpretation of results, big data, training data, and the adaptation of existing methods to specific geological conditions are among these.

Nevertheless, it can be confidently stated that AI will continue to play an increasingly important role in geology contributing to the development of new approaches to subsurface exploration and providing more accurate and efficient solutions to objectives related to the search and exploration of mineral resources.

REFERENCES

- Brown A.R. Interpretation of Three-Dimensional Seismic Data. Translated from English. Society of Exploration Geophysicists (SEG). Moscow, 2011 (in Russian).
- Dobrynin V.M., Vendelstein B.Yu., Kozhevnikov D.A. Interpretation and modeling of geophysical data. Nedra. Moscow, 2009, 456 p. (in Russian).
- Easyoffer.ru. What is model overfitting. URL: <https://easyoffer.ru/question/5440> (accessed: 10.10.2023).
- Hastie T., Tibshirani R., Friedman J. The elements of statistical learning: Data mining, inference, and prediction. 2nd ed. Springer. New York, 2009, 745 p.
- Introduction to machine learning. URL: <https://habr.com/ru/post/448892/> (accessed: 3.09.2019) (in Russian).
- Keras: The Python Deep Learning API. Official Documentation. URL: <https://keras.io/>.
- Kolbikova E.S. Lithofacies analysis and prediction of properties based on geophysical and seismic data using machine learning methods.: Roxar Paradigm – Software and Solutions LLC. Moscow, 2021, 120 p. (in Russian).
- KPMG Caucasus and Central Asia. Technological Research 2024. KPMG. February 2025.
- Merembayev T., Kurmangaliyev B., Bekbauov B., Amanbek Ye. A comparison of machine learning algorithms in predicting lithofacies: Case studies from Norway and Kazakhstan. Energies. Vol. 14, No. 7, 2021, p. 1896, DOI: <https://doi.org/10.3390/en14071896>.
- Neural networks for beginners. Part 1. Habr. URL: <https://habr.com/ru/articles/312450> (accessed: 10.10.2023) (in Russian).
- Neural networks. Psy.Wikireading. URL: <https://psy.wikireading.ru/12215> (accessed: 10.10.2023) (in Russian).
- Ng A. Artificial Intelligence (AI) for Everyone. Deep Learning.AI. 2023, URL: <https://www.deeplearning.ai> (accessed: 10.10.2023).
- Prietzhev I.I., Taikulakov E.E., Kayumov I.L., Leonov A.V., Gorbach D.A., Miroshkin V.G., Ovechkina V.Yu. Direct neural network prediction of reservoir properties based on seismic data: A case study of clinoform deposits in Western Siberia. PRONeft. Professionalno o nefti, Vol. 8, No. 2, 2023, pp. 28-39, DOI: <https://doi.org/10.51890/2587-7399-2023-8-2-28-39> (in Russian).
- Prietzhev I. I., Veeken P. C. H., Egorov S.V., Nikiforov A.N., Strecker U. Seismic waveform classification based on Kohonen 3D neural networks with RGB visualization. First Break, Vol. 37, No. 2, 2019, pp. 37-43.
- Scikit-learn: Machine Learning in Python. Официальная документация. URL: https://scikit-learn.org/stable/user_guide.html.
- Браун А.Р. Интерпретация трехмерных сейсмических данных. Пер. с англ. Общество инженеров-геофизиков (SEG), Москва, 2011.
- Введение в машинное обучение. URL: <https://habr.com/ru/post/448892/> (дата обращения: 3.09.2019).
- Добрынин В.М., Вендельштейн Б.Ю., Кожевников Д.А. Интерпретация и моделирование геофизических данных. Недра. Moscow, 2009, 456 с.
- Keras: The Python Deep Learning API. Официальная документация. URL: <https://keras.io/>.
- Колбикова Е.С. Литофацальный анализ и возможности прогнозирования свойств по данным геофизических исследований и сейсморазведки методами машинного обучения. ООО «Роксар Парадайм – ПО и Решения». Москва, 2021, 120 с.
- KPMG Кавказ и Центральная Азия. Технологическое исследование 2024. KPMG. Февраль 2025.
- Нейронные сети для начинающих. Часть 1. Habr. URL: <https://habr.com/ru/articles/312450> (дата обращения: 10.10.2023).
- Нейронные сети. Psy.Wikireading. URL: <https://psy.wikireading.ru/12215> (дата обращения: 10.10.2023).
- Приезжев И.И., Тайкулов Е.Е., Каюмов И.Л., Леонов А.В., Горбач Д.А., Мирошкин В.Г., Овчакина В.Ю. Прямой нейросетевой прогноз коллекторских свойств пласта по данным сейсморазведки на примере клиноформных отложений Западной Сибири. PROНефть. Профессионально о нефти, Т. 8, №. 2, 2023, с. 28-39, DOI: <https://doi.org/10.51890/2587-7399-2023-8-2-28-39>.
- Шамаев С.Д. Применение методов искусственного интеллекта при обработке и интерпретации данных геофизических методов. Известия УГГУ, № 1 (65), 2022, с. 86-101.

ЛИТЕРАТУРА

- Easyoffer.ru. Что такое переобучение модели. URL: <https://easyoffer.ru/question/5440> (дата обращения: 10.10.2023).
- Hastie T., Tibshirani R., Friedman J. The elements of statistical learning: Data mining, inference, and prediction. 2nd ed. Springer. New York, 2009, 745 p.
- Merembayev T., Kurmangaliyev B., Bekbauov B., Amanbek, Ye. A comparison of machine learning algorithms in predicting lithofacies: Case studies from Norway and Kazakhstan. Energies. Vol. 14, No. 7, 2021, p. 1896, DOI: <https://doi.org/10.3390/en14071896>.
- Ng A. Artificial Intelligence (AI) for Everyone. Deep Learning.AI. 2023, URL: <https://www.deeplearning.ai> (дата обращения: 10.10.2023).
- Prietzhev I.I., Veeken P.C.H., Egorov S.V., Nikiforov A.N., Strecker U. Seismic waveform classification based on Kohonen 3D neural networks with RGB visualization. First Break, Vol. 37, No. 2, 2019, pp. 37-43.
- Scikit-learn: Machine Learning in Python. Официальная документация. URL: https://scikit-learn.org/stable/user_guide.html.
- Браун А.Р. Интерпретация трехмерных сейсмических данных. Пер. с англ. Общество инженеров-геофизиков (SEG), Москва, 2011.
- Введение в машинное обучение. URL: <https://habr.com/ru/post/448892/> (дата обращения: 3.09.2019).
- Добрынин В.М., Вендельштейн Б.Ю., Кожевников Д.А. Интерпретация и моделирование геофизических данных. Недра. Moscow, 2009, 456 с.
- Keras: The Python Deep Learning API. Официальная документация. URL: <https://keras.io/>.
- Колбикова Е.С. Литофацальный анализ и возможности прогнозирования свойств по данным геофизических исследований и сейсморазведки методами машинного обучения. ООО «Роксар Парадайм – ПО и Решения». Москва, 2021, 120 с.
- KPMG Кавказ и Центральная Азия. Технологическое исследование 2024. KPMG. Февраль 2025.
- Нейронные сети для начинающих. Часть 1. Habr. URL: <https://habr.com/ru/articles/312450> (дата обращения: 10.10.2023).
- Нейронные сети. Psy.Wikireading. URL: <https://psy.wikireading.ru/12215> (дата обращения: 10.10.2023).
- Приезжев И.И., Тайкулов Е.Е., Каюмов И.Л., Леонов А.В., Горбач Д.А., Мирошкин В.Г., Овчакина В.Ю. Прямой нейросетевой прогноз коллекторских свойств пласта по данным сейсморазведки на примере клиноформных отложений Западной Сибири. PROНефть. Профессионально о нефти, Т. 8, №. 2, 2023, с. 28-39, DOI: <https://doi.org/10.51890/2587-7399-2023-8-2-28-39>.
- Шамаев С.Д. Применение методов искусственного интеллекта при обработке и интерпретации данных геофизических методов. Известия УГГУ, № 1 (65), 2022, с. 86-101.

Simplified explanation of the new Kolmogorov-Arnold network from MIT. Habr. 2024. URL: <https://habr.com/ru/articles/817547> (accessed: 10.10.2023) (in Russian).

Упрощённое объяснение новой сети Колмогорова-Арнольда из МИТ. Набр. 2024. URL: <https://habr.com/ru/articles/817547> (дата обращения: 10.10.2023).

ПРИМЕНЕНИЕ МЕТОДОВ МАШИННОГО ОБУЧЕНИЯ И НЕЙРОННЫХ СЕТЕЙ В ЗАДАЧАХ КАРТИРОВАНИЯ ЛИТОФАЦИЙ И ОЦЕНКИ КОЛЛЕКТОРСКИХ СВОЙСТВ: АНАЛИЗ И ВЫБОР МЕТОДОВ

Абетов А.Е.¹, Сейтжанов А.К.², Семенов Е.Р.¹

¹Казахский национальный исследовательский технический университет имени К. И. Сатпаева, Казахстан
Ул. Сатпаева 22, Алматы, 050013

²Казахстанско-Британский Технический Университет, Казахстан
Ул. Толеби, 59, Алматы, 050000: ansar.seitzhanov.98@mail.ru

Резюме. В статье рассмотрены аспекты применения методов искусственного интеллекта (ИИ) для решения задач картирования лиофаций и оценки коллекторских свойств пород. При этом выбор метода ИИ зависит от характера данных, целей исследования (классификация, регрессия, кластеризация, сегментация изображений), требований к конечным результатам интерпретации и моделирования. Проведен анализ различных алгоритмов машинного обучения, таких как метод опорных векторов, случайный лес, нейронные сети и другие. Оценена эффективность каждого их перечисленных методов на основе открытых источников и геологических данных. Проанализированы их преимущества и недостатки, а также идентифицированы факторы, влияющие на выбор метода ИИ. Представлена классификация геологических задач и соответствующих методов ИИ, включая SVM, RF, линейную и полиномиальную регрессию, k-means, иерархическую кластеризацию и CNN. Представлены платформы машинного обучения с открытым исходным кодом, такие как TensorFlow, PyTorch и Keras, а также факторы, влияющие на выбор оптимального метода ИИ для лиофациального анализа и оценки коллекторских свойств. Предложены рекомендации по выбору оптимальных методов ИИ для решения конкретных задач. Подчеркнута важность объема и качества данных для выбора метода ИИ и предотвращения переобучения модели. Наибольшую результативность в условиях Юго-Восточного Прикаспия могут продемонстрировать метод опорных векторов, случайный лес и нейронные сети, каждый из которых обладает уникальными преимуществами. В работе отмечены ключевые проблемы, связанные с качеством исходных данных, интерпретируемостью результатов и адаптацией методов к конкретным геологическим условиям, а также переобучение. В обсуждении и заключении представлена информация касательно применения каждого метода машинного обучения под конкретные задачи и условия.

Ключевые слова: искусственный интеллект, машинное обучение, классификация геологических задач, линейная и полиномиальная регрессия, кластеризация лиофаций, коллекторские свойства

LİTOFASIYALARIN XƏRİTƏLƏNDİRİLMƏSİ VƏ KOLLEKTOR XÜSUSİYYƏTLƏRİNİN QİYMƏTLƏNDİRİLMƏSİ TAPŞIRIQLARINDA MAŞIN ÖYRƏNMƏSİ VƏ NEYRON ŞƏBƏKƏ METODLARININ TƏTBİQİ: METODLARIN TƏHLİLİ VƏ SEÇİMİ

Abetov A.E.¹, Seyidzhanov A.K.², Samenov E.R.¹

¹K. İ. Satpayev adına Qazax Milli Tədqiqat Texniki Universiteti, Qazaxistan
Satpayev küç., 22, Almatı, 050013

²Qazaxstan-Britaniya Texniki Universiteti, Qazaxistan
Tolebi küç., 59, Almatı, 050000: ansar.seitzhanov.98@mail.ru

Xülasə. Məqalədə süni intellekt (Sİ) metodlarının litofasiyaların xəritələşdirilməsi və səxurların kollektor xüsusiyyətlərinin qiymətləndirilməsində tətbiq imkanları araşdırılmışdır. Sİ metodunun seçimi məlumatların xarakterindən, tədqiqatın məqsədlərindən (təsnifat, regressiya, klasterləşmə, təsvirlərin seqmentasiyası), eləcə də interpretasiya və modelləşdirməyə qoyulan tələblərdən asılı olaraq müəyyən edilir. SVM, RF və CNN və digər maşın öyrənməsi alqoritməri təhlil olunmuşdur. Bu metodların effektivliyi açıq mənbəli məlumatlar və real geoloji verilənlər əsasında qiymətləndirilmiş, onların üstünlükleri və məhdudiyyətləri müəyyən edilmişdir. Süni intellekt metodlarının seçimini təsir edən əsas amillər müəyyənənləşdirilmiş və geoloji vəzifələrin təsnifatına uyğun metodlar təqdim edilmişdir. Bunlara SVM, RF, xətti və polinomial regressiya, k-means klasterləşməsi, iyerarxik klasterləşmə və konvolyusion neyron şəbəkələr (CNN) daxildir. TensorFlow, PyTorch və Keras kimi açıq mənbə kodlu maşın öyrənməsi platformaları təqdim olunmuş və litofasiyaların analizi ilə kollektor xüsusiyyətlərinin qiymətləndirilməsi üçün optimal metodun seçimini təsir göstərən amillər müzakirə edilmişdir. Müəyyən geoloji məsələlərin həlli üçün konkret metodlara dair tövsiyələr verilmişdir. Modelin həddindən artıq öyrədilməsi (overfitting) riskinin qarşısının alınması məqsədilə verilənlərin həcmi və keyfiyyətinin əhəmiyyəti xüsusi vurgulanmışdır. Cənub-Şərqi Xəzər regionunun geoloji şəraitində dəstək vektorları metodu, təsadüfi meşə və neyron şəbəkələrin yüksək nəticə verdiyi müəyyən edilmişdir. Hər bir metodun spesifik üstünlükleri qeyd olunmuşdur. Araşdırında ilkin məlumatların keyfiyyəti, nəticələrin interpretasiya imkanları və metodların konkret geoloji şəraitə uyğunlaşdırılması ilə yanaşı, modelin həddindən artıq öyrədilməsi ilə bağlı əsas problemlər də nəzərdən keçirilmişdir. Müzakirə və nəticələr bölməsində isə maşın öyrənməsi metodlarının konkret geoloji məsələlər və onların tətbiq oluna biləcəyi şəraitə uyğun istifadəsi ətraflı təhlil olunmuşdur.

Açar sözlər: süni intellekt, maşın öyrənməsi, geoloji vəzifələrin təsnifati, xətti və polinomial regressiya, litofasiyaların klasterləşdirilməsi, kollektor xüsusiyyətləri

НОВЫЙ ПОДХОД К НЕФТЕГАЗОГЕОЛОГИЧЕСКОМУ РАЙОНИРОВАНИЮ ТЕРРИТОРИИ АЗЕРБАЙДЖАНА

Керимов В.Ю.^{1,2}, Юсубов Н.П.¹, Гулиев И.С.⁴, Кадиров Ф.А.^{1,3}

¹Министерство науки и образования Азербайджанской Республики,
Институт нефти и газа, Азербайджан

AZ1000, Баку, ул. Ф. Амирова, 9: vagif.kerimov@mail.ru

²Российский государственный геологоразведочный университет
имени Серго Орджоникидзе, Россия

117997, Москва, ул. Миклухо-Маклая, 23

³Министерство науки и образования Азербайджанской Республики,
Институт геологии и геофизики, Азербайджан

AZ1073, Баку, просп. Г.Джавида, 119

⁴Президиум Национальной академии наук Азербайджана, Азербайджан
Ул. Истиглалийят, 30, Баку, AZ1001

A NEW APPROACH TO THE OIL AND GAS GEOLOGICAL ZONING OF THE TERRITORY OF AZERBAIJAN

Kerimov V.Yu.^{1,2}, Yusubov N.P.¹, Guliyev I.S.⁴, Kadirov F.A.^{1,3}

¹Ministry of Science and Education of the Republic of Azerbaijan, Institute of Oil and Gas, Azerbaijan
9, F.Amirov str., Baku, AZ1000: vagif.kerimov@mail.ru

²Sergo Ordzhonikidze Russian State University for Geological Prospecting, Russian Federation
23, Miklouho-Maclay str., Moscow, 117997

³Ministry of Science and Education of the Republic of Azerbaijan, Institute of Geology and Geophysics, Azerbaijan
119, H.Javid av., Baku, AZ1073

⁴Presidium of the Azerbaijan National Academy of Sciences, Azerbaijan
30, Istiglaliyyat str., Baku, AZ1001

Keywords: Oil and gas geological zoning, Azerbaijan, basin, province, hydrocarbon systems, oil and gas bearing areas

Summary. The theoretical foundations have been developed and a scheme of oil and gas geological zoning of Azerbaijan has been created based on the introduction of "basin" characteristics into the nomenclature of elements allocated in the "provincial" approach. The novelty in the proposed scheme of oil and gas geological zoning is the allocation of a hierarchical level – "hydrocarbon systems". The Caspian-Kura oil and gas province (megabasin) is distinguished on the territory and in water area of Azerbaijan. As the next hierarchical level of oil geological zoning within the oil and gas province (megabasin), three oil and gas areas (basins) have been identified – the Middle Kur, South Caspian and Middle Caspian areas (basins). The next category of hierarchically subordinate elements in the systematics of zoning objects is the hydrocarbon system (HS), which distinguishes the proposed scheme of oil and gas geological zoning of Azerbaijan. The results of the analysis and numerical modeling of hydrocarbon systems in the South Caspian oil and gas basin reveal three classical generation-accumulation hydrocarbon systems (GAHS): Eocene-Pliocene GAHS; Maikop-Pliocene GAHS and Miocene-Pliocene GAHS. Within the basin, there are also three unconventional (shale) HS: Eocene, Maikop and diatomaceous HS. In the Middle-Kura region, there are two GAHS: Eocene and Maikop GAHS; two unconventional (shale) HS – Eocene and Maikop. In the Middle Caspian region, there are three GAHS: Eocene-Pliocene, Maikop-Pliocene and Maikop-Cretaceous GAHS. There are also three unconventional HS – Cretaceous, Eocene and Maikop.

© 2025 Earth Science Division, Azerbaijan National Academy of Sciences. All rights reserved.

Успешность решения задачи, прогнозирование и оценка нефтегазоперспективности исследуемых территорий и акваторий во многом опре-

деляется знанием общих закономерностей формирования и объёмного – по площади и в разрезе изучаемого геологического региона – распреде-

ления углеводородных скоплений. Результаты прогноза выражаются в выявлении и геологическом обосновании нефтегазоперспективности изученного участка недр, а эффективность решения задачи прогнозирования – в её практическом подтверждении бурением на уровне геологически определённых территорий: области, района, зоны или отдельного локального объекта.

Первой ступенью прогноза и оценки перспектив нефтегазоносности недр на уровне континентального или морского региона в целом или его части является его нефтегазогеологическое районирование. Оно представляет собой разделение территории или акватории на нефтегазоносные/перспективные площадные объекты разного масштаба и взаимного соподчинения на основе анализа совокупности геологических данных о структуре, стратиграфическом содержании, вещественном составе разреза рассматриваемого региона, об условиях его формирования и нефтегазогеологических свойствах.

В зависимости от особенностей геологического строения территорий и акваторий, при выделении объектов нефтегазогеологического районирования, ключевую роль могут играть структурно-тектонические, литологические или комплексные факторы.

Проблема нефтегазогеологического районирования территорий и акваторий имеет большое научное и практическое значение, поскольку от правильности выбора модели и построения соответствующей карты или схемы районирования зависит правильность прогноза перспектив региона, правильность выбора и эффективность применения методики поисковых и разведочных работ в его пределах, обоснованность и исполнимость долгосрочных планов и программ освоения ресурсов региона и развития отрасли в целом.

Принципы и задачи нефтегазогеологического районирования

Разработкой принципов выделения и классификации нефтегазоносных территорий занимались многие учёные, в числе которых М.В.Абрамович, Б.К.Бабазаде, А.А.Бакиров, Ф.М.Багир-Заде, И.О.Брод, М.И.Варенцов, Н.Б.Вассоевич, И.В.Высоцкий, И.М.Губкин, Н.А.Ерёменко, В.Ю.Керимов, С.П.Максимов, Ш.Ф.Мехтиев, С.Г.Салаев, Х.Б.Юсуфзаде, А.Н.Гусейнов, К.М.Керимов, Ш.С.Кочарли, М.М.Зейналов, Н.П.Юсубов и другие исследователи (Kerimov et al., 2014; 2017; 2019; 2023; Kerimov и др., 2016; 2019).

Нефтегазогеологическое районирование является научной основой для решения следующих задач:

– выяснения связей размещения регионально нефтегазоносных территорий с теми или иными типами крупных геоструктурных элементов земной коры и приуроченными к ним формациями;

– дифференцированной оценки перспектив нефтегазоносности различных частей изучаемой территории с учетом особенностей строения и формирования её крупных геоструктурных элементов;

– выявления геологических условий размещения прогнозируемых ресурсов нефти и газа в различных частях изучаемой территории, в том числе зон наибольших концентраций этих ресурсов;

– выбора оптимальных направлений и методов поисково-разведочных работ на нефть и газ.

Существует два основных, устоявшихся в теоретическом и практическом отношении и достаточно активно применяемых принципиальных подходов к выделению и классификации нефтегазоносных и перспективных территорий и акваторий, один из которых основан на выявлении в геологической структуре земной коры нефтегазоносных бассейнов, а другой – нефтегазоносных провинций.

Подход, или принцип, условно определяемый как "бассейновый", состоит в выделении упомянутых выше нефтегазоносных бассейнов (НГБ), которые, согласно данному И.О.Бродом определению, представляют собой замкнутые или частично замкнутые впадины, разнообразные по строению и истории геологического развития, содержащие в разрезе осадочной толщи свиты, которые заключают в себе залежи нефти и газа (Брод, 1964). Этот подход развивается по трём направлениям, одно из которых выделяет НГБ по характеру их обрамления и возрасту фундамента, второе основывается на их классификации по тектоническим принципам, третье исходит из необходимости первоочередного рассмотрения условий генерации и аккумуляции углеводородов.

Иерархически подчинёнными элементами в систематике объектов районирования при "бассейновом" подходе являются ареал и зона нефтегазонакопления, месторождение и залежь.

Подход, основанный на выделении нефтегазоносных провинций ("провинциальный" подход, или принцип), а в их составе нефтегазоносных областей, районов и более дробных классификационных единиц был предложен И.М.Губкиным и в дальнейшем развит А.А.Бакировым, его коллегами и последователями (Бакиров и др., 1971). Этот подход давно и плодотворно применяется в практике нефтегазогеологического районирования, рекомендуется к применению современными методическими изданиями, используется в спра-

вочниках и официальных картографических документах, характеризующих фактическую нефтегазоносность российских территорий и акваторий.

Необходимо отметить, что рассмотренные подходы к районированию не являются антагонистами по отношению друг к другу. Более того, на уровне таких элементов классификации, как зоны нефтегазонакопления, месторождения и залежи они идентичны. Их различия на уровне крупных классификационных единиц заключаются в роли, которая отводится факторам тектоники, геодинамики, онтогенеза нефти и другим – при выделении и установлении конфигурации нефтегазоносной территории. В этом отношении "провинциальный" подход представляется более всеобъемлющим по комплексу учитываемых факторов и в связи с этим менее зависимым от индивидуальной позиции исследователя относительно интеграции и истолкования геологических данных (Керимов и др., 2019; 2024а,б). Учитывая, что осадочные бассейны в составе нефтегазоносной провинции являются неотъемлемыми и важными участниками процесса формирования её углеводородного потенциала, необходимо вкратце остановиться на характеристике их общих черт. Одной из оптимальных схем классификации осадочных бассейнов, осно-

ванной на ранжировании структурно-тектонических элементов, образующих тектоническую основу разномасштабных осадочных бассейнов и их геодинамическую характеристику, является иерархическая классификация, построенная по "морфометрическому" принципу (форма-размер). Пример укрупнённой морфологической классификации бассейновых образований в сопоставлении с разноранговыми структурно-тектоническими элементами подвижных (складчато-орогенных) и стабильных (платформенных) территорий приведён в таблице 1.

Эта таблица отображает корреляцию бассейновых образований в земной коре, выделяемых по морфологическому признаку с теми, которые определяются на основании структурно-тектонического анализа геологических данных. Из неё следует, что структурно-тектоническим элементам глобального, субглобального и отчасти надрегионального ранга морфологически соответствуют отрицательные элементы, имеющие ранг осадочного мегабассейна. Морфометрической категорией осадочного бассейна описываются отрицательные элементы надрегионального, регионального и субрегионального ранга, а категорией суббассейна – субрегиональные и локальные элементы.

Таблица 1

Иерархическая классификация отрицательных (бассейновых) структурных элементов
(извлечение из общей классификации по (Иерархическая классификация..., с дополнениями, 2018))

Ранг структурно-тектонических элементов	Геодинамическая характеристика		Примерная корреляция с морфометрическим «бассейновым рядом»
	Подвижные территории	Стабильные территории	
Глобальный	Складчатая область (система)	Платформа	
Субглобальный	Складчатый (орогенный) пояс	Плита	МЕГАБАССЕЙН
Надрегиональный	Синклиниорная зона	Синеклиза и авлакоген	
Региональный (I порядка)	Мегасинклиниорий	Впадина и прогиб	БАССЕЙН
Субрегиональный (II порядка)	Синклиниорий	Депрессия и котловина	
Локальный (III порядка)	Синклиналь	Локальные отрицательные структуры	СУББАССЕЙН

Исходя из этой структурной корреляции профессор В.Ю.Керимов в предложенной схеме (рис. 1) нефтегазогеологического районирования ввел соответствующую "бассейновую" характеристику в номенклатуру элементов, выделяемых при «провинциальном» подходе, и установил, таким образом, примерное ранговое соответствие между ними и элементами, которые выделяются при районировании по "бассейновому" принципу. Другой новизной в предложенной схеме нефтегазогеологического районирования является выделение иерархического уровня – "углеводородные системы". Таким образом, в нефтегазоносных бассейнах выделяются генерационные-аккумуляционные углеводородные системы (ГАУС) – естественная система углеводородных флюидов, которая включает в себя очаг генерации (т.е. область развития активных нефтематеринских пород), все связанные с ним углеводороды, все значимые элементы и процессы, необходимые для возникновения скоплений нефти и газа. Элементами углеводородных систем наряду с нефтематеринскими породами являются вмещающие породы, ловушки, резервуары и коллекторы, покрышки, перекрывающие толщи, а процессы — это генерация, миграция и

аккумуляция скоплений УВ. Неразрывность связей таких элементов углеводородной системы, как очаг генерации нефти и газа, зон его миграции и аккумуляции является важным условием, определяющим корректность нефтегазогеологического районирования и прогноза нефтегазоносности. Такой подход позволяет придерживаться важного принципа, который может быть сформулирован как "принцип неразрывности связей между элементами углеводородной системы", который основан на концепции углеводородных систем, разработанной в период 80-90-х годов XX в. (Magoon, Dow, 1994; Magoon, 2004).

Далее в пределах углеводородных систем выделяются зоны нефтегазонакопления (плеи) – ассоциация смежных и сходных по геологическому строению месторождений нефти и газа, приуроченных в целом к единой группе генетически связанных между собой ловушек, месторождение – ассоциация залежей, приуроченных к одной или нескольким ловушкам, расположенным на одной локальной площади, залежь – естественное локальное единичное скопление УВ в одном или группе пластов, контролируемое единым (общим) водонефтяным (ВНК) или газоводяным (ГВК) контактом.



Рис. 1. Общая схема нефтегазогеологического районирования

Нефтегазогеологическое районирование проводится не только по латерали. Основными единицами вертикального нефтегазогеологического расчленения разреза нефтегазоносных территорий являются нефтегазоносная формация, региональный, субрегиональный, зональный нефтегазоносный комплексы. В связи с этим наряду с морфологическими и структурно-тектоническими характеристиками осадочных бассейнов, дающими представления о сопоставимости геологических образований изучаемой территории в плане, используются и другие характеристики (или классификационные категории) осадочных бассейнов, пример которых приведён в таблице 2.

Использование в процессе выделения элементов нефтегазогеологического районирования и обоснования их контуров этих и других характеристик геологического строения изучаемой территории является залогом построения оптимальной модели её нефтегазоперспективности.

Опыт нефтегазогеологического районирования Азербайджана и о необходимости его пересмотра

Общая площадь нефтегазоносных и перспективно-нефтегазоносных районов Азербайджана оценивается порядка 92.8 тыс. км². Первая “Карта месторождений нефти и газа и перспективных площадей Азербайджанской ССР” была издана в 1958 г. под редакцией М.В.Абрамовича, Б.К.Бабазаде и Ш.Ф.Мехтиева. В 1985 г. под редакцией академиков АН Азербайджанской ССР Ш.Ф.Мехтиева и Ф.М.Багир-Заде (рис. 2) коллективом авторов: А.И.Алиев, Ф.М.Багир-Заде, З.А.Буниат-Заде, А.Н.Гусейнов, Ф.Г.Дадашев, Ш.Ф.Мехтиев, С.Г.Салаев, Х.Б.Юсуфзаде (Алиев и др., 1985) была составлена “Карта месторождений нефти и газа перспективных структур Азербайджанской ССР”. При составлении этой карты использовались: “Тектоническая карта Азербайджанской ССР” 1981 г. и “Карта грязевых вулканов нефтегазоносных областей Азербайджанской ССР” 1978 г. издания.

Таблица 2
Возможные классификационные категории осадочных бассейнов

Классификационные категории	Некоторые примеры признаков (свойств) бассейна
Условия осадкообразования	Континентальные, озерные, лагунные, окраинно-континентальные, глубоководные, разных климатических зон и т.д.
Литолого-формационный состав отложений	Молассы, флиш, эвапориты, красноцветы, угленосные формации и т.д.
Происхождение	«Эпигеосинклинальный», «эпиплатформенный», рифтогенный (внутриконтинентальный, межконтинентальный), надрифтовая (эпирифтовая) депрессия и т.д.
Морфология	Нелинейные (изометричные) удлиненные, линейные и т.д.
Тектоника (структура)	Синеклиза, впадина, грабен, наложенная впадина, перикратонное погружение, краевой (передовой) прогиб и т.д.
История развития (погружения)	Устойчивое, прерывистое, с остановками или кратковременными поднятиями, быстрое или медленное, в морских или иных обстановках
Геодинамика	Характеристики направленности и интенсивности основных и сопутствующих процессов в области осадконакопления в зависимости от ее положения внутри литосферных плит или на их дивергентных, конвергентных или трансформных границах (в условиях действия сил растяжения, сжатия или сдвига)
Положение относительно других элементов структуры земной коры	Внутриплатформенные, окраинно-платформенные, периконтинентальные, периокеанические, шовные, пограничные и т.д.

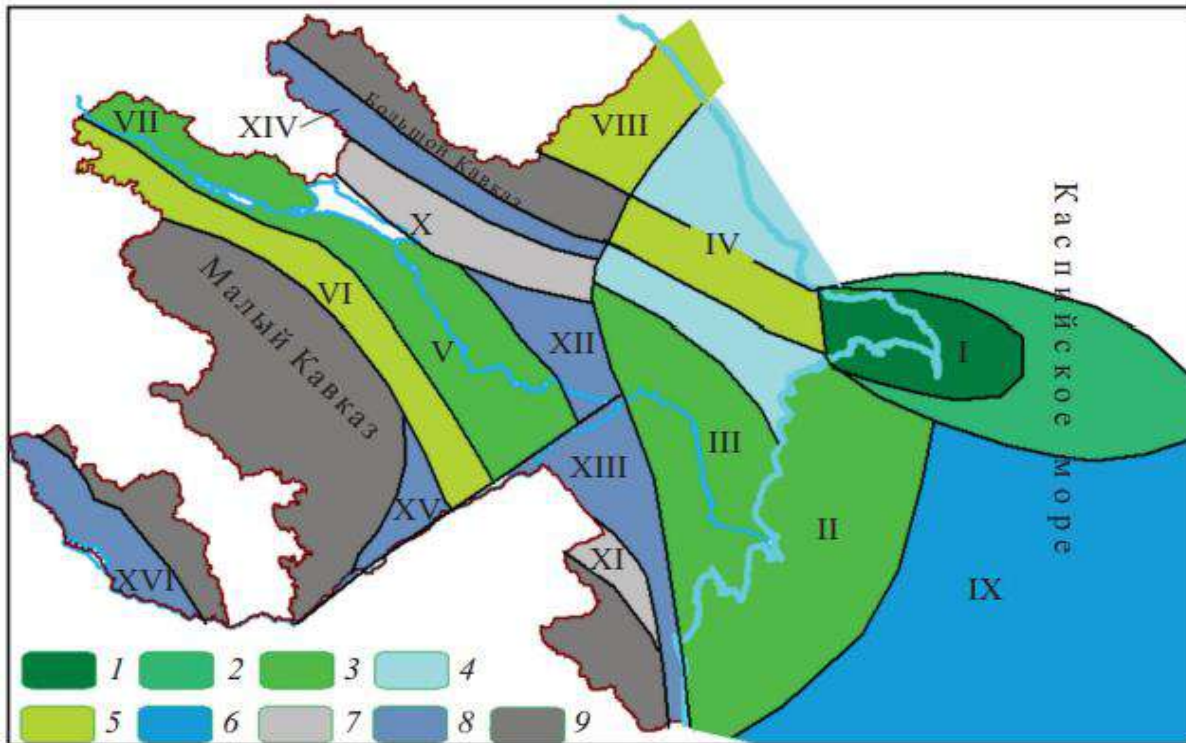


Рис. 2. Нефтегазогеологическое районирование Азербайджанской ССР (Алиев и др., 1985). Нефтегазоносные районы: I – Абшеронский; II – Бакинский архипелаг; III – Нижнекуринский; IV – Шамаха-Гобустанский; V – Евлах-Агджабединский; VI – Гяндзинский; VII – междуречье Куры и Габырры; VIII – Прикаспийско-Губинский. Перспективно-нефтегазоносные территории (акватории); IX – Глубоководная часть Южного Каспия; Возможно-перспективные территории; X – Аджиноурская; XI – Джалилабадская; Территория с невыясненными перспективами нефтегазоносности; XII – Джарлы-Саатлинская; XIII – Мильско-Муганьская; XIV – Алазано-Агричайская; XV – Аразская; XVI – Нахчыванская.

Районы: 1 – с реализацией начальных потенциальных ресурсов более 80%; 2 – высокоперспективные; перспективные; 3 – I категории; 4 – II категории; 5 – III категории; 6 – перспективно-нефтегазоносные территории (акватории); 7 – возможно-перспективные территории; 8 – территории с невыясненными перспективами нефтегазоносности; 9 – бесперспективные территории.

При оценке перспектив нефтегазоносности отдельных районов за основу были приняты следующие критерии: удельный вес потенциальных ресурсов и плотность перспективных и прогнозных запасов нефти и газа отдельных районов; степень реализации (т.е. перевода в промышленные категории) начальных потенциальных ресурсов углеводородов; результативность поисково-разведочных работ; состояние изученности основных перспективно нефтегазоносных комплексов и достоверность полученной геологической информации; палеогеографические условия накопления осадков и особенности геотектонического развития нефтегазоносных районов; геохимические условия нефтегазообразования; наличие благоприятной фации коллекторов для скопления нефти и газа; наличие надежных покрышек для сохранения залежей нефти и газа (Алиев и др., 1985; Алиев А.И., Алиев Э.А., 2011).

Следует отметить, что рассмотренные выше подходы к районированию не являются антагонистическими друг другу. Более того, на уровне та-

ких элементов классификации, как зоны нефтегазонакопления, месторождения и залежи, они идентичны. Их различия на уровне крупных единиц классификации заключаются в роли, отводимой тектонике, геодинамике, онтогенезу нефти и другим факторам – в выявлении и установлении конфигурации нефтегазоносной территории.

Результаты этих двух направлений отражены в картах тектонического и нефтегазоносного районирования территории Азербайджана и представлены на рис. 3 и 4. Они основаны на обобщении результатов предыдущих исследований (Алиев А.И., Алиев Э.А., 2011; Гаджиев и др., 1983; Керимов и др., 2002; 2003) с учетом результатов геолого-геофизических работ, проведенных в период 1985-2002 гг.

Совокупность приведенных геологических критериев позволила авторам выделить на территории Азербайджана высокоперспективные и перспективные I, II, III категории нефтегазоносные районы, перспективно-нефтегазоносные и возможно-перспективные территории (аквато-

рии), а также территории с невыясненными перспективами. Следует подчеркнуть, что наличие такой карты очень помогло при определении наиболее эффективных направлений и размещения объемов поисково-разведочных работ на нефть и газ.

Использование геолого-геофизической информации, накопленной за период с 1985 по 2003 гг. группой авторов, в 2003 г. были составлены и изданы тектоническая и нефтегазогеологическая карты (Керимов и др., 2002; 2003). Вторая карта (рис. 4), как и предшествующие, составлена также на тектонической основе.

В ней отмечены: главные структурные элементы депрессионных зон; основные глубинные разломы и региональные разрывы в осадочном чехле; изогипсы поверхности консолидированной коры; выявленные структуры и месторождения по плиоцен-четвертичному, палеоген-миоценовому и мезозойскому этапам; структурные схемы по кровле продуктивной толщи сред-

него плиоцена (основной этаж нефтегазоносности) и по поверхности мезозоя (Керимов, 2019; Mustaev et al., 2023; Kadirov et al., 2024; Eppelbaum et al., 2024).

Особо подчеркиваем, что во всех работах, направленных на составление карт нефтегазогеологического районирования Азербайджана в основу положен геотектонический принцип с учетом мощности и фациально-geoхимических условий осадочного выполнения, степени изученности района и надежности основных критерии оценки перспектив нефтегазоносности.

Проведенные исследования с использованием сейсморазведочных данных позволили сделать вывод о том, что поля тектонических напряжений в осадочном чехле, создающие разрывные нарушения активизировались в течение двух интервалов геологического времени (Юсубов, 2023). Первый период активизации, создавший вертикальные (или субвертикальные) разломы, действовал в основном до начала палеогена.

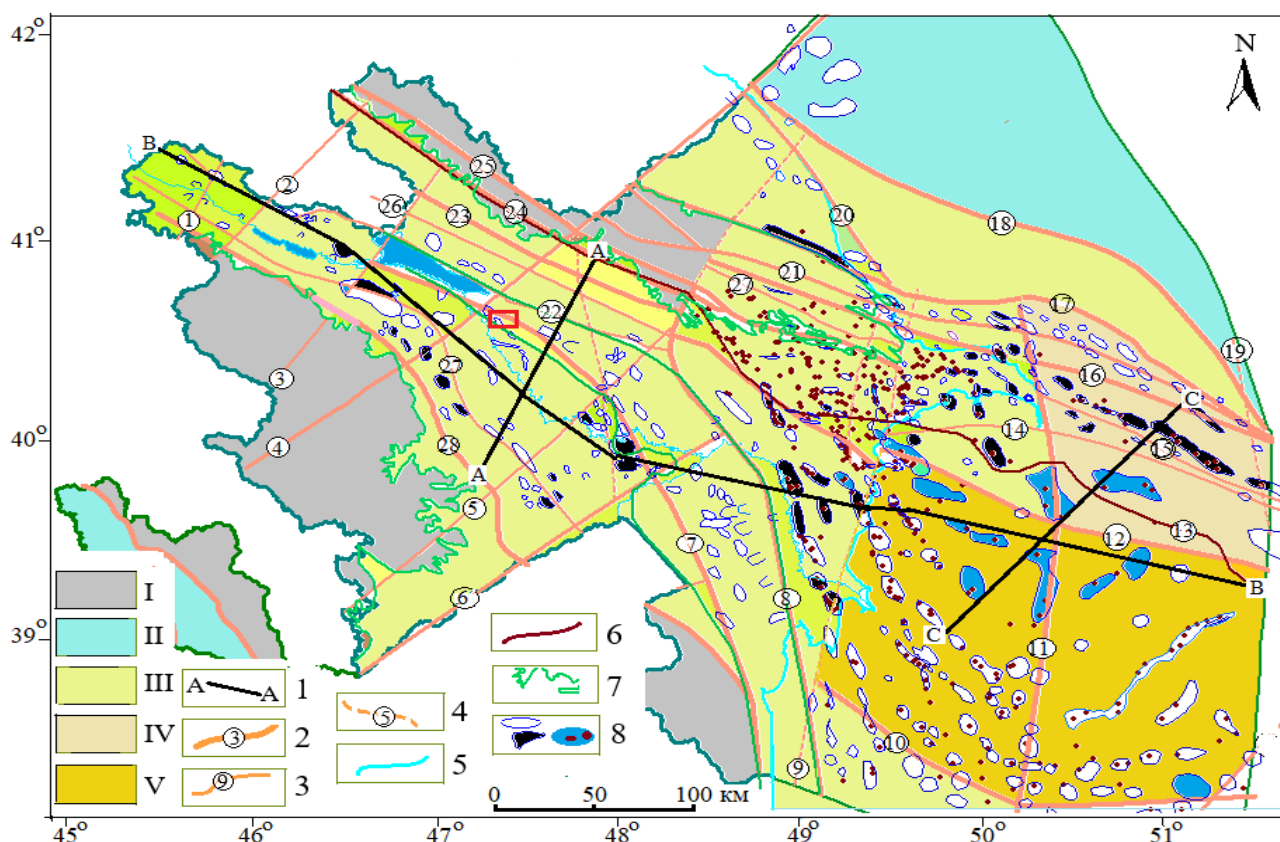


Рис. 3. Карта тектонического районирования нефтегазоносных районов Азербайджана (Керимов и др., 2002). На карте цветом показан предполагаемый возраст фундамента: I – складчатые горные системы; II – раннепротерозойский; III – позднепротерозойско-кембрийский; IV – архейско-палеозойский; V – позднепротерозойский.

Условные обозначения: 1 – линии сейсмических профилей (рис. 5, 6, 7); 2 – глубинные разрывы; 3 – крупные тектонические разломы; 4 – флексуры или предполагаемые разломы; 5 – береговая линия Каспийского моря; 6 – тектонический разлом по данным сейсмологии, сейсморазведки и геологии; 7 – выходы мезозойских отложений; 8 – антиклинальные объекты, месторождения нефти и газоконденсата

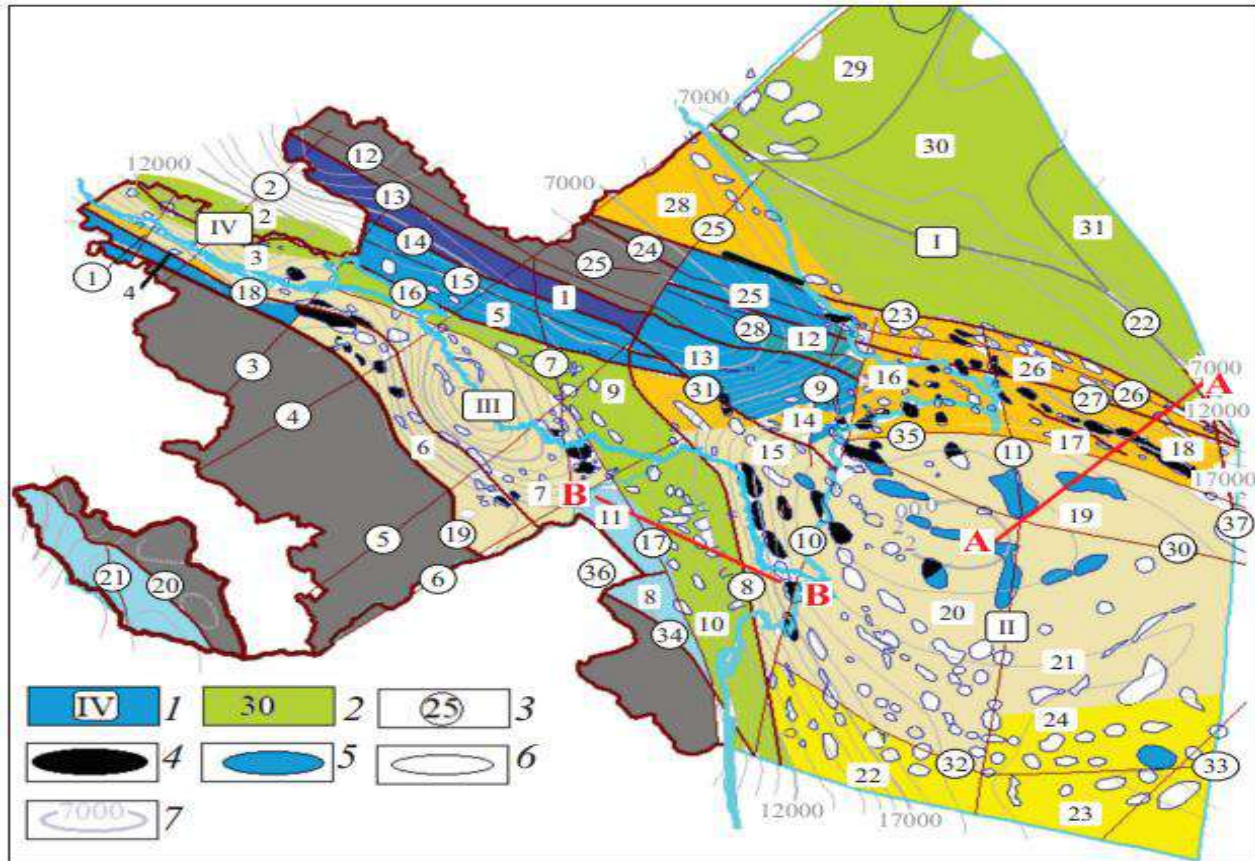


Рис. 4. Карта нефтегазогеологического районирования и перспектив нефтегазоносности Азербайджана (Керимов и др., 2003)
Условные обозначения: 1 – крупные прогибы (I – Средне-Каспийский, включающий Прикаспийско-Губинский район, как часть Терско-Каспийского прогиба и Северо-Абшеронской синклинали, II – Южно-Каспийский с Абшеронской, Гобустанской и Нижнекуринской зонами, III – Евлах-Агджабединский с Гянджинской и Саатлы-Гейчайской зонами, IV – Габырры-Аджиноурский с Аджиноурской зоной и междуречьем Куры и Габырры), 2 – нефтегазоносные, перспективные, высокоперспективные и возможно-перспективные с невыясненными перспективами районы, 3 – тектонические разломы по фундаменту и осадочному комплексу мезо-кайнозоя, 4 – нефтяные месторождения, 5 – газовые месторождения, 6 – антиклинальные постройки, 7 – изолинии по поверхности фундамента

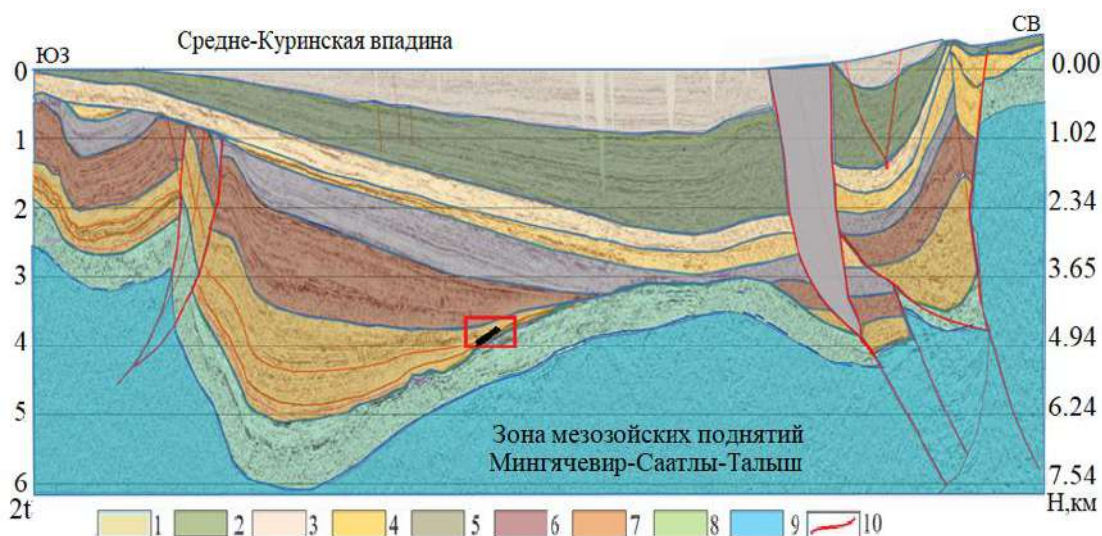


Рис. 5. Временной разрез по линии А-А (рис. 1). В левой и правой частях профиля отмечаются Куринский, Предмалокавказский и Предбольшекавказский тектонические разломы. Расчеты показывают, что Предмалокавказский разлом амплитудой более 1.5 км образовался в результате эмиграции углеводородов в песчаные резервуары, расположенные в базальных майкопских горизонтах, сформировавшихся в майкопских породах.
Условные обозначения: 1 – голоцен; 2 – плейстоцен; 3 – агчагыл; 4 – плиоцен; 5 – миоцен; 6 – майкоп; 7 – палеоген; 8 – мел; 9 – юрский период; 10 – тектонические разломы.

Образованные в этом интервале геологического времени разломы охватили разрез ниже поверхности мезозойских отложений. Второй период, начавшийся с конца миоцена, создавал и создает субвертикальные тектонические разрывы в кайнозойской части разреза.

При этом разломы по нижнему этажу практически не испытывают каких-либо изменений, в результате тектонических событий, происходящих в кайнозое, что подтверждается данными современной сейсморазведки, охватывающей весь стратиграфический интервал мезо-кайнозоя (см. рис. 5, 6, 7).

Прошло около 20 лет со времени издания (2003 г.) последних карт – “Тектоническая карта нефтегазоносных районов Азербайджана” и “Нефте-

газогеологического районирования и перспектив нефтегазоносности Азербайджана”. За прошедшее время: появились 2D сейсмические данные регионального масштаба при плотности сети сейсмических профилей 2.5x2.5 км и 3D сейсморазведки, выполненной в Каспийском море; на территории (суша) Азербайджана был отработан ряд региональных сейсморазведочных профилей и на некоторых площадях выполнена 3D сейсморазведка с использованием инновационных технологий; появились новые результаты глубокого бурения (Керимов и др., 2012). По результатам производственных и научных исследований уточнено геологическое строение территории Азербайджана, в том числе отдельных площадей депрессионных зон и акватории азербайджанского сектора Каспийского моря.



Рис. 6. Сейсмогеологический профиль СЗ-ЮВ направление (рис. 1, линия В-В)

Условные обозначения: 1 – слой воды; 2 – голоцен + плейстоцен; 3 – агчагыл; 4 – плиоцен; 5 – миоцен; 6 – майкоп; 7 – палеоген; 8 – мел; 9 – юрский период; 10 – тектонические разломы.

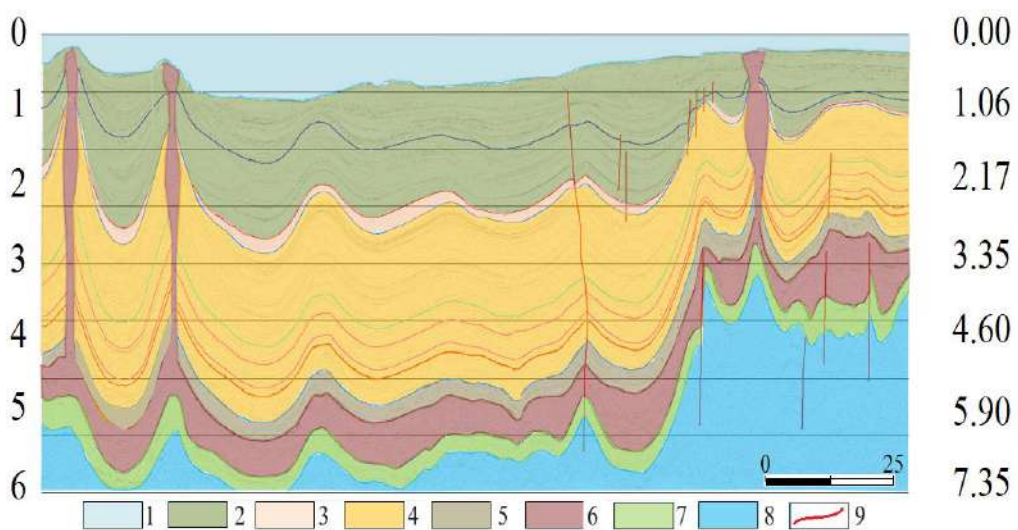


Рис.7. Временной разрез в Южно-Каспийском море (см.: по линии С-С на рис. 1). На рисунке показано пересечение линии профиля с разломом, выявленным по сейсмологическим и сейсмическим данным. На этом участке разлом отмечен малоамплитудным смещением, которое из-за его масштаба не заметно.

Условные обозначения: 1 – слой воды; 2 – голоцен + плейстоцен; 3 – агчагыл; 4 – плиоцен; 5 – миоцен; 6 – майкоп; 7 – палеоген; 8 – мел; 9 – юрский период; 10 – тектонические разломы

Результаты этих работ показали, что ряд выводов предыдущих исследований устарели и принципы, вложенные в основу нефтегазогеологического районирования, не учитывают современные достижения фундаментальной нефтегазогеологической науки и практики и требуют пересмотра.

В целом в работах, посвящённых нефтегазогеологическому районированию, нет четкости, и присутствует большая путаница при выделении объектов. Так в работе (Авербух, 1995) автор некоторые НГР называет зонами – зона Нижнекуринской впадины, Среднекуринская зона, Туркменская нефтегазоносная зона, зона центральной части ЮКБ.

Не используется концепция углеводородных систем, разработанная в период 80-90-х годов XX в. и позволяющая комплексно, системно подойти к определению и полноценной характеристике перспективной территории или акватории с учётом всей совокупности данных о геологическом строении и составе разреза, его физических параметрах, особенностях тектоники и геодинамики, истории геологического развития и изменений во времени геологической среды и использовании современных методов и технологий анализа и моделирования (Kerimov et al. 2021; Kadirov et al., 2023). В соответствии с этим принципом в осадочных бассейнах должны выделяться естественные углеводородные системы.

Во всех схемах районирования территории Азербайджана в качестве части нефтегазоносной области выделяются нефтегазоносные районы. При этом у разных авторов их количество колеблется в широком интервале. Это прежде всего связано с тем, что в основу выделения нефтегазоносных районов вложены различные критерии – геологоструктурные или географические, а в большинстве случаев – по административному или промышленно-административному признакам.

Как отмечено в статье (Юсубов, 2023), устаревшие выводы – это те, которые относятся в основном к выводам, связанным с тектоническим строением осадочного комплекса мезо-кайнозоя и углеводородной системы, составными частями которой являются: наличие в земной коре условий для первичного образования углеводородов (нефтеринские породы); наличие пористых (проницаемых) горных пород (коллекторов), каналов для миграции углеводородов в верхние слои, пластовых покрышек, состоящих из непроницаемых горных пород, ограничивающих перемещение нефти и газа по вертикали (экранов или покрышек).

Результаты сейсморазведочных работ и глубокое поисковое бурение за более чем 30 лет не приводили к дополнению имеющегося структурного фонда. В то же время по данным 3D сейсморазвед-

ки удалось в значительной степени уточнить геометрические и прогнозировать петрофизические параметры выявленных ранее в результате геолого-геофизических исследований антиклиналей, представляющих интерес с точки зрения обнаружения в них месторождений (Юсубов, 2020; 2022).

Заключение

Схема нефтегазогеологического районирования Азербайджана

Как было отмечено выше, осадочные бассейны в составе нефтегазоносной провинции являются неотъемлемыми и важными областями процесса формирования её углеводородного потенциала. Известно, что на территории и в акватории Азербайджана размещаются (выделяются) части двух крупных – Каспийского и Куриńskiego мегабассейнов, нефтегазоносность которых является установленной. Исходя из этого авторы предлагают выделить **Каспийско-Куриńskую нефтегазоносную провинцию (мегабассейн)**.

Согласно представлениям авторов, применение данного подхода к нефтегеологическому районированию не отрицает возможности выделения наряду с нефтегазоносными бассейнами также и нефтегазоносных провинций. Классификацией разномасштабных осадочных бассейнов, включющей углеводородные системы соответствующего уровня, формирующей внутреннюю структуру нефтегазоносных провинций и определяющей возможность их разделения на дробные элементы районирования, является иерархическая классификация, построенная по "морфометрическому" принципу (форма-размер). Из неё следует, что структурно-тектоническим элементам глобального, субглобального и отчасти надрегионального ранга морфологически соответствуют отрицательные элементы, имеющие ранг осадочного мегабассейна. Морфометрической категорией осадочного бассейна описываются отрицательные элементы надрегионального, регионального и субрегионального ранга, а категорией суббассейна – субрегиональные и локальные элементы.

В связи с вышеизложенным в качестве следующего иерархического уровня нефтегеологического районирования в составе нефтегазоносной провинции (мегабассейна) выделяются **нефтегазоносные области (бассейны)**. В пределах Каспийско-Куринского нефтегазоносного бассейна (провинция) выделяются три нефтегазоносные области (бассейна) – **Средне-Куринская, Южно-Каспийская и Средне-Каспийская области (бассейны)** (рис. 8). В этих областях создались весьма уникальные условия для эволюции и распространения генерационно-аккумуляционных углеводородных систем.

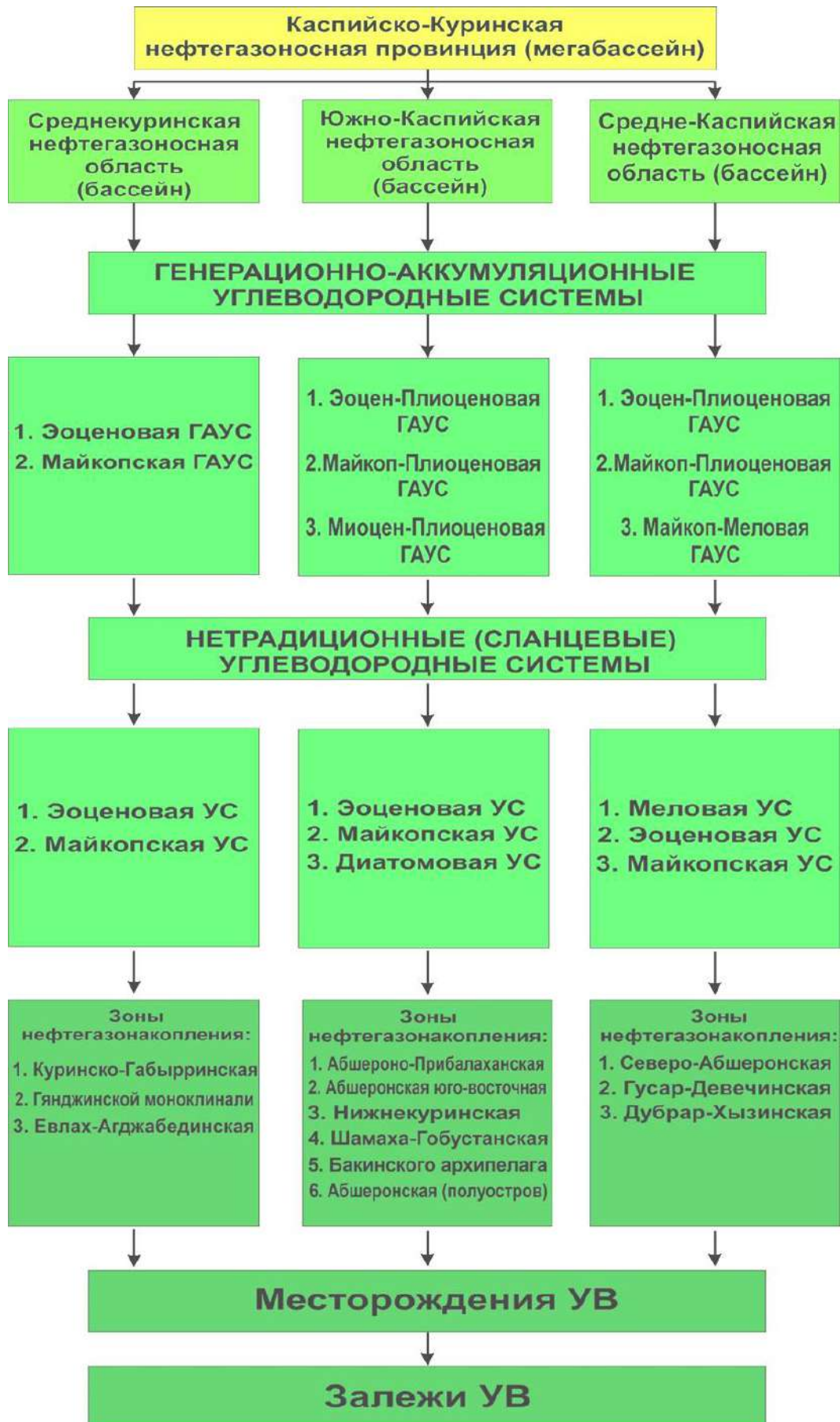


Рис. 8. Схема нефтегеологического районирования Каспийско-Куринской НГП

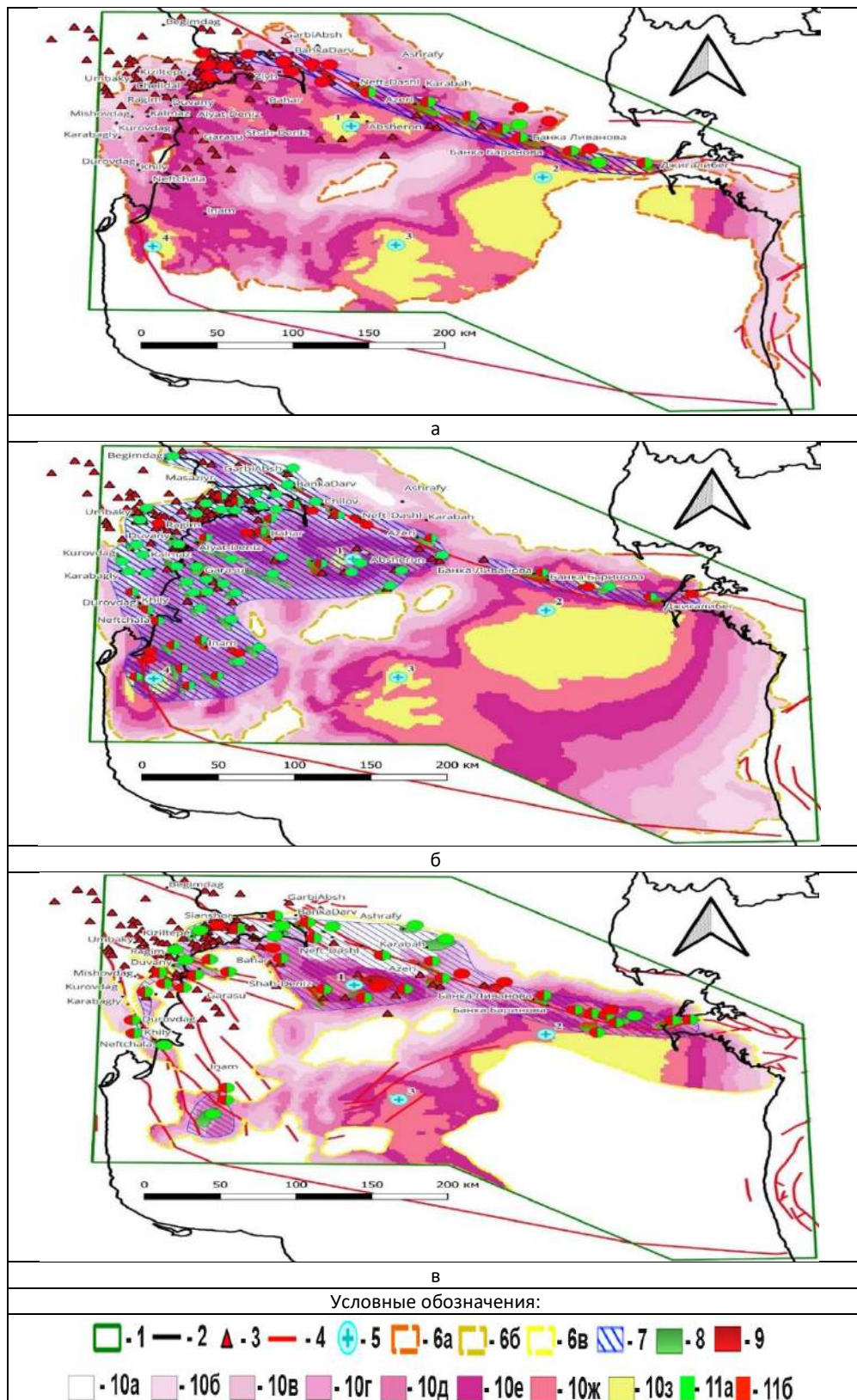


Рис. 9. Генерационно-аккумуляционные углеводородные системы ЮКБ

Условные обозначения: Генерационно-аккумуляционные углеводородные системы: а – эоцен-плиоценовая, б – майкоп-плиоценовая, в – миоцен-плиоценовая; 1 – область исследования, 2 – современная береговая линия, 3 – грязевые вулканы, 4 – разломы, 5 – псевдоскважины, 6 – граница ГАУС: 6а – эоцен-плиоценовой, 6б – майкопско-плиоценовой, 6в – миоцен плиоценовой, 7 – зоны аккумуляций (зоны нефтегазонакопления), 8 – области аккумуляции жидких УВ, 9 – области аккумуляции газообразных УВ, 10 – зрелость ОВ в очаге (R0,%): 10а – меньше или равно 0,5%, 10б – от 0.55 до 0.75%, 10в – от 0.75 до 1%, 10г – от 1 до 1.3%, 10д – от 1.3 до 2%, 10е – от 2 до 3%, 10ж – от 3 до 4%, 10з – от 4 до 5%, 11 – фактические месторождения: 11а – нефтяные, 11б – газовые.

Следующей категорией иерархически подчинённых элементов в систематике объектов районирования при "бассейновом" подходе, являются "углеводородные системы (УС)" (рис. 8 и 9), что отличает предложенную схему нефтегазогеологического районирования Азербайджана. В результате проведенного анализа и численного моделирования углеводородных систем в Южно-Каспийском нефтегазоносном бассейне выделяются три классических ГАУС: эоцен-плиоценовая; майкоп-плиоценовая и миоцен-плиоценовая углеводородные системы (рис. 9). В пределах бассейна выделяются также три нетрадиционных (сланцевых) УС: эоценовая, майкопская и диатомовая УС. В Средне-Куринской области выделяются две ГАУС: эоценовая и майкопская; две нетрадиционные (сланцевые)

УС – эоценовая и майкопская. В Средне-Каспийской области выделяются три ГАУС: эоцен-плиоценовая, майкоп-плиоценовая и майкоп-меловая ГАУС. Здесь выделяются также три нетрадиционных УС – меловая, эоценовая и майкопская.

Далее в пределах углеводородных систем выделяются **зоны нефтегазонакопления (плеи)** – ассоциация смежных и сходных по геологическому строению месторождений нефти и газа, **месторождения** – ассоциация залежей, приуроченных к одной или нескольким ловушкам, расположенным на одной локальной площади, **залежь** – естественное локальное единичное скопление УВ.

На основании вышеизложенного нами предлагается карта нефтегазогеологического районирования Азербайджана (рис. 10).

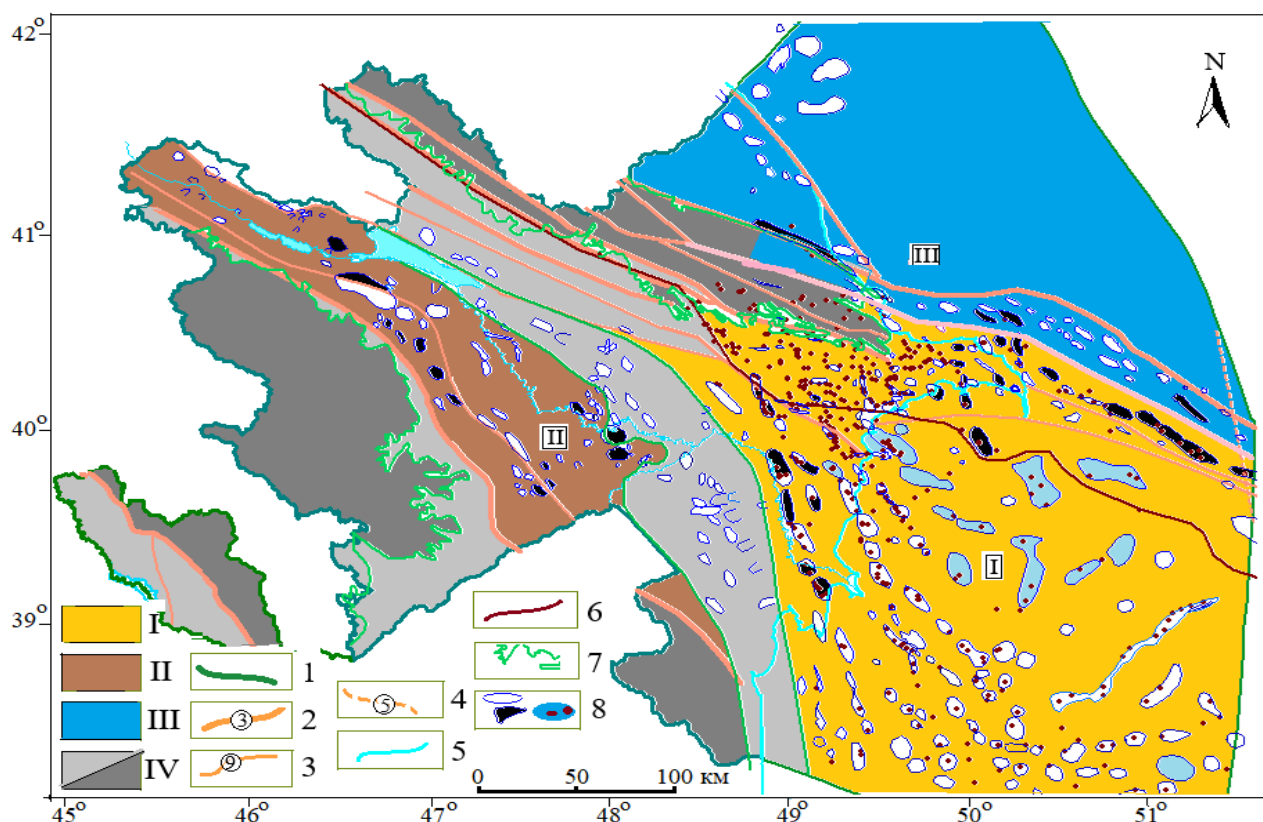


Рис. 10. Нефтегазогеологическое районирование Азербайджана. Куриńskо-Каспийская нефтегазоносная провинция (мегабассейн). I – Южно-Каспийская; II – Средне-Куринская; III – Средне-Каспийская нефтегазоносная область (бассейны); IV – бесперспективные и горно-складчатые районы.

Условные обозначения: 1 – Государственная граница; 2 – глубинные разрывы; 3 – крупные тектонические разломы; 4 – флексуры или предполагаемые разломы; 5 – береговая линия Каспийского моря; 6 – тектонический разлом по данным сейсмологии, сейморазведки и геологии; 7 – выходы на поверхность мезозойских отложений; 8 – антиклинальные объекты, нефтяные и газоконденсатные месторождения

ЛИТЕРАТУРА

Авербух Б.М. Нефтегазогеологическое районирование сложно построенных регионов с использованием ретроспективного анализа эволюции осадочно-породных бассейнов. Геология нефти и газа, №. 1, 1995, <https://geolib.narod.ru/Journals/OilGasGeo/1995/01/Stat/02/ht>.

REFERENCES

Abdullayev N.R., Guliyev I.S., Kadirov F.A., Huseynova Sh.M., Javadova A.S., Maharramov B., Mukhtarov A.Sh. Novel interpretation of the crustal structure and hydrocarbon evolution within the South Caspian and Kura sedimentary basins, Azerbaijan, Geofizicheskiy Zhurnal, Vol. 46, No. 3, 2024, pp. 146-161, <https://doi.org/10.24028/gj.v46i3.306357>.

- Алиев А.И., Алиев Э.А. Нефтегазоносность больших глубин. Проблемы прогнозирования, поисков и разведки. Оскар. Баку, 2011, 420 с.
- Алиев А.И., Багир-Заде Ф.М., Буниат-Заде З.А., Гусейнов А.Н., Дадашев Ф.Г., Мехтиев Ф.Ш., Салаев С.Г., Юсуфзаде Х.Б. Месторождения нефти и газа и перспективные структуры Азербайджанской ССР. Элм. Баку, 1985, 108 с.
- Бакиров А.А., Варенцов М.И., Бакиров Э.А., Нефтегазоносные провинции и области зарубежных стран. Недра. Москва, 1971, 544 с.
- Брод И.О. Основы учения о нефтегазоносных бассейнах. Недра. Москва, 1964, 60 с.
- Гаджиев Т.Г., Гусейнов А.Н., Ахмедов А.М., Юсуфзаде Х.Б., Гасанов И.С., Андреев Д.Н. Зейналов А.М., Касумова А.Н., Кулиева А.Р. Атлас нефтегазоносных и перспективных структур Азербайджана. Азернешр. Баку, 1983, 80 с.
- Иерархическая классификация бассейновых структурных элементов. Ранг структурно-тектонических элементов. Геодинамическая характеристика. Москва, Российский Государственный университет нефти и газа, 2018, <https://miloserdovalv.narod.ru> poisk > lekcija_2.
- Керимов К.М., Гусейнов А.Н., Гаджиев Ф.М., Гасанов И.С., Гусейнов Г.А., Кочарли Ш.С., Зейналов М.М. Карта тектонического районирования нефтегазоносных районов Азербайджана. Фабрика картографии. Баку, 2002.
- Керимов К.М., Гусейнов А.Н., Гаджиев Ф.М., Гасанов И.С., Гусейнов Г.А., Кочарли Ш.С., Зейналов М.М. Карта нефтегазогеологического районирования и перспектив нефтегазоносности Азербайджана. Баку, 2003.
- Керимов К.М., Новрузов А.К., Данешвар С.Н. Глубинные разломы и некоторые особенности размещения нефтегазовых месторождений в Южно-Каспийской мегавпадине, Вести Бакинского Университета, 2012, №. 3, с. 69-78.
- Керимов В.Ю., Гулиев И.С., Джавадова А.С., Кадиров Ф.А., Мустаев Р.Н., Гурбанов В.Ш., Гусейнова Ш.М. Характеристика нефтегазоматеринских толщ и особенности углеводородных систем Южно-Каспийского бассейна. ANAS Transactions, Earth Sciences, 2024a, №. 1, с. 77-92.
- Керимов В.Ю., Гулиев И.С., Джавадова А.С., Мустаев Р.Н., Гурбанов В.Ш., Гусейнова Ш.М. Сланцевые нефтегазовые системы Южно-Каспийской впадины. ANAS Transactions, Earth Sciences, №. 2, 2024b, с. 123-140.
- Керимов В.Ю., Осипов А.В., Мустаев Р.Н., Минлигалиева Л.И., Гусейнов А.А. Условия формирования и развития пустотного пространства на больших глубинах. Нефтяное хозяйство, №. 4, 2019, с. 22-27.
- Керимов В.Ю., Шилов Г.Я., Мустаев Р.Н., Дмитриевский С.С. Термобарические условия формирования скоплений углеводородов в сланцевых низкопроницаемых коллекторах хадумской свиты Предкавказья. Нефтяное хозяйство, №. 2, 2016, с. 8-11.
- Юсубов Н.П. К вопросу о разломной тектонике депрессионных зон Азербайджана по данным сейсморазведки. SOCAR Proceedings, №. 3, 2020, с. 011-017.
- Юсубов Н.П. О необходимости пересмотра карт тектонического и нефтегазогеологического районирования депрессионных зон Азербайджана. Азербайджанское нефтяное хозяйство, №. 3, 2023, с. 63-72.
- Юсубов Н.П., Гулиев И.С. Грязевой вулканализм и углеводородные системы Южно-Каспийской впадины (по новейшим данным геофизических и геохимических исследований). Элм. Баку, 2022, 168 с.
- Abdullayev N.R., Guliyev I.S., Kadirov F.A., Huseynova Sh.M., Javadova A.S., Maharramov B., Mukhtarov A.Sh. Novel interpretation of the crustal structure and hydrocarbon evolution within the South Caspian and Kura sedimentary basins, Azerbaijan, Geofizicheskiy Zhurnal, Vol. 46, No. 3, 2024, pp. 146-161, <https://doi.org/10.24028/gj.v46i3.306357>.
- Aliyev A.I., Aliyev E.A. Oil and gas potential of great depths. Problems of forecasting, prospecting and exploration. Oscar. Baku, 2011, 420 p. (in Russian).
- Aliyev A.I., Baghir-Zade F.M., Buniat-Zade Z.A., Huseynov A.N., Dadashev F.G., Mekhtiev F.Sh., Salayev S.G., Yusufzade H.B. Oil and gas fields and prospective structures of the Azerbaijan SSR. Elm. Baku, 1985, 108 p. (in Russian).
- Averbukh B.M. Oil and gas geological zoning of complex regions using retrospective analysis of sedimentary-rock basin evolution. Oil and gas geology, No. 1, 1995, <https://geolib.narod.ru/Journals/OilGasGeo/1995/01/Stat/02/ht> (in Russian).
- Bakirov A.A., Varentsov M.I., Bakirov E.A. Oil and gas provinces and regions of foreign countries. Nedra. Moscow, 1971, 544 p. (in Russian).
- Brod I.O. Fundamentals of the doctrine of oil and gas basins. Nedra. Moscow, 1964, 66 p. (in Russian).
- Eppelbaum L., Katz Y., Kadirov F. The relationship between the paleobiogeography of the northern and southern sides of the Neotethys and the deep geodynamic processes. ANAS Transactions, Earth Sciences, 2024, No.1, pp. 57-76.
- Gadzhiev T.G., Huseynov A.N., Akhmedov A.M., Yusufzade H.B., Hasanov I.S., Andreev D.N. Zeynalov A.M., Kasumova A.N., Kuliyeva A.R. Atlas of oil and gas bearing and prospective structures of Azerbaijan. Azerneshr. Baku, 1983, 80 p. (in Russian).
- Hierarchical classification of basin structural elements. Rank of structural-tectonic elements. Geodynamic characteristics. Russian State university of oil and gas, Moscow, 2018, <https://miloserdovalv.narod.ru> poisk > lekcija_2 (in Russian).
- Kadirov F., Yetirmishli G., Safarov R., Mammadov S., Kazimov I., Floyd M., Reilinger R., King R. Results from 25 years (1998-2022) of crustal deformation monitoring in Azerbaijan and adjacent territory using GPS. ANAS Transactions, Earth Sciences, 2024, No.1, pp. 28-43.
- Kadirov F.A. Klokočník J., Eppelbaum L.V., Kostelecký J., Bezděk A. Bouguer gravity data and satellite gravity transformation integration in the Caspian region: an introduction. ANAS Transactions, Earth Sciences, 2023, No. 1, pp. 11-16.
- Kerimov K.M., Huseynov A.N., Gadzhiev F.M., Gasanov I.S., Huseynov G.A., Kocharli Sh.S., Zeynalov M.M. Map of tectonic zoning of oil and gas bearing regions of Azerbaijan. Cartography Factory. Baku, 2002 (in Russian).
- Kerimov K.M., Huseynov A.N., Gadzhiev F.M., Gasanov I.S., Huseynov G.A., Kocharli Sh.S., Zeynalov M.M. Map of oil and gas geological zoning and prospects of oil and gas content of Azerbaijan. Baku, 2003 (in Russian).
- Kerimov K.M., Novruzov A.K., Daneshvar S.N. Deep faults and some features of oil and gas fields in the South Caspian megadepression. Baku University News, 2012, No. 3, pp. 69-78 (in Russian).
- Kerimov V., Kosyanov V., Serikova U. Efficiency and safety of prospecting, exploration and development of oil and gas fields in the waters of the world ocean. Marine Technologies, Gelendzhik, 2019, pp. 10-14.
- Kerimov V., Osipov A.V., Mustaev R.N., Minligalieva L.I., Huseynov D.A. Conditions of formation and development of the void space at great depths. Neftyanoe Khozyaystvo - Oil Industry, 2019, No. 4, pp. 22-27 (in Russian).
- Kerimov V.Y., Bondarev A.V., Mustaev R.N. Estimation of geological risks in searching and exploration of hydrocarbon deposits. Neftyanoe Khozyaystvo - Oil Industry, No. 8, 2017, pp. 36-41, DOI:10.24887/0028-2448-2017-36-41 (in Russian).
- Kerimov V.Y., Osipov A.V., Mustaev R.N., Monakova A.S. Modeling of petroleum systems in regions with complex geological structure. The 16th Science and Applied Research Conference on Oil and Gas Geological Exploration and Development, GEOMODEL-2014, 2014.

- Eppelbaum L., Katz Y., Kadirov F. The relationship between the paleobiogeography of the northern and southern sides of the Neotethys and the deep geodynamic processes. ANAS Transactions, Earth Sciences, 2024, No. 1, pp. 57-76.
- Kadirov F.A. Klokočník J., Eppelbaum L.V., Kostecký J., Bezděk A. Bouguer gravity data and satellite gravity transformation integration in the Caspian region: an introduction. ANAS Transactions, Earth Sciences, 2023, No. 1, pp. 11-16.
- Kadirov F., Yetirmishli G., Safarov R., Mammadov S., Kazimov I., Floyd M., Reilinger R., King R. Results from 25 years (1998-2022) of crustal deformation monitoring in Azerbaijan and adjacent territory using GPS. ANAS Transactions, Earth Sciences, 2024, No. 1, pp. 28-43.
- Kerimov V.Y., Bondarev, A.V., Mustaev R.N. Estimation of geological risks in searching and exploration of hydrocarbon deposits Neftyanoe Khozyaystvo - Oil Industry, No. 8, 2017, pp. 36-41.
- Kerimov V., Kosyanov V., Serikova U. Efficiency and safety of prospecting, exploration and development of oil and gas fields in the waters of the world ocean. Marine Technologies, Gelendzhik, 2019, pp. 10-14.
- Kerimov V.Y., Mustaev R.N., Etirmishli G.D., Yusubov N.P. Influence of modern geodynamics on the structure and tectonics of the Black Sea-Caspian region. Eurasian Mining, 2021, Vol. 35, No. 1, pp. 3-8.
- Kerimov V.Y., Osipov A.V., Mustaev R.N., Monakova A.S. Modeling of petroleum systems in regions with complex geological structure. 16th Science and Applied Research Conference on Oil and Gas Geological Exploration and Development, GEOMODEL 2014, 2014.
- Kerimov V.Y., Senin B.V., Serikova U.S., Mustaev R.N., Romanov P.A. Assessment of the conditions of formation and distribution of structural, lithological, stratigraphic and combined traps in the Black Sea – Caspian region. ANAS Transactions, Earth Sciences, No. 1, 2023, pp. 81-99.
- Magoon L.B., Dow W.G. The petroleum system – From source to trap. American Association of Petroleum Geologists, Tulsa. Memoir, Vol. 60, 1994, 655 p.
- Magoon L.B. Petroleum system: Nature's distribution system for oil and gas. In: (Cleveland, C.J., Ed.) Encyclopedia of Energy, Elsevier Science. Amsterdam, 2004, pp. 823-836.
- Mustaev R.N., Kerimov V.Y., Senin B.V., Lavrenova E.A. Structural-geodynamic and hydrocarbon systems in the Black Sea-Caspian region. ANAS Transactions, Earth Sciences, Special Issue, 2023, pp. 41-45.
- Kerimov V.Y., Guliyev I.S., Javadova A.S., Kadirov F.A., Mustaev R.N., Gurbanov V.Sh., Huseynova Sh.M. Characteristics of source rocks and features of petroleum systems of the South Caspian basin. ANAS Transactions, Earth Sciences, 2024, No.1, pp. 77-92 (in Russian).
- Kerimov V.Y., Guliyev I.S., Javadova A.S., Mustaev R.N., Gurbanov V.Sh., Huseynova Sh.M. Shale oil and gas systems of the South Caspian depression. ANAS Transactions, Earth Sciences, No. 2, 2024, pp. 123-140 (in Russian).
- Kerimov V.Y., Mustaev R.N., Etirmishli G.D., Yusubov N.P. Influence of modern geodynamics on the structure and tectonics of the Black Sea-Caspian region. Eurasian Mining, 2021, Vol. 35, No. 1, pp. 3-8.
- Kerimov V.Y., Senin B.V., Serikova U.S., Mustaev R.N., Romanov P.A. Assessment of the conditions of formation and distribution of structural, lithological, stratigraphic and combined traps in the Black Sea – Caspian region. ANAS Transactions, Earth Sciences, No.1, 2023, pp. 81-99 (in Russian).
- Kerimov V.Y., Shilov G.Ya., Mustaev R.N., Dmitrievsky S.S. Thermobaric conditions for the formation of hydrocarbon accumulations in low-permeable oil reservoirs of the Khadum formation of the Pre-Caucasus. Neftyanoe Khozyaystvo - Oil Industry, No. 2, 2016, pp. 8-11 (in Russian).
- Magoon L.B. Petroleum System: Nature's distribution system for oil and gas. In: (Cleveland C.J., Ed.) Encyclopedia of Energy, Elsevier Science. Amsterdam, 2004, pp. 823-836. DOI:org/10.1016/B0-12-176480-X/00251-5.
- Magoon L.B., Dow W.G. The petroleum system – From source to trap. American Association of Petroleum Geologists, Tulsa. Memoir, Vol. 60, 1994, 585 p., doi/org/10.1306/M60585.
- Mustaev R.N., Kerimov V.Y., Senin B.V., Lavrenova E.A. Structural-geodynamic and hydrocarbon systems in the Black Sea-Caspian region. ANAS Transactions, Earth Sciences, Special Issue, 2023, pp. 41-45.
- Yusubov N.P. To the question of the breaking depressional tectonics of Azerbaijan's zone according to seismic exploration data. SOCAR Proceedings, No. 3, 2020, pp. 14-20 (in Russian).
- Yusubov N.P. On the necessity of reviewing maps of tectonic and oil-gas geological zoning of depressive regions of Azerbaijan. Azerbaijan oil industry, 2023, No. 3, pp. 63-72 (in Russian).
- Yusubov N.P., Guliyev I.S. Mud volcanism and hydrocarbon systems of the South Caspian Basin (according to the latest data from geophysical and geochemical studies). Elm. Baku, 2022, 168 p. (in Russian).

НОВЫЙ ПОДХОД К НЕФТЕГАЗОГЕОЛОГИЧЕСКОМУ РАЙОНИРОВАНИЮ ТЕРРИТОРИИ АЗЕРБАЙДЖАНА

Керимов В.Ю.^{1,2}, Юсубов Н.П.¹, Гулиев И.С.⁴, Кадиров Ф.А.^{1,3}

¹Министерство науки и образования Азербайджанской Республики, Институт нефти и газа, Азербайджан
AZ1000, Баку, ул. Ф. Амирова, 9: vagif.kerimov@mail.ru

²Российский государственный геологоразведочный университет имени Серго Орджоникидзе, Россия
117997, Москва, ул. Миклухо-Маклая, 23

³Министерство науки и образования Азербайджанской Республики, Институт геологии и геофизики, Азербайджан
AZ1073, Баку, просп. Г.Джавида, 119

⁴Президиум Национальной академии наук Азербайджана, Азербайджан
Ул. Истиглалият, 30, Баку, AZ1001

Резюме. Разработаны теоретические основы и создана схема нефтегазогеологического районирования территории Азербайджана на основе введения "бассейновой" характеристики в номенклатуру элементов, выделяемых при "провинциальном" подходе. Новизной в предложенной схеме нефтегазогеологического районирования является выделение иерархического уровня – "углеводородные системы". На территории и в акватории Азербайджана выделяется Каспийско-Куринская нефтегазоносная провинция (мегабассейн). В качестве следующего иерархического уровня нефтегазогеологического районирования в составе нефтегазоносной провинции (мегабассейна) выделены три нефтегазоносные области (бассейны) – Средне-Куринская, Южно-Каспийская и Средне-Каспийская области (бассейны). Следующей категорией иерархически подчинённых элементов в систематике объектов районирования является углеводородная система (УС). В нефтегазоносных бассейнах выделяются генерационные-аккумуляционные углеводородные системы (ГАУС) – естественная система углеводород-

ных флюидов, которая включает в себя очаг генерации, все связанные с ним углеводороды, все значимые элементы и процессы, необходимые для возникновения скоплений нефти и газа. Элементами углеводородных систем наряду с нефтепаринскими породами являются вмещающие породы, ловушки, резервуары и коллекторы, покрышки, перекрывающие толщи, а процессы — это генерация, миграция и аккумуляция скоплений УВ. Неразрывность связей таких элементов углеводородной системы, как очаг генерации нефти и газа, зон его миграции и аккумуляции является важным условием, определяющим корректность нефтегазогеологического районирования и прогноза нефтегазоносности. Такой подход позволяет придерживаться важного принципа — "принципа неразрывности связей между элементами углеводородной системы", основанного на концепции углеводородных систем. В Южно-Каспийском нефтегазоносном бассейне выделяются три классические генерационно-аккумуляционные углеводородные системы: эоцен-плиоценовая; майкоп-плиоценовая и миоцен-плиоценовая. В пределах бассейна выделяются также три нетрадиционные (сланцевые) углеводородные системы: эоценовая, майкопская и диатомовая. В Средне-Куринской области выделяются две углеводородные системы: эоценовая и майкопская; две нетрадиционные (сланцевые) — эоценовая и майкопская. В Средне-Каспийской области выделяются три углеводородные системы: эоцен-плиоценовая, майкоп-плиоценовая и майкоп-меловая, а также три нетрадиционные УС — меловая, эоценовая и майкопская.

Ключевые слова: Нефтегазогеологическое районирование, Азербайджан, бассейн, провинция, углеводородные системы, нефтегазоносные области

AZƏRBAYCAN ƏRAZİSİNİN NEFT-QAZ SAHƏLƏRİNİN GEOLOJİ RAYONLAŞDIRILMASINA YENİ YANAŞMA

Kərimov V.Yu.^{1,2}, Yusubov N.P.¹, Quliyev İ.S.⁴, Qədirov F.A.^{1,3}

¹Azərbaycan Respublikasının Elm və Təhsil Nazirliyi, Neft və Qaz İnstitutu, Azərbaycan
AZ1000, Bakı şəh., F. Əmirov küç., 9: vagif.kerimov@mail.ru

²Sergo Ordjonikidze adına Rusiya Dövlət geologi kəşfiyyat Universiteti, Rusiya
117997, Moskva şəh., Mikluso-Maklay küç., 23

³Azərbaycan Respublikasının Elm və Təhsil Nazirliyi, Geologiya və geofizika İnstitutu, Azərbaycan
AZ1073, Bakı şəh., H.Cavid pr., 119

⁴Azərbaycan Milli Elmlər Akademiyasının Rəyasət Heyəti, Azərbaycan
İstiqlaliyyət küç., 30, Bakı, AZ1001

Xülasə. "Hövzə" xarakteristikasının "Vilayət" yanaşması zamanı ayrılan elementlərin nomenklaturasına daxil edilməsi əsasında Azərbaycanın ərazisinin neft-qaz-geoloji rayonlaşdırılması sxemi işlənib və hazırlanmışdır. Təklif olunan neft və qaz – geoloji rayonlaşdırma sxemindəki yenilik iyerarxik səviyyənin - "karbohidrogen sistemləri"nin ayrılmışdır. Azərbaycanın ərazisində və akvatoriyasında Xəzər-Kür neft-qaz vilayəti (meqahövzə) ayrılır. Neft – qaz vilayətinin (meqahövzə) tərkibində neft-qaz rayonlaşdırmasının növbəti iyerarxik səviyyəsi kimi üç neft-qaz vilayəti (hövzələri)-Orta Kür, Cənubi Xəzər və Orta Xəzər vilayətləri (hövzələri) müəyyən edilmişdir. Rayonlaşdırma obyektlərinin sistematikasında iyerarxik olaraq tabe olan elementlərin növbəti kateqoriyası karbohidrogen sistemidir. Neft və qaz hövzələrində generativ-akkumulyator karbohidrogen sistemləri fərqlənir – generasiya mərkəzini (yəni aktiv neft-qaz süturlarının inkişaf sahəsi), onunla əlaqəli bütün karbohidrogenlər, neft və qaz yiğilmasının baş verməsi üçün lazım olan bütün əhəmiyyətli elementlər və proseslər. Karbohidrogen sistemlərinin elementləri, ana süturları ilə yanaşı, tələləri, kollektorları, qalınlığı üst və proseslər – karbohidrogen qruplarının yaranması, miqrasiyası və yiğilmasıdır. Neft və qazın yaranma Mərkəzi, onun miqrasiya və yiğilma zonaları kimi karbohidrogen sisteminin bu cür elementlərinin əlaqələrinin davamlılığı neft-qaz-geoloji rayonlaşdırmanın düzgünlüğünü və neft-qaz hasilatının proqnozunu müəyyən edən vacib şərtidir. Bu yanaşma, karbohidrogen sistemləri konsepsiyasına əsaslanan "karbohidrogen sisteminin elementləri arasındaki əlaqələrin davamlılığı principi" kimi formalasdırıla bilən vacib bir principle riayət etməyə imkan verir. Karbohidrogen sistemlərinin təhlili və ədədi modeləşdirilməsinin nəticələrinə görə Cənubi Xəzər Neft və qaz hövzəsində üç klassik generativ-akkumulyativ karbohidrogen sistemi müəyyən edilir: Eosen-plioen; Maykop-plioen və Miosen-plioen. Hövzə daxilində üç qeyri-ənənəvi (şist) karbohidrogen sistemi də müəyyən edilir: Eosen, Maykop və Diatom. Orta Kür bölgəsində iki karbohidrogen sistemi müəyyən edilir: Eosen və Maykop; iki qeyri – ənənəvi (şist) - Eosen və Maykop. Orta Xəzər bölgəsində üç karbohidrogen sistemi müəyyən edilir: Eosen-plioen, Maykop-plioen və Maykop-təbaşir. Burada üç qeyri – ənənəvi karbohidrogen sistemi müəyyən edilir – Təbaşir, Eosen və Maykop.

Açar sözlər: Neft-qaz geoloji rayonlaşdırma, Azərbaycan, hövzə, Vilayət, karbohidrogen sistemləri, neft-qaz rayonları

СРАВНИТЕЛЬНАЯ ХАРАКТЕРИСТИКА ЗОЛОТОНОСНОСТИ ТЕРРИГЕННО-КАРБОНАТНЫХ ОТЛОЖЕНИЙ АЛМАЛЫКСКОГО РУДНОГО РАЙОНА С МЕСТОРОЖДЕНИЯМИ КАРЛИНСКОГО ТИПА

Мундузова М.А.¹, Сайитов С.С.¹, Нурходжаев А.К.²

¹Государственное Учреждение «Институт минеральных ресурсов», Узбекистан
100164, Ташкент, ул. Олимлар, д. 64: mavlyuda.munduzova1956@gmail.com

²Государственное Учреждение «Институт геологии и геофизики»
имени Х.М.Абдуллаева, Узбекистан
100164, Ташкент, ул. Олимлар, д. 64

COMPARATIVE CHARACTERISTICS OF THE GOLD CONTENT IN TERRIGENOUS-CARBONATE DEPOSITS OF THE ALMALYK ORE REGION WITH DEPOSITS OF THE KARLIN TYPE

Munduzova M.A.¹, Sayitov S.S.¹, Nurkhodjaev A.K.²

¹Institute of Mineral Resources, Uzbekistan
64, Olimlar str., Tashkent, 100164: mavlyuda.munduzova1956@gmail.com

²Institute of Geology and Geophysics named after H.M.Abdullayev, Uzbekistan
64, Olimlar str., Tashkent, 100164

Keywords: Gold content, terrigenous-carbonate deposits, dolomites, comparison, Almalyk, Karlin, manifestations, deposits

Summary. For the first time in Uzbekistan, studies on gold content in terrigenous-carbonate deposits of the Almalyk ore region were conducted by M.A.Munduzova, S.T.Badalov and others. The gold content was determined both – in the rocks composing these strata and individual occurrences within them. Gold mineralization in terrigenous-carbonate strata can be one of the unconventional sources of gold mineralization. The selected samples from gray, black dolomites containing organic compounds (bituminous) were analyzed both in laboratories of the Republic of Uzbekistan and in laboratories of the USA. The convergence of the results obtained in the laboratories of the two countries was confirmed. Gold mineralization in terrigenous-carbonate rocks in both provinces is finely dispersed, difficult to diagnose and difficult to extract. The author continues the laboratory and technological research on the extraction of gold from terrigenous-carbonate rocks, including studies to determine the relationship of thin, scattered gold with organic matter in black, bituminous dolomites. Gold in sedimentary terrigenous-carbonate rocks is finely disseminated with organic matter. Carlin-type gold deposits are hosted in carbonate sediments and are represented by fine-grained sulfide mineralization. Varieties of gold are distinguished: films on the surface of pyrite and amorphous carbon, gold-organic compounds, native gold, gold in realgar and native arsenic. The most favorable prospecting and predictive signs of such mineralization in the Chatkal-Kurama region are lithological and structural factors, certain formations and areas of conjugation of multidirectional faults and interformational positions in the form of scanning, ferruginization, crushing and other secondary changes.

© 2025 Earth Science Division, Azerbaijan National Academy of Sciences. All rights reserved.

Золоторудные месторождения Карлинского типа являются сингенетично-эпигенетическими, вкрашенными, золотоносными пиритовыми (марказитовыми или арсенопиритовыми) месторождениями, характеризующимися измененными карбонатными породами – аргиллитизированными, сульфидизированными и окремненными (Hofstra, Cline, 2000). Месторождения встречаются в рудных узлах (клusterах), сосредоточенных вдоль достаточно протяженных разломов (Волков, Галямов, 2020).

Месторождения золота Карлинского типа с более 10 000 т запасами составляют около 9-10% мирового производства золота (Волков, Сидоров, 2016). Запасы золота на месторождении Карлинского типа в северной Неваде – 5500 т и по значимости уступают только таковому Витватерсранду в Южной Африке. Месторождение Карлинского типа в районе Дянь-Цянь-Гуй в Западной части Циньлин на юге Китая характеризуются запасами 400 т (Saunders et al., 2014). В

районе Голд Бар (Gold Bar) размещены пять золотоносных месторождений Карлинского типа, которые по совокупности запасов золота достигают 1.6 млн. унций (Yigit, Hofsra, 2003).

Месторождения Карлинского типа размещаются в пределах золоторудного пояса штата Невада (Birak, Hawkins, 1985) и встречаются в сложной геологической обстановке в северо-центральной части Невады, которую обычно называют протерозойской рифтовой западной окраиной Северо-Американского кратона (Hollingsworth et al., 2018). Месторождения золота Карлинского типа являются золото-полисульфидными, тонковкрапленные золотосульфидные руды находятся в ассоциации с реальгаром, аурипигментом и антимонитом (Ибламинов, 2019). В джаспероидах большинство трещин и каверн заполнено друзовым кварцем и могут содержать каолинит, антимонит, барит, кальцит (Cline et al., 2005).

Геохимический профиль руды – Au–Tl–As–Hg–Sb–(Te)–Ba – характеризуется низкими содержаниями Ag и полиметаллов (Волков, Сидоров, 2016). Распределение растворенных рудных компонентов отражает реакции между магматическими гидротермальными флюидами, богатыми Na, и вмещающими породами, богатыми Ca и Mg (Jin et al., 2021). Результаты исследований Йигита и Хофстра показали, что изменение литохимических показателей рудовмещающих пород свидетельствуют о прогрессирующем окремнении, декарбонизации (декальцитизации и дедоломитизации), аргиллизации (иллит) и сульфидизации в зависимости от минерализации золота (Yigit, Hofsra, 2003).

В последнее время проводятся многочисленные работы по выявлению золоторудных месторождений на территории СНГ. А.С.Борисов оценил перспективы золотой минерализации Карлинского типа участка Охловской в Пермском крае. Золото – тонковкрапленное с содержанием органического вещества (Борисов, 2018). Результаты анализа геофизических моделей земной коры показали сходство геодинамических обстановок формирования невадийских и сакындженских месторождений Карлинского типа, что подтверждает высокие перспективы открытия крупных месторождений в этом арктическом районе Якутии (Волков и др., 2020).

Предпосылки обнаружения золотосульфидного оруденения в палеозойских терригенно-карбонатных толщах Момонтайской площади Магаданской области установлены Рязановым К. По среднему течению ручья Ясный выявлены комплексные аномалии золота, бария, сурьмы, ртути и других элементов, которые характерны для месторождений Карлинского типа (Рязанов,

Енгалычев, 2020). Результаты работ Хомича и Борискиной свидетельствуют о сопоставимости тектоно-стратиграфических факторов и геодинамических позиций, повлиявших на формирование месторождений Карлинского типа в Неваде (США) и в юго-западных провинциях Китая и Приамурья (РФ) (Хомич, Борискина, 2020).

Для Восточного Казахстана впервые выделены новые апокарбонатные формационные типы золотоносных джаспероидов. На примере Байбуринского рудного поля изучены структурно-геологические особенности рудных тел золотоносных джаспероидов (Кузьмина, 2015).

В Узбекистане впервые было выявлено несколько объектов золота, размещенных в карбонатных отложениях и представленных тонкозернистой сульфидной минерализацией в горах Букантау, Чакилкаян, Чаткало-Кураме. Нетрадиционные апокарбонатные типы золотого оруденения (Карлинский тип) в Узбекистане довольно широко рассмотрены в работе В.Д. Цоя (Цой, 2010; Цой и др., 2011), М.А.Мундузовой (2004; Цой и др., 2011). Построенная модель формирования апокарбонатного золотого оруденения отражает привнос рудоносных растворов $\text{SiO}_2 + \text{Al}_2\text{O}_3$ (Au, WO₃) вдоль рудоподводящего разлома, наложение их на доломиты с образованием кварца, шеелита и золота (Цой, 2010; Цой и др., 2011).

Черты сходства с металлогеническими позициями (наличие золоторудной провинции) Привинции Бассейнов и Хребтов Западного Тянь-Шаня по комплексу признаков охарактеризованы Поповым (1958). Алмалыкский рудный район расположен на северных склонах Кураминского хребта и входит в состав Кураминской подзоны Чаткало-Кураминской структурно-фацальной зоны (Акбаров, Умарходжаев, 1978).

Особенности геологического строения месторождений Карлинского типа

Карлинский тип характеризует часть мезозойско-кайнозойской золотоносной провинции, протянувшейся с севера на юг вдоль западной части Северной Америки, к которой относятся месторождения коренного золота различных геолого-промышленных типов. Карлинская залежь, находящаяся в Центре рудного поля, стала типовой для класса осадочных мелковкрапленных золотоносных месторождений, обычно известных как «залежи Карлинского типа». Открытое в 1960 г. геологами «Ньюмонт Майнинг», оно стало первым в мире крупным месторождением золота, разрабатывавшимся методом открытой добычи. С того времени в районе было обнаружено более 30 отдельных месторождений.

Золотое оруденение типа Карлин локализуется в существенно карбонатных породах во всем стратиграфическом диапазоне от ордовика до позднего триаса включительно. Здесь выявлено тонкодисперсное золото субмикроскопических размеров, аккумулированное в пирите. Околорудные процессы представлены окварцеванием, аргиллитизацией пород, переотложением углеродистого вещества (Clark, 1970; Radtke, 1985).

Формирование месторождений Карлинского типа связывают с постмагматическими флюидами. Данные о распределении растворенных веществ свидетельствуют о реакции флюид-породы между богатыми Na магматическими гидротермальными флюидами и вмещающими породами, богатыми Ca и Mg (Акбаров, Умарходжаев, 1978).

Исследование мантийных плюмов месторождения типа Карлин в пределах бассейна Юцзян в восточной части крупной магматической провинции Эмэйшань указывает на возраст 260 млн. лет (Zhu et al., 2020).

Rb-Sr изотопный анализ золотосодержащих кварцевых флюидных включений золоторудного месторождения Нибао в Китае определяет его Rb-Sr изохронный возраст 142 ± 3 и 141 ± 2 млн. лет (Lulin Zheng et al., 2019).

Месторождение Карлин находится в северной части штата Невада, примерно в 50 км к западу от г. Элко. Месторождение располагается у восточного края тектонического окна Линн в зоне надвига Робертс-Маунтинс. В районе выделяется 8 таких окон с собственными наименованиями.

Тектоническое окно Линн представляет собой выход на поверхность карбонатных пород лежачего бока надвига (автохтона). Оруденение приурочено к верхней части формации Робертс-Маунтин, представленной илистыми тонкослоистыми известняками, доломитистыми известняками, содержащими глинистый и песчанистый материал (рис.1).

Между разломами заключено все золотое оруденение, представленное Восточным, Главным и Западным рудными телами пластовой формы, в целом согласными со слоистостью. На стыке Главного и Восточного рудных тел пластовые залежи размещаются в два яруса друг над другом.

Выделяются разновидности золота:

- пленочные, на поверхности пирита и аморфного углерода;
- золотоорганические соединения;
- самородное золото;
- золото в реальгаре и самородном мышьяке.

Основная масса золота тяготеет к пириту и как бы пропитывает его.

На месторождении выделяются два типа рудных тел:

- согласные со слоистостью пластиообразные залежи;
- залежи в сбросах и придайковом пространстве, сопряженные с пластовыми телами и удаленные от них.

Разведанные запасы руд, пригодные для открытой разработки, составляют 10 млн. тонн при среднем содержании золота 1.1 г/т.

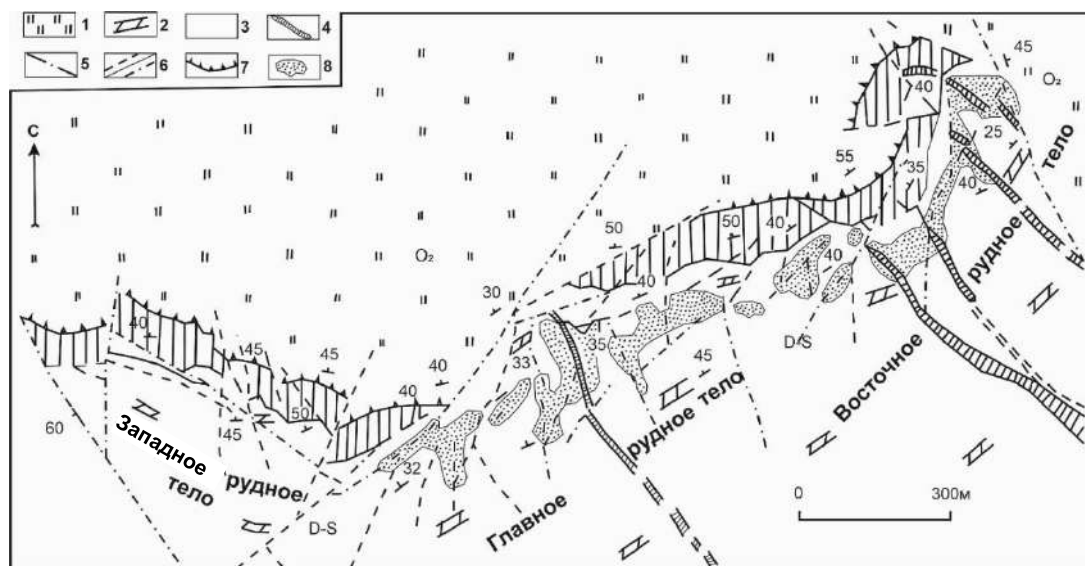


Рис. 1. Геологическая карта месторождения Карлин (по материалам A.S.Radtke, (Radtke, 1985))

1 – кремнистые и углисто-глинистые сланцы (O_2); 2 – глинистые доломиты (D-S); 3 – известняки (D₁); 4 – дайки гранодиорит-порфиров (J₃-K); 5 – протяженные, возможно рудоконтролирующие разломы; 6 – непротяженные разломы: а) прослеженные участки, б) фланговые участки; 7 – взброс Роберт Маунтине; 8 – золоторудные залежи

Месторождение Гэтчел расположено в северо-восточной части штата Невада (рис. 2). К зоне дробления сброса приурочено 2200-метровое ленточное тело север-северо-западного направления с апофизами, проникающими в гранодиориты. Максимальные мощности рудных тел в аргиллитах и на контактах этих пород с известняками – 35 м. Отрабатывались руды с содержаниями более 3-5 г/т золота. В руде часть золотинок имеет размер до 4 мкм.

Месторождение Кортек залегает в доломитизированных известняках, насыщенных синге-

нетическим пиритом. Золотое оруденение приурочивается к зонам разломов и горизонтам выщелачивания. Субмикроскопическое золото размером от 0.2 до 10 микронов устанавливается в халцедоне, кварце, лимонитизированном пирите и гидрослюдах.

В Алмалыкском рудном районе (Центральный блок) в геолого-структурном отношении и по метасоматическим преобразованиям рудопроявление Балантепе сходно с месторождением Кортек (рис. 3, 4).

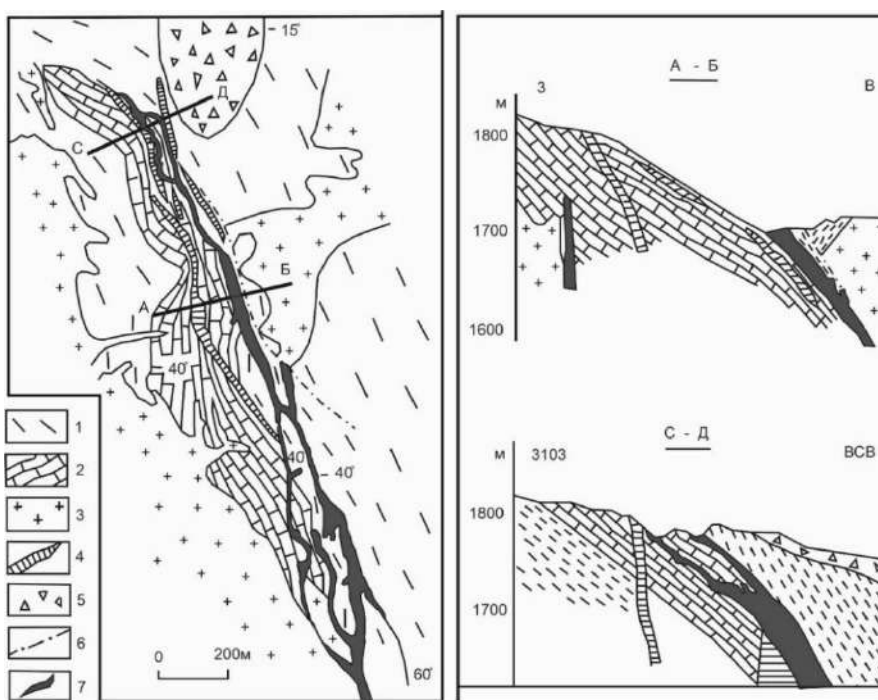


Рис. 2. Геологическая схема месторождения Гэтчел
(по материалам Е.М.Некрасова, (Некрасов, 1988))

1 – аргиллитовые сланцы, 2 – известняки, 3 – гранодиориты, 4 – андезитовые порфиры, 5 – риолитовые туфы, 6 – разрывы, 7 – залежи прожилково-вкрашенных руд

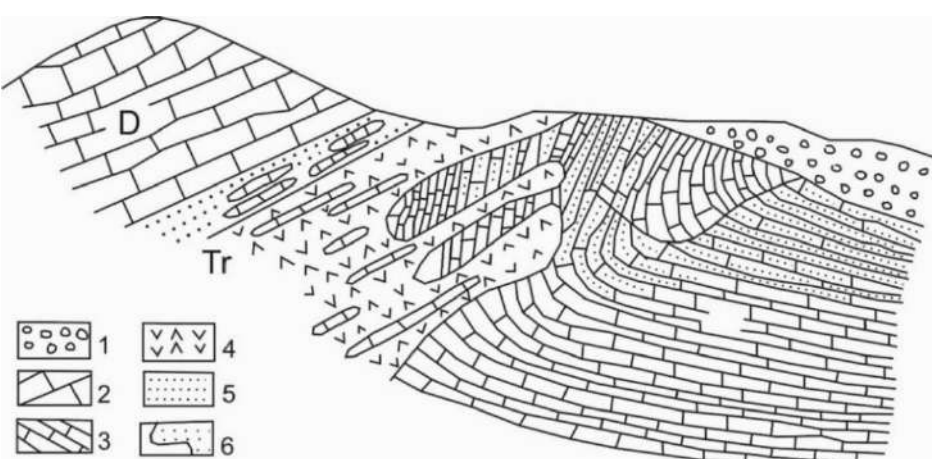


Рис. 3. Геологический разрез через месторождение Кортек

1 – четвертичные отложения; 2 – известняки формации Венбан; 3 – известняки и известковистые алевролиты формации Роберт Маунтин; 4 – биотит-кварцевые порфиры; 5 – зона измененных (окремненных, осветленных окрашенных гидроокислами железа в бурый свет) известняков; 6 – золотоносные тела

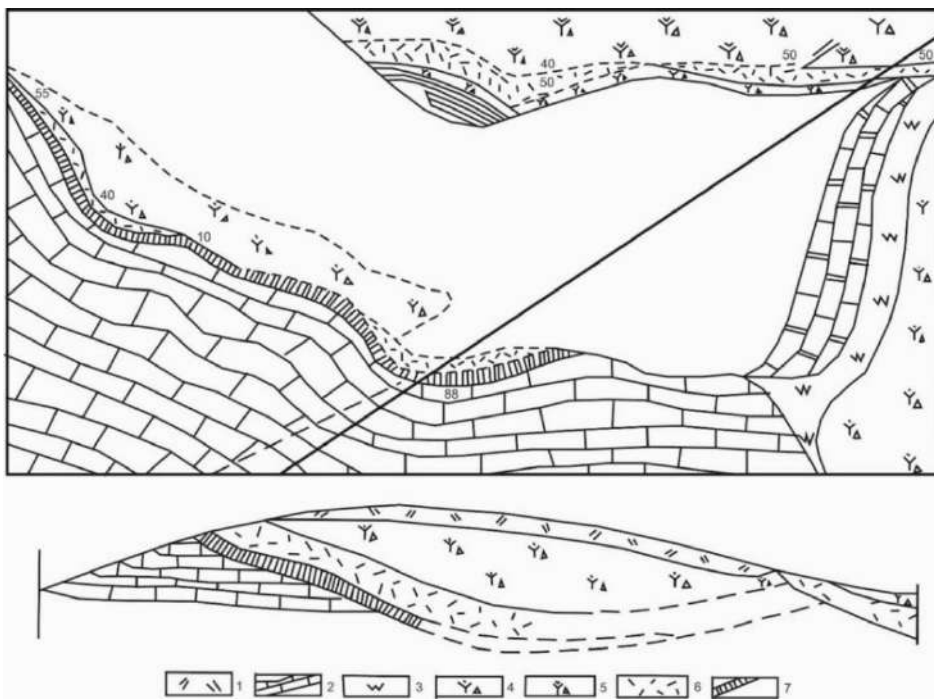


Рис. 4. Схема геологического строения рудопроявления Балантепе
(по материалам М.А.Мундузовой, 2004)

1 – нансы; 2 – карбонаты Дз; 3 – монокварциты; 4 – брекции андезито-дацитового состава С₂; 5 – андезито-дацитовые порфириты; 6 – зоны дробления; 7 – зоны окварцевания

Е.М.Некрасов Карлинский тип относит к месторождениям углеродсодержащих карбонатных и терригенных (вулканогенных) карбонатных толщ. Он подчеркивает, что географически месторождения этого типа размещаются в пределах золоторудного пояса штата Невада. На других территориях США рудные объекты рассматриваемого типа чрезвычайно редки (Некрасов, 1988).

Специфика месторождений Карлинского типа, как подчеркивает А.И.Кривцов, заключается в том, что оруденение в большинстве случаев оказывается представленным пластовыми залежами кварцевых метасоматитов джаспероидного типа, тонко- и даже скрытокристаллического облика (Кривцов, 1988). Залежи содержат обильную вкрапленность пирита и сульфидов сурьмы, мышьяка, ртути, преобладающих над сульфидами цветных металлов. Почти все известные месторождения возникают в активизированных зонах передовых прогибов складчатых систем или окраин кратонов, платформ.

Месторождения обладают специфическими чертами:

- представляют собой минералого-геохимическую ассоциацию при нахождении мышьяка преимущественно в виде реальгара и аурипигмента;

- характеризуются тонкодисперсной формой нахождения золота в рудах и его парагенезисом с кварцем, глинисто-гидрослюдистыми минералами и «битумами»;

– вне зависимости от структурно-морфологических типов рудных тел, трещинные или пластообразные, все они локализуются в горизонтах определенного литологического состава.

Месторождения типа Карлин локализуются в известняках, доломитах, известковистых сланцах различного возраста: ордовик (месторождение Джеррит Каньон), девон (Карлин, Гэтчел, Голд Акресс, Бутстрон, Манхэттен, Меркур и др.), триас (Релайф-Каньон), ордовик, силур, девон, триас (Магги Крик) (рис. 5).

Эксплуатирующиеся руды имеют предельно бедные содержания, иногда ниже 1г/т. Поэтому в разведку вовлекаются только те объекты, которые могут разрабатываться открытым способом с применением кучного выщелачивания руд. А.С.Radtke относит Карлинский тип месторождений к стратиформным и допускает длительность формирования месторождений с выделением сингенетического этапа рудонакопления и эпигенетического этапа перераспределения руд. Главным фактором прогноза подобных объектов следует считать литолого-стратиграфический контроль оруденения, его приуроченность к определенным фациям и формациям. Основные признаки, контролирующие размещение месторождений типа Карлин:

- литологический признак – размещение месторождений в известняках, доломитах, известковистых сланцах, конгломератах, обогащенных углеродсодержащим веществом;

– геотектонический признак – размещение в геосинклинально-складчатой системе с наложенным континентальным рифтом;

– металлогенический признак – размещение месторождений в золотоносной провинции, где наряду с месторождениями золота типа Карлин имеются золотосодержащие месторождения других формаций (скарновая, медно-порфировая, полиметаллическая и медно-колчеданная);

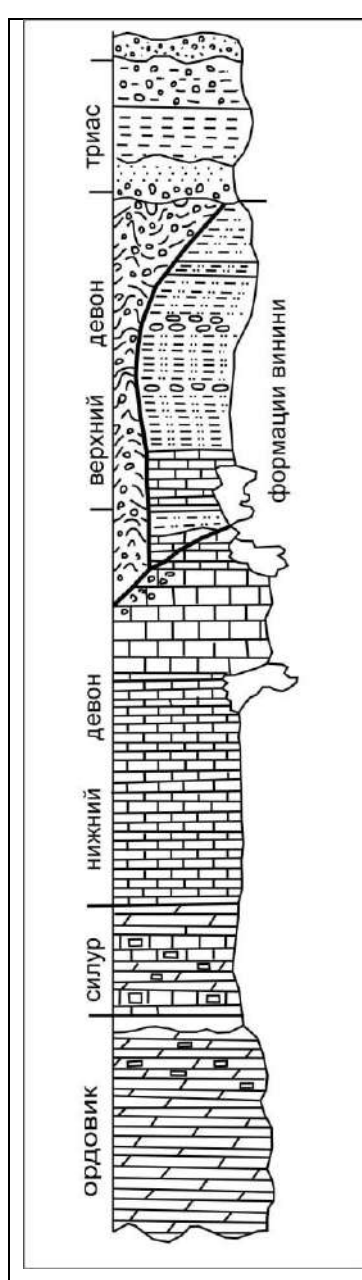
– структурный признак – оруденение контролируется крупными региональными нарушениями. Практически всё оруденение локализуется в подэкранных позициях. Размещение рудных тел приурочено к сколовым нарушениям. Наличие этих признаков в других регионах является

достаточным для положительной оценки их металлогенического потенциала на Карлинский тип месторождений золота.

Признаки геологической общности территорий и месторождений Карлинского типа и Алмалыкского рудного района (Центральный блок)

По результатам сопоставления региональных геологических и металлогенических особенностей западной части североамериканского континента с Чаткало-Кураминским регионом для оценки металлогенического потенциала территории на золотое оруденение Карлинского типа можно заключить следующее.

Аллювий
Карлинская формация 550' выветрелые гуфы, озерные вулканокластические осадки, гравий и коллювий, кварцевые монцониты, монцониты, дайки.
Пачка Quarry 700' Переслаивание аргиллитов, кремнистых образований, глинистых сланцев, известняков и песчаников.
Пачка James Creek 200 -400' Переслаивание черных тонкослоистых кремнисто-известковистых сланцев, доломитов и аргиллитов.
Девонские известняки 100 -400' средне-тонкослоистые известняки, илистые и глинистые образования.
Формация Роберт Маунтинс 1000'-1500' средне-тонкослоистые серые известняки и доломиты, глинистые и доломитистые алевролиты.
Формация Hanson Creek 600 -900 Окварцованные черные битуминозные известковистые сланцы, переходящие в битуминозные известняки.



The stratigraphic column diagram illustrates the geological sequence from bottom to top:

- Ордовик (Ordovician):** Shows alternating layers of horizontal and wavy patterns.
- Силур (Silurian):** Shows horizontal layers with some internal cross-hatching.
- Нижний девон (Lower Devonian):** Shows thick, horizontal layers.
- Верхний девон (Upper Devonian):** Shows thin, horizontal layers.
- Девон (Devonian):** Shows thick, horizontal layers.
- Триас (Triassic):** Shows horizontal layers with small circular features.

A diagonal line labeled "формации винини" (Vining Formation) runs through the Devonian and Lower Carboniferous layers.

Рис. 5. Генеральная стратиграфическая колонка Магги Креек Subdistrict (по материалам геохимической конференции по Карлинскому тренду, 1991).

На Американском континенте месторождения типа Карлин находятся в Провинции Бассейнов и Хребтов, которая в геотектоническом плане представляет собой континентальный рифт на геосинклинально-складчатой системе Кордильер.

Территория Кураминской подзоны представляет собой геосинклинально-складчатую область, подвергшуюся континентальному рифтогенезу в позднем палеозое. Рудовмещающие толщи формировались в близких палеогеографических условиях. Это морские мелководные и лагунные бассейны, где формировались толщи, состоящие из различного чередования известняков, доломитов, песчаников, алевролитов с прослойками гипсов, с резкой сменой гидродинамических и гидрохимических режимов. Для них характерна интенсивная насыщенность отдельных ритмов органическим веществом. Особый палеотектонический режим, наличие крупных долгоживущих разломов обусловили обогащение осадков, в первую очередь содержащих органическое вещество, сингенетичными концентрациями золота, свинца, цинка и других элементов.

Вещественный состав и минералогические особенности руд, типичные для Карлинского типа, мало изучены в Алмалыкском рудном районе. Химико-аналитическими исследованиями терригенно-карбонатных пород Алмалыкского рудного района установлено наличие ртути, варьирующей от 0.09 до 2.1 г/т. Контрольные анализы карбонатных пород, проведенные в лаборатории «Newmont» (1998), показали тот же порядок содержаний ртути от 0.8 до 4.5 г/т. (табл. 1, 2). Низкие содержания ртути в карбонатных породах Алмалыкского рудного района, по сравнению с Карлинским типом, объясняются металлогеническими особенностями исследуемого региона, характеризующегося активной магматической деятельностью в палеозойское время.

Ртуть является элементом широкого рассеяния, поэтому она для районов с активным магма-

тизмом не характерна. Ртутные месторождения, как правило, являются телетермальными, удаленными от магматизма (Мундузова, 2020).

Для Алмалыкского рудного района и Карлинского типа характерны: первое – сквозной характер золоторудной минерализации, которая встречается как в самих высокотемпературных (скарны), так и средне- (порфировые руды) и низкотемпературных (зоны окварцевания и доломитизации) образований. Это – единое «рудное дерево». Второе – четко выраженная структурно-генетическая позиция оруденения, его связь в данном случае с более высокотемпературными образованиями. В этом случае, по-видимому, можно выстроить единый ряд золоторудных формаций – эпискарновый, медно-порфировый, полиметаллический и, собственно золоторудный, с объектами низкотемпературного тонкодисперсного золота. Третье – связь золотого оруденения Алмалыкского рудного района с определенными типами пред- и внутрирудных метасоматитов: зонами окварцевания, развивающимися на фоне блоков пород, подвергшихся предрудной доломитизации.

В Алмалыкском рудном районе проявления золота размещаются в карбонатных породах верхнего девона (франский и фаменский ярусы). Обязательными элементами являются пологие структуры экранирования. В районе Карлинского типа это пологие надвиги (формация Виннини, фация Попович), в Алмалыкском рудном районе – подошва вулканитов верхнего палеозоя. В Алмалыкском рудном районе роль пологих экранов могут играть подошвы пород с различными физическими свойствами: контакт кварцевых порфиров D₂ и карбонатных толщ D₃ (участок Карасай), то же наблюдается в районе Карлинского типа (Кортец-фация Попович, формация Виннини). Аналогичные примеры можно привести — это месторождение Булуткан в Кызылкумах, месторождения Бургунда, Скальное, Джаманкудук в Таджикистане (рис. 6.).

Таблица 1

Результаты нейтронно-активационного анализа карбонатных пород
по данным ОАО «ANALIT – SERVIS», на золото и ртуть, в г/т

№№ п/п	Название породы	Au	Hg
1	Аргиллит окварцованный	0.4	0.4
2	Доломит окварцованный	2.5	2.1
3	Песчаник окварцованный	1.3	0.5
4	Доломит окварцованный	1.2	1.4
5	Доломит ожелезненный, окварцованный	1.1	1.4
6	Известняк окварцованный	1.5	0.1
7	Доломит ожелезненный, окварцованный	2.0	0.5
8	Доломит ожелезненный, окварцованный	1.4	0.4
21	Песчаник ожелезненный	2.3	0.09
29	Аргиллит ожелезненный, окварцованный	0.05	0.09
29/1	Известняк ожелезненный	0.3	0.05
32	Доломит ожелезненный, окварцованный	0.3	0.1

Таблица 2

Вариации содержания основных элементов в карбонатных породах Алмалыкского рудного района, по данным лаборатории «Newmont», в г/т

Название пород	Au	Sb	As	Ba	Ca	Cr	Cu	Pb	Mn	Hg	Mo	Ag	Zn
Карбонатная порода	1-3	2.9-130	14-1245	20-37	1>15%	83-566	13-171	22-4580	80>10000	0.8-4.5	2.6-27.6	0.12-22.2	16-4390

В обоих районах пространственно и во времени месторождения связаны с проявлениями магматической деятельности. В Алмалыкском рудном районе это кварцевые порфиры, гранодиориты, сиенито-диориты Сз, в Карлинском типе – третичные субинтрузивные породы, представленные кварцевыми монцонитами, гранодиоритами.

Вещественный состав рудных тел, минеральные ассоциации, типоморфные особенности слагающих их минералов имеют как сходства, так и отличия:

– обладают нераспознаваемыми признаками осадочного золота, именуемыми «микроскопическим золотом» или «невидимым тонкодисперсным золотом»;

– характеризуются геолого-структурными условиями размещения оруденения;

– имеет место широкое развитие процессов окварцевания, доломитизации, аргиллитизации, низкотемпературного кварц-серийцитового метасоматоза;

– состав вмещающей среды – терригенно-карбонатные образования;

– обладают близким минеральным составом руд умеренно- и малосульфидных месторождений Алмалыкского рудного района (Каратагата, Карасай, Серая Скала, Бургунда, Южный-П) с типичными месторождениями Карлинского типа (Гэтчел, Эврика, Батл Маунтин);

– выявлен одинаковый литолого-стратиграфический контроль оруденения.

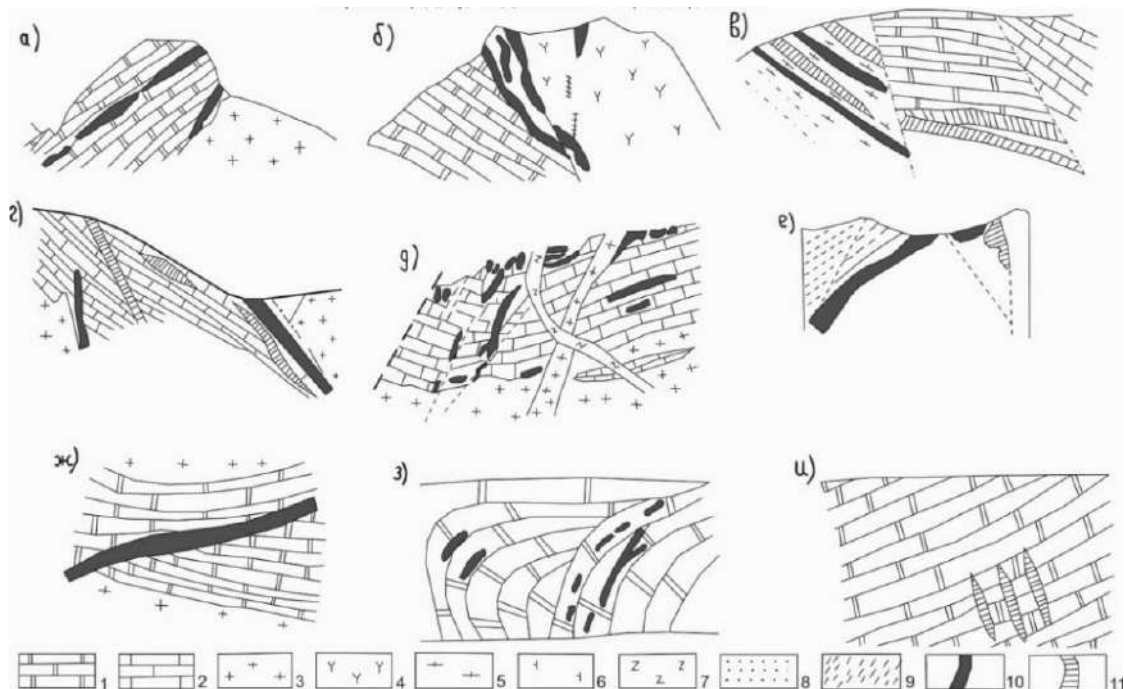


Рис.6. Структурно-морфологические особенности размещения рудных тел на примере Алмалыка (а, б, в), Карлина (г,д,е), Таджикистана (ж,з,и)

1 – доломиты; 2 – известняки; 3 – гранодиориты; 4 – андезито-дацитовые порфиры; 5 – кварцевые порфиры; 6 – туфы с подчиненными конгломератами, песчаниками, известняками; 7 – риолиты; 8 – формация Роберта Маунтинс; 9 – глинистые сланцы; 10 – рудные тела; 11 – зона окварцевания, джаспероиды

Выводы

Вещественный состав рудных тел, минеральные ассоциации, типоморфные особенности слагающих их минералов имеют как сходства, так и отличия:

- обладают нераспознаваемыми признаками осадочного золота, именуемого «микроскопическим золотом» или «невидимым тонкодисперсным золотом»;
- характеризуются геолого-структурными условиями размещения оруденения;
- имеет место широкое развитие процессов окварцевания, доломитизации, аргиллитизации, низкотемпературного кварца-серицитового метасоматоза;
- обладают близким минеральным составом руд умеренно- и малосульфидных месторож-

дений Алмалыкского рудного района (Карасай, Серая Скала, Бургунда, Южный-II) с типичными месторождениями Карлинского типа (Гэтчел, Батл Маунтин, Кортен);

- выявлен одинаковый литолого-стратиграфический контроль оруденения;
- установлена близкая геохимическая характеристика руд (за исключением Hg);

Разновозрастные рудные образования на разных континентах вряд ли будут полностью идентичны. Они сходны в главном – в литолого-стратиграфическом контроле оруденения, в геотектоническом режиме формирования как рудовмещающих толщ, так и рудных тел, а также в парагенезисе рудных формаций.

ЛИТЕРАТУРА

- Акбаров Х.А., Умарходжаев М.У. и др. Типы геолого-структурных позиций, рудных полей и месторождений Чаткало-Кураминского региона. В кн.: Структурные условия размещения руд, методы их прогнозирования, оценки и разведки, Среднеаз. Научн.-исслед. Ин-т геологии и минерального сырья (САИГИМС). Ташкент, вып.1, 1978, с 44-51.
- Борисов А.С. Особенности распределения золота в терригено-карбонатных комплексах на западном склоне Урала. В: Стратегия и процессы освоения георесурсов. Сборник научных трудов, Пермь, выпуск 16, 2018, с. 70-74.
- Волков А.В., Галямов А.Л. Геофизическая модель земной коры, геодинамические обстановки и перспективы открытия месторождений золота карлинского типа в Арктической зоне Республики Саха (Якутия). Арктика: экология и экономика. №. 1 (37), 2020, с. 82-94, DOI: 10.25283/2223-4594-2020-1-82-94.
- Волков А.В., Галямов А.Л., Лобанов К.В. Перспективы открытия новых крупных месторождений стратегических металлов в Арктической зоне России. Труды Ферсмановской научной сессии, ГИ КНЦ РАН, №.17, 2020, с. 89-96, <https://doi.org/10.31241/FNS.2020.17/017>.
- Волков А.В., Сидоров А.А. Геолого-генетическая модель месторождения золота карлинского типа. Литосфера, №. 6, 2016, с. 145-165.
- Ибламинов Р.Г. Геология месторождений полезных ископаемых (Геология и генезис месторождений эндогенной серии. 2-я часть). Издательский центр Пермского государственного национального исследовательского университета. Пермь, 2019, 232 с.
- Кривцов А.И. Основные тенденции развития минерально-сырьевой базы цветных и благородных металлов за рубежом. Советская геология, №. 2, 1988, с. 37-46.
- Кузьмина О.Н. Геология, минералогия и условия формирования золото-сульфидного оруденения восточного Казахстана (на примере Байбуринского и Жайминского рудных полей). Автореферат диссертации на соискание ученой степени к.г.-м.н., Новосибирск, 2015, 240 с.
- Мундузова М.А. Золотоносность среднепалеозойских терригенно-карбонатных толщ Алмалыкского рудного района (Центральный блок). Ташкент, Диссертация на соискание ученой степени кандидата геолого-минералогических наук. 2004, 109 с.
- Некрасов Е.М. Зарубежные эндогенные месторождения золота. Недра. Москва, 1988, 286 с.
- Попов В.И. История депрессий и поднятий Западного Тянь-Шаня. Ташкент, 1958, 135 с.

REFERENCES

- Akbarov H.A., Umarkhodjaev M.U., et al. Types of geological and structural locations, ore fields and deposits of the Chatkal-Kurama region. In: Structural conditions of ore placement, methods of their prediction, evaluation and exploration, Tashkent, Central Asian scientific-research Institute of Geology and Mineral Raw Materials, issue 1, 1978, pp. 44-51 (in Russian).
- Birak D.J., Hawkins R.B. The geology of the Enfield Bell mine and the Jerritt Canyon district, Elko county, Nevada. US Geol. Surv. Bull., No. 1646, 1985, pp. 95-106.
- Borisov A.S. Features of gold distribution in terrigenous-carbonate complexes on the western slope of the Urals. In: Strategy and processes of development of georesources. Collection of scientific papers, Perm, issue 16, 2018, pp. 70-74 (in Russian).
- Clark W.B. Gold districts of California. Bull Calif. Division of mines and geology, Vol. 193. 1970, 186 p.
- Cline J.S., Hofstra A.H., Muntean J.L., Tosdal R.M., Hickey K.A. Carlin-type gold deposits in Nevada: Critical geologic characteristics and viable models. Society of Economic Geologists, Inc. Economic Geology 100th Anniversary Volume, 2005, pp. 451-484.
- Hofstra A.H., Cline J.S. Characteristics and models for Carlin-type gold deposits. SEG Reviews, Vol. 13, 2000, p. 163-200.
- Hollingsworth E.R., Ressel M.W., Henry Ch.D. Age and depth of Carlin-type gold deposits in the Southern Carlin Trend: Eocene mountain lakes, big volcanoes, and widespread, shallow hydrothermal circulation. Geological Society of Nevada field trip guidebook: Shallow expressions of Carlin-type gold deposits: Alligator Ridge and Emigrant mines, Nevada. 2018, pp. 149-173.
- Iblaminov R.G. Geology of mineral deposits (Geology and genesis of endogenous series deposits. 2nd part). Publishing Center of Perm State National Research University. Perm, 2019, 232 pp. (in Russian).
- Jin X., Yang C., Liu J., Wu Y. Source and evolution of the ore-forming fluids of Carlin-type gold deposit in the Youjiang Basin, South China: Evidences from solute data of fluid inclusion extracts. Journal of Earth Science, Vol. 32, No.1, 2021, pp. 185-194, DOI: 10.1007/s12583-020-1055-x.
- Khomich V.G., Boriskina N.G. Potential prospects of detection of noble metal mineralization of the Carlin type in the Gonzhinsky district of the Amur region. Advances in modern natural science, No. 7, 2020, pp. 168-173, DOI:10.17513/use.37449 (in Russian).
- Kravtsov A.I. Main tendencies in the development of the mineral resource base of non-ferrous and precious metals abroad. Soviet Geology, No. 2, 1988, pp. 37-46 (in Russian).

- Рязанов К.П., Енгалычев С.Ю. Перспективы выявления объектов золотосульфидного оруденения Карлинского типа в палеозойских терригенно-карбонатных толщах Момонтайской площади (Север Магаданской области). Структура, вещества, история литосферы Тимано-Североуральского сегмента. Материалы 29-й научной конференции Института геологии Коми НЦ УрО РАН, Сыктывкар, 2020, с. 94-97.
- Хомич В.Г., Борискина Н.Г. Потенциальная перспективность обнаружения благороднометалльного оруденения карлинского типа в Гонжинском районе Приамурья. Успехи современного естествознания, №. 7, 2020, с. 168-173, DOI:10.17513/use.37449.
- Цой В.Д. Апокарбонатная модель формирования золотого оруденения Узбекистана. Матер. Всерос. Конф. «Самородное золото, типоморфизм минеральных ассоциаций, условия образования месторождений, задачи прикладных исследований». ИГЕМ РАН. Москва, Том II, 2010, с. 289-291.
- Цой В.Д., Королёва И.В., Мундузова М.А., Захидов А.Р. Нетрадиционный апокарбонатный тип золотого оруденения Узбекистана. (Отв. Ред. Исоков М.У.). Госком РУЗ по геологии и минеральным ресурсам, Госпредприятие «Научно-исследовательский институт минеральных ресурсов». Ташкент, 2011, 174 с.
- Birak D.J., Hawkins R.B. The geology of the Enfield Bell mine and the Jerritt Canyon district, Elko county, Nevada. US Geol. Surv. Bull., No. 1646, 1985, pp. 95-106.
- Clark W.B. Gold districts of California. Bull Calif. Division of mines and geology, Vol. 193. 1970, 186 p.
- Cline J.S., Hofstra A.H., Muntean J.L., Tosdal R.M., Hickey K.A. Carlin-type gold deposits in Nevada: Critical geologic characteristics and viable models. Society of Economic Geologists, Inc. Economic Geology 100th Anniversary Volume, 2005, pp. 451-484.
- Hofstra A.H., Cline J.S. Characteristics and models for Carlin-type gold deposits. SEG Reviews, Vol. 13, 2000, p. 163-200.
- Hollingsworth E.R., Ressel M.W., Henry Ch.D. Age and depth of Carlin-type gold deposits in the Southern Carlin Trend: Eocene mountain lakes, big volcanoes, and widespread, shallow hydrothermal circulation. Geological Society of Nevada field trip guidebook: Shallow expressions of Carlin-type gold deposits: Alligator Ridge and Emigrant mines, Nevada. 2018, pp. 149-173.
- Jin X., Yang C., Liu J., Wu Y. Source and evolution of the ore-forming fluids of Carlin-type gold deposit in the Youjiang Basin, South China: Evidences from solute data of fluid inclusion extracts. Journal of Earth Science, Vol. 32, No.1, 2021, pp. 185-194, DOI: 10.1007/s12583-020-1055-x.
- Lulin Zheng, Ruidong Yang, Junbo Gao, Jun Cheng, Jianzhong Liu, Depeng Li. Quartz Rb-Sr isochron ages of two type orebodies from the Nibao Carlin-Type Gold Deposit, Guizhou, China. Minerals, Vol. 9(7), 399, 2019, pp. 3-15, DOI:10.3390/min9070399.
- Radtke A.S. Geology of the Carlin gold deposit, Nevada. US Geol. Surv. Profess. Paper. No. 1267, 1985, 124 p., <https://doi.org/10.3133/pp1267>.
- Saunders J.A., Hofstra A.H., Goldfarb R.J., Reed M.H. Geochemistry of hydrothermal gold deposits. Treatise on Geochemistry, 2nd Edition, Vol. 13, 2014, pp. 383-424, DOI:10.1016/B978-0-08-095975-7.01117-7.
- Yigit O., Hofstra A.H. Lithogeochemistry of Carlin-type gold mineralization in the Gold Bar district, Battle Mountain-Eureka trend, Nevada. Ore Geology Reviews, Vol. 22, No. 3-4, 2003, pp. 201-224, DOI:10.1016/S0169-1368(02)00142-7.
- Zhu J., Zhang Z.C., Santosh M., Jin Z.L. Carlin-style gold province linked to the extinct Emeishan plume. Earth and Planetary Science Letters, Vol. 530, No. 115940, 2020, <https://doi.org/10.1016/ersl.2019.115940>.
- Kuzmina O.N. Geology, mineralogy and conditions of formation of gold-sulfide mineralization of the eastern Kazakhstan (on the example of Bayburin and Zhaimin ore fields). Abstract of the dissertation on the degree of candidate of geological and mineralogical sciences, Novosibirsk, 2015 (in Russian).
- Lulin Zheng, Ruidong Yang, Junbo Gao, Jun Cheng, Jianzhong Liu, Depeng Li. Quartz Rb-Sr isochron ages of two type orebodies from the Nibao Carlin-Type Gold Deposit, Guizhou, China. Minerals, Vol. 9(7), 399, 2019, pp. 3-15, DOI:10.3390/min9070399.
- Munduzova M.A. Gold content of the Middle Paleozoic terrigenous-carbonate strata of the Almalyk ore region (Central block). Dissertation on the degree of candidate of geological and mineralogical sciences, Tashkent, 2004, 109 p. (in Russian).
- Nekrasov E.M. Foreign endogenous gold deposits. Nedra. Moscow, 1988, 286 p. (in Russian).
- Popov V.I. History of depressions and uplifts of the Western Tien Shan. Tashkent, 1958, 135 p. (in Russian).
- Radtke A.S. Geology of the Carlin gold deposit, Nevada. US Geol. Surv. Profess. Paper. No. 1267, 1985, 124 p., <https://doi.org/10.3133/pp1267>.
- Ryazanov K., Engalichev S.Y. Prospects of identifying objects of gold-sulfide mineralization of the Carlin type in the Paleozoic terrigenous-carbonate strata of the Momontai area (North of the Magadan region). Structure, substance, history of the lithosphere of the Timan – North Ural segment. Proceedings of the 29th scientific conference of the Institute of Geology of the Komi Scientific Center of the Ural Branch of the Russian Academy of Sciences, Syktyvkar, 2020, pp. 94-97 (in Russian).
- Saunders J.A., Hofstra A.H., Goldfarb R.J., Reed M.H. Geochemistry of hydrothermal gold deposits. Treatise on Geochemistry, 2nd Edition, Vol. 13, 2014, pp. 383-424, DOI:10.1016/B978-0-08-095975-7.01117-7.
- Tsoi V.D. Apocarbonate model of the formation of gold mineralization in Uzbekistan. Proc. All-Russian Conf. "Native gold, typomorphism of mineral associations, conditions of deposit formation, tasks of applied researches". Institute of geology of ore deposits, petrography, mineralogy and geochemistry of the Russian Academy of Sciences. Moscow, Vol. II, 2010, pp. 289-291 (in Russian).
- Tsoi V.D., Koroleva I.V., Munduzova M.A., Zakhidov A.R. Non-traditional apocarbonate type of gold mineralization in Uzbekistan (Ed. Isokov M.U.). State Committee of the Republic of Uzbekistan on Geology and Mineral Resources, State Enterprise "Research Institute of Mineral Resources". Tashkent, 2011, 174 p. (in Russian).
- Volkov A.V., Galyamov A.L. Geophysical model of the Earth's crust, geodynamic conditions and prospects for discovering Carlin-Type ore deposits in the Arctic Zone of the Republic Of Sakha (Yakutia). Arctic: Ecology and Economy, No. 1(37), 2020, pp. 82-94 (in Russian).
- Volkov A.V., Galyamov A.L., Lobanov K.V. Prospects for discovery of new large strategic metals deposits in the Arctic zone of Russia. Proceedings of the Fersman Scientific Session, No.17, 2020, pp. 89-96, <https://doi.org/10.31241/FNS.2020.17/017> (in Russian).
- Volkov A.V., Sidorov A.A. The geological-genetic model of Carlin type gold deposits. Lithosphere, No. 6, 2016, pp. 145-165 (in Russian).
- Yigit O., Hofstra A.H. Lithogeochemistry of Carlin-type gold mineralization in the Gold Bar district, Battle Mountain-Eureka trend, Nevada. Ore Geology Reviews, Vol. 22, No. 3-4, 2003, pp. 201-224, DOI:10.1016/S0169-1368(02)00142-7.
- Zhu J., Zhang Z.C., Santosh M., Jin Z.L. Carlin-style gold province linked to the extinct Emeishan plume. Earth and Planetary Science Letters, Vol. 530, No. 115940, 2020, <https://doi.org/10.1016/ersl.2019.115940>.

СРАВНИТЕЛЬНАЯ ХАРАКТЕРИСТИКА ЗОЛОТОНОСНОСТИ ТЕРРИГЕННО-КАРБОНАТНЫХ ОТЛОЖЕНИЙ АЛМАЛЫКСКОГО РУДНОГО РАЙОНА С МЕСТОРОЖДЕНИЯМИ КАРЛИНСКОГО ТИПА

Мундузова М.А.¹, Сайитов С.С.¹, Нурходжаев А.К.²

¹Государственное Учреждение «Институт минеральных ресурсов», Узбекистан

100164, Ташкент, ул. Олимп, д. 64: mavlyuda.munduzova1956@gmail.com

²Государственное Учреждение «Институт геологии и геофизики» имени Х.М.Абдуллаева, Узбекистан

100164, Ташкент, ул. Олимп, д. 64,

Резюме. Впервые в Узбекистане исследования по золотоносности в терригенно-карбонатных отложениях Алмалыкского рудного района проводили М.А.Мундузова, С.Т. Бадалов и др. Была определена золотоносность как непосредственно пород, слагающих эти толщи, так и отдельных проявлений в них. Актуальность этих исследований будет в дальнейшем способствовать расширению минерально-сырьевой базы Республики Узбекистан. Золотая минерализация в терригенно-карбонатных толщах может быть одним из нетрадиционных источников золотого оруденения. Сравнительную характеристику золотоносности терригенно-карбонатных пород Алмалыкского рудного района с проявлениями и месторождениями Карлинского типа впервые дала автор статьи М.А. Мундузова в своей диссертационной работе. Отобранные пробы из серых и черных органосодержащих (битуминозных) доломитов проанализированы как в лабораториях Республики Узбекистан, так и в лабораториях США. Подтверждена сходимость полученных результатов по лабораториям двух стран. Золотая минерализация в терригенно-карбонатных породах в обеих провинциях имеет тонкодисперсный характер выделений, трудно диагностируется и сложно извлекается. Продолжаются лабораторно-технологические исследования по извлечению золота из терригенно-карбонатных пород, в том числе и исследования по определению связи тонких, рассеянных золотин с органическим веществом в черных, битуминозных доломитах. Золото в осадочных терригенно-карбонатных породах тонков-крапленное с содержанием органического вещества. Золотые объекты типа Карлин, размещены в карбонатных отложениях и представлены тонкозернистой сульфидной минерализацией. Выделяются разновидности золота: пленочные на поверхности пирита и аморфного углерода, золото-органические соединения, самородное золото, золото в реальгаре и самородном мышьяке. Наиболее благоприятными поисково-прогнозными признаками подобных оруденений в Чаткало-Кураминском регионе являются литолого-структурные факторы, определенные свиты и участки сопряжения разнонаправленных разрывных нарушений и межформационные позиции в виде сканирования, ожелезнения, дробления и другие вторичные изменения.

Ключевые слова: золотоносность, терригенно-карбонатные отложения, доломиты, сравнение, Алмалык, Карлин, проявления, месторождения

KARLİN TİPLİ YATAQLARA MALİK ALMALIK FİLİZ RAYONUNUN TERRİGEN-KARBONAT ÇÖKÜNTÜLƏRİNİN QIZILLILIĞININ MÜQAYİSƏLİ SƏCİYYƏSİ

Munduzova M.A.¹, Sayitov S.S.¹, Nurhocayev A.K.²

¹“Mineral ehtiyatlar İnstituťu” Dövlət müəsissəsi, Özbəkistan

Daşkənd, Olimlar küç., 64, 100164: mavlyuda.munduzova1956@gmail.com

²“Geologiya və Geofizika İnstituťu” Dövlət müəsissəsi, Özbəkistan

100164, Daşkənd, Olimlar küç., 64

Xülasə. Munduzova M.A., Bədəlov S.T. və başqları ilk dəfə Özbəkistanda Almalık filiz sahəsinin terrigen-karbonat çöküntülərinin qızılığının tədqiqatlarını aparmışlar. Həm birbaşa bu qatlardı təşkil edən sūxurların, həm də onların ayrı-ayrı təzahürlerinin qızılılığı təyin edilmişdir. Bu tədqiqatların aktuellüyü göləcəkdə Özbəkistan Respublikasının mineral-xammal bazasını genişləndirməyə imkan verəcəkdir. Terrigen-karbonat qatlarda qızıl mineralallaşması qızıl filizləşməsi mənbəyinin qeyri-ənənəvi növü ola bilər. Məqalə müəllifi M.A.Munduzova ilk dəfə öz dissertasiya işində Karlin tipli yataq və təzahürlərə malik Almalık filiz rayonunun terrigen-karbonat çöküntülerinin qızılığının müqayisəli səciyyəsini aparmışdır. Orqanik tərkibli (bitumlu) boz və qara dolomitlərdən götürülmüş sınaqlar həm Özbəkistan Respublikasının, həm də ABŞ-nin laboratoriyalarında təhlil edilmişdir. İki dövlətin laboratoriya nəticələrinin uyğunluğu təsdiqlənmişdir. Terrigen-karbonat qatlarda qızıl mineralallaşması hər iki əyalətdə incədispers səciyyə daşıyır, çətin diaqnozlaşdırılır və çıxarılması mürəkkəbdür. Müəllif terrigen-karbonat sūxurlardan qızılın çıxarılması üçün laborator-texnoloji tədqiqatları, həmçinin orqanik maddəyə malik qara, bitumlu dolomitlərdə incə, səpinti qızılın təyini üzrə araşdırmaçıları davam etdirir. Əvvəllər aparılmış işlərlə Özbəkistanda Bükantau, Çakılıkalyan, Çatkal-Kuram dağlarında karbonat çöküntülərində yerləşmiş və incədənəli sulfid mineralallaşması ilə təqdim olunmuş Karlin tipli qızıl obyektləri ayrılmışdır. Qızılın pirit və amorf karbon üzərində pərdə şəklində müxtəliflikləri, üzvi maddələr, sərbəst qızıl, realqar və sərbəst mərgümüşdə qızıl ayrılır. Çatkal-Kurama regionunda belə filizləşmənin ən əlverişli axtarış-proqnoz əlamətləri – litoloji-struktur amillər, müxtəlif istiqamətləri qırılma pozulmalarının qovuşma məntəqələri və müəyyən lay dəstələri, skarnlaşma, dəmirləşmə, doğranma və başqa dəyişmələr şəklində formasiyalarası mövqelərdən ibarətdir.

Açar sözlər: Qızıl tərkibli, terrigen-karbonat çöküntüləri, dolomitlər, müqayisə, Almalık, Karlin, təzahür, yataqlar

AQUIFER ZONE DELINEATION USING CORRELATION BETWEEN MICROTREMOR METHODS AND GEOFECTRICITY

Yuliyanto G., Nurwidjanto M.I.N., Harmoko U., Yulianto T., Fernando G.A.

*Department of Physics, Faculty of Science and Mathematics, Diponegoro University, Indonesia
Semarang 50275, Indonesia: gatoty@fisika fsm.undip.ac.id*

Keywords: microtremor, geoelectric, resistivity, HVSR, aquifer zone, Poisson's ratio, Grabang Magelang

Summary. Geoelectric and microtremor are geophysical methods that can be used to determine subsurface conditions, especially in determining the presence of aquifer zones. This study aims to determine the potential and presence of aquifer rocks in the Grabag District area through microtremor and geoelectric methods and to compare the results of the two methods. The area of the Grabag District is very limited in conducting geoelectrical research because it is related to narrow topographical contours, so a microtremor method is needed to determine the condition of the aquifer below the ground surface. Measurements in this study resulted in 3 geoelectric trajectories and 20 microtremor measurement stations. The results of microtremor and geoelectric measurements have a good correlation between the two. The geoelectrical method uses resistivity parameters while the HVSR method uses v_s and Poisson's ratio parameters. There are several anomalies that can be suspected as the presence of aquifer zones such as surface water found at station 2, unpressured aquifers at stations 16 and 19, depressed aquifers at stations 1, 10 and 20 and water loss zones at stations 4, 2 and 13. Based on the advantages of the two methods in collecting data in the field, microtremor is more flexible and better used in narrower conditions like in this study and the depth of microtremor does not depend on how long the stretch is like geoelectric.

© 2025 Earth Science Division, Azerbaijan National Academy of Sciences. All rights reserved.

Introduction

Groundwater is very necessary and increasing population will lead to a reduction in available groundwater reserves. The increasing number of people requires a sufficient amount of water. An area that has limited water is difficult to meet the needs of a high population, especially during the dry season. According to Sadjad et al. (2012) groundwater is stored in an aquifer, which is a water-saturated geological formation that has the ability to store and release water economically and in sufficient quantities. Investigation of water catchment areas in an area is inseparable from its geological conditions, which include rock composition, rock properties and geological structure. The subsurface geological conditions of an area can be determined through geophysical measurements.

Geophysics is a branch of geology that applies physical principles in understanding and finding solutions to geological problems (Alile, Amadasun, 2008). Some examples of methods from geophysics that can be used for groundwater exploration are electrical resistivity, seismic refraction and electromagnetic methods. The resistivity method is carried out using an artificial current source, which is transmitted below the ground surface (Sheriff, Gel-

dart, 1995). Geoelectricity can provide information about the structure of groundwater and can determine vertical variations in subsurface electrical properties that can be related to the geology of the area (Omada, Obayomi, 2012). Based on research by Kasidi (2017), the geoelectric method can be used to determine groundwater potential, namely by using the VES method, so that groundwater potential is obtained which includes VES 1, 5, 7, 9, 11, 12, 16, 17, and 18 at depths ranging from 40 – 80 m.

The microtremor method is used to support the analysis of groundwater aquifers, which is carried out using the geoelectric method. The 1D profile from the geoelectric method will be correlated with the 2D profile from the microtremor method on the same line. Yuliyanto and Nurwidjanto (2021) introduced a geophysical method that can be used to identify potential groundwater aquifers by utilizing microwaves using the microtremor method. The parameters used to determine the existence of an aquifer are v_s and Poisson's ratio. Based on his research, the potential for subsurface water sources is below microtremor point 9 with a v_s value of 840 m/s with a Poisson's ratio value > 0.3 at a depth of 70 m.

This research will provide an overview of the potential and existence of aquifer rocks in the Grabag

District area using geophysical methods, namely microtremors using v_s parameters and Poisson's ratio. Apart from that, this research will also provide a comparison of the results of microtremor and geoelectric survey methods to determine the aquifer.

Theory

Geological structure

Based on the Magelang-Semarang geological map sheet (Thanden et al., 1996) it can be explained that Grabag's geological conditions are composed of Merbabu volcanic rock (Qme) composed of igneous rock composed of olivine and andesite augite, Andong and Kendil (Qak) volcanic rock composed of hornblende-augite andesite breccias and Gilipetung volcanic rocks (Qg) which are composed of hollow lava flows, the three rock units are the result of volcanic activity while the sedimentary rocks that compose this area are the Kaligetas Formation (Qpkg) which is composed of volcanic breccias, lava flows, tuff, tuffaceous sandstone and claystone.

Groundwater can be found in permeable soil known as aquifers which are water-binding formations that allow large enough amounts of water to move through them. Glacial sand and gravel deposits, floodplain alluvial fans and sand delta deposits are all excellent water sources. The aquifer system is controlled by several aspects which can be lithology, stratigraphy, and geological structure of geological sedimentary materials and formations (Kodoatie, 1996). These hydrogeological boundaries determine three important elements in the anatomy of a hydrogeological basin, namely recharge area, flowing area, and discharge area. The various types of aquifers that will determine the distribution of groundwater in hydrogeological mapping can be divided into 4 parts, namely:

1. Unconfined aquifer
2. Confined Aquifer
3. Semi Confined Aquifer
4. Semi Unconfined Aquifer

Microtremor

Microtremor is a low amplitude vibration of around 0.1-1 microns and a speed amplitude of 0.0001-0.01 cm/second at the ground surface caused by various natural factors such as wind, sea waves, vehicle noise, and others (Mirzaoglu, Dykmen, 2003). Microtremor, also called background seismic (ambient vibration), is a ground vibration caused by natural or artificial events that has relatively low energy and low amplitude which is always present in every seismic recording and can describe geological conditions near the surface (Tokimatsu, 1995). In the study of seismic engineering, softer lithology has a higher risk of being shaken by earthquake waves, this

is because it experiences greater wave amplification compared to more compact rocks (Kanai, 1983).

The HVSR (Horizontal to vertical spectrum ratio) transfer function of microtremors introduced by Nakamura (1989) can be expressed by equation 1.

$$SE(\omega) = \frac{HS(\omega)}{HB(\omega)} \quad (1)$$

where $HS(\omega)$ is the horizontal component microtremor spectrum on the surface while $HB(\omega)$ is the horizontal component microtremor spectrum found in the bedrock. The wave amplification contained in the vertical component can be referred to as the spectrum ratio of the vertical component at the surface and in the bedrock which can be written in equation 2.

$$AS(\omega) = \frac{VS(\omega)}{VB(\omega)} \quad (2)$$

where $VS(\omega)$ is the vertical component microtremor spectrum on the surface, and $VB(\omega)$ is the vertical component microtremor spectrum in the bedrock. Normalization is carried out to reduce the source effect contained in the horizontal gain spectrum $SE(\omega)$ on the source spectrum $AS(\omega)$ to obtain equation 3. $SM(\omega)$ is the transfer function for the soil layer.

$$SM(\omega) = \frac{SE(\omega)}{AS(\omega)} \quad (3)$$

Poisson's ratio (σ) can be interpreted as a ratio of transverse strain or contraction to longitudinal strain or extension due to changes in normal stress due to compression or dilation. The form of comparison related to the propagation speed of the longitudinal wave v_p to the shear wave v_s can be written as (Lay, Wallace, 1995).

$$\sigma = \frac{v_p^2 - 2v_s^2}{2(v_p^2 - v_s^2)} \quad (4)$$

Geoelectric

Geoelectric is one of the geophysical methods to determine the resistivity value of the rock layers below the soil surface. Measurements are made by flowing an electric current into the ground using 2 metal electrodes (current electrodes) commonly known as current electrodes A and B. If the ground is dry, water should be sprinkled around the electrodes to improve the current relationship. The electric voltage that occurs between the two electrodes is also measured with 2 metal electrodes (potential electrodes) known as potential electrodes M and N. The value of rock resistivity is a representation of variations in the physical and chemical characteristics of the rock.

Apparent resistivity can be interpreted as the resistivity measured over a layered medium which has a difference in resistivity and layer thickness which is considered to be isotropically homogeneous. The earth consists of layers with different ρ at each depth, so that the measured potential is the influence of these depth layers. This will mean that the measured resistivity is not the resistivity value for just one layer. This apparent resistivity is formulated by equation 5 (Sharma, 1997; Telford et.al., 1990):

$$\rho_{(a)} = K \frac{\Delta V}{I} \quad (5)$$

$\rho_{(a)}$ is the apparent resistivity with units of Ωm (ohmmeter), K is the geometry factor of the electrode configuration, ΔV is the measured potential between potential electrodes with units of V (volts), and I is the measured electric current between current electrodes with units of A (amperage). Geometry factors vary depending on the type of configuration used during the data collection process in the field. For the resistivity geoelectric method used, the Schlumberger configuration aims to identify vertical resistivity continuity (Telford et.al., 1990). The geometric factor of the Schlumberger configuration is shown by equation 6 (Sharma, 1997; Telford et.al., 1990):

$$K = \frac{\pi}{4} \left[\frac{(AB)^2 - (MN)^2}{MN} \right] \quad (6)$$

where K is the configuration geometric factor, π is a constant (3.14), AB is the distance from current source A to current source B (m), and MN is the distance from potential source M to potential source N (m). The inversion method is a method that can obtain actual resistivity values where the earth has heterogeneous resistivity. According to Jupp and Vozoff (1976), inversion is generally described by a model or point with a layered earth structure.

Research methods

Research on estimating the aquifer zone at the study site was carried out using several tools. Microtremor data collection uses 3 sets of data loggers, 3-component digital seismograph VHL PS 2B, global positioning system (GPS), and compass to determine the North - South direction from data collection. Software that can be used later for data processing in microtremor (HVSR) method is Microsoft Excel, Notepad, Notepad++, Geopsy, and Dinver (Irham et al., 2021) (Arintalofa et al., 2022). Raw microtremor data will be obtained in the form of a file in CSV format which can be opened in Microsoft Excel. This data shows the response of microtremors in showing subsurface images with several compo-

nents, namely horizontal East-West component, horizontal North-South component, and then vertical component. These three components will then be processed using Geopsy software to produce an HV curve, dominant frequency and amplification factor (Yuliyanto, Yulianto, 2023). These results can be processed again using dinver software to produce v_p , v_s , density and depth values (Yulianto, Yuliyanto, 2023). The results of v_p and v_s will later be used in determining the Poisson's ratio value.

Table 1

2D trajectories of microtremor measurements

Trajectory	Microtremor measurement station
A – A'	4, 8, 3, 9, 2, 1
B – B'	5, 16, 17, 18, 13
C – C'	6, 20, 19, 14, 12
D – D'	7, 15, 10, 11
E – E'	7, 6, 5, 4
F – F'	7, 20, 16, 8
G – G'	15, 19, 17, 3
H – H'	10, 14, 18, 9
I – I'	11, 12, 13, 2

Table 1 explains the 2D trajectories used in microtremor data analysis. The microtremor measurement stations in Table 1 show the name and sequence of the track used, while the trajectory shows the name of the track. Data modeling uses Golden Software: Surfer which is used for 2D modeling.

Retrieving geoelectrical data using Naniura NRD-300. Software that can be used to process geoelectrical data is Res1DInv. The configuration method used in this research uses the Schlumberger configuration. In this study, the path length AB/2m from each line 1, 2, and 3 from geoelectric measurements is 250 m, 180 m, and 180 m. Figure 1(a): 3 geoelectrical path measurements were carried out together with (b) 20 microtremor measurement stations due to the limitations of the field area (length and width) of the study location on the length of the geoelectric cable stretch at the site location. Both locations use a geographic coordinate system (decimal degree system) with S 7.405560° to S 7.400735° and E 110.40247° to E 110.407774°. The microtremor method uses 3 sets of tools, each microtremor requiring 10 minutes of recording at each station location. Meanwhile, the geoelectric method uses 1 set of tools and takes around 90 minutes for a path length (AB/2) 80 m (depending on the length of the track).

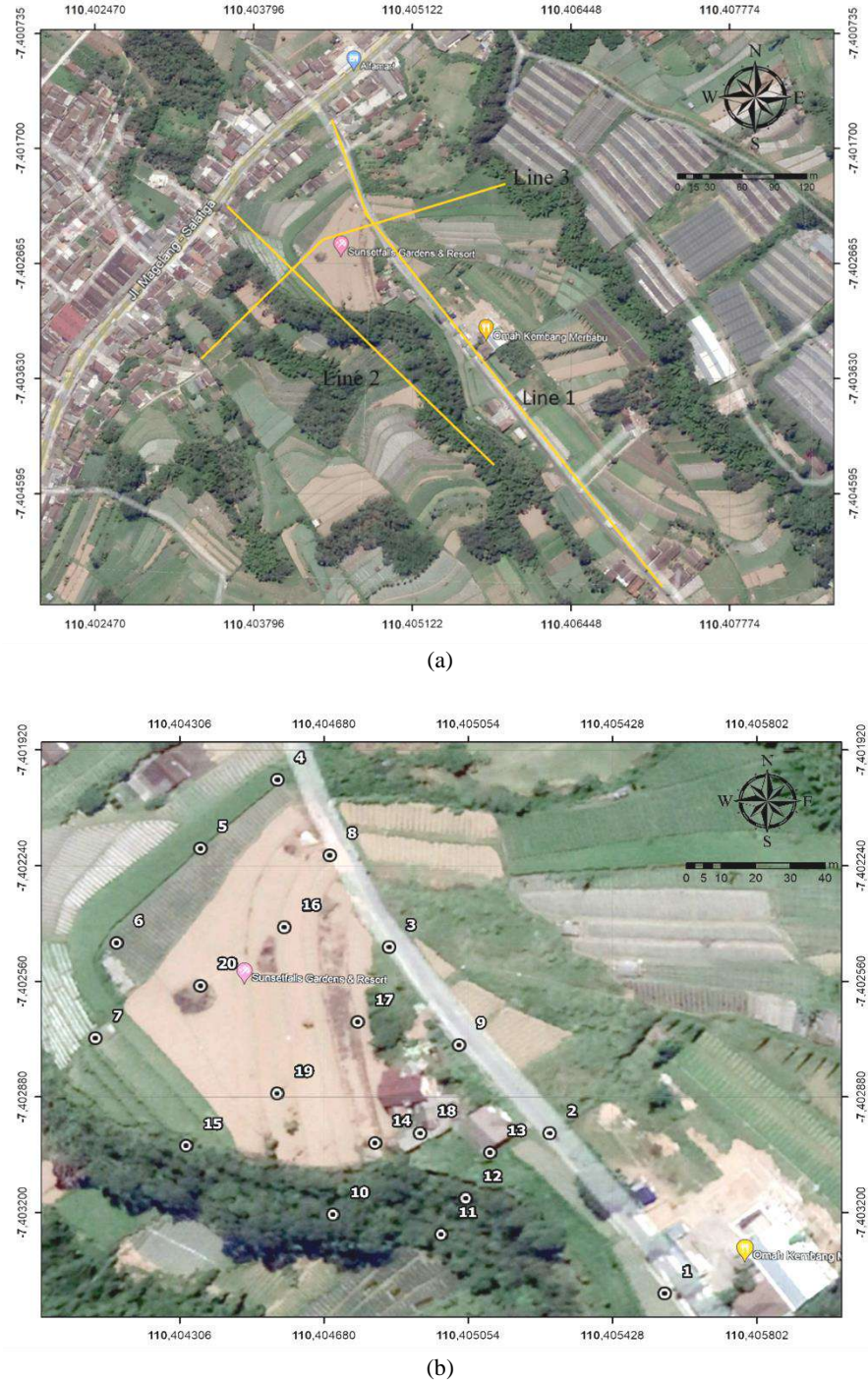


Fig. 1. Measurement trajectory for (a) Geoelectric, (b) Microtremor

Results and discussion

2D modeling was carried out by adjusting the straight trajectory of each microtremor station according to Figure 1 (b) and Table 1. The results of 1D microtremor data processing (v_p , v_s , and density) will be imaged in 2D using modeling with kriging as a geostatistical analysis. The concept of kriging itself is estimating a value at a point that is not sampled based on surrounding sample points by paying attention to spatial correlation using spatial weighting whose correlation is shown through a

variogram (Bahtiyar et al., 2014). The results of modeling using kriging are in the form of 2D images on each trajectory in Figure 1 (b), which is explained in detail in Table 1, imaged as in Figures 4 and 5. These images show that the modeling was carried out using kriging so that 2D contours were obtained from cross-correlation data in the research area.

The results of the field data processing that has been carried out and the cross-sectional resistivity obtained can then be correlated with local geological conditions. Figure 2 is the result of geoelectric

processing with the x-axis as $AB/2$ and the y-axis as the apparent resistivity and actual resistivity values. Figure 2 (a) shows the measurement results on Line 1, Figure 2 (b) shows the measurement results on Line 2 and Figure 2 (c) shows the measurement results on Line 3. Figure 3 is a cross-section of the 3 lines with the x-axis as the distance between them, line and y-axis as depth based on geoelectrical measurements.

Interpretation of aquifer potential is obtained through the presence of a value in Geoelectric measurements (Yuliyanto, Nurwidjanto, 2021). Referring to Wahyono et al. (2023) and Telford et al. (1990) research, water soil has a resistivity of around 0.5-300 Ωm , clay has a resistivity range of 10-45 Ωm , and sandstone has a resistivity of 45-333 Ωm . The results are in Figure 2 (a). There is an aquifer potential at a depth of 38 to 81 m from the ground surface with resistivity values of 53 and 71.5 Ωm (Sandstone lithology). Figure 2 (b) shows the potential for an aquifer at a depth of 24 to 44 m from the ground surface for geoelectric measurements with a resistivity value of 78.6 Ωm (Sandstone lithology). Figure 2 (c) shows that there is an aquifer potential at a depth of 40 m below the ground surface for geoelectric measurements with a resistivity value of 2.78 Ωm . This can be influenced by the surrounding geological conditions, namely the presence of several rocks that have good porosity and permeability as water carriers.

Based on Figure 4 and Figure 5 the results of microtremor modeling and processing obtained 20 measurement stations and from these 20 stations, there can be 9 microtremor modeling paths. One indication of the presence of water can be known by using the Poisson's ratio parameter (Equation 4.). The Poisson's ratio used in determining groundwater has a value of > 2.5 (Yuliyanto, Nurwidjanto, 2021). Track 1 in Figures 4 (a) and 5 (a) shows a Poisson's ratio contour with a value of 0.3 below station 2 in the form of surface water and confined aquifers at station 1 at a depth of 40-120 m below the ground surface. Track 2 in Figures 4 (b) and 5 (b) has a Poisson's ratio contour of 0.3 below station 16 with a depth of 70 m in the form of an unconfined aquifer. Track 3 in Figures 4 (c) and 5 (c) shows a Poisson's ratio contour of 0.3 below station 20 with a depth of 105-190 m in the form of a confined aquifer and below station 19 in the form of an unconfined aquifer to a depth of 90 m. Track 4 in Figures 4 (d) and 5 (d) has an anomaly in the form of a water loss zone at a depth of 90-140 m at station 4. Track 5 in Figures 4 (e) and 5 (e) at station 10 has an aquifer potential at a depth of 60-125 m with a Poisson's ratio > 0.25 . Track 6 in Figures 4 (f) and 5 (f) found a Poisson's ratio contour with a value of 0.3 below station 20 with a depth of 105-190 m in the form of a confined aquifer and below station 16 in the form of an aquifer that is not depressed to depth 70 m.

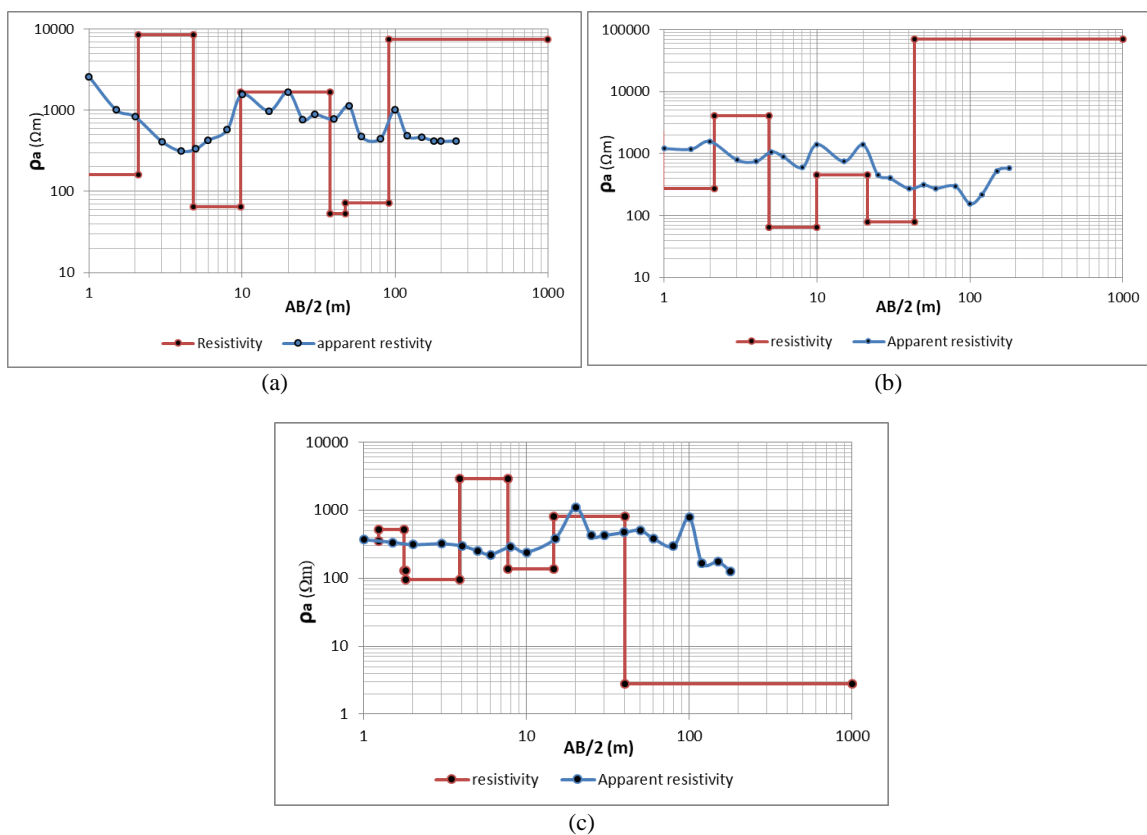


Fig. 2. Geoelectric processing results (a) Line 1 (b) Line 2 (c) Line 3

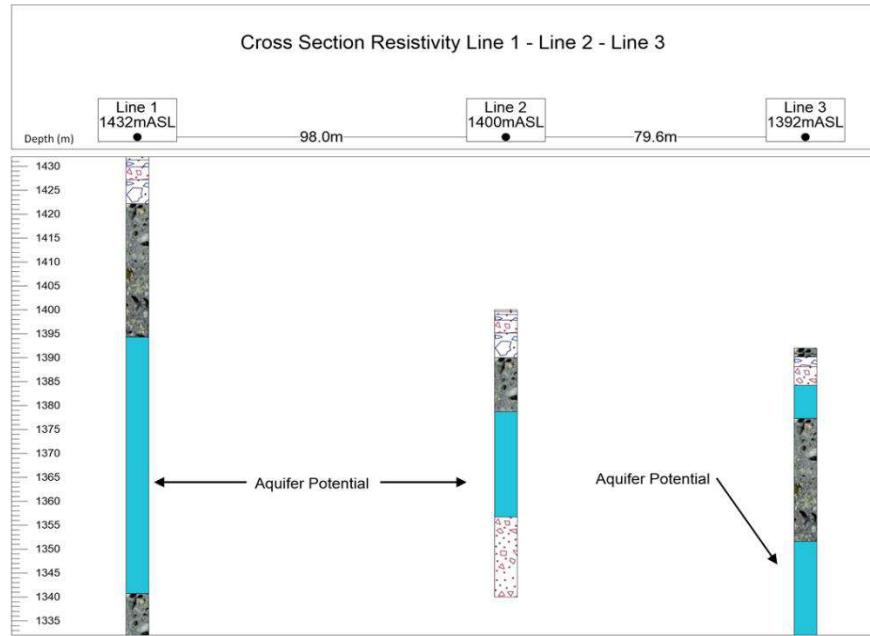


Fig. 3. Cross section of the soil layer resistivity

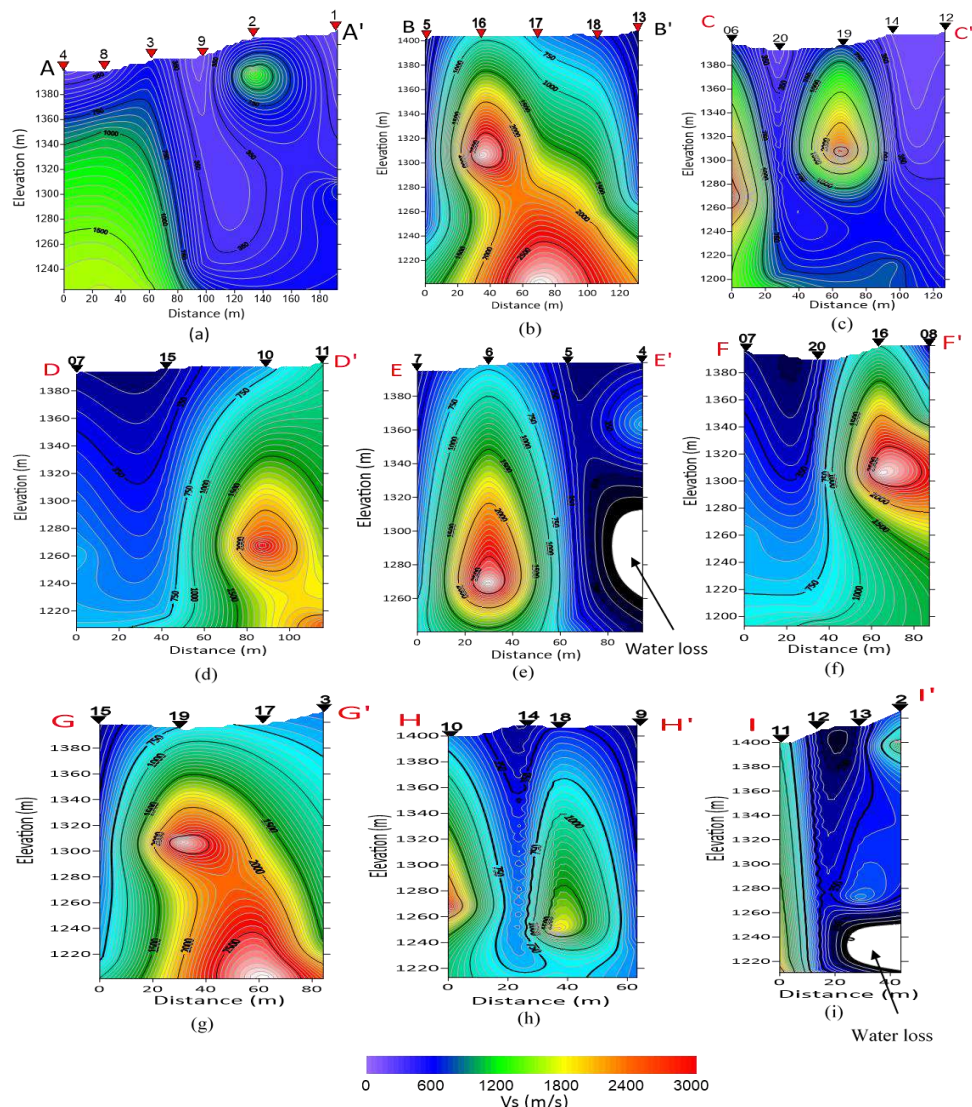


Fig. 4. Modeling v_s on each path: (a) A-A', (b) B-B', (c) C-C', (d) D-D', (e) E-E', (f) F-F', (g) G-G', (h) H-H', (i) I-I'

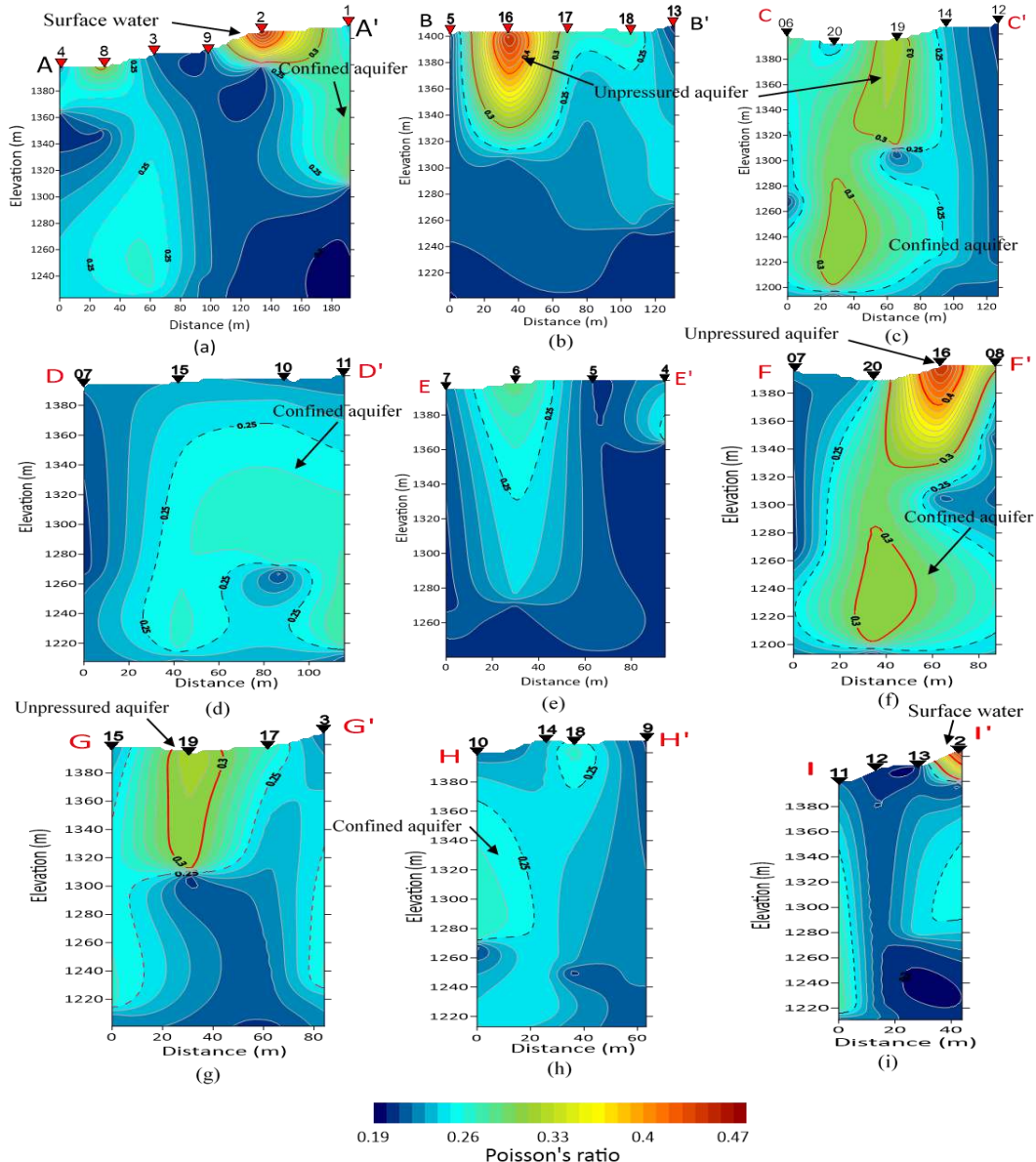


Fig. 5. Poisson's Ratio modeling on each path (a) A-A', (b) B-B', (c) C-C', (d) D-D', (e) E-E', (f) F-F', (g) G-G', (h) H-H', (i) I-I'

Track 7 in Figures 4 (g) and 5 (g) found a Poisson's contour ratio of 0.3 below station 19 in the form of an unconfined aquifer to a depth of 80 m. On track 8 in Figures 4 (h) and 5 (h), there is station 10 which has an aquifer potential at a depth of 60-125 m with a Poisson's ratio value > 0.25 . Track 9 in Figures 4 (i) and 5 (i) has an anomaly in the form of a water loss zone at a depth of 180-230 m at stations 2 and 13.

Figure 6 (a) is a correlation between microtremor measurements at station 20 and geoelectricity at line 1, while Figure 6 (b) is a correlation between microtremor measurements at station 10 and geoelectricity at line 2. The imaged correlation is the correlation of the hv curve of the microtremor which has frequency value as the x-axis and the average value of the horizontal to vertical mean values which are weighted as the y-axis. The correlation of geo-

lectricity in images (a) and (b) has depth values as the x-axis and weighted resistivity values as the y-axis. Weighting is carried out to obtain a correlation regarding the response of microtremor values from the HV curve and geoelectricity form resistivity.

According to Yuliyanto et al. (2017) one of the methods to determine the condition and physical properties of the soil using a geophysical approach is the microtremor method which has a fairly good correlation between data and measurement data using the geoelectric resistivity method. Based on the two analyzes regarding the search for aquifer zones, the two methods (microtremor and resistivity) provide a compatible solution (Yulianto et al., 2021) and shows a suitable response in showing the response of subsurface imagery to search for groundwater by using corelation hv curve and resistivity (Figure 6).

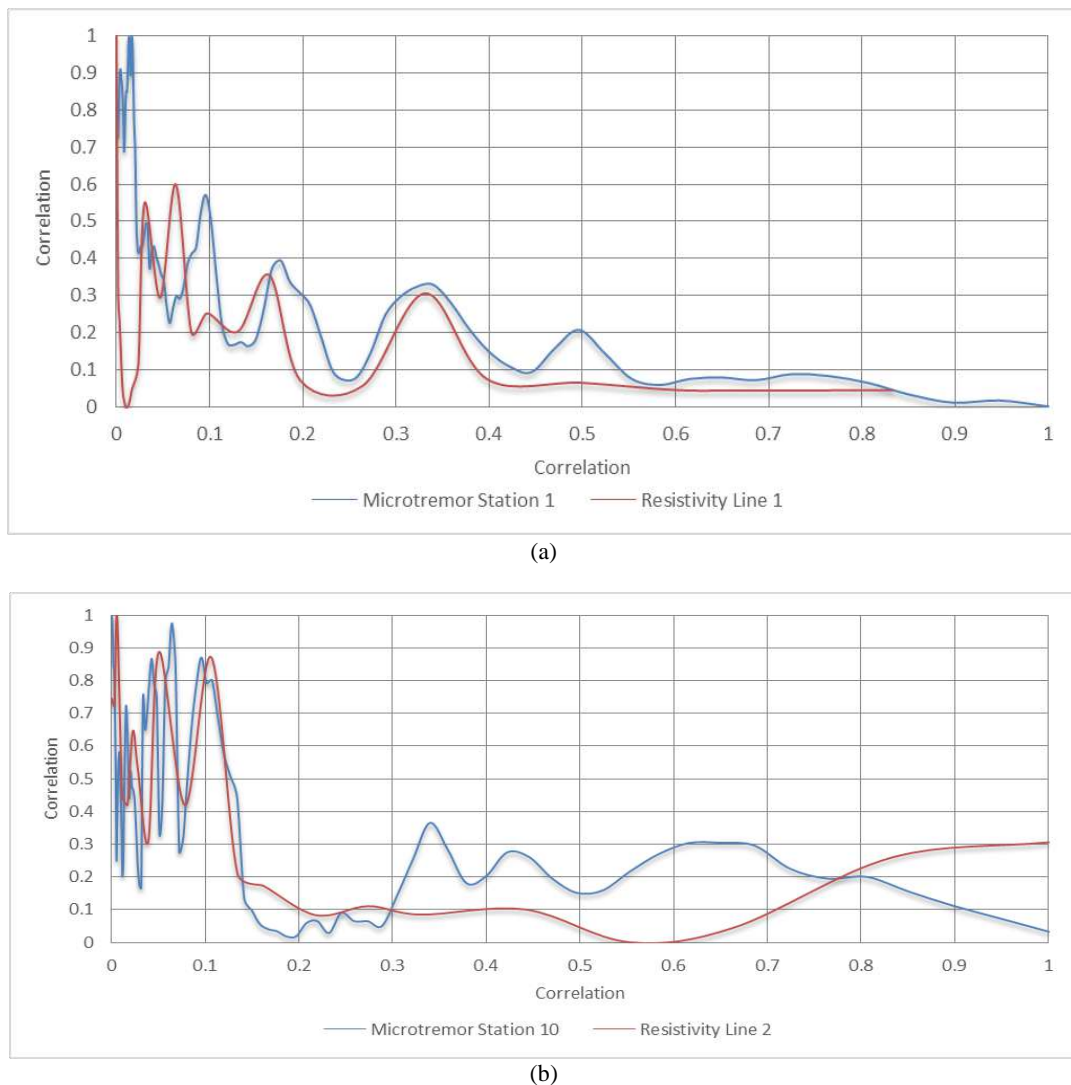


Fig. 6. Correlation between Geoelectricity and Microtremor: (a) measurement 1 (b) measurement 2

The geoelectrical resistivity and the Poisson's ratio on microtremor indicate an accuracy in knowing the aquifer zone. However, when viewed from the amount of data obtained and the flexibility in data collection, microtremor has more advantages than geoelectric. Retrieval of data on the Geoelectric method requires a long enough path length to determine subsurface conditions that are deep enough, while data collection on microtremor can easily be used in narrower conditions and the depth of microtremor does not depend on how long the stretch is like geoelectric.

Conclusion

The results of research that has been carried out using geoelectric and microtremor with the HVSR

method can identify the potential presence of aquifer layers. Based on the research results, it was found:

1. The results of microtremor and geoelectric measurements have a good correlation between the two. There are several anomalies that can be suspected as the presence of aquifer zones such as surface water found at station 2, unpressured aquifers at stations 16 and 19, confined aquifers at stations 1, 10 and 20 and water loss zones at stations 4, 2 and 13.

2. Based on The advantages of both methods in collecting data in the field, microtremor is more flexible and better used in narrower conditions such as in this study and the depth of microtremor does not depend on how long the stretch is like geoelectric.

REFERENCES

- Alile O.M., Amadasun C.V.O. Investigation of direct currents beneath the earth's surface to search for water bearing layers in Oredo Local Government Area, Edo State, Nigeria. Nigeria journal of Applied Science, Vol. 25, 2008, pp. 107-116.

ЛИТЕРАТУРА

- Alile O.M., Amadasun C.V.O. Investigation of direct currents beneath the earth's surface to search for water bearing layers in Oredo Local Government Area, Edo State, Nigeria. Nigeria journal of Applied Science, Vol. 25, 2008, pp. 107-116.

- Arinalofa V., Yuliyanto G., Harmoko U. Subsurface characterization of Diwak Derekan geothermal field by HVSR analysis method based on microtremor data. AIP Conference Proceedings, 2296, 020057, 2020, <https://doi.org/10.1063/5.0030356>.
- Bahtiyar A.D.R., Hoyyi A., Yasin H. Ordinary kriging in rainfall estimation in Semarang City. Gaussian Journal, 2014, Vol. 3, No. 2, pp. 151-159.
- Irham M.N., Zainuri M., Yuliyanto G., Wirasatriya A. Measurement of ground response of Semarang coastal region risk of earthquakes by Horizontal To Vertical Spectral Ratio (HVSR) microtremor method. IOP Publishing Journal of Physics: Conference Series, Vol. 1943, 012031, 2021, DOI:10.1088/1742-6596/1943/1/012031.
- Jupp D.B.L., Vozoff K. Two-Dimensional Magnetotelluric Inversion. Geophysical Journal International, 1976, Vol. 50(2), 2007, pp. 333-352, DOI:10.1111/j.1365-246X.1977.tb04177.x.
- Kanai K. Engineering Seismology. University of Tokyo Press. Japan, 1983, 251 p.
- Kasidi S. Groundwater exploration using the electrical resistivity method case study in the Federal Capital Territory (FCT) Abuja, Nigeria. International Journal of Engineering and Applied Sciences (IJEAS), Vol. 4, No.10, 2017, 1-8 p.
- Kodoatje J.R. Introduction to Hydrogeology. Yogyakarta: ANDI, Yogyakarta, 1996.
- Lay T., Wallace T.C. Modern global seismology. Academic Press. California. United States, 1995, 521 p.
- Mirzaoglu M., Dykmen U. Journal of the Balkan Geophysical Society, Vol. 6, No. 3, 2003, pp.143-153.
- Nakamura Y. A Method for dynamic characteristic estimation of subsurface using microtremor on the ground surface, Quarterly Report of RTRI, Vol. 30, No.1, 1989, pp. 25-33.
- Omada J.I., Obayomi O.O. An assessment of groundwater resources in the basement complex of Gwarinpa-Kafé area in Abuja Metropolis, Central Nigeria. Advances in applied science research, Vol. 3, No.1, 2012, pp. 393-398.
- Sadjab B., As'ari A., Adey T. Mapping of groundwater aquifers in Prambanan District, Sleman Regency, Special Region of Yogyakarta using the geoelectrical resistivity method. UNSRAT Online Mathematics and Natural Sciences Journal, Vol. 1(1), 2012, pp. 37-44.
- Sharma P.V. Environmental and engineering geophysics. Cambridge University Press. Cambridge, United Kingdom, 1997, 475 p.
- Sheriff R.E., Geldart L.P. Exploration seismology. Second Edition, Cambridge University Press. Cambridge, 1995, 592 p.
- Telford W.M., Geldart L.P., Sheriff R.E., Keys D.A. Applied geophysics. Cambridge University Press. Cambridge, 1990, 770 p.
- Tokimatsu K. Geotechnical site characterization using surface waves. In: Proc. 1st Intern. Conf. Earthquake Geotechnical Engineering, 1995 (Ishihara, ed.), Balkema. Rotterdam, 1997, pp. 1333-1368.
- Thanden R.E., Sumadiredja H., Richards P.W., Sutisna K., Amin T.C. Geological map of the Magelang and Semarang Sheets, Jawa, Geological Research and Development Centre. Bandung, Indonesia, 1996.
- Wahyono S.C., Siregar S.S., Putri R.A., Sari N., Wianto T., Nasrulloh A.V. Identifying and classifying andesite rocks based on resistivity in Tanah Bumbu County, South Kalimantan. ANAS Transaction. Earth sciences, No.1, 2023, pp. 3-10.
- Yulianto T., Yuliyanto G. Microtremor data and HVSR method in the kaligarang fault zone Semarang, Indonesia, Data In Brief, Vol. 49, 109428, 2023a, <https://doi.org/10.1016/j.dib.2023.109428>.
- Yulianto T., Sasongko D.P., Yuliyanto G., Indriana R.D., Setyawan A., Widada S. Correlation of Vp/Vs ratio against the resistivity value to determine the aquifers presence estimation in Jetak Subvillage, Getasan Sub-District, Semarang regency, IOP Publishing Journal of Physics: Conference Proceedings, 2296, 020057, 2020, <https://doi.org/10.1063/5.0030356>.
- Bahtiyar A.D.R., Hoyyi A., Yasin H. Ordinary kriging in rainfall estimation in Semarang City. Gaussian Journal, 2014, Vol. 3, No. 2, pp. 151-159.
- Irham M.N., Zainuri M., Yuliyanto G., Wirasatriya A. Measurement of ground response of Semarang coastal region risk of earthquakes by Horizontal To Vertical Spectral Ratio (HVSR) microtremor method. IOP Publishing Journal of Physics: Conference Series, Vol. 1943, 012031, 2021, DOI:10.1088/1742-6596/1943/1/012031.
- Jupp D.B.L., Vozoff K. Two-Dimensional Magnetotelluric Inversion. Geophysical Journal International, 1976, Vol. 50(2), 2007, pp. 333-352, DOI:10.1111/j.1365-246X.1977.tb04177.x.
- Kanai K. Engineering Seismology. University of Tokyo Press. Japan, 1983, 251 p.
- Kasidi S. Groundwater exploration using the electrical resistivity method case study in the Federal Capital Territory (FCT) Abuja, Nigeria. International Journal of Engineering and Applied Sciences (IJEAS), Vol. 4, No.10, 2017, 1-8 p.
- Kodoatje J.R. Introduction to Hydrogeology. Yogyakarta: ANDI, Yogyakarta, 1996.
- Lay T., Wallace T.C. Modern global seismology. Academic Press. California. United States, 1995, 521 p.
- Mirzaoglu M., Dykmen U. Journal of the Balkan Geophysical Society, Vol. 6, No. 3, 2003, pp.143-153.
- Nakamura Y. A Method for dynamic characteristic estimation of subsurface using microtremor on the ground surface, Quarterly Report of RTRI, Vol. 30, No.1, 1989, pp. 25-33.
- Omada J.I., Obayomi O.O. An assessment of groundwater resources in the basement complex of Gwarinpa-Kafé area in Abuja Metropolis, Central Nigeria. Advances in applied science research, Vol. 3, No.1, 2012, pp. 393-398.
- Sadjab B., As'ari A., Adey T. Mapping of groundwater aquifers in Prambanan District, Sleman Regency, Special Region of Yogyakarta using the geoelectrical resistivity method. UNSRAT Online Mathematics and Natural Sciences Journal, Vol. 1(1), 2012, pp. 37-44.
- Sharma P.V. Environmental and engineering geophysics. Cambridge University Press. Cambridge, United Kingdom, 1997, 475 p.
- Sheriff R.E., Geldart L.P. Exploration seismology. Second Edition, Cambridge University Press. Cambridge, 1995, 592 p.
- Telford W.M., Geldart L.P., Sheriff R.E., Keys D.A. Applied geophysics. Cambridge University Press. Cambridge, 1990, 770 p.
- Tokimatsu K. Geotechnical site characterization using surface waves. In: Proc. 1st Intern. Conf. Earthquake Geotechnical Engineering, 1995 (Ishihara, ed.), Balkema. Rotterdam, 1997, pp. 1333-1368.
- Thanden R.E., Sumadiredja H., Richards P.W., Sutisna K., Amin T.C. Geological map of the Magelang and Semarang Sheets, Jawa, Geological Research and Development Centre. Bandung, Indonesia, 1996.
- Wahyono S.C., Siregar S.S., Putri R.A., Sari N., Wianto T., Nasrulloh A.V. Identifying and classifying andesite rocks based on resistivity in Tanah Bumbu County, South Kalimantan. ANAS Transaction. Earth sciences, No.1, 2023, pp. 3-10.
- Yulianto T., Yuliyanto G. Microtremor data and HVSR method in the kaligarang fault zone Semarang, Indonesia, Data In Brief, Vol. 49, 109428, 2023a, <https://doi.org/10.1016/j.dib.2023.109428>.
- Yulianto T., Sasongko D.P., Yuliyanto G., Indriana R.D., Setyawan A., Widada S. Correlation of Vp/Vs ratio against the resistivity value to determine the aquifers presence estimation in Jetak Subvillage, Getasan Sub-District, Semarang regency, IOP Publishing Journal of Physics: Conference Proceedings, 2296, 020057, 2020, <https://doi.org/10.1063/5.0030356>.

- ence Series, Vol. 1943, 2021, 012028, DOI:10.1088/1742-6596/1943/1/012028.
- Yuliyanto G., Yulianto T. Microtremor data and HVSR method of geothermal manifestation of Mt. Telomoyo, Central Java, Indonesia, Data In Brief, 51, 109428, 2023b, <https://doi.org/10.1016/j.dib.2023.109721>.
- Yuliyanto G., Harmoko U., Widada S. Identify the slip surface of land slide in Wirogomo Banyubiru Semarang Regency using HVSR method. Int. J. Appl. Environ. Sci., 2017, Vol. 12, No. 12, pp. 2069-2078.
- Yuliyanto G., Nurwidjantoro M.I. Integrated survey to identify potential groundwater aquifers in Jabungan Semarang using geoelectric and microtremor methods. IOP Publishing Journal of Physics: Conference Series, Vol.1943, 2021, 012026, DOI:10.1088/1742-6596/1943/1/012026.
- Yuliyanto G., Nurwidjantoro M.I. Integrated survey to identify potential groundwater aquifers in Jabungan Semarang using geoelectric and microtremor methods. IOP Publishing Journal of Physics: Conference Series, Vol.1943, 2021, 012026, DOI:10.1088/1742-6596/1943/1/012026.
- Yuliyanto G., Nurwidjantoro M.I. Integrated survey to identify potential groundwater aquifers in Jabungan Semarang using geoelectric and microtremor methods. IOP Publishing Journal of Physics: Conference Series, Vol.1943, 2021, 012026, DOI:10.1088/1742-6596/1943/1/012026.

ВЫДЕЛЕНИЕ ЗОН ВОДОНОСНЫХ ГОРИЗОНТОВ С ИСПОЛЬЗОВАНИЕМ КОРРЕЛЯЦИОННОГО АНАЛИЗА РЕЗУЛЬТАТОВ МИКРОТРЕМОРНОГО И ГЕОЭЛЕКТРИЧЕСКОГО МЕТОДОВ

Юлияントо Г., Нуривидяントо М.И.Н., Хармоко У., Юлиантонто Т., Фернандо Г.А.

Кафедра физики, Факультет естественных наук и математики, Университет Дипонегоро, Индонезия
Семаранг 50275, Индонезия: gatoty@fisika fsm.undip.ac.id

Резюме. Геоэлектрический и микротреморный методы – это геофизические методы, которые можно использовать для определения подземных условий, особенно при определении наличия зон водоносных горизонтов. Это исследование направлено на определение потенциала и наличия водоносных пород в районе Грабагского района с помощью микротреморного и геоэлектрического методов, а также на сравнение результатов этих двух методов. Территория Грабагского района очень ограничена для проведения геоэлектрических исследований, так как связана с узкими топографическими контурами, поэтому для определения состояния водоносного горизонта под поверхностью Земли необходимо использование микротреморного метода. В рамках данного исследования были определены три геоэлектрических профиля и выполнены измерения на 20 станциях микротреморных наблюдений. Результаты микротреморных исследований и геоэлектрических измерений показывают их хорошую согласованность между собой. В геоэлектрическом методе используются параметры удельного сопротивления, в то время как в методе HVSR (горизонтально-вертикальные спектральные отношения) используются параметры v_s и коэффициент Пуассона. Есть несколько аномалий, в которых можно предположить наличие зон водоносных горизонтов, таких как поверхностные воды, обнаруженные на станции 2, безнапорные водоносные горизонты на станциях 16 и 19, депрессивные водоносные горизонты на станциях 1, 10 и 20 и зоны потери воды на станциях 4, 2 и 13. Основываясь на преимуществах двух методов сбора данных в полевых условиях, микротреморный метод обладает большей гибкостью и лучше подходит для работы в сложных условиях, как и показано в данном исследовании. В отличие от геоэлектрического метода, глубина микротреморных исследований не зависит от длины профиля.

Ключевые слова: микротремор, геоэлектрический, удельное сопротивление, HVSR, водоносный горизонт, коэффициент Пуассона, Grabang Magelang

MİKRO TREMOR VƏ GEOLEKTRİK ÜSULLARDAN ƏLDƏ EDİLƏN NƏTİCƏLƏRİN KORRELYASIYA ANALİZİ İSTİFADƏ EDİLMƏKLƏ SUSAXLAYAN HORİZONTLARIN AYRILMASI

Yuliyanto G., Nurwidjantoro M.İ.N., Harmoko U., Yulianto T., Fernando G.A.

Diponegoro Universiteti, Elm və Riyaziyyat Fakültəsi, Fizika kafedrası
Semarang 50275, İndoneziya: gatoty@fisika fsm.undip.ac.id

Xülasə. Mikrotremor və geolektrik, yeraltı şəraiti müəyyən etmək üçün, xüsusən də sulu təbəqə zonalarının mövcudluğunu müəyyən etmək istifadə edilə bilən geofiziki üsullardır. Bu tədqiqat mikrotremor və geolektrik üsullarla Qrabəq rayonu ərazisində sulu təbəqə səxurlarının potensialını və mövcudluğunu müəyyən etmək və iki metodun nəticələrini müqayisə etmək məqsədi daşıyır. Qrabəq rayonunun ərazisi geolektrik tədqiqatlarının aparılmasında çox məhduddur, çünkü o, dar topoqrafik konturlarla bağlıdır, ona görə də yer səthinin altındaki su qatının vəziyyətini müəyyən etmək üçün mikrotremor metoduna ehtiyac var. Bu tədqiqatda ölçmələr 3 geolektrik trayektoriya və 20 mikrotremor ölçmə stansiyası ilə nəticələndi. Mikrotremor və geolektrik ölçmələrin nəticələri ikisi arasında yaxşı korrelyasiyaya malikdir. Geolektrik üsul müqavimət parametrlərindən istifadə edir, HVSR metodu isə VS və Poisson nisbəti parametrlərindən istifadə edir. 2-ci stansiyada aşkar edilmiş səth suları, 16 və 19-cu stansiyalarda təzyiqsiz sulu laylar, 1, 10 və 20-ci stansiyalarda çökək sulu laylar və 4, 2 və stansiyalarda su itkisi zonaları kimi sulu təbəqə zonalarının olması kimi bir neçə anomaliyadan şübhələnmək olar. 13-cü sahədə məlumatların toplanmasında iki metodun üstünlüklerinə əsaslanaraq, mikrotremor daha çevikdir və bu tədqiqatda olduğu kimi daha dar şəraitdə daha yaxşı istifadə olunur və mikrotremorun dərinliyi uzanmanın geolektrik kimi nə qədər uzun olmasına asılı deyil.

Açar sözlər: Mikrotremor, Geolektrik, Rezistivlik, HVSR, Aquifer zonası, Puasson nisbəti, Grabang Magelang

APPLICATION OF SEISMIC REFRACTION SURVEY FOR ENGINEERING SITE CHARACTERIZATIONS OF WEYTO DAM CONSTRUCTION SITE, SOUTHERN ETHIOPIA

Mulualem A.¹, Demsie T.¹, Shano L.², Getahun E.², Solomon H.³

¹*Department of Geology, College of Natural Sciences, Debre Markos University, Debre Makos, Ethiopia: abraham_mulualem@dmu.edu.et/muluabr4114@gmail.com*

²*Department of Geology, College of Natural Sciences, Injibara University, Injibara, Ethiopia*

³*Addis Ababa Design and Construction Works Bureau, Addis Ababa, Ethiopia*

Keywords: Dam, geophysical survey, subsurface, compressional wave, foundation

Summary. The study area is geographically situated within the Southern Nations, Nationalities, and Peoples' Region (SNNPR), specifically encompassing portions of the Segen Zone and the South Omo Zone. It lies within the Benetsemay Woreda, in close proximity to the established urban center of Weyto Town. The terrain of the study area presents a topographically rugged landscape. Notably, this region forms an integral segment of the extensive Southern Main Ethiopian Rift System, a significant geological feature marked by considerable tectonic activity. To gain a comprehensive understanding of the subsurface characteristics at the proposed Weyto Dam construction site, a series of seismic refraction surveys were meticulously conducted. The geophysical survey was executed utilizing a sophisticated 24-channel refraction wave instrument, the Seis-24, a tool specifically designed to generate detailed velocity sections of the subsurface at the prospective dam construction location. The study area is distinguished by a multifaceted geological setting, exhibiting a diverse array of intricate tectonic structures and a variety of distinct geological formations. These formations include fine-grained aphanitic basalt, various clastic sediments, metamorphic gneiss, porphyritic basalt and accumulations of pyroclastic deposits. The application of the seismic refraction survey proved instrumental in effectively identifying the different subsurface units based on the analysis of their compressional wave velocity values and the determined thicknesses of these layers. The acquired data revealed that the seismic refraction survey successfully achieved a maximum depth of investigation reaching approximately 100 meters within the defined study area, providing valuable insights into the subsurface architecture relevant to the proposed dam project.

© 2025 Earth Science Division, Azerbaijan National Academy of Sciences. All rights reserved.

1. Introduction

The main purpose of constructing a dam is to impound water for several reasons, such as flood control, human water supply, irrigation, livestock water supply, and energy generation. They also provide an enhanced environment and recreation purpose (Long term benefits ..., 2004). In most parts of the country, Ethiopian people faced a strong moisture shortage. To increase crop production, the residents were forced to use irrigation. To overcome the aim of irrigation, the governments of Ethiopia proposed and constructed dams at different times (Bihon, 2015). Preliminary insufficient investigation of geological structures, lithological types, soil strengths and seismic zones leads to a short lifespan of dam sites (Ivan, Samuel, 1987).

Dam failures are usually caused by inadequate design, improper construction, or inadequate maintenance.

Failure of the dam can cause considerable loss of capital investment, income, possible property damage, and loss of life. Loss of the reservoir can cause severe hardship for those dependent on it for their livelihood and can upset the ecological balance of the area; therefore, it requires the detailed investigation of the foundation for the construction of safe and sustainable dam structures.

Geophysical methods are extensively used in dam investigations, both on dam construction projects and in the assessment of the condition of existing dam structures. These methods help in identifying local areas of concern that have no surface expression. Moreover, the methods help to delineate boundaries between residual soils, weathered rocks and fresh rock. It is also possible to locate anomalous foundation features such as dykes, cavities, fault zones and buried river channels (Fell et al., 2005).

Geophysics has many disciplines, of which seismology being the largest, especially in exploration geophysics. Refraction seismology measures arrival time of seismic waves at fixed positions on the ground after their generation at the focus. A small explosive charge or sledgehammer can be used for shallow seismic refraction investigations to generate seismic energy, which moves through the subsurface at a velocity depending on the subsurface material. Some of waves that travel through the subsurface are refracted at the interface between two layers back to the surface, where they are detected by geophones at fixed locations. These signals then are sent to a seismograph, which records the arrival time for signals. The arrival time depends on the velocity of waves in the layer it travels through, so knowing the time of arrival and the distance from the focus to the geophone, the velocity of the wave can be determined. The velocity of a particular earth material can vary over a wide range as a function of its age, depth of burial, degree of fracturing or porosity, and whether water or air fills the voids (Telford et al., 1976).

The velocity variation can also aid in determining the number of layers the wave has travelled through and their elastic properties, thus informing the engineer or geologist on the kind of material to expect at different depths within the subsurface. This research seeks to use the seismic refraction survey method to obtain the subsurface condition of the dam site. Boreholes, trenches and other invasive methods are conventionally used to investigate the subsurface, but they are discrete and may cause serious omissions in an attempt to delineate the

boundaries of geological structures and the nature of the subsurface. This is a major issue in engineering site investigations that seismic refraction surveys address by providing more continuous data on the subsurface based on which engineering decisions can be made with some degree of certainty. A seismic refraction survey also gives the various layers in the subsurface by using the velocities of the seismic waves in the subsurface, thereby helping to reduce the number of boreholes that are required for subsurface investigation at a site. This reduces the cost involved in subsurface investigation. Seismic refraction is nondiagnostic like all geophysical methods, and a specific conclusion of the material making up the subsurface cannot be drawn from the results of seismic refraction survey alone. Therefore, it is very important that the investigation be supplemented with some boreholes and knowledge of the geology of the area so that the possible material makeup of the subsurface can readily be inferred (Bawuah et al., 2018).

2. Location and accessibility of the study area

The Weyto proposed dam is located in the SNNPR, which is specifically between Benetsemay Woreda and Ale Special Woreda near Weyto town. It is approximately 580 km Southwest of Addis Ababa. Geographically, the study area is bounded by the coordinates of 280589-288230 m E and 605700-613890 m N and covers an area of 76 square km (Fig. 1). The study area is accessible through the Addis Ababa-Araba Minch-Jinka main road and newly constructed dry weather road that branches from the Addis Ababa-Weyto asphalt road (25 km from Weyto Bridge).

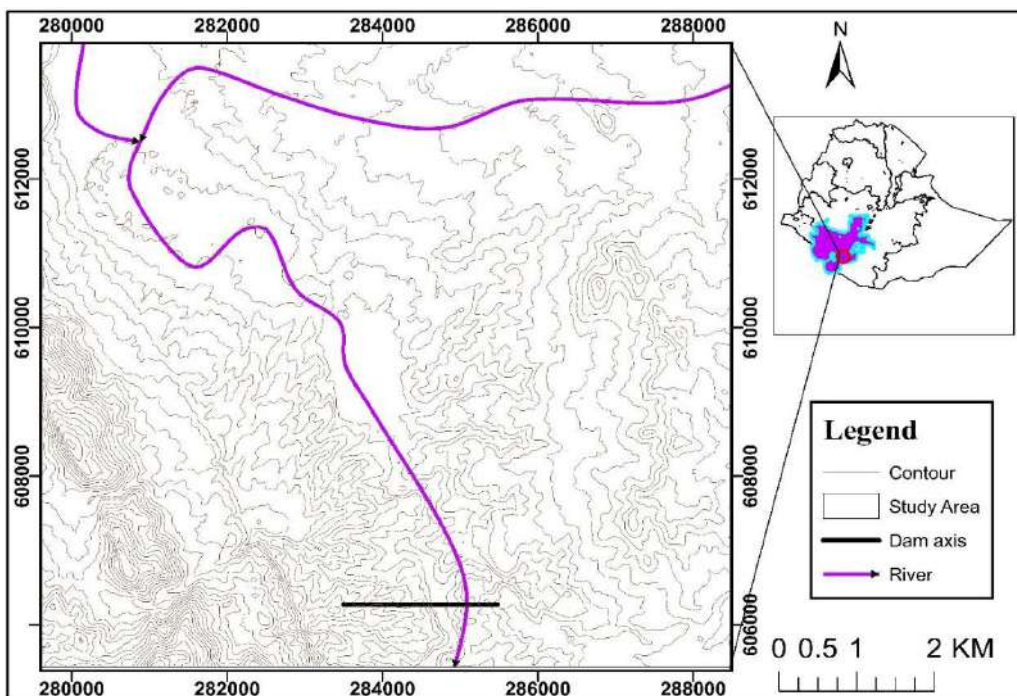


Fig. 1. Location map of the study area

The geophysical survey area is located between UTM (Adindan, Zone 37N) coordinates 281000 to 286500 m E and 604500 to 610500 m N. The locations of the proposed geophysical survey lines in the study area are shown in Fig. 2. The study area is located approximately 25 km upstream of the Weyto River Bridge and can be reached by 4 WD vehicles using dry weather roads that branch from the main high way connecting Arba Minch and Jinka Towns.

3. Geology of the study area

The geology of the study area belongs to the southern Ethiopian rift system, which is characterized by rift basins with fully defined margins and 300 km wide broad rifted zones characterized by half grabens and basin range-type tectonic features (Levitte et al., 1974). Precambrian basement rocks, Tertiary volcanic successions, Tertiary sediment deposits and Quaternary superficial deposits are major stratigraphic successions in the study area.

The crystalline basement rocks are overlaid by red sandstone, which is overlaid by volcanic flows. The detailed mapping of the area outlined lithologic units comprising superficial deposits, siliciclastic sediments, porphyritic basalt, felsites, pyroclastic deposits, aphanitic basalt and gneissic rock units. The crystalline basement rocks are part of the gneissic complexes consisting of quartzo feldspathic and biotite layered quartzo feldspathic gneiss. They outcrop in the central-eastern mapped area, and the left margin of the Weyto River is mainly uplifted by a series of faults with several orientations. The average foliation trend of this rock unit is 45-55/270-300 degrees in the eastern part of the map and 50/070 in the western part. The aphanitic basalt unit is described as dark gray to black in its fresh state and a brownish gray to greenish gray color on its weathered surfaces. It has a fine-grained texture, and its minerals are hardly seen in field lenses. It is highly and spherically weathered and at places completely decomposed to soil with only remnants of some core stones. Pyroclastic deposits are described as pinkish gray to brownish red and yellowish brown, fine grained, massive to layered, reworked, felsic volcano-sediments interlayered by ignimbrite layers. Felsites are mapped as light color (greenish gray, light gray to pinkish gray colored rock unit in its fresh state), fine grained in texture; and at places it is vesicular, intermediate composition. It is a volcanic flow unit consisting of intermediate to felsic lava flows and centers with localized lava flows forming NS-trending scarped plugs mainly following riverbanks of the Weyto River. Porphyritic basalt with well-developed olivine crystals within fine ground mass is mapped capping felsites and pyroclastic sediments in the central part of the project area found in the eastern portion of the Weyto River. It has

dark grey weathered and black fresh surfaces. It is fine grained with phenocrysts in it. Generally, it is massive and has a thickness of 3 to 13 meters at the top of small hill topographies. Siliciclastic sediment deposits which thickness is in the range of tens of meters cover the majority of the project area, particularly the map peripheries of both the northern and southern maps. Most of the mapped outcrops of this unit show alternating layers of coarser and finer clastic beds. They are found as hybrid beds of clast-supported sediments with disturbed grading, possibly because they are continuously reworked materials. The unit in general is light brown, medium to coarse grained, massive to bedded, slightly consolidated, compositionally matured and unsorted and consists of sand and minor silt supported by pebble gravel.

4. Field procedure

The geophysical observations were made along survey lines, which had been laid out at the preselected sites. In the surveying work, the direction and layout of seismic lines and locations of seismic shot points and geophones were determined. The distance between geophones was 10 m, whereas the shot point intervals were 25 m, 50 m, 55 m, 100 m and 110 m. Survey work was planned and conducted at 2 sites, dam site option 1 and dam site option 2 along 20 lines. The layouts of these profiles are shown in Fig. 2. All seismic refraction lines were laid down on the ground.

5. Instrumentation and spread layout

The instrument used for the seismic refraction survey was the specialized engineering seismic wave-prospecting instrument known as the Seis-24 channel seismograph. The instrument accessories used during the fieldwork include a multichannel cable, trigger geophone cable and 25 pieces of geophones. Twenty-four pieces of geophones were set (Fig.3), each geophone at equal intervals driven into the ground so, that it would be in a straight line and connected with a multichannel cable to the main instrument. A trigger geophone was set at an approximately 2-4 m distance from a shot point. The interval between measuring geophones and shot points was more than 5 m. Explosives were used as a source of seismic energy and deployed with different weight ranges from 200 gm to 2000 gm depending on the position of the shot point. The stations of optimal offset shot points and weights of the optimal explosive were determined after field testing progressed enough. The methods of nine shots/spread (-95, 5, 30, 55, 80, 105, 130, 155, 180, 205, 305) and seven shots/spread (-105, 5, 60, 115, 170, 225, 335) were applied in the area of investigations and were found to be adequate. During the survey work, two to four geophone stations overlapped for every line; that is, an inline-profiling survey technique was conducted.

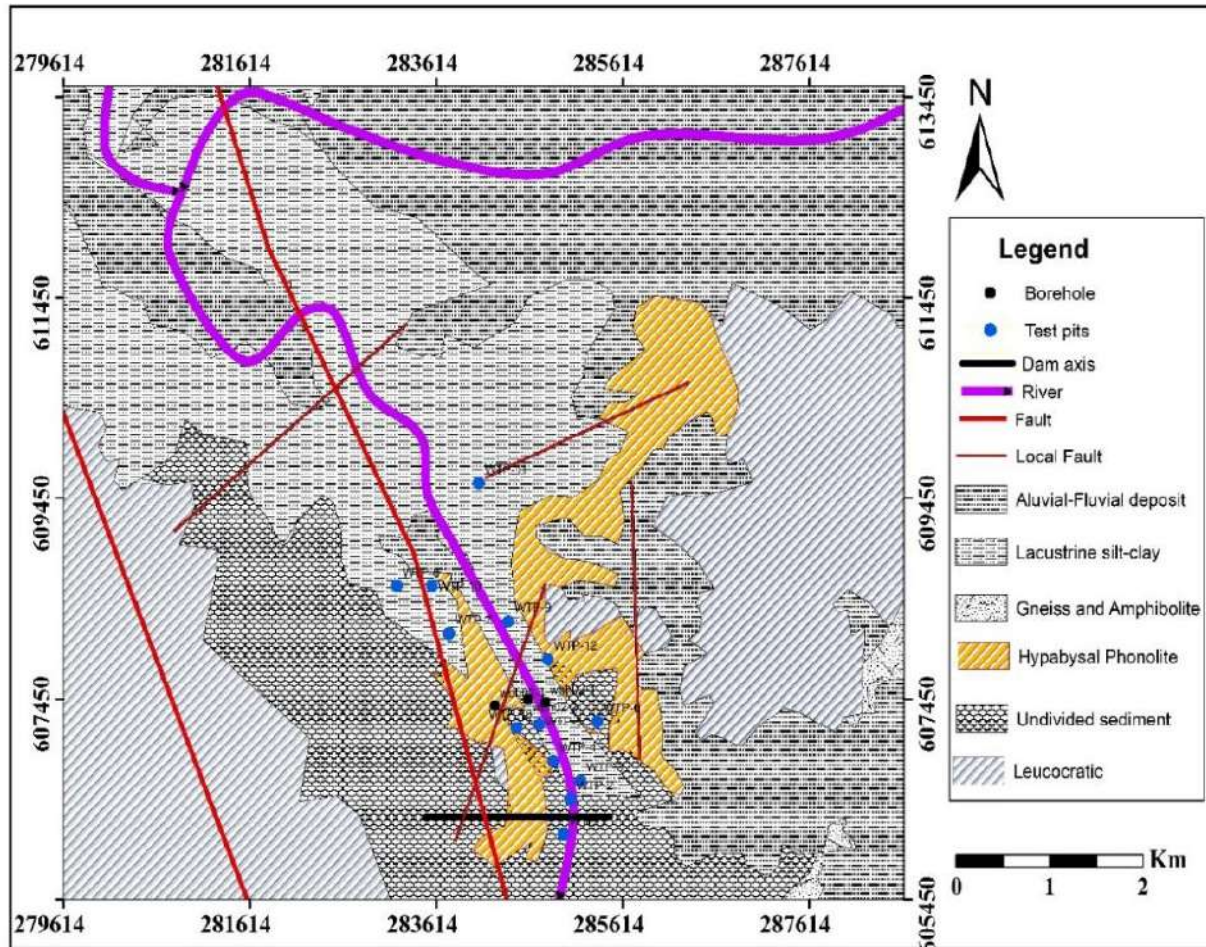


Fig. 2. Geological map study area

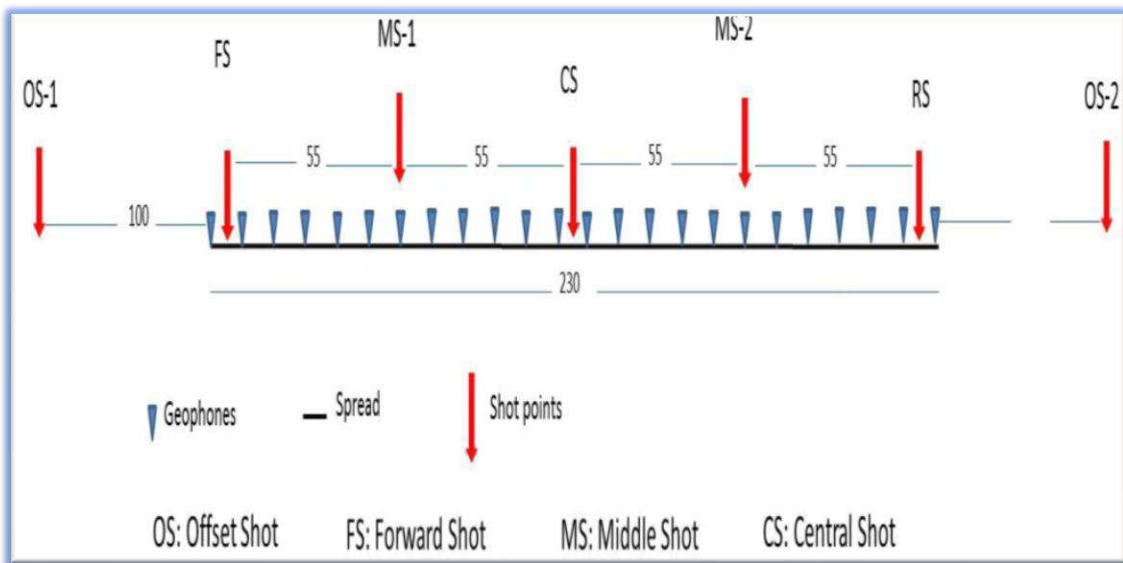


Fig. 3. Geometry of seismic refraction survey setup

6. Field parameters, data processing and data quality

The refraction seismic data were acquired using field parameters selected on site (Fig.4). These pa-

rameters enabled the acquisition of good-quality data (Table 1). Moreover, at some places, the repeated measurements were made to refine the data quality after correcting envisaged problems.

Table 1
Parameters of seismic refraction used

Energy source	Explosive
Geophone distance	10 m
Length of spread	230 m
Shot position	-105, 5, 60, 115, 170, 225, 330 -95, 5, 30, 55, 80, 105, 130, 155, 180, 205, 305
Recording time	1500 microseconds(ms)
Sampling	0.5
Filter	Open

The acquired seismic wave field can be described in two parts: travel times and amplitudes. Seismic amplitudes are more prone to the detrimental effects of noise compared to travel times. As such, travel time inversion is a very robust and accurate method to estimate the P-wave velocity-depth model of geological columns. Therefore, noise is filtered out from the wave signal until a high signal-to-noise ratio is obtained, and first arrivals are selected to produce the tomography section. The accuracy of interpretation depends on several factors, such as the scale of investi-

tigation, topography, geology and surrounding noise. All the above mentioned factors are possible contributors, as deeper depth was investigated with wide geophone spacing in topographically widely varying terrain and complex geologic conditions. The correlation of available borehole logs with seismic results indicates very good data for the upper, medium and bottom units. A comparison of seismic interpretation results and borehole logs shows that the difference between depths obtained from interpretation and borehole logs is less than 10%.

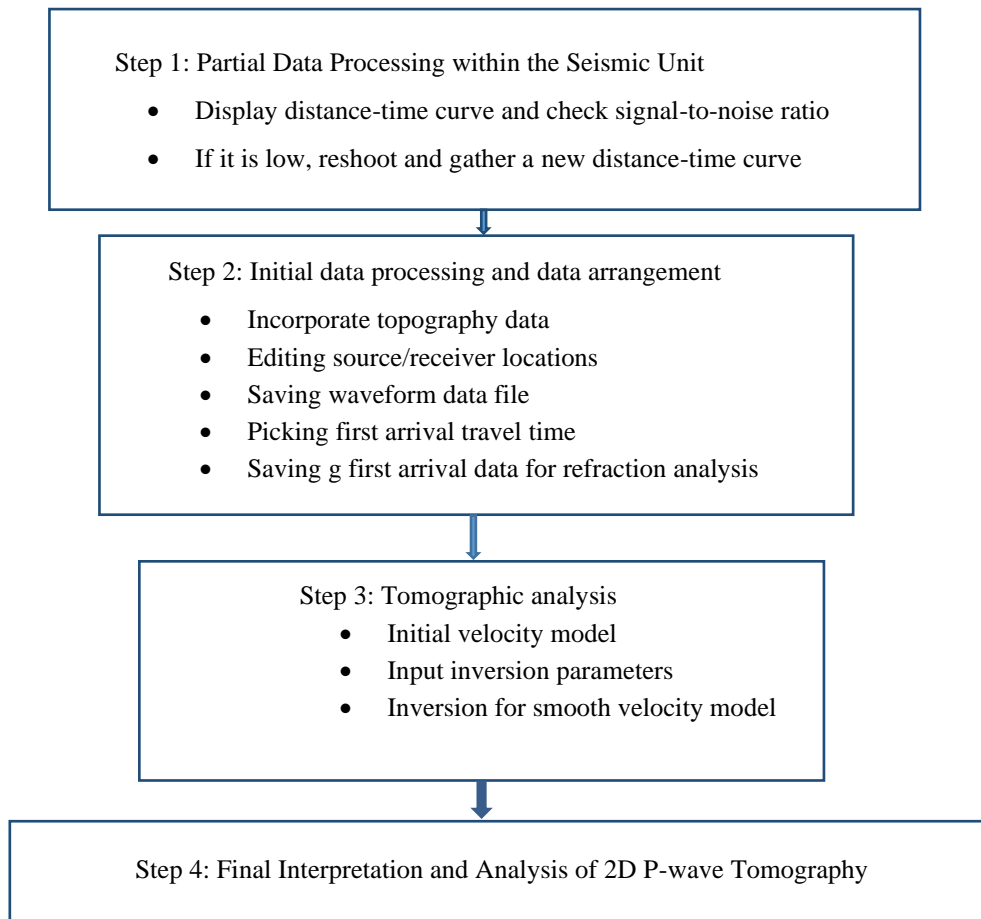


Fig. 4. Summary of data processing steps

7. Interpretation of seismic refraction data

Ten survey lines (Fig. 5) with a total length of 10512 m were conducted to characterize the geological features of foundations at the Dam Site.

Spread line-1

This line (Fig. 6) is acquired on the right side of the proposed dam with a survey direction NE-SW orientation with a turning point at SP-6. There are 20 shot points with 55 m source intervals along the line and two offset shots with 100 m distances from two ends of the line. The line extends from the UTM geographic coordinate of 284578E, 606022N (SP-1) to the SW direction and turns at SP-8 (284485E, 60519N) almost to the south direction and ends at 284606E, 605176N (SP-20). Topographically, the line is along a very ragged and sloppy surface, and it crosses the river between SP-15 and SP-16. This line is traversed by lines 10, 9, 8, 7, and 6 on the left and right sides of the Weyto River. The first layer is mapped with a wide range of thicknesses throughout the section. The thickest part of this layer is detected at the plateau between SP-3 and SP-11, where there is the minimum degree of erosion. The maximum thickness is measured to be approximately 40 m at

and around SP-7. This weak material with P-wave velocity of < 1500 m/s could be related to the clastic sediments, which comprise fine sandy silt. The underlying layer with P-wave velocity measured in the range of 1500 m/s to 2500 m/s could correspond to highly weathered gneiss or clastic with consolidated gravels. This layer is either left with minimum thickness or totally eroded along the fault plane. Similar to the overlaying formation, this layer reaches its maximum thickness of approximately 20-25 m in the elevated part of the section.

The third layer, which looks at a constant thickness in the entire section with velocity values ranging between 2500 m/s and 4000 m/s, is correlated to highly or moderately weathered gneiss or fractured basalt. The bottom layer, which has a P-wave velocity value greater than 4000 m/s could be related to the slightly weathered basalt, and the slightly weathered gneiss is 114 m deep at SP 9 and 41 m just beneath the river channel. Successive normal faults that mimic the regional normal faults of the region are selected in the middle of the section. The other major structure identified from this section is two normal faults that created uplift from SP-3 to SP-14.

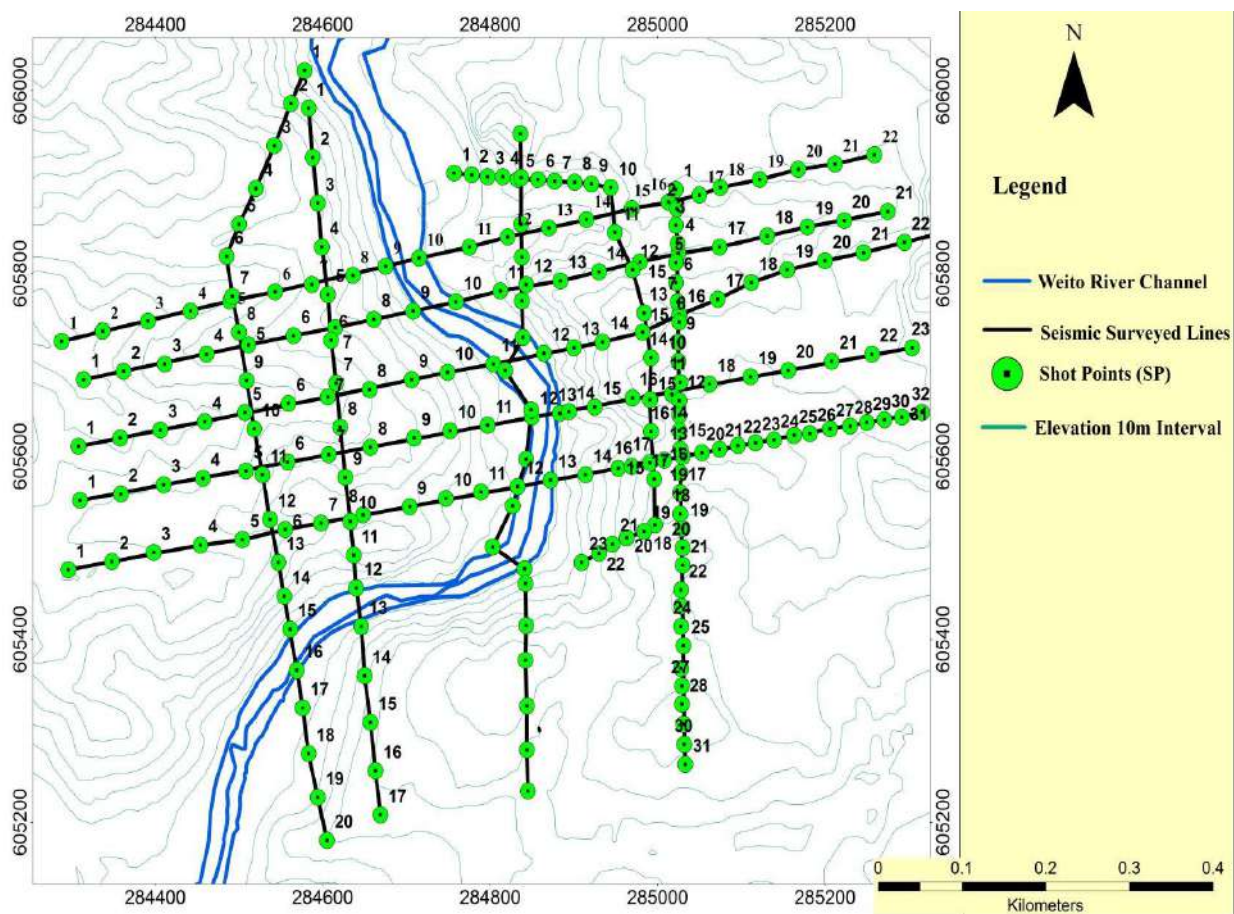


Fig. 5. Seismic Refraction Surveyed lines on Option-1

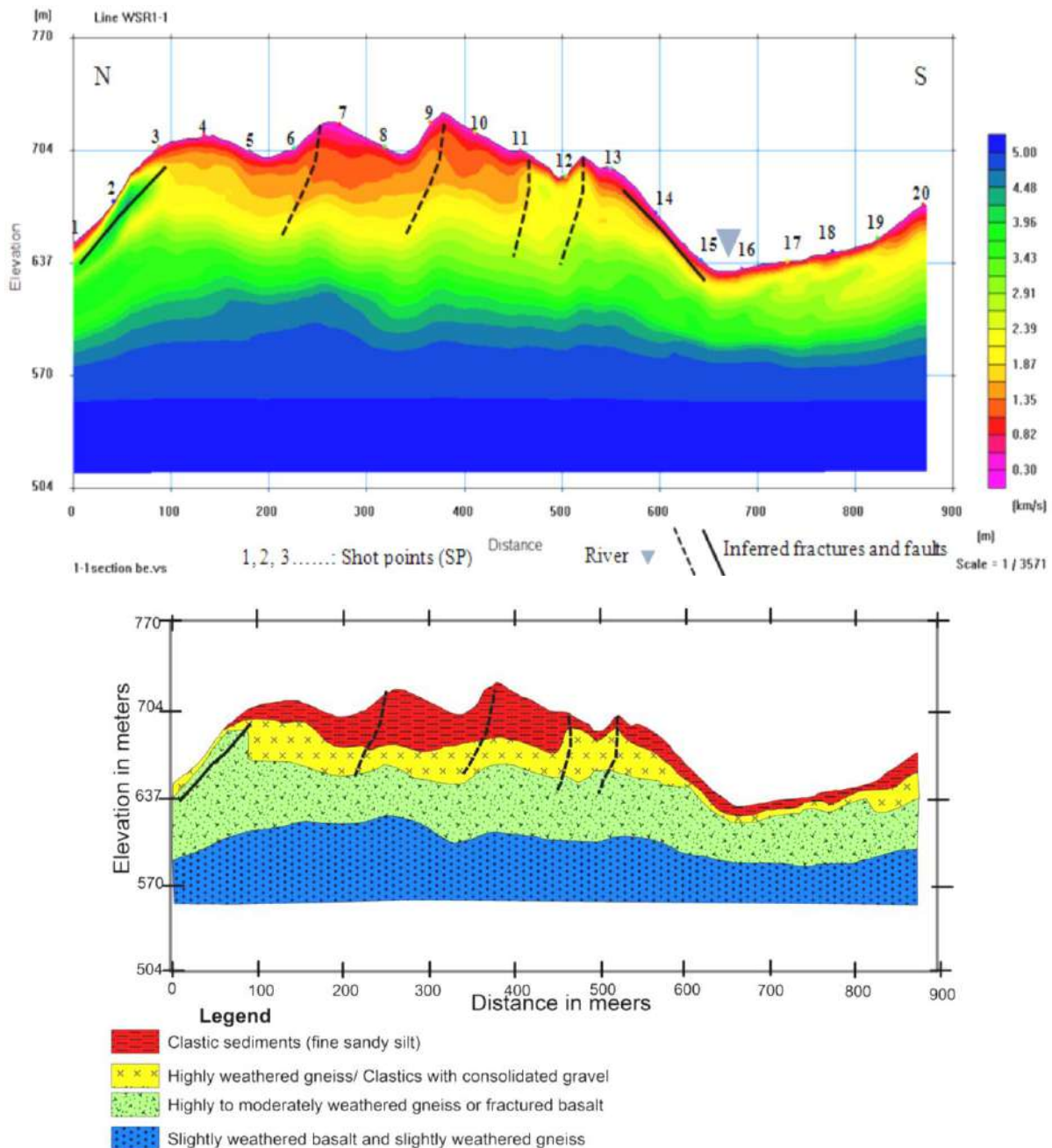


Fig. 6. Geo-seismic section of line-1

Spread line-2

This line is located on the right bank of the dam site acquired in the N-S direction. There are 19 shot points with 55 m intervals except the two offset shots, which are located 100 m away from two ends of the line. The line extends from UTM coordinates of 284583E, 605981N (SP-1) to 284669E, 605204N (SP-17). This line intersected all the dip lines (6, 7, 8, 9 and 10) and WBH1-3 between SP-7 and SP-8. Log data of WBH1-3 were used as priori data in data interpretation, and the interpreted parameters are comparable with the log data around the borehole. The section (Fig.7) revealed a layer with low p-wave velocity (> 1500 m/sec having a constant thickness

of 6-10 m almost throughout the section. This low-velocity layer could be related to clastic sediments that comprise fine sandy silt.

The second layer with p-wave velocities between 1500 m/sec and 2500 m/sec is associated with highly weathered gneiss or clastic with consolidated gravels. This layer has a maximum thickness of 30 m around SP-7 and almost vanishes along slant surfaces, which could be the fault plane (between SP-11 and SP-12). This layer is relatively thick to the south part of the river. The third layer, which could slightly be related to moderately weathered gneiss filled by quartz or pegmatite veins with P-wave velocity range between 2500 and 4000 m/sec., is detected at

different depths in the section. In areas such as fault planes, the third layer is either underlain by the thin portion of clastic sediments or exposed to the surface without the above mentioned two layers. Its maximum thickness is identified in the northern part of the section, which is measured to be approximately 60 m, while the eastern side of the river is relatively thin with a thickness of only 30 m. The bottom layer that has P-wave velocity greater than 4000

m/s has been detected at a shallow depth of 45 m at the river channel and gets down deep to 100 m depth at the WBH1-3 location. This layer could correspond to slightly weathered gneiss or fractured basalt. Weak zones are identified around SP-5 and SP-8 bounded by the low velocity layer within these inferred fractured zones. The other possible structure picked in this section is a fault which is located between SP-11 and SP-12.

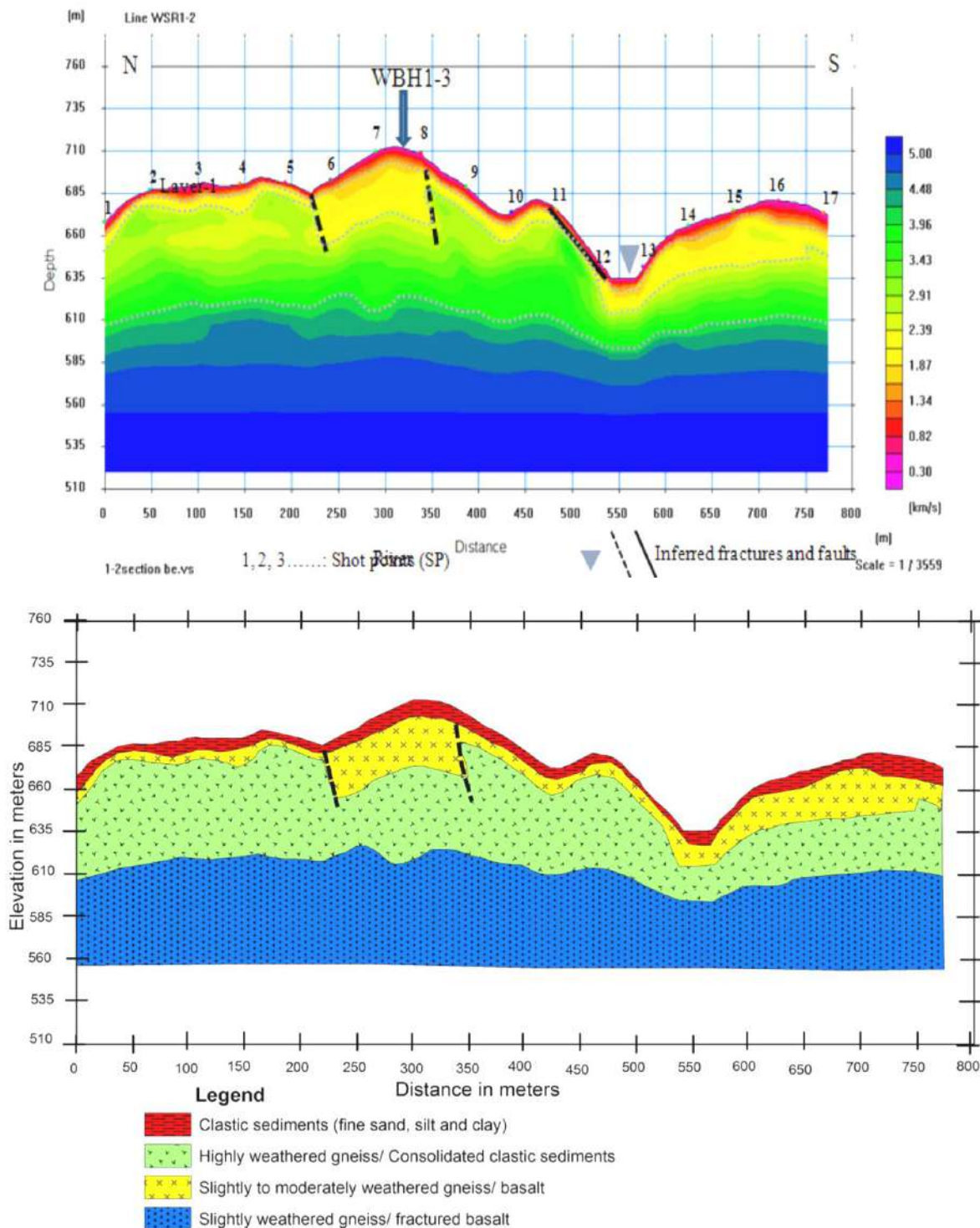


Fig 7. Geo-seismic section of line-2

Spread Line-3

Line-3 is surveyed in the N-S orientation, and it crosses the river at two places (SP-6 and SP-12). There are 18 shot points with 55 m intervals except the two offset shots, which are located 100 m away from two ends of the line. The line extends from UTM coordinates of 284836E, 605958N (SP-1) to 284845E, 605229N (SP-18) with a total ground survey length of 910 m. This line (Fig.8) is traversed by lines 4, 10, 9, 8, 7, and 6 from the upstream to downstream direction. Topographically, the central part of the line is situated in a flat surface following the river channel. Apart from the central part, the other portion

of the line is located on a hilly and ragged surface. Since the central part of the line is acquired along the river channel where there is high energy attenuation because of thick alluvial sand, it was difficult to obtain deeper data. To solve this problem, a large amount of explosive was deployed in a deep shot hole. The top layer with a P-wave velocity value greater than 1500 m/sec has almost a constant 6 m thickness in the central part of the section and reaches its maximum thickness of 20 m at SP-15. This low-velocity layer is related to colluvium sediments, which are composed of fine sand, silt and clay according to borehole data and field observations.

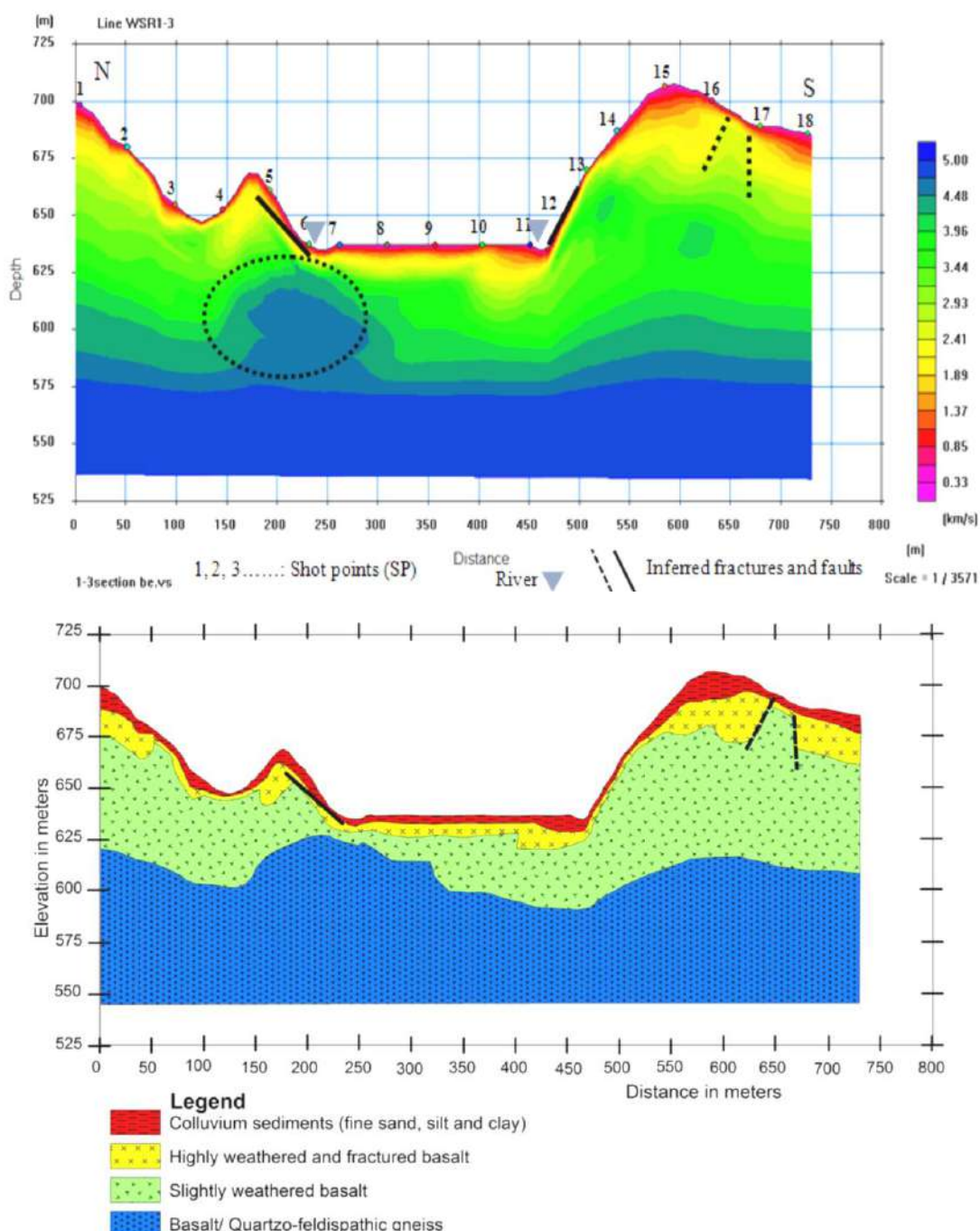


Fig. 8. Geo-seismic section of line-3

The second layer with P-wave velocities ranging from 1500 m/s to 2500 m/s, which could be related to the highly weathered and fractured basaltic rock, is spotted only in a few parts of the section. This formation is missing in the slope areas and some points, such as SP-3, SP-4, SP-6 and SP-7. At the hill tops (SP-1, between SP-4 & SP-5 and SP-15), this formation reaches its maximum thickness of 20 m. The third layer has P-wave velocity ranging from 2500 m/s to 4000 m/s, which could be related to the slightly weathered basaltic rock identified at various depths. It is detected at a shallow depth at SP-6 with a thickness of less than 10 m, gets deep towards the south side of the section and measures approximately 50 m in thickness on both ends of the section. The bottom layer with P-wave velocity value of more than 4000 m/s may be correlated to basalt rock or quartz-feldspathic gneiss with pegmatite or quartz vein intrusions. At the river crossing between SP-7 and SP-6, this layer could be exposed or detected at shallow depths similar to the overlain formation. The minimum depth to its top surface is 20 m along the river channel, whereas the maximum depth is located at SP-15, which is measured more than 90 m.

Spread line-4

Due to the design of this line, it can be divided into four segments based on the orientation of the line. The first and fourth segments are surveyed along almost the E-W direction. The second and third segments extending from SP-10 to SP-19 are surveyed in the N-S and NW-SE orientations, respectively. All segments of the line are surveyed on the left side of Option-1 with a total length of 920 m. There are 23 shot points with 55 m intervals for the central segments (Segments 3 and 4) and 25 m intervals for segments 1 and 4. This line is traversed by lines 10, 9, 8, 7, and 6 on the left side of the Weyto River. The line (Fig. 9) extends from UTM geographic coordinates of 284754E, 605910N (SP-1) to 284904E, 605482N (SP-23). The interpretation for this line is controlled by WBH1-1, which is situated between SP-14 and SP-13 of this line.

The top layer with P-wave velocity value of less than 1500 m/s is identified only in some parts of the section corresponding to clastic sediments, which comprise sand, clay and silt. This layer is missed almost in parts between SP-8 and SP-11 of the section; however, it is identified from SP-1 to SP-8 and around the borehole location, which has a thickness of approximately 10 m. At the north end of the section, this layer measured 20 m in thickness, while the maximum thickness of approximately 45 m was noticed around SP-18. There are clear structures picked at two different places, SP-16 and SP-5, which could be faults and that is the reason to dis-

cover a wide variation in thickness of this layer within a few meter intervals. Most structures can manifest on the surface, such as the above mentioned two faults, while few cannot have surface signatures and die in the ground. The underlying layer where its occurrence is more or less similar to the top low velocity layer is mapped at different portions with a very wide range of thicknesses. Its velocity is demarcating between 1500 m/s and 4000 m/s, which corresponds to highly or moderately weathered and fragmented volcanic rocks. Even if its degree of weathering decreases with depth, this layer goes to a depth of 75 m around the borehole location with poor rock quality. It could be exposed to the surface in the portion between SP-7 and SP-11. The bottom layer, which is related to slightly weathered basalt rocks that have P-wave velocity of more than 4000 m/s is placed at a depth of between 75 m and 105 m from the surface.

Spread Line-5

This line is surveyed along the N-S direction parallel to the Weyto River extending from UTM coordinates of 285022E, 605918N (SP-1) to 285032E 605225N (SP-32). There are 32 energy source points with 25 m intervals that are acquired to the left side of the river. All the dip lines (parallel to the dam axis) are traversed by this line. Successive valleys and hills are encountered across the 830 m length. Topographically, the line (Fig.10) is situated on the elevation variation from 723 m to 685 m above mean sea level. WBH1-1 is located just 40 m to the west side of SP-9, and it is conceivable to constrain the interpretation of this line by the borehole data based on the 2D P-wave velocity tomography section of Line 5. Four layers have been identified. The first top layer having P-wave velocity value of less than 1500 m/s is interpreted as either clastic sediments comprising sand, silt and clay or highly weathered trachyte basalt, or it could be both formations. This layer is identified at the south end of the line with a maximum thickness of 41 m for a length of approximately 180 m. Its thickness decreases when it goes towards the center of the section and is almost lost at SP-14. Near the WBH1-1 location, an average thickness of 20 m is measured on the northern part of the line. The underlying layer characterized by P-wave velocity ranging from 1500 m/s to 2500 m/s possibly represents highly weathered or fractured and decomposed basaltic rock. From SP-4 to SP-24, except of the intrusion of the high velocity layer in the central part, the thickness of the second layer somehow ranges from 20 to 30 m. On the south side underneath the thick top layer, the second layer has a constant thickness of approximately 14 m.

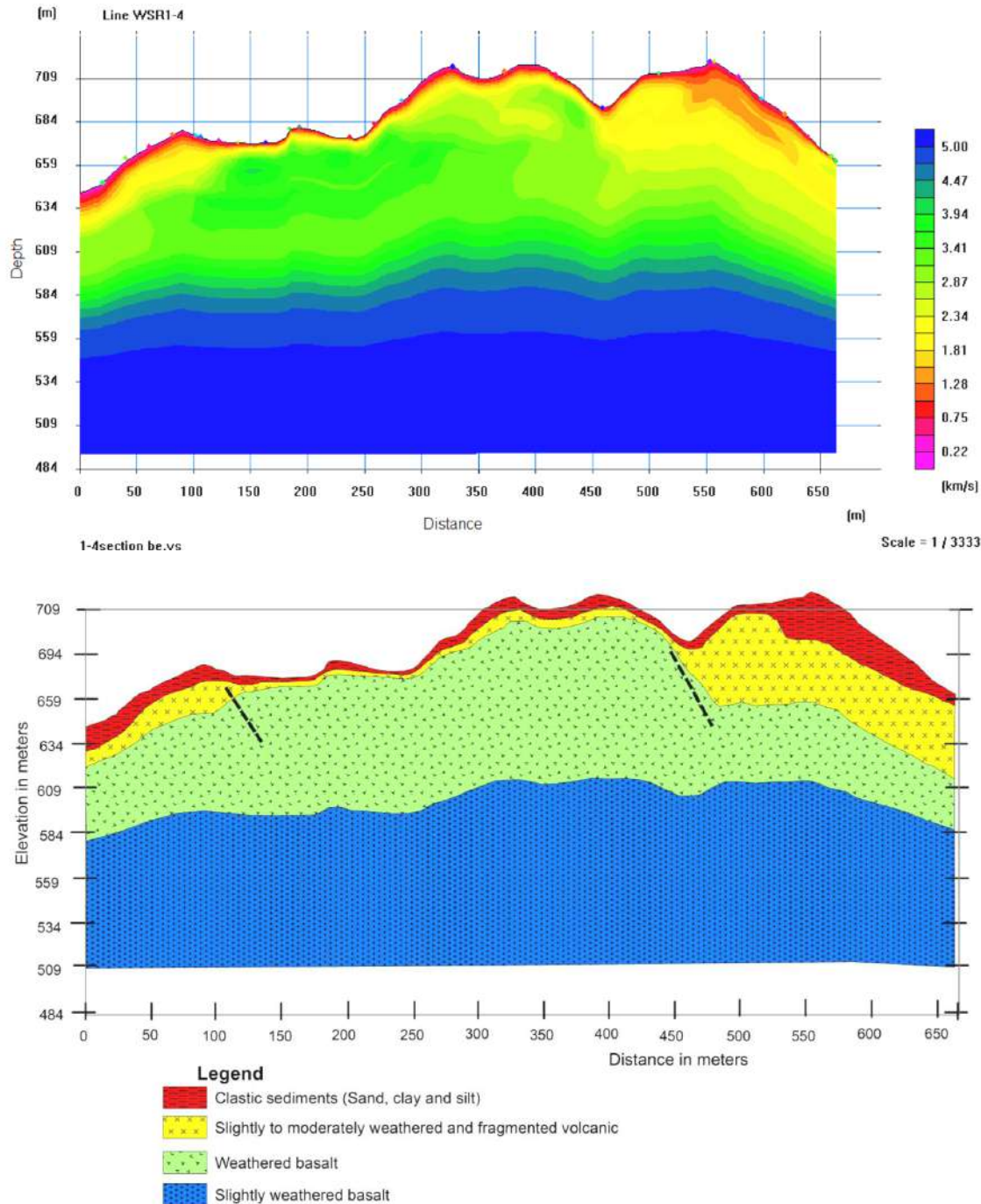


Fig. 9. Geo-seismic section of line-4

The third velocity layer has compressional wave velocities between 2500 m/s and 4000 m/s, which could be related to the slightly weathered aphanitic basalt intercalated with a highly weathered rock matrix. It is mapped near or exposed to the surface around SP-14, although it is found deep down to 55 m in the southern part of the line. It is unconformably underlain by the above layer. Regarding its thickness distribution, apart from the north end and SP-16 of the line where it has a maximum thickness of 46 m thickness, it has a constant thickness of 15-20 m

throughout the section. The bottom layer that has P-wave velocity value of more than 4000 m/s is detected at a depth of 55 m to 85 m from the surface. This layer could be similar to the overlying layer with only varying degrees of weathering of the basalt rock and/or the rock matrix, or it could be related to slightly weathered gneiss. According to the borehole data, the formation encountered from 26 m to the final depth of the borehole is mafic volcanic rock.

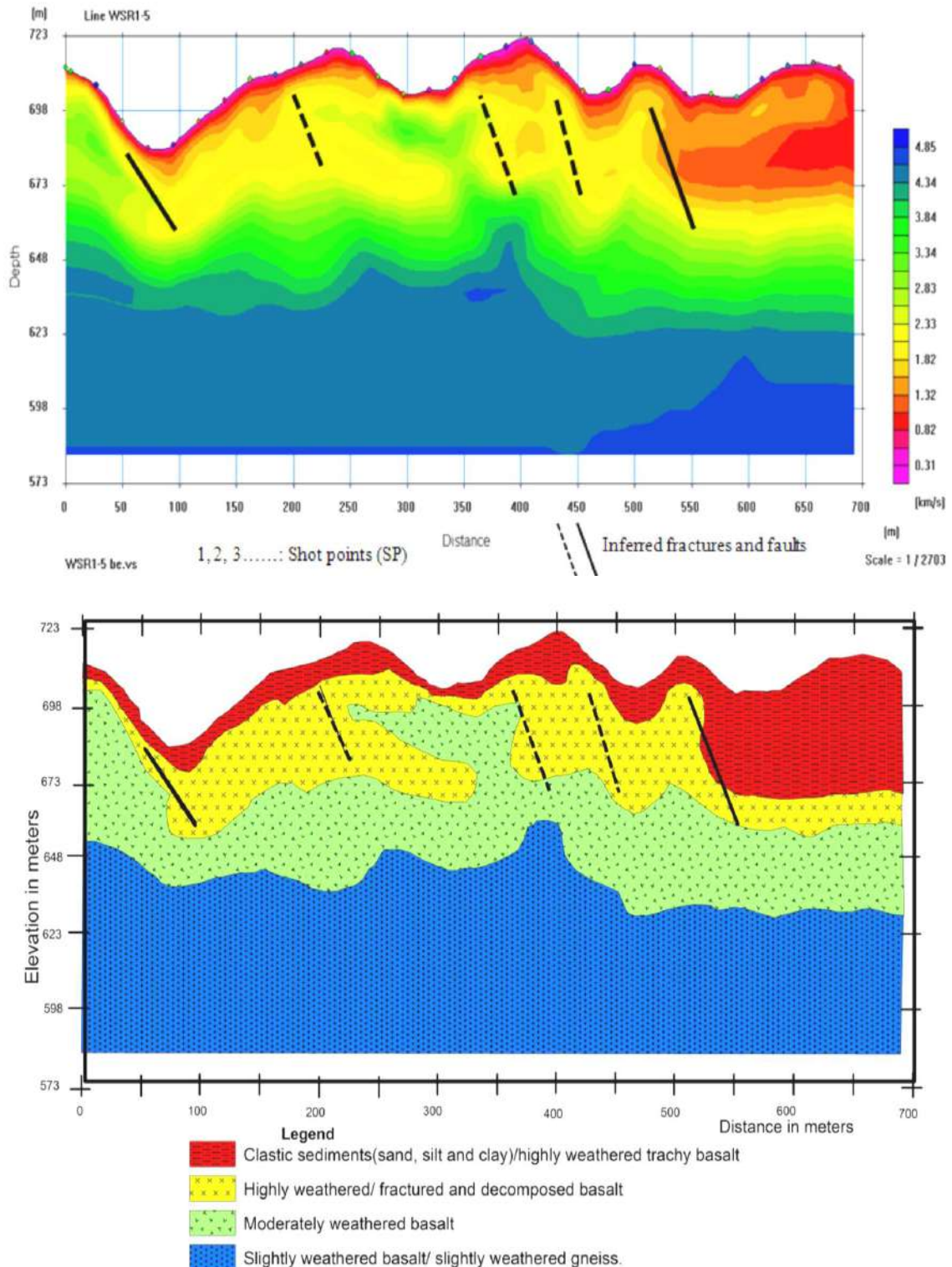


Fig. 10. Geo-seismic section of line-5

Spread Line-6

Line WSR1-6 is surveyed parallel to the dam axis along the E-W direction, which intersects the river at SP-13. This line extends from UTM coordinates of 284296E, 605476N (SP-1) to 285321E 605648N (SP-32) situated to the downstream side of the proposed dam axis. There were two setups for explosive shot point intervals; the whole right

side of the section and the sloppy part of the left part were surveyed with 55 m source interval, while the other part of the line was surveyed with 25 m source interval. Line 6 is intersected by lines 1, 2 and 3 to the west side of the river and lines 4 and 5 to the left side. Four seismic layers have been identified that correspond to different geological layers. As always, the first layer that has P-wave

velocity below 1500 m/s is identified at different parts of the line with a wide range of thicknesses. The section (Fig.11) of the first 200 m length from the right side has predominantly composed of clastic sediment or highly weathered and fractured rock, which could be denoted by this low velocity layer. Around this part of the section, the top layer has a maximum thickness of 33 m; however, at slant areas, just at both sides of the river channel has no chance to preserve these weathered and loose clastic sediments. This layer has a constant thickness of approximately 8 m on the plateau area to the eastern part of the river. The underlying layer that has relatively higher P-wave velocity is repre-

sented by compressional wave velocities on the order of 1500 m/s-2500 m/s, which are associated with highly weathered and fractured basaltic rock. Its thickness varies from very thin or possibly vanishes at the slant surface to 33 m at the plateau areas. There is a thin squashed layer mapped with high velocity from SP-5 to SP-10, which could be due to a volcanic layer overlay on palaeosoils or volcanic clastic. The third layer, which is characterized by a compressional velocity ranging from 2500 m/s to 4000 m/s is exposed to the surface at the river valley or identified profoundly when it goes away from the river channel. This layer is related to slightly or moderately weathered basalt or moderately weathered gneiss.

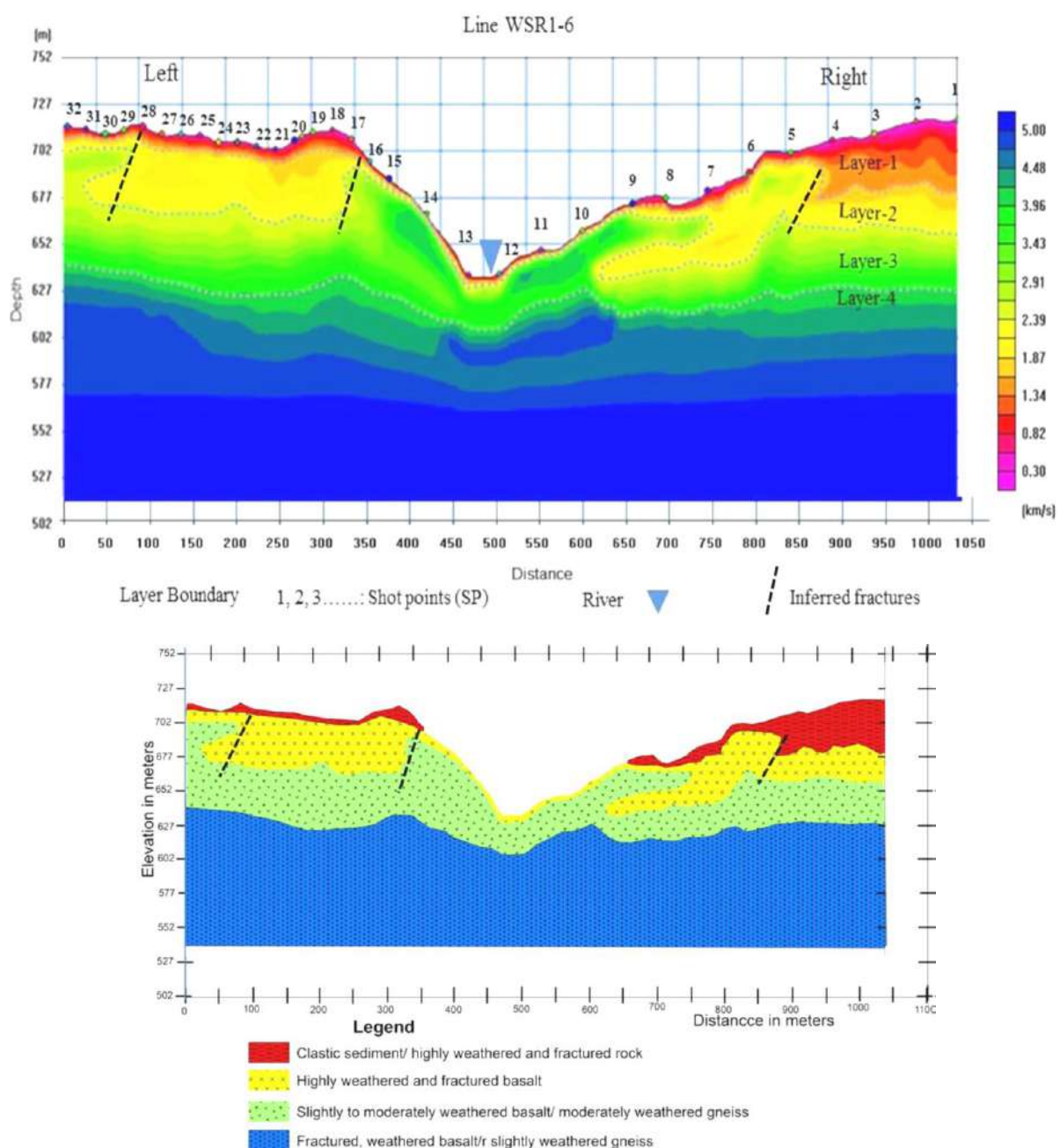


Fig. 11. Geo-seismic section of line-6

Its thickness varies from its least thickness of 20 m at SP-12 to maximum value of 62 m thickness at SP-16. The isolated spot with an inverted velocity distribution mapped beneath SP-10 to SP-14 could be related to the existence of water in the fractured basalt rock. It can be observed from 2D P-wave velocity tomography section of Line WSR1-6 that the bottom layer is generally represented by over 4000 m/s velocity. The depth to basement is near the river channel, which is only 30 m deep; however, it is traced between 80 and 96 m depth around the elevated areas. This layer could be related to fractured, weathered basalt or slightly weathered gneiss.

Spread Line-7

Line 7 is surveyed along the E-W orientation and crosses the river between SP-13 and SP-14. There are 23 shot points with 55 m intervals except two offset shots, which are located 100 m away from two ends of the line. The line extends from UTM geographic coordinates of 284310E, 605552N (SP-1) to 285307E, 605719N (SP-23) with a total ground survey length of 1190 m. This line (Fig.12) is traversed by lines 5 and 4 to the left side, while lines 3, 2 and 1 cross the right side of the river.

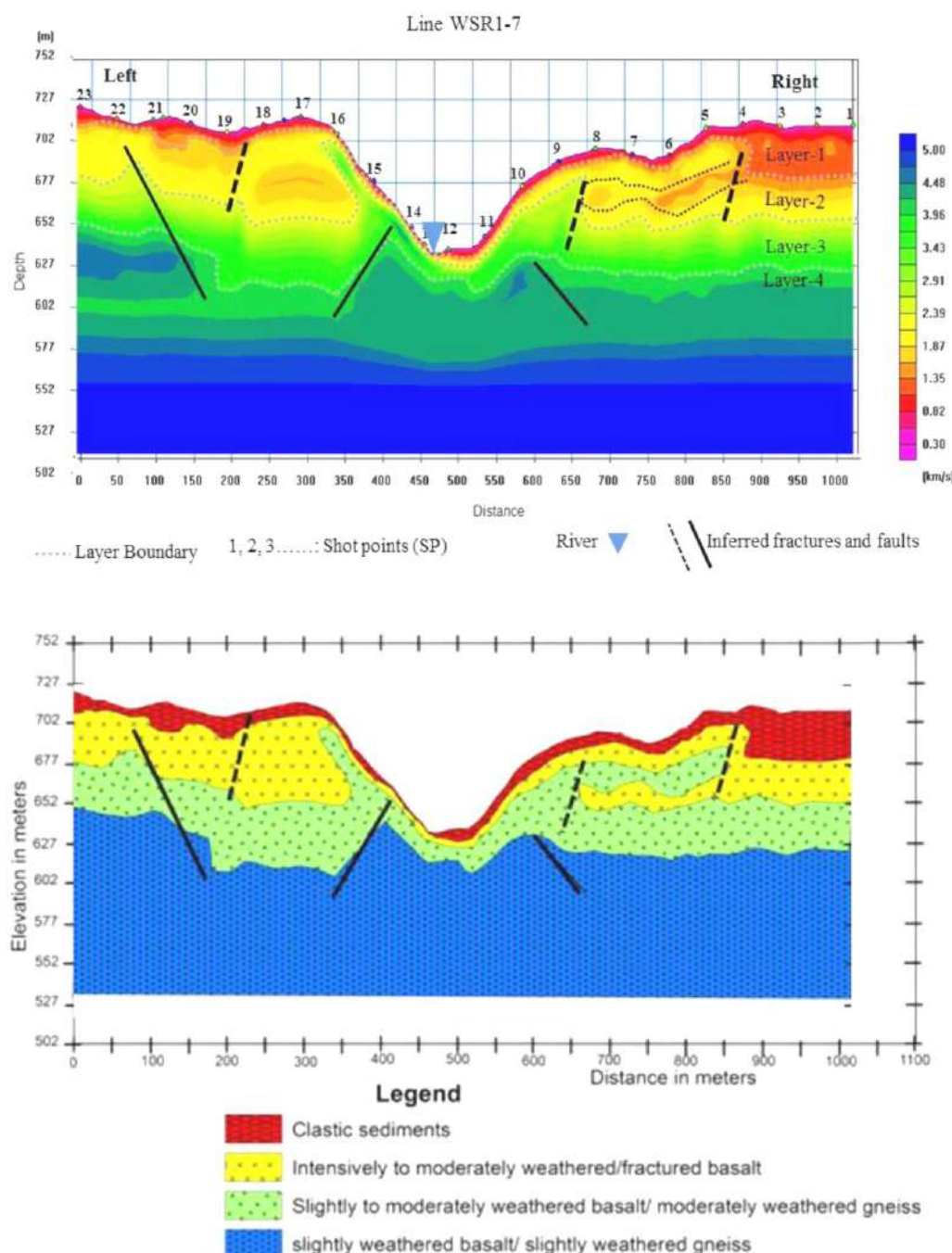


Fig. 12. Geo-seismic section, Line WSR1-7

The top layer outlined by P-wave velocity value of less than 1500 m/s is identified throughout the section except the slope surface to the left side of the river. This seismic layer corresponds to clastic sediments that comprise sand, clay and silt. The thickest part of this layer is found to the right end of the section with a thickness of 40 m. This layer has almost a constant thickness between 5-10 m from SP-5 to the river channel and from SP-17 to the left end of the section. Since highly weathered rocks and loose sediments could not exist on a highly inclined surface, this top clastic sediment was missed in parts between SP-14 and SP-17. In some parts, the underlying layer is squeezed within this layer (see SP-4 to SP-9). The underlying layer characterized by P-wave velocity between 1500 m/s and 2500 m/s is traced in almost all parts of the section. This layer is attributed to intensively or moderately weathered/fractured basalt having very poor rock mass quality or highly weathered gneiss. Relatively, it is very thick to the left side of the section than to the right side. The thickness varies from 50 m at SP-18 to very thin or completely absent along the slant surface of the left side of the river. The third layer characterized by a compressional velocity ranging from 2500 m/s to 4000 m/s is exposed to the surface at the river valley or detected profoundly when it goes away from the river channel. This layer corresponds to slightly or moderately weathered basalt or moderately weathered gneiss. Its thickness varies from its least thickness of 7 m at the river channel to maximum thickness of 50 m at SP-10. The bottom layer that has P-wave velocity value of more than 4000 m/s is detected at a depth of 17 m beneath the river channel to 102 m at SP-18 from the surface. This layer could be similar to the overlaying layer with only varying degrees of weathering of the basalt rock, or it could be related to slightly weathered gneiss. There are inferred structures at various depths of the section that could be faults or fracture zones. Based on the 2D P-wave tomography section and field observations, these structures are not manifested on the surface. The two inferred faults are picked inside the third and bottom layers, while the fractures are displayed in the first two layers.

Spread Line-9

This line (Fig.13) extends from W (SP-1) to E (SP-21) marked by UTM geographic coordinates of 284314E and 605683 N and 285280 E and 605869 N, respectively. It is surveyed parallel to the dam axis, which crosses lines 1 and 2 to the right and Lines 3, 4 and 5 to the left side of the river. There are 21 shot points with 55 m intervals and offset shots placed 100 m away from the first and last geophone locations. One borehole (WBH1-2) is located between SP-10

and Sp-11 of this line. The interpretation of this line is well constrained by these core drilling data. The top layer, which is characterized by a compressional P-wave velocity value of less than 1500 m/s is identified all over the section with various thicknesses. The left part of the section has constant thickness of approximately 7 m, while the right part shows from 45 m around SP-3 to 10 m towards the valley. This velocity layer could be related to clastic sediments and highly weathered and fractured basalt or gneiss along the slant surface. The underlying unit is characterized by P-wave velocities varying between 1500 m/s and 2500 m/s, which could be associated with intensively fractured and weathered gneiss or highly fractured basalt. This layer could be missed around SP-11 and become thick at two specific points; in the right part, 35 m thickness is identified for more than 100 m lateral distance, and to the left side, it has similar thickness but has small area coverage. The third velocity unit covers the entire section and is clearly indicated by 2500 m/s to 4000 m/sec velocity related to slightly or moderately weathered basalt with poor rock mass quality or weakly to moderately weathered gneiss. The thickness varies from 20 m at SP-7 to 70 m around SP-15. This layer could be exposed at an inclined surface and identified at depth of approximately 75 m to the right end of the section. In some areas, slightly weathered and fractured basalt rock is found between low-velocity layers. This could be due to volcanic layer overlay on paleosoils or ground water being detected. According to the 2D P-wave velocity tomography section of line WSR1-9, the fourth layer is represented by velocity value greater than 4000 m/s, which is attributed to slightly weathered gneiss or slightly to moderately weathered basalt. The depth of the bedrock surface varies between 40 m at the central part and 100 m to the right end. The inferred structures that could be fractured or fault zones have been identified on both sides of the river around SP-7 and SP-18.

8. Discussion

Refraction seismic investigations were carried out with objective of the determining the thickness of the overburden materials, identifying the subsurface layers, and estimating the depth to the bedrock, presence of geologic structures and ground-water conditions. It is well understood that types of rocks, degree of weathering and geological structures are the main controlling factors for dam site selection. To address these controlling factors, seismic refraction investigation is the primary choice over other geophysical investigation methods. Therefore, the results from such seismic measurements may assist in dam site selection and rock engineering.

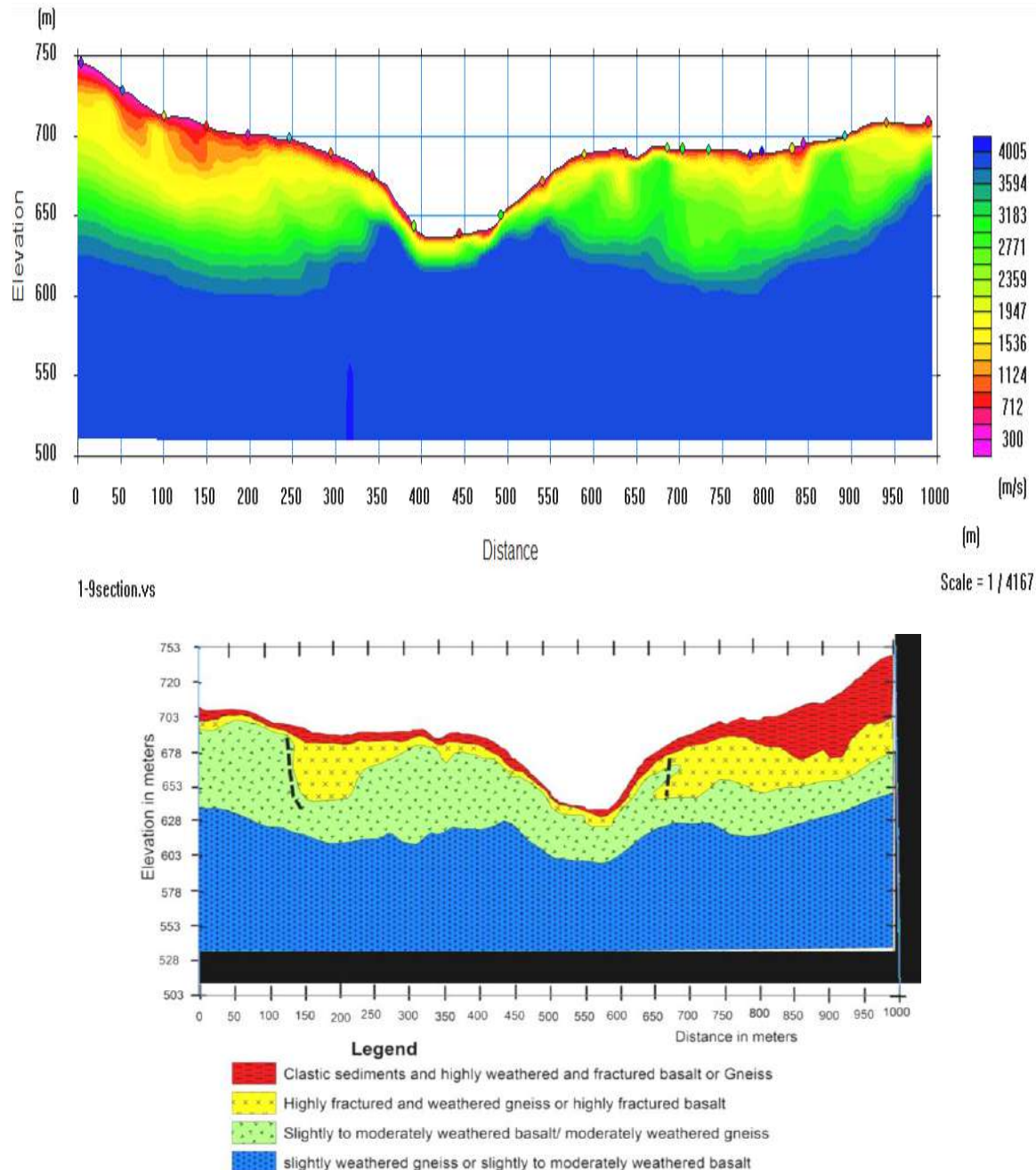


Fig. 13. Geo-seismic section of line-9

Practically, if any dam site shows any occurrence of active faulting irrespective of its attitude (i.e., dip & strike) under no circumstances, dam construction should not be undertaken. The Weyto dam sites are geologically and tectonically complex and characterized by faults and fracture zones that are identified in almost all seismic sections. Furthermore, the project is located in the southwestern part of the Main Ethiopian Rift, which is tectonically an active area. It has been recognized that most of the seismic sections and the borehole data except WBH1-2 do not show groundwater, at least up to the drilling depth. Therefore, the absence of groundwater in most parts of the project site will minimize the risk of dam failure.

The most identified faults from seismic tomography sections exist on both upstream and downstream sides and frequently dip towards the downstream side, which will decrease the suitability of sites for dam construction. The foundation rock or rock mass under the dam axis and reservoir area has to provide stable support with little or no deformation and avoid settlement under all conditions of saturation and loading. Igneous and metamorphic rocks are the most desirable rocks at the dam site. These are strong and durable due to their dense character, interlocking texture, hard silicate mineral composition, occurrence of negligible porosity and permeability, absence of any inherent weak planes,

resistance to weathering and tendency to occur over wide areas. However, it should be checked that the selected rocks are not affected by weathering or fracturing or dykes or any geological structures such as shearing, faulting and jointing. Thus, all plutonic rocks, such as granites, syenites, diorites and gabbro, are very competent and desirable rocks for the foundation at the dam site. However, another consideration should be taken into account; volcanic rocks, which are generally vesicular or amygdaloidal, are not desirable since they will be permeable and contribute to porosity and hollowness, in turn contributing to the weakness of rocks. Massive basalts, which are very fine grained, are one of the toughest rocks in nature. However, they can be adversely affected when they are vesicular and permeable. The seismic section revealed thick loose sediments in most parts of the dam sites apart from the central

part along the river channel and the slope areas. From the core drilling data and geological mapping, the types of rocks dominating the dam sites are fractured and weathered gneiss and igneous rocks.

10. Conclusion

The seismic refraction investigations were carried out along topographically surveyed lines. The interpreted results satisfactorily met the objectives and depths of investigations (over 100 m) despite the complexity of the study area. Accordingly, maximum depth of approximately 110 m is attained by the refraction seismic survey in the right and left parts of dam site. Based on the results of the refraction, seismic investigation in conjunction with the available borehole logging data, the seismic layers and their respective geological layers are summarized below.

Table 2
Seismic layers with corresponding geological layers

Seismic Layers	P-wave velocity (m/sec)	Geological layers
Layer-1	<1500	Clastic sediment consists of gravels, boulder size of rock fragments and fines, fluvial deposit, sandy silt gravelly sandy silt
Layer-2	1500-3000	Intensively to moderately weathered and fractured basalt and gneiss, having very poor rock mass quality
Layer-3	2500-4000	Moderately to slightly weathered and fractured basalt and gneiss, having poor rock mass quality
Layer-4	>4000	Moderately to slightly weathered and slightly fractured and fragmented to fresh basalt and slightly weathered gneiss

REFERENCES

- Bawuah G., Baffoe E., Darko B., Hadir I. A.A., Ogbetuo D. The use of seismic refraction survey in geotechnical investigations. International Journal of Engineering Research and Science, Vol. 4(7), 2018, pp. 6-17.
- Bihon K. Factors affecting agricultural production in Tigray region, Northern Ethiopia. PhD thesis, University of South Africa, 2015.
- Fell R., MacGregor P., Stapledon D. Geotechnical engineering of dams. Taylor and Francis Group PLC. London, UK, 2005, pp. 180-181.
- Ivan A., Samuel H. Techniques for prevention and detection of leakage in dams and reservoirs, Venezuela, 1987.
- Levitte D., Columba J., Mohr P. Reconnaissance geology of the Amaro horst, Southern Ethiopian rift. Geological society of America Bulletin, Vol. 85(3), 1974, pp. 417-422.
- Long-term benefits and performance of dams. British Dam Society 13 Conference, 2004, Canterbury, Kent, Thomas Telford. London, 676 p.
- Telford W.M., Geldart L.P., Sheriff R.E., Keys D.A. Applied geophysics. Cambridge University Press. 1976.

ЛИТЕРАТУРА

- Bawuah G., Baffoe E., Darko B., Hadir I. A.A., Ogbetuo D. The use of seismic refraction survey in geotechnical investigations. International Journal of Engineering Research and Science, Vol. 4(7), 2018, pp. 6-17.
- Bihon K. Factors affecting agricultural production in Tigray region, Northern Ethiopia. PhD thesis, University of South Africa, 2015.
- Fell R., MacGregor P., Stapledon D. Geotechnical engineering of dams. Taylor and Francis Group PLC. London, UK, 2005, pp. 180-181.
- Ivan A., Samuel H. Techniques for prevention and detection of leakage in dams and reservoirs, Venezuela, 1987.
- Levitte D., Columba J., Mohr P. Reconnaissance geology of the Amaro horst, Southern Ethiopian rift. Geological society of America Bulletin, Vol. 85(3), 1974, pp. 417-422.
- Long-term benefits and performance of dams. British Dam Society 13 Conference, 2004, Canterbury, Kent, Thomas Telford. London, 676 p.
- Telford W.M., Geldart L.P., Sheriff R.E., Keys D.A. Applied geophysics. Cambridge University Press. 1976.

ПРИМЕНЕНИЕ СЕЙСМИЧЕСКОЙ СЪЕМКИ МЕТОДОМ ОТРАЖЕННЫХ ВОЛН ДЛЯ ОПРЕДЕЛЕНИЯ ИНЖЕНЕРНЫХ ХАРАКТЕРИСТИК УЧАСТКА СТРОИТЕЛЬСТВА ПЛОТИНЫ ВЕЙТО, ЮЖНАЯ ЭФИОПИЯ

Мулуалем А.¹, Демси Т.², Шано Л.², Гетахун Э.², Соломон Х.³

¹Кафедра геологии, Колледж естественных наук, Университет Дебре Маркос,

Дебре Макос, Эфиопия: muluabr4114@gmail.com

²Кафедра геологии, Колледж естественных наук, Университет Инджисибара, Инджисибара, Эфиопия

³Бюро проектно-строительных работ, Аддис-Абеба, Эфиопия

Резюме. Выделенный район исследования, являющийся центром важнейших геологических исследований, географически расположен в Регионе южных наций, национальностей и народов (SNNPR), в частности, охватывая части зоны Сеген и зоны Южный Омо. Точнее, он находится на территории вореда Бенетсемай в непосредственной близости от городского центра Вейто Таун. Располагаясь в пределах скромной долины, местность района исследования представляет собой топографически пересеченный ландшафт. Примечательно, что этот регион является составной частью обширной Южной Главной Эфиопской рифтовой системы, характеризующейся значительной тектонической активностью. Чтобы получить полное представление о характеристиках грунта на предполагаемом месте строительства плотины Вейто, была проведена серия сейсморазведочных исследований. Основными целями этих геофизических исследований были достижение достаточной глубины проникновения и точное определение глубины залегания коренных пород. Кроме того, исследования были направлены на оценку качества недр и выявление наличия и распределения геологических трещин – важнейших параметров, определяющих структурную целостность плотины. Было выявлено, что объекты плотины Вейто имеют сложную геологическую и тектоническую структуру и характеризуются наличием разломов и зон трещин, которые выявлены почти на всех сейсмических разрезах. Геофизические исследования проводились с помощью высокоточного 24-канального прибора преломляющихся волн Seis-24, разработанного с целью получения скоростных разрезов на участке строительства плотины. Территория исследования отличается многогранной геологической обстановкой, демонстрирующей разнообразные сложные тектонические структуры и множество различных геологических формаций. Эти образования включают мелкозернистый афанитовый базальт, различные обломочные осадки, метаморфический гнейс, порфировый базальт и скопления пирокластических отложений, образовавшихся в результате вулканической деятельности.

Ключевые слова: плотина, геофизические исследования, недра, волны сжатия, фундамент

VEYTO BƏNDİNİN TİKİNTİ SAHƏSİNDE MÜHƏNDİSLİK XÜSUSİYYƏTLƏRİNİN MÜƏYYƏNLƏŞDİRİLMƏSİ ÜÇÜN ƏKS OLUNAN DALĞALARIN ÜSULU ƏSASINDA SEYSMİK TƏDQİQATIN TƏTBİQİ, CƏNUBİ EFIÖPIYA

Mulualem A.¹, Demsi T.², Şano L², Getahun E², Solomon H.³

¹Geologiya kafedrası, Təbiət Elmləri Kolleci, Debre Markos Universiteti, Debre Markos, Efiopiya: muluabr4114@gmail.com

²Geologiya kafedrası, Təbiət Elmləri Kolleci, İncibara Universiteti, İncibara, Efiopiya

³Layihə-tikinti işləri bürosu, Addis-Abeba, Efiopiya

Xülasə. Araşdırma üçün seçilmiş ərazi mühüm geoloji tədqiqatlarının mərkəzi olmaqla, coğrafi baxımdan Cənubi Millətlər, Milliyetlər və Xalqlar Regionunda (SNNPR), xüsusilə Seqen zonası ilə Cənubi Omo zonasının bəzi hissələrini əhatə edir. Daha dəqiq desək, bu sahə Benetsemay Voreda ərazisində, artıq formalasılmış şəhər mərkəzi olan Veyto qəsəbəsinin birbaşa yaxınlığında yerləşir. Ərazi nisbəton dərin vadidə yerləşməklə, mürəkkəb və dağlıq relyefə malikdir. Qeyd olunmalıdır ki, bu region yüksək tektonik aktivliklə səciyyələnən geniş Əsas Efiopiya Rift Sisteminin tərkib hissəsini təşkil edir. Veyto bəndinin nəzərdə tutulan tikinti sahəsində yeraltı qatların xüsusiyyətlərini öyrənmək məqsədilə seysmik tədqiqatlar aparılmışdır. Bu geofiziki tədqiqatların başlıca məqsədi sükür qatlarına kifayət qədər dərin nüfuz etməklə, əsas (bərk) sükürlerin yerləşmə dərinliyinin dəqiq müəyyən edilməsindən ibarət olmuşdur. Eyni zamanda, aparılan tədqiqatlar yerin dərinliklərindəki mühəndis-geoloji xüsusiyyətlərin qiymətləndirilməsi, geoloji çatların mövcudluğu və onların ərazi üzrə paylanması müəyyənleşdirilməsi məqsədi daşıyır. Bu amillər bəndin struktur dayanıqlığını müəyyən edən əsas geoloji göstəricilər hesab olunur. Tədqiqat nticələri göstərmişdir ki, Veyto bəndi üçün nəzərdə tutulan ərazi mürəkkəb geoloji və tektonik quruluşu malikdir. Demək olar ki, bütün seysmik profillərdə qırılma və çat zonaları müşahidə olunmuşdur. Bəndin tikinti sahəsində sürət kəsimlərinin qurulması məqsədilə geofiziki ölçmələr Seis-24 markalı 24-kanallı refraksiya cihazı vasitəsilə həyata keçirilmişdir. Tədqiqat sahisi müxtəlif mürəkkəb tektonik strukturları və zəngin litoloji tərkibi ilə səciyyələnən çoxşaxəli geoloji mühitə malikdir. Buraya incə dənəli bazaltlar, müxtəlif mənşəli çöküntü və dağıntı materialları, metamorfik qneyslər, porfirli bazaltlar və vulkanik fəaliyyət nəticəsində formalasılmış piroklastik yığıntılar daxildir.

Açar sözlər: bənd, geofiziki tədqiqatlar, yerin təki, sıxılma dalgaları, təməl

ANALYSIS OF COMPLEX GEODYNAMIC INTERACTIONS IN THE EASTERN PART OF CENTRAL GONDWANA AND EURASIA

Eppelbaum L.^{1,2}, Katz Y.³, Kadirov F.^{4,5}, Guliyev I.⁶, Ben-Avraham Z.¹

¹Dept. of Geophysics, Faculty of Exact Sciences, Tel Aviv University, Israel

Ramat Aviv 6997801, Tel Aviv, Israel: levap@tauex.tau.ac.il

²Azerbaijan State Oil and Industry University, Baku, Azerbaijan

20 Azadlig Ave., Baku AZ1010

³Steinhardt Museum of Natural History & National Research Center,

Faculty of Life Sciences, Tel Aviv University, Israel

Ramat Aviv 6997801, Tel Aviv

⁴Ministry of Science and Education of the Republic of Azerbaijan,

Oil and Gas Institute, Azerbaijan

9, F.Amirov ave., Baku, AZ1000

⁵Ministry of Science and Education of the Republic of Azerbaijan,

Institute of Geology and Geophysics, Azerbaijan

119, H.Javid av., Baku, AZ1073

⁶Presidium of the Azerbaijan National Academy of Sciences, Azerbaijan

30, Istiglaliyyat str., Baku, AZ1001

Keywords: the Eastern Mediterranean mantle structure, the Iranian lithospheric plate, the South Caspian Basin, Eurasia-Gondwana boundary, geodynamic rotation and displacement

Summary. The eastern part of Central Gondwana and Eurasia is a tectonically complex region where several large tectonic plates interact – Eurasian, African, Arabian, Aegean-Anatolian, Iranian, and Sinai. However, consideration of only these plate interactions is insufficient. In addition to this interface, other regional geodynamic factors exist: the mantle rotating counterclockwise structure (MRCS), the Ural-African geoid anomaly, and the critical Earth latitude 35°. The Eurasia-Gondwana boundary divides the western part – the Aegean-Anatolian Plate and Mesozoic Terrane Belt (MTB) associated with the comparatively young Neoproterozoic Belt – and the eastern part, the Iranian Plate, whose terranes are fragments of the Archean-Early Proterozoic Arabian craton. The Iranian lithospheric plate, a key player at the boundary between Eurasia and Gondwana, holds significant implications in the tectonic-geodynamic context. It tectonically influenced the South Caspian Basin (SCB) and recently revealed MTB. Novel tectonic, satellite-derived gravity, and magnetic maps of the Iranian Plate have been developed. Geodynamically, the considered tectonic units are located above the central and eastern parts of the MRCS. The Iranian Plate is above the eastern (periclinal) zone of the MRCS and, under its influence, moves northward. The movement of the western part and complex form of the Iranian Plate force the clockwise rotation of the SCB. A complex geodynamic-geophysical interaction of the central tectonic-geodynamic units in the region is shown. The influence of the recent geodynamic event – Akchagylian hydrodynamic maximum on the ancient hominin dispersal in the region is exhibited. The carried analysis is essential to understand the role of the complex geodynamic interface in a transition zone between Eurasia and Gondwana.

© 2025 Earth Science Division, Azerbaijan National Academy of Sciences. All rights reserved.

1. Introduction

The status and history of the formation of the Iranian lithospheric plate have been considered mainly at a narrow regional level. Therefore, its classification validity (legitimacy) as a supraregional structure is not a generally accepted factor

in the plate tectonics and geodynamics of the transition zone between Eurasia and Gondwana. Based on these positions, we propose analyzing the available data on plate tectonics of this large region, deep geophysics, and geodynamics, as indicated in Figure 1.

Figure 1 clearly shows that the vast Eurasian plate to the south relates to a complex of different-sized, differentially elongated lithospheric plates of Gondwana, oriented in either the latitudinal or meridional direction: Anatolian (Aegean-Anatolian), Iranian, Sinai, Nubian, Victorian, Somalian, Arabian, and Indian. The boundaries between the lithospheric plates belong to geodynamically heterogeneous zones and correspond to manifestations of collision, spreading, transform shears, and rotation. GPS data, paleomagnetic patterns, and geodynamic reconstructions reflect the latter phenomena. However, consideration of only these plate interfaces is insufficient. In this region there are other significant regional geodynamic factors: the mantle rotating counterclockwise structure (MRCS), the Ural-African geoid anomaly, and the critical Earth latitude 35°.

The discovery of a mantle rotating counterclockwise structure (MRCS) (Eppelbaum et al., 2021) based on multifactor geophysical data (GPS, gravity, magnetic, paleomagnetic, seismotomographic, etc.) caused the need to reconsider geodynamic evolution of this region. It is necessary to underline that earlier, Le Pichon and Gaurier (1988) distinguished the rotation of Arabia and the Levant fault system only based on the tectonic-structural data.

Geodynamically, the Iranian Plate (Motaghi et al., 2015) is considered to occur above the eastern part of the MRCS (Eppelbaum et al., 2021). The lithosphere blocks above the MRCS eastern branch rotation initiate northern displacement of the Iranian Plate. The maps and schemes are based on the previous comprehensive regional geophysical, geodynamic, and paleobiogeographic studies (Alizadeh et al., 2016; Eppelbaum et al., 2018, 2021; 2024a, 2024b; Kadirov et al., 2024).

It is seen that the high magnitude seismogenic zone (Figure 1) is under the MRCS influence (the structure long-term rotation initiates a stress in the above lithosphere) and is nearly such geodynamic factors as the Eastern Anatolian Fault (EAF), distal part of the Mesozoic Terrane Belt (MTB), Ural-African tectonic step, Earth's critical latitude, and the western ending of the Iranian Plate. Besides this, the seismogenic zone is at the boundary between the MTB and Alpine-Himalayan tectonic belt (Eppelbaum et al., 2024a).

The regional scheme presented in Figure 1 allows considering combination of geodynamic elements of Gondwana several larger radial zones in this complex associated with the features of the historical development of this supercontinent: (1) Western Gondwana, located to the rear of the spreading zone of the Red Sea and East Africa, (2) Central Gondwana – lying on the eastern side of the East African – the Red Sea spreading zone, and (3) Eastern Gondwana; articulated with

the Central Gondwana by a deep shear zone and represented in the extreme east of the region as a fragment of the Indian lithospheric plate.

The given tectonic-geophysical analysis is essential for assessing and understanding the role of the sublatitudinal lithospheric plates – the Iranian and Aegean-Anatolian—as transition zones between Eurasia and Gondwana. The complex tectonic-geodynamic and geophysical peculiarities of the region under study required the examination of works by numerous authors (see Section 2 below). A combined examination of literature sources and analyses of developed gravity, magnetic, tectonic-geodynamic, and topography/bathymetry maps allowed extending our geodynamic knowledge of the region.

For example, the multidimensional statistical analysis applied to the satellite-derived gravity data (Figure 2) (after Eppelbaum et al., 2018) indicates two significant anomalies (in arbitrary units): to the west of the Afar triangle and inside the central part of the Iranian Plate. This fact indicates the plate's geodynamic significance of the plate.

2. Materials and Methods

Such an investigation requires the acquisition of various geophysical and geological data. The satellite-derived gravity and topographic (bathymetry) data for this study were acquired from the World Gravity Database as retracked from the Geosat and European Remote Sensing (ERS) missions (Sandwell and Smith, 2009). Initial ΔZ magnetic data recalculated to one ordinary level of 2.5 km above the mean sea level (msl) were acquired from <https://geomag.colorado.edu/magnetic-field-model-mf7.htm>. Several independent works were examined for the GPS data analysis (e.g., Reilinger et al., 2006; Khorrami et al., 2019; Kadirov et al., 2015; 2024). In addition, various seismic (e.g., Ben-Avraham, 2002; Abdullayev et al., 2017; Teknik et al., 2019; Mousavi and Fullea, 2020; Alizadeh et al., 2024; Teknik, 2024; Corchete, 2025), thermal (e.g., Eppelbaum and Pilchin, 2006; Goutorbe et al., 2011; Mukhtarov, 2018; Mousavi and Andestani, 2023; Teknik, 2024), gravity (Kadirov, 2000; Ben-Avraham et al., 2002; Kadirov and Gadirov, 2014; Eppelbaum et al., 2018, 2021; Kadirov et al., 2023; Teknik, 2024), paleomagnetic (Issayeva and Khalafli, 2006; Mattei et al., 2019; Eppelbaum et al., 2021; Mousavi and Andestani, 2023), and magnetic (Eppelbaum and Katz, 2015; Eppelbaum et al., 2023, 2024a; Eppelbaum, 2024) data sources were analyzed. The following works were examined in the paleobiogeographical studies: Arkell, 1956; James and Wynd, 1965; Makridin et al., 1968; Ализаде, 1972; Ализаде и др., 1983; Feldman, 1987; Hirsch, 1988; Hirsch and Picard, 1988; Cooper, 1989; Kazmer, 1993; Hall et al., 2005; Alizadeh et al., 2016.

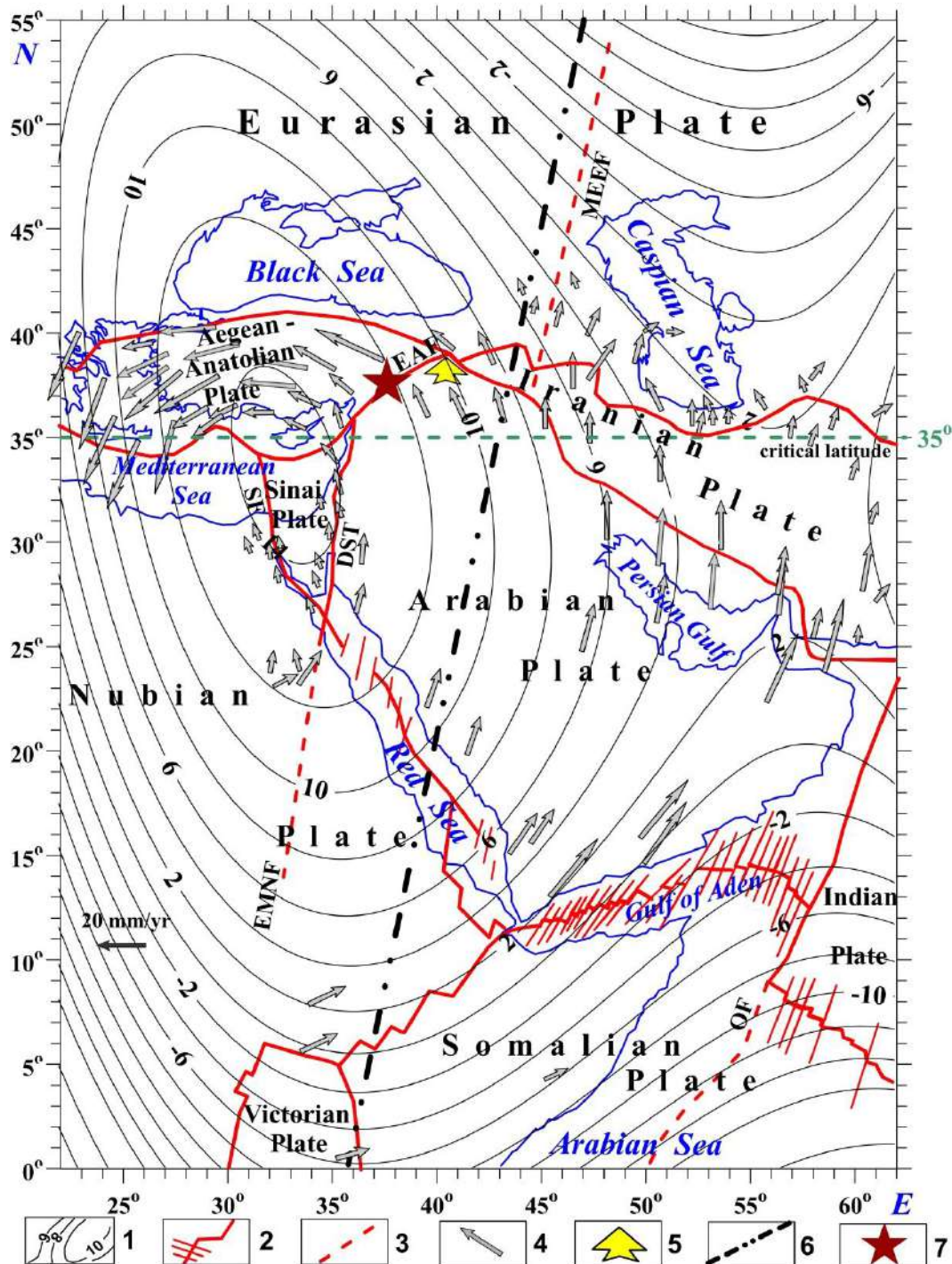


Fig. 1. Geophysical-geodynamic map of the area under study.

(1) isolines of the residual satellite-derived gravity field, (2) main interplate faults, (3) main intraplate faults, (4) GPS vector behavior (mainly after Reilinger et al., 2006; Khorrami et al., 2019; Kadirov et al., 2024), (5) a distal part of the Mesozoic Terrane Belt, (6) averaged position of the Ural-African tectonic step, (7) high-magnitude seismogenic zone in Eastern Turkey (February 06, 2023). SF, Sinai Fault; DST, Dead Sea Transform; MEEF, Main Eastern European Fault; EMNB, Eastern Mediterranean Nubian Belt; OF, Owen Fault

Among the analyzed tectonic-geodynamic sources, we can mention the following works: Le Pichon and Gaurier, 1988; Tselentis and Drakopoulos, 1990; Ben-Avraham and Ginzburg, 1990; Scotese, 1991; Alavi, 1994; Ismail-Zade, 1996; Mangino and Priestley, 1998; Ben-Avraham et al., 2002; Nalbant et al., 2002; Stampfli and Borel, 2002; Brunet et al.,

2003; Hall et al., 2005; Хайн, 2005; Şengör et al., 2005; Jimenez-Munt et al., 2006; Artyushkov, 2007; Zakariadze et al., 2007; Гулиев и др., 2009; Леонов и др., 2010; Goutorbe et al., 2011; Kaz'min and Verzhbitskii, 2011; Vergés et al., 2011; Eppelbaum and Katz, 2012; Eppelbaum et al., 2014; Moghadam and Stern, 2014; Kadirov et al., 2015; Motaghi et al.,

2015; Alizadeh et al., 2016; Abdullayev et al., 2017, 2024; Eppelbaum and Katz, 2017; Mattei et al., 2017, 2019; Eppelbaum et al., 2018; Malekzade, 2018; Le Pichon et al., 2019; Tugend et al., 2019; Bagheri and Gol, 2020; Trifonov et al., 2020; Eppelbaum and Katz, 2021; Eppelbaum et al., 2021, 2024a, 2024b; Rashidi et al., 2022; Mousavi and

Ardestani, 2023; Alizadeh et al., 2024; Koshnaw et al., 2024; Nouri et al., 2024; Teknik, 2024; Eppelbaum et al., 2025.

The investigation methods are based on integration of geophysical, tectonic-structural, and paleobiogeographical data (including anthropological materials).

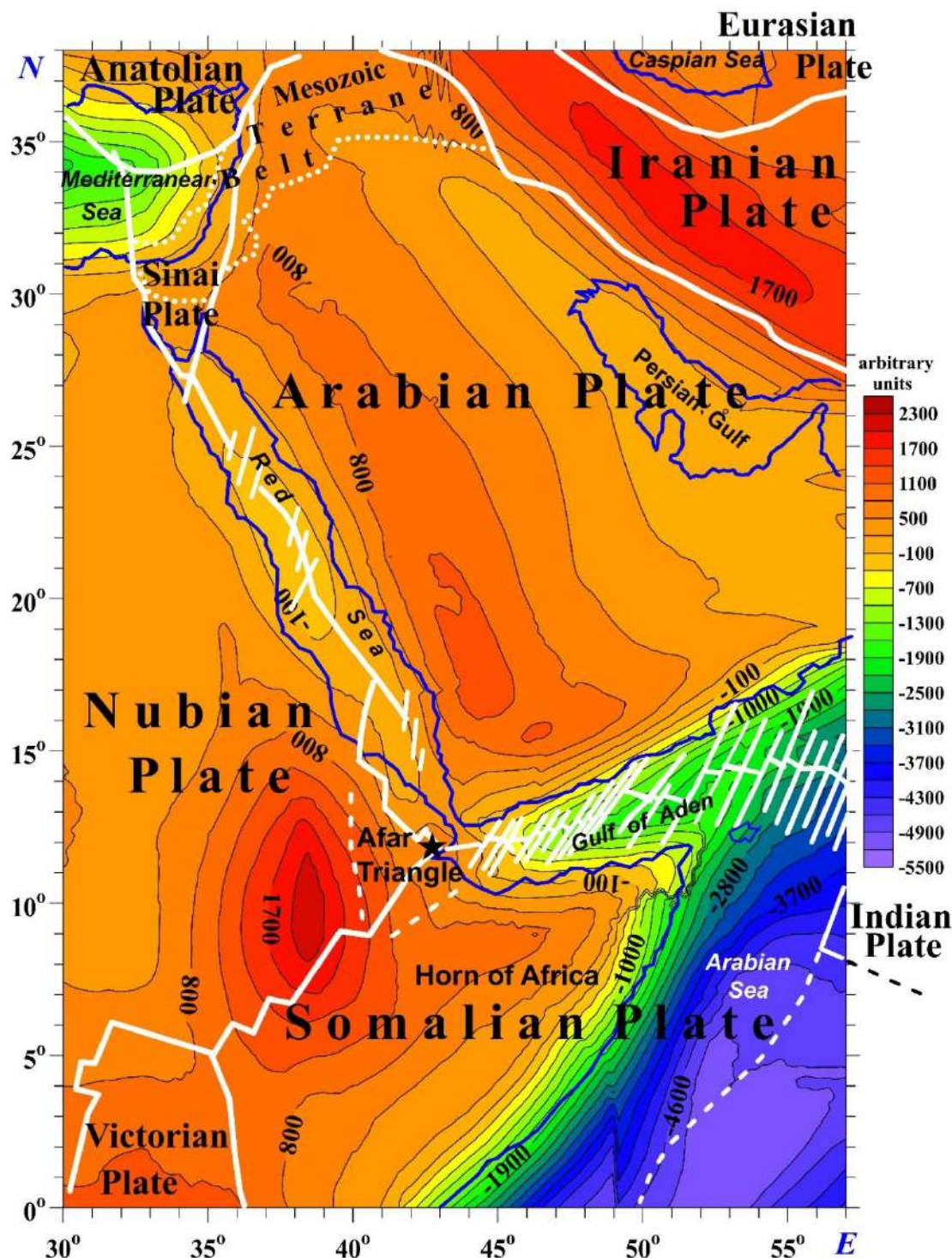


Fig. 2. The map of the satellite-derived gravity field transformed using multidimensional statistical analysis, accompanied by the main plate tectonics units. White lines indicate fault systems, and blue lines show boundaries between the land and marine areas; white points contour the Mesozoic Terrane Belt (supplemented and modified after Eppelbaum et al., 2018).

3. Geodynamic Interaction: A Brief Description

3.1. The Eastern Mediterranean giant mantle rotating structure

The first evidence of a giant mantle rotating counterclockwise structure (MRCS) in the Eastern Mediterranean was provided by Eppelbaum et al. (2021). The center of this structure is located under the island of Cyprus, at the Earth's critical latitude of 35° . The identification of this structure was demonstrated based on: (1) GPS data, (2) satellite gravity data recalculated to the sea/land surface (Figure 1), (3) Bouguer gravity anomalies were observed in the region, (4) geoid anomalies mostly co-

inciding with the GPS (Figure 3) and gravity anomalies, (5) numerous paleomagnetic data showing mostly counterclockwise rotation of tectonic blocks within the projection of the deep structure onto the surface, (6) primary analysis of paleobiogeographic data, (7) initial analysis of seismotomographic data, (8) tectonic-structural analysis, (9) petrological and mineralogical analysis. In the present paper, the results of the quantitative analysis of the residual satellite gravity anomaly are reinterpreted. Additional essential confirmation is provided by the circular pattern of anomalies of the regional magnetic field ΔZ recalculated to 2.5 km above the sea level (Eppelbaum et al., 2024a).

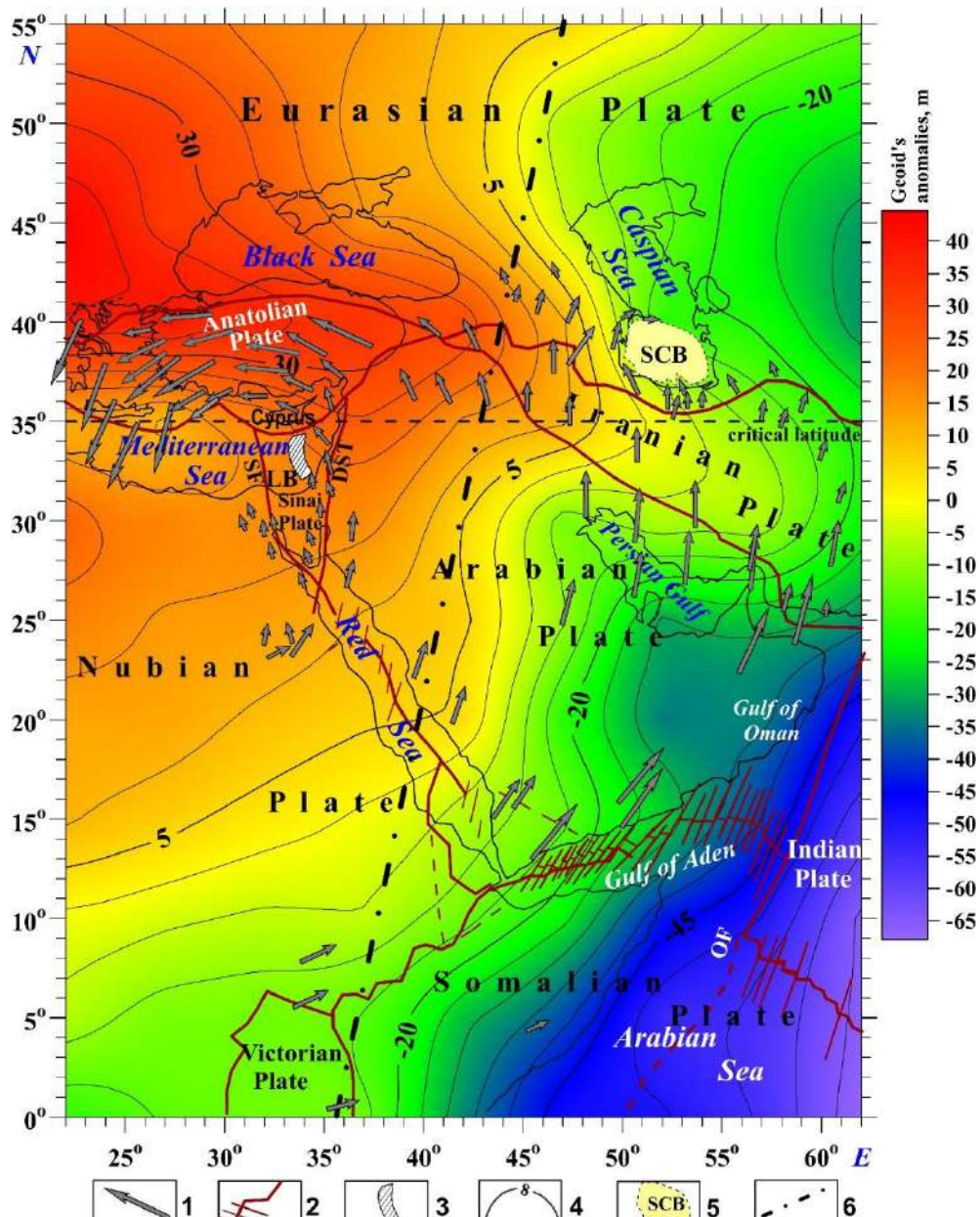


Fig. 3. Geoid map of the African-Arabian-Eurasian region with the tectonic-geodynamic features.

(1) GPS vector distribution, (2) faults, (3) block of oceanic crust relating to the Kiama paleomagnetic hyperzone, (4) geoid's isolines, (5) South Caspian Basin, (6) average position of the Ural-African tectonic step. SF, Sinai Fault, DST, Dead Sea Transform, OF, Owen Fault, LB, Levant Basin, SCB, South Caspian Basin.

The synthesis of seismic tomography profiles enabled the construction of a seismic tomographic scheme for locating the deep structure, which aligns well with the results of other geophysical methods. The integrative combination of all these factors makes it unambiguously proven to detect an anomalous deep structure under the Eastern Mediterranean and surrounding regions. The first constructed paleobiogeographic map (Figure 4) clearly shows the displacement of the typical Ethiopian fauna to

the northwest counterclockwise. The relationship between the rotating deep structure and the occurrence of rock stress before the catastrophic Turkish earthquakes ($M = 7.9$ and 7.8) that occurred on 06.02.2023 (the seismogenic zone, as shown in Figure 1, is at the crossing and nearly several significant tectonic and geodynamic features) (Eppelbaum et al., 2024a). Thus, MRCS is the leading profound geodynamic factor in the region under study.

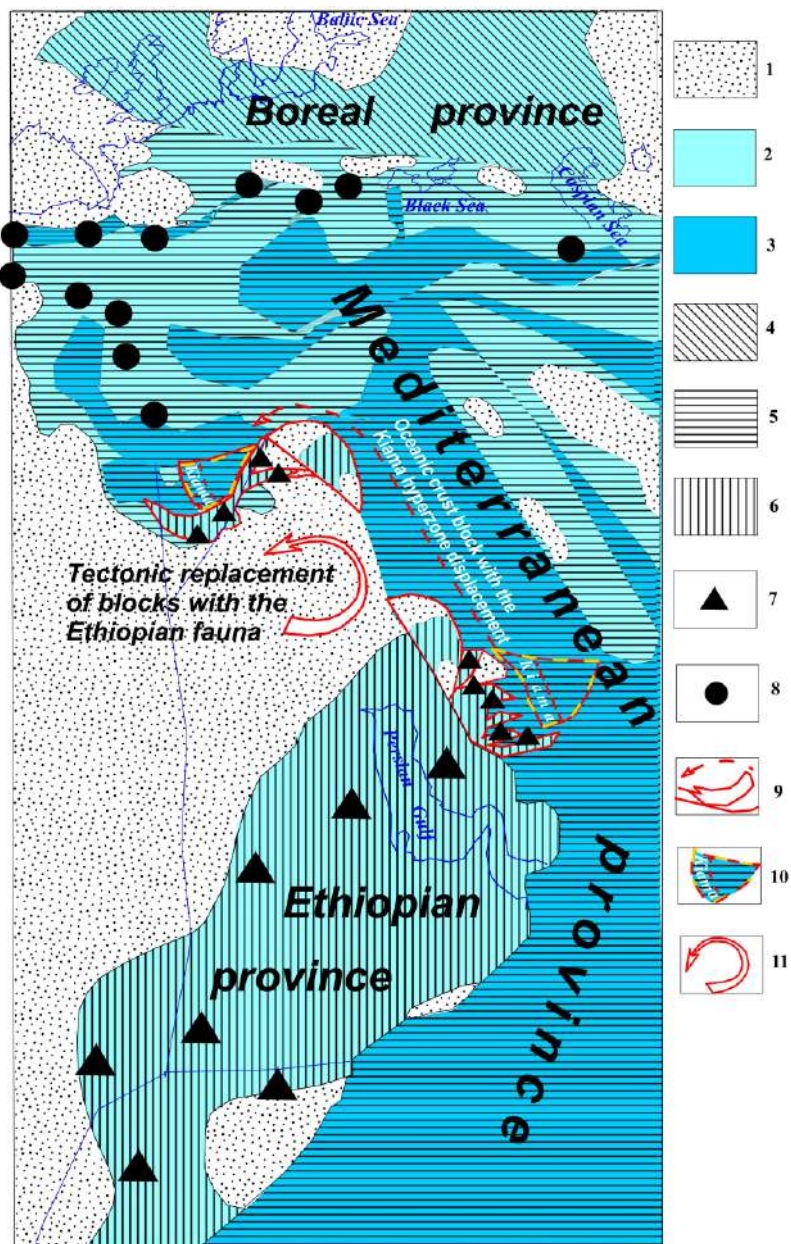


Fig. 4. The schematic Late Jurassic paleobiogeographical map of the transitional region between Eurasia and Gondwana with elements of the subsequent Early Cretaceous geodynamics in the MTB. The blue lines show boundaries between the seas and land. For construction of this map paleobiogeographic data were used from (Arkell, 1956; James and Wynd, 1965; Макридин и др., 1968; Feldman, 1987; Hirsch, 1988; Hirsch and Picard, 1988; Cooper, 1989; Alizadeh et al., 2016; Eppelbaum et al., 2024b) and tectonic-geodynamic data from (Scotesse, 1991; Hall et al., 2005; Stampfli and Kozur, 2006; Eppelbaum et al., 2021).

(1) land, (2) continental shields and arcs, (3) oceanic plateaus and rifts, (4) Boreal paleobiogeographic province, (5) Mediterranean paleobiogeographic province, (6) Ethiopian paleobiogeographic province, (7) points with the Ethiopian brachiopods *Septirhynchia-Somalirhynchia*, (8) location points with the Mediterranean brachiopods *Pygope*, (9) tectonic lines of the discordant paleobiogeographic replacements, (10) block of the oceanic crust with the Kiama hyperzone, (11) counterclockwise rotated tectonic blocks.

3.2. The Iranian lithospheric plate

A new generalized tectonic map of the Iranian lithospheric plate and surrounding regions has been developed (Figure 5). This map reflects the tectonic position of the Central Gondwana and the southern Eurasian plates. The most crucial element here is the boundary between the Iranian and Arabian lithospheric plates, as this collision zone corresponds to the once vast expanse of the Neotethys Ocean that existed in this region. This essential structural element has long been referred to as the Zagros zone. Our regional tectonic studies (Eppelbaum and Katz, 2017) have shown that the Zagros uplift (e.g., Alavi, 1994) is merely the easternmost block of the vast MTB.

The younger Alpine-Himalayan folded-block belt of the transition zone between Gondwana and Eurasia lies to the north of the MTB (formed in the middle of the Early Cretaceous), composed of a

complex of continental and oceanic crust with the ancient Kiama paleomagnetic zone (Eppelbaum et al., 2014). The Iranian lithospheric plate is part of this extensive belt and occupies its southern and eastern parts on the map (Figure 5). The structure of this plate is asymmetric. To the southeast of the Caspian Basin meridian, submeridional block structures and belts are developed: Yanz, Tabas, Lut, and Afghanistan blocks. On the border with Kopet Dagh, sublatitudinal structures are concentrated north of these structures: the Central Iranian Massif and the Ala-Dagh and Binalud folded belts (Mattei et al., 2017). Elongated narrow sublatitudinal structures are developed in the south of the Iranian Plate, directly near the border with the Arabian Plate (Figure 5). Here, the plateau of Southern Iran stands out (Motaghi et al., 2015), composed of the Sanandaj-Sirjan zone (SS).

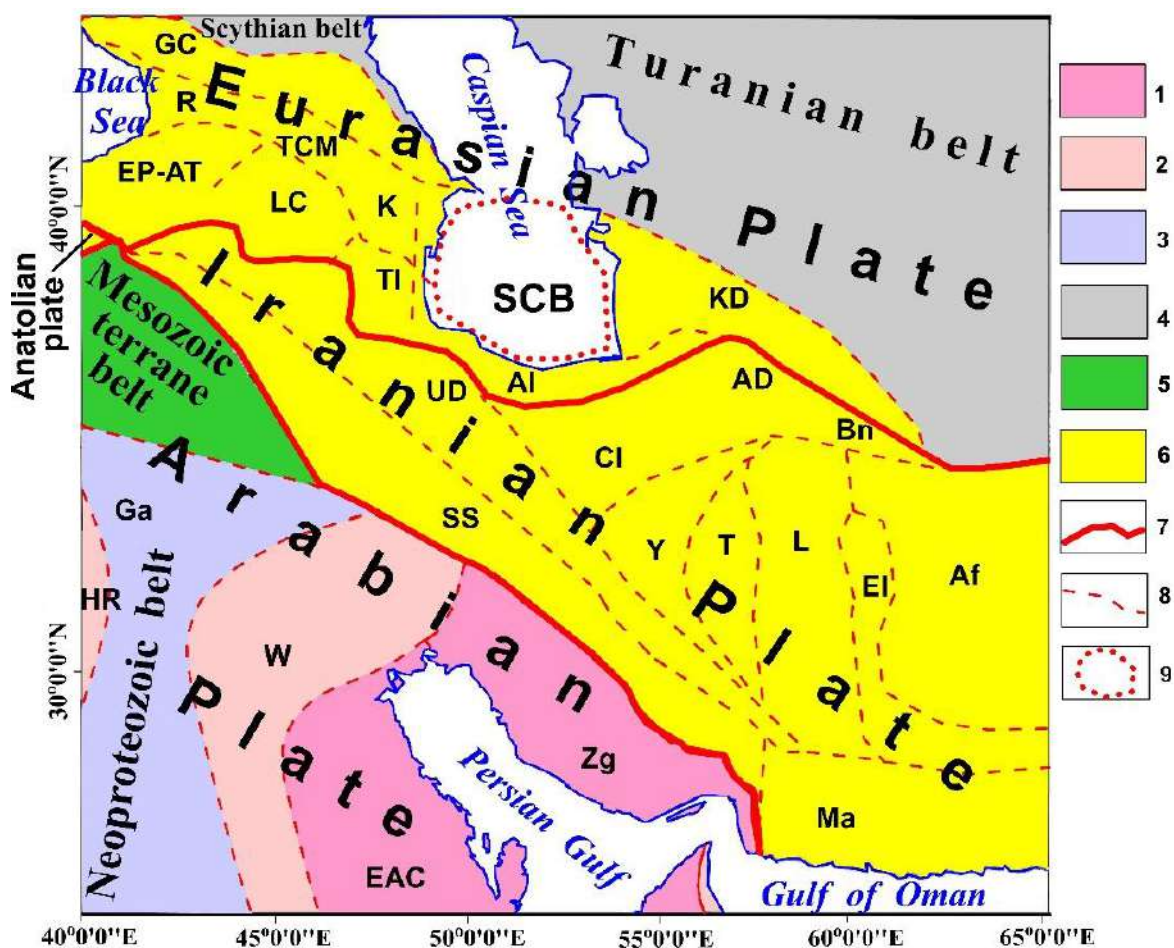


Fig. 5. The tectonic-geodynamic map of the region under study (based on Alavi, 1994; Zakariadze et al., 2007; Moghadam and Stern, 2014; Motaghi et al., 2015; Mattei et al., 2017; Eppelbaum et al., 2018; Malekzade, 2018; Bagheri and Gol, 2020; Trifonov et al., 2020; Eppelbaum et al., 2021, 2024b).

(1) Archean cratons, (2-4) folded belts: (2) Paleo-Mesoproterozoic, (3) Neoproterozoic, (4) Late Paleozoic (Hercynian), (5) Mesozoic Terrane Belt, (6) Alpine-Himalayan orogenic belt, (7) lithospheric plates boundaries, (8) folded belts and massifs boundaries, (9) boundary of the South Caspian Basin. Indexes of the structural zones: AD, Ala Dagh, Af, Afghanistan block, Al, Alborz Mts., BN, Binalud Mts., CI, Central Iran massif, EAC, Eastern Arabian craton, EI, Eastern Iranian orogen, EP-AT, Eastern Pontides-Adjaro-Trialet zone, G, Ga'ara belt, GC, Greater Caucasian belt, HR, Hall-Rutbah massif, KD, Kopet-Dagh Mts., L, Lut block, LC, Lesser Caucasus, Ma, Makran accretional zone, SCB, South Caspian Basin, SS, Sanandaj-Sirjan zone, T, Tabas block, TCM, Transcaucasian Massif, TI, Talysh zone, UD, Urumieh-Dochtar Magmatic Arc, W, Widyan belt, Y, Yazd belt, Zg, Zagros Folded zone

To the east of this subduction zone, the Macran accretionary obduction zone, composed of the Mesozoic ophiolites, is developed. Geotectonically, these elongated belts mark the most intense zone, corresponding to the once vast absorbed space of the Neotethys Ocean. The northern boundary of the Iranian lithospheric plate is less contrasting. It reflects the process of less significant phenomena associated with tectonic collision, an important characteristic of terrane tectonics. In the west of the Iranian Plate, its elongated belts discordantly touch the structures of the Caucasian belt (Figure 5). According to the satellite-derived gravity map (Figure 6), the Eurasian Plate is sharply separated from the Iranian Plate by increased values of the gravity field within a vast belt stretching from the Lesser Caucasus to the Kope-Dagh. In the western part, between the Black Sea and Caspian basins to the north of the Lesser Caucasus back island arc, the submerged belt of the Transcaucasian massif is developed with marks with reduced field values, and to the north of it – the folded structure of the Greater Caucasus with sharply increased marks of the gravity field values. Thus,

the Eurasian Plate in the study area is characterized by sharp indicators of changes in gravity compared to the adjacent lithospheric plates.

The ΔZ magnetic map (Figure 7) clearly shows the dominant striped nature of the magnetic zones distribution, which partially levels out the structural plan of the region (Figure 5). Nevertheless, each of the three lithospheric plates (Eurasian, Iranian, and Arabian) has a specific distribution of magnetization indices in the form (topology) and the ΔZ amplitudes.

The Eurasian Plate differs sharply from the Iranian and Arabian plates in its striped spatial nature and in the contrast and intensity of the magnetic amplitudes. Unlike the gravity distribution stripes, the magnetic field stripes are not directly associated with the structural belts or stable zones that pass near them. Nevertheless, it should be noted that the ΔZ amplitudes differ within the western part of the Eurasian Plate, where the folded belts of the Caucasus are developed, from the eastern – Transcaspian part of the plate, where the epi-Hercynian stable plateau of the Turanian belt dominates.

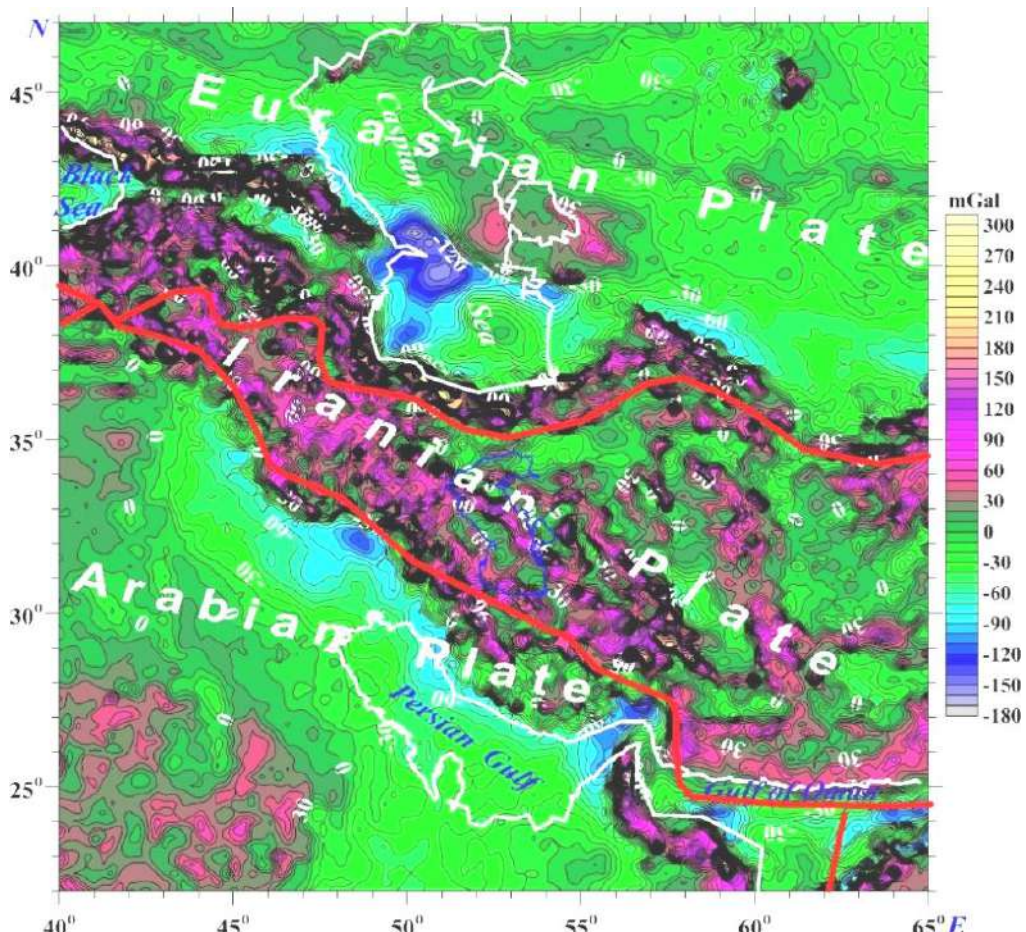


Fig. 6. Gravity satellite-derived map with the main tectonic elements. The bold red lines designate the plates' boundaries (based on Alavi, 1994; Zakariadze et al., 2007; Moghadam and Stern, 2014; Motaghi et al., 2015; Mattei et al., 2017; Eppelbaum et al., 2018; Malekzade, 2018; Bagheri and Gol, 2020; Trifonov et al., 2020; Eppelbaum et al., 2021, 2024b), and the white lines – the land-sea boundaries.

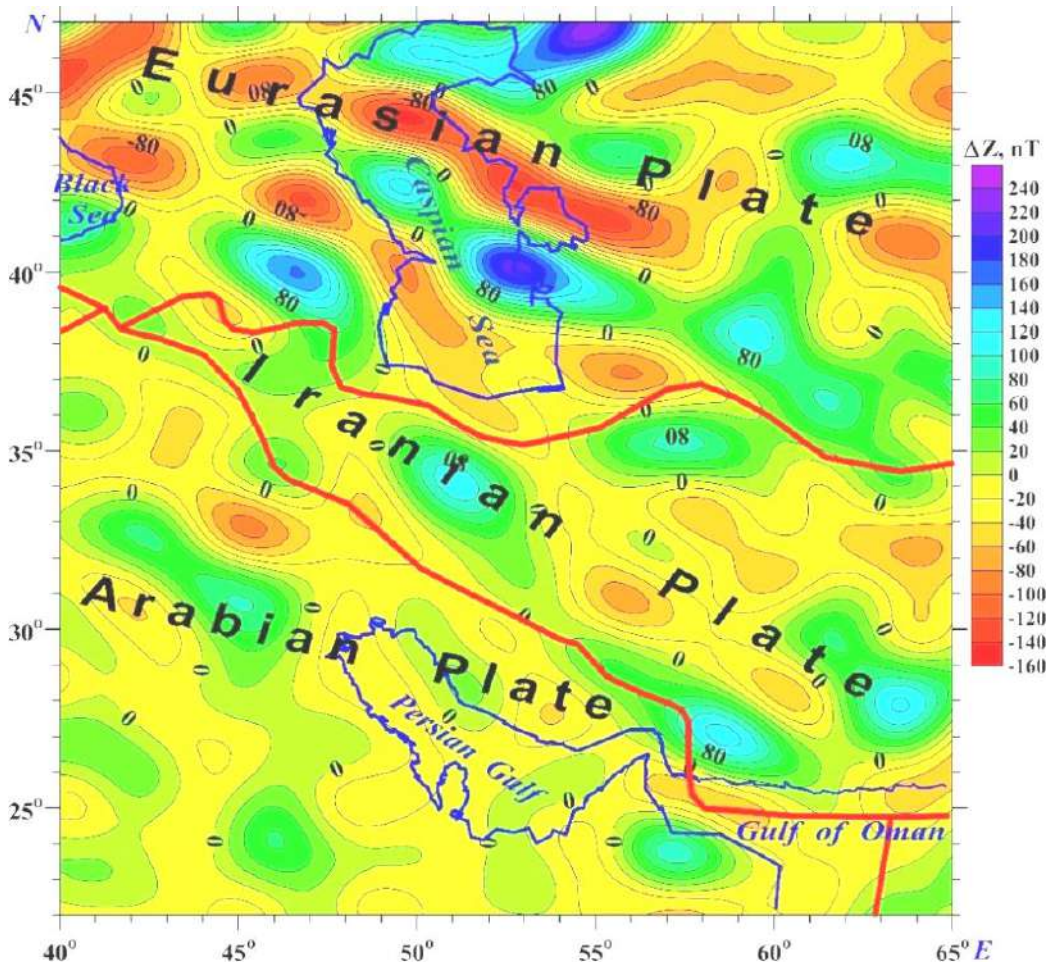


Fig. 7. ΔZ magnetic map (recalculated to 2.5 km above the Earth's surface) with the main tectonic elements. The bold red lines designate the plates' boundaries (based on Alavi, 1994; Zakariadze et al., 2007; Moghadam and Stern, 2014; Motagh et al., 2015; Mattei et al., 2017; Eppelbaum et al., 2018; Malekzade, 2018; Bagheri and Gol, 2020; Trifonov et al., 2020; Eppelbaum et al., 2021, 2024b), and the blue lines – the land-sea boundaries

The Iranian lithospheric plate is characterized by a strident discordance of the junction of magnetization zones in the northern boundary (with the Eurasian Plate) and in the south (with the Arabian Plate) regarding the magnetic pattern. This peculiarity is of fundamental importance since both boundaries under consideration are zones of absorption for the Neotethys oceanic structures between Eurasia and Gondwana. On the other hand, the western part of the Iranian Plate differs from its eastern part by the ΔZ pattern due to tectonic and geodynamic differences in the region and the lithospheric plate itself.

The Arabian lithospheric plate differs significantly from the Eurasian and Iranian plates in terms of its high homogeneity and stability. The banded nature of the distribution of magnetic field zones is practically not manifested here, and the ΔZ amplitude fluctuates near the zero line.

Regional topography data also proved highly informative and productive in structural and geodynamic terms (Figure 8). A clear contrast was revealed at the boundary of the Arabian and Iranian lithospheric

plates – the central subduction zone of the Neotethys Ocean. In addition, the topography map indicates the boundary of the northern Iranian Plate.

3.3. South Caspian Basin

The comprehensive seismic data suggest a fundamental compositional difference between the crust of the South Caspian Basin (SCB) and the surrounding region (Mangino and Priestley, 1998). The SCB has been sufficiently studied structurally and geodynamically based on drilling data, seismic profiling, gravity, thermal, magnetic, and paleomagnetic data, and remote sensing (Гулиев и др., 2009; Kadirov et al., 2015, 2024; Abdullayev et al., 2017, 2024; Alizadeh et al., 2024).

As a result, a structural-tectonic map was compiled (Artyushkov, 2007; Abdullayev et al., 2017), where the age and geodynamic type of various SCB zones were clearly defined. In this paper, this map was generally used as a basis (Figure 9) but slightly modified by incorporating data from adjacent areas of Turkmenistan and the eastern SCB area (Леонов

и др., 2010; Nouri et al., 2024) and the latest geodynamic data based on GPS analysis (Kadirov et al., 2024). The presented structural-tectonic map (Figure 9) effectively reflects the deep structure of the SCB and its adjacent areas. According to the distribution of the thickness of the sedimentary cover, the difference between the SCB and the North Caspian Basin, which belong to tectonic zones of different ages, is sharply manifested. The first is part of the Alpine-Himalayan belt, and the second is the epi-Hercynian Scythian-Turanian belt. The SCB basin is sharply separated from the Hercynides and the adjacent Alpine structures by a system of deep faults. All this is emphasized by the anomalously high thickness of the SCB sedimentary layer, reaching a maximum (28.5 km) near the Absheron ridge. It is the boundary structure between the Hercynides and the Alpines (Хайн, 2005). The structural map indicates that the

arcuately curved zone of high sedimentary rock thicknesses suggests a thrust of the space of its highest thicknesses under the Absheron Ridge fault system. The fault-displaced Jurassic trough system (Artyushkov, 2007; Abdullayev et al., 2017) confirms this tectonic-geodynamic model. The displaced southeastern part of the trough is not so contrasting geodynamically, and the thickness of the sedimentary layer here is 8-10 km less than in the north.

The eastern part of the SCB is characterized by sharply reduced sedimentary layer thicknesses, up to 8 km near the Caspian coastline. According to the distribution of isopachs, the basin itself forms a plateau, which is why it was called TST—Turkmenian Structural Terrace. Near the coastline (Figure 9), this terrace gives way to the GOS—Gorgan' dag—Okarem Step scarp (Леонов и др., 2010).

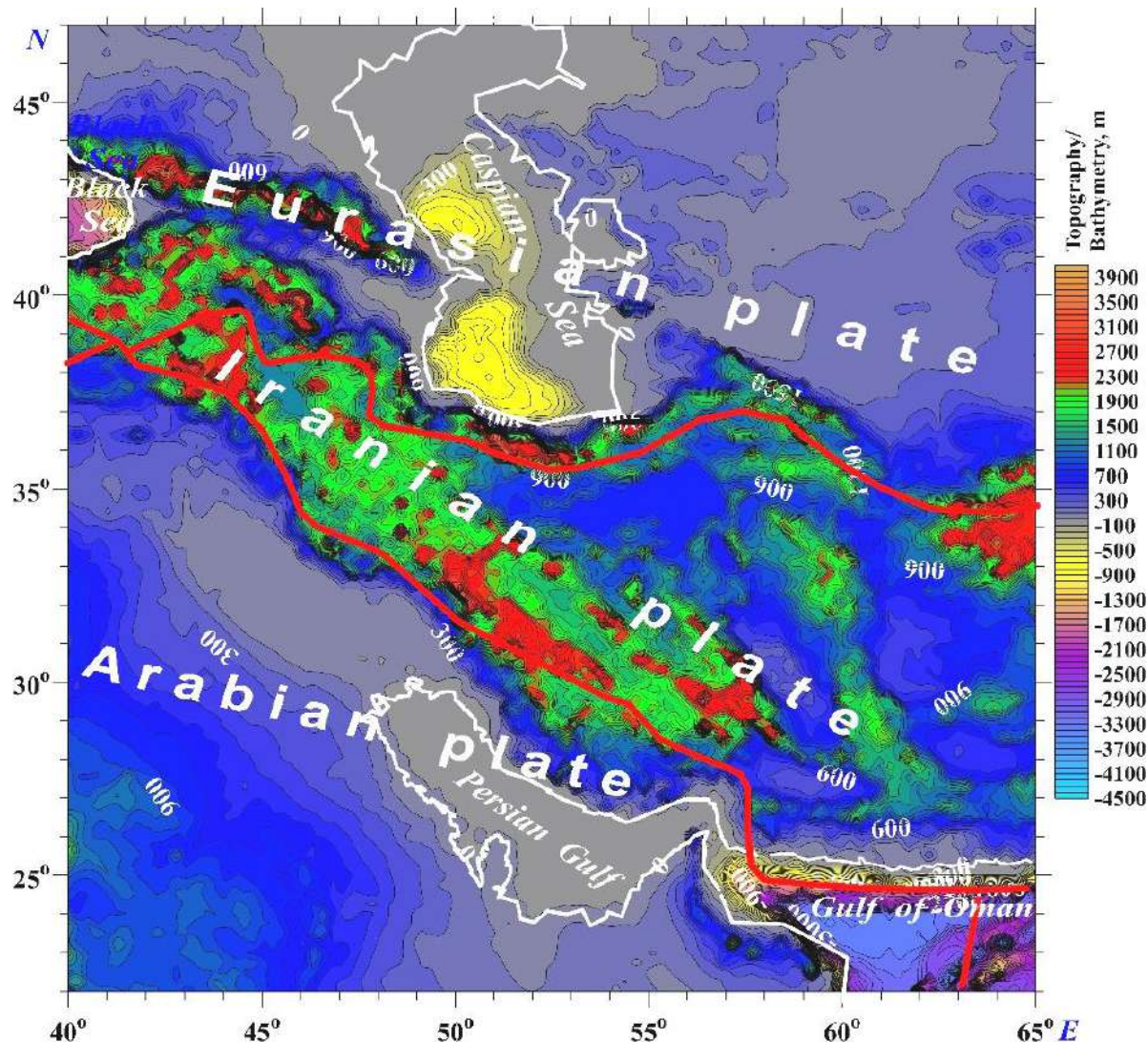


Fig. 8. Topography-bathymetric map with the main tectonic elements. The bold red lines designate the plates' boundaries (based on Alavi, 1994; Zakariadze et al., 2007; Moghadam and Stern, 2014; Motaghi et al., 2015; Mattei et al., 2017; Eppelbaum et al., 2018; Malekzade, 2018; Bagheri and Gol, 2020; Trifonov et al., 2020; Eppelbaum et al., 2021, 2024b), and the white lines – the land-sea boundaries

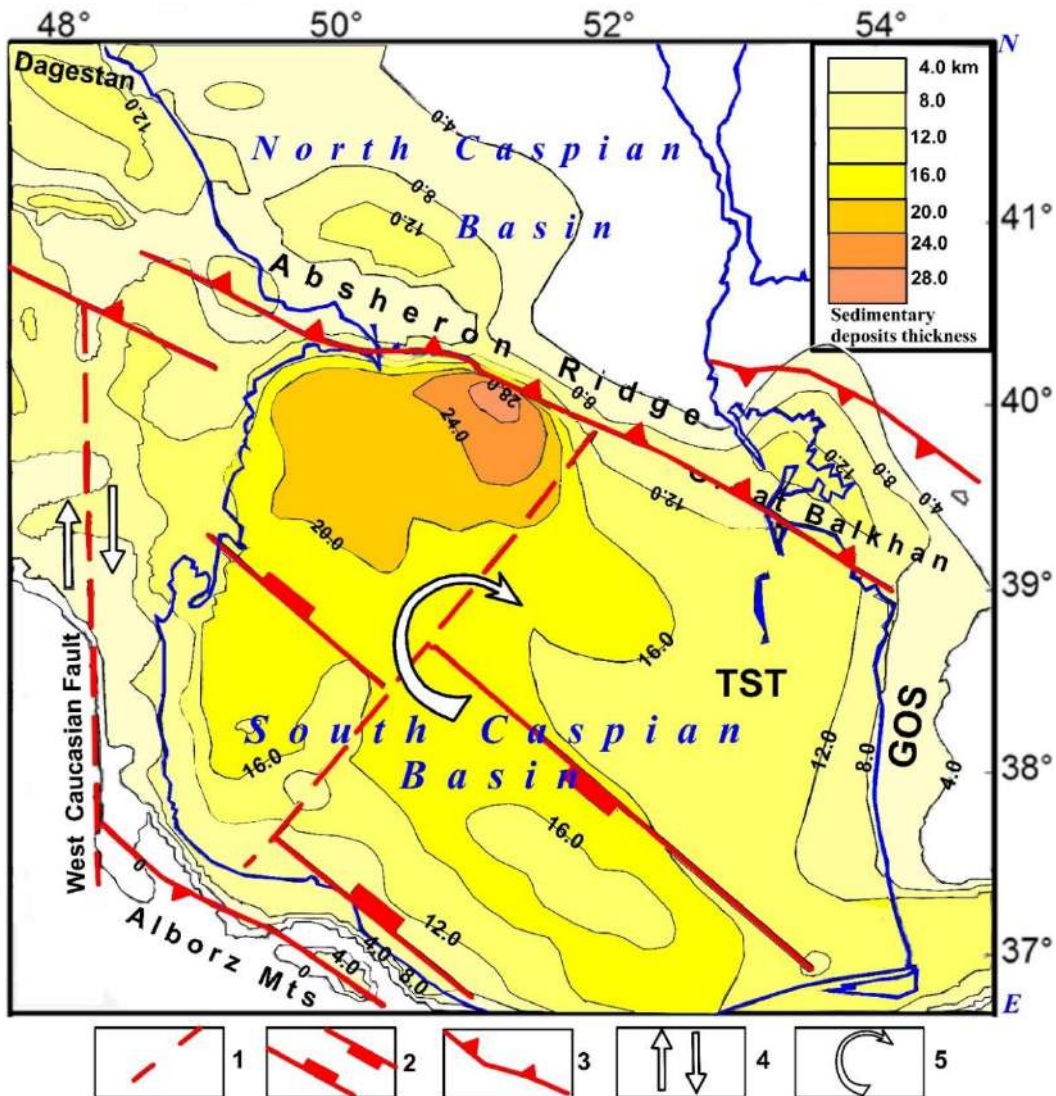


Fig. 9. Structural-geodynamic map of the SCB (after Леонов и др., 2010; Abdullayev et al., 2017; Trifonov et al., 2020; Abdullayev et al., 2024; Kadirov et al., 2024; Nouri et al., 2024).

(1) shear zones, (2) Jurassic rift zone, (3) thrust and underthrust zones, (4) direction of strike-slip displacement, (5) clockwise rotation of blocks.

Al, Alborz Mts, GC, Greater Caucasian belt, GOS, Gorgan'dag – Okerem Step, KD, Kopet-Dagh Mts, LC, Lesser Caucasus, TCM, Transcaucasian Massif, Tl, Talysh zone, TST, Turkmenian Structural Terrace. The black lines show boundaries between the land and sea

The distribution of the thickness of the sedimentary cover and fault systems indicates the geodynamic nature that created the complex structure of the SCB. The data suggests a clockwise rotation of the western part of this sedimentary basin. A more detailed analysis of this cartographically recorded phenomenon requires geophysical materials since seismic profiling and GPS analyses have been well-studied in this area (Kadirov et al., 2024).

The data from the gravity anomaly studies were used for the structural-geodynamic analysis of the SCB. First, the Bouguer gravity anomaly map is considered (Figure 10). It indicates the difference between the SCB and the adjacent structures of the Alpine-Himalayan belt and the epi-Hercynian Turanian belt. The Bouguer anomalies within the Alpine

belt are characterized mainly by negative values (Kadirov and Gadirov, 2014; Kadirov et al., 2023).

At the same time, shallow values from -120 to -200 mGal are concentrated on the boundary of the Eurasian and Iranian lithospheric plates. Somewhat less extreme (from -100 to -120) are the negative Bouguer anomalies on the boundary between the Alpines of the Absheron Ridge and the Hercynides of the Turanian belt. The maximum values of the Bouguer anomalies (from about +40 to values over +60 mGal) are widely developed in the Kara-Bugaz arch of the Hercynides. In the Alpines, anomalies of this kind are created only to the west of the SCB – near the fault zone on the border with the Talysh uplift (e.g., Кадиров, 2000).

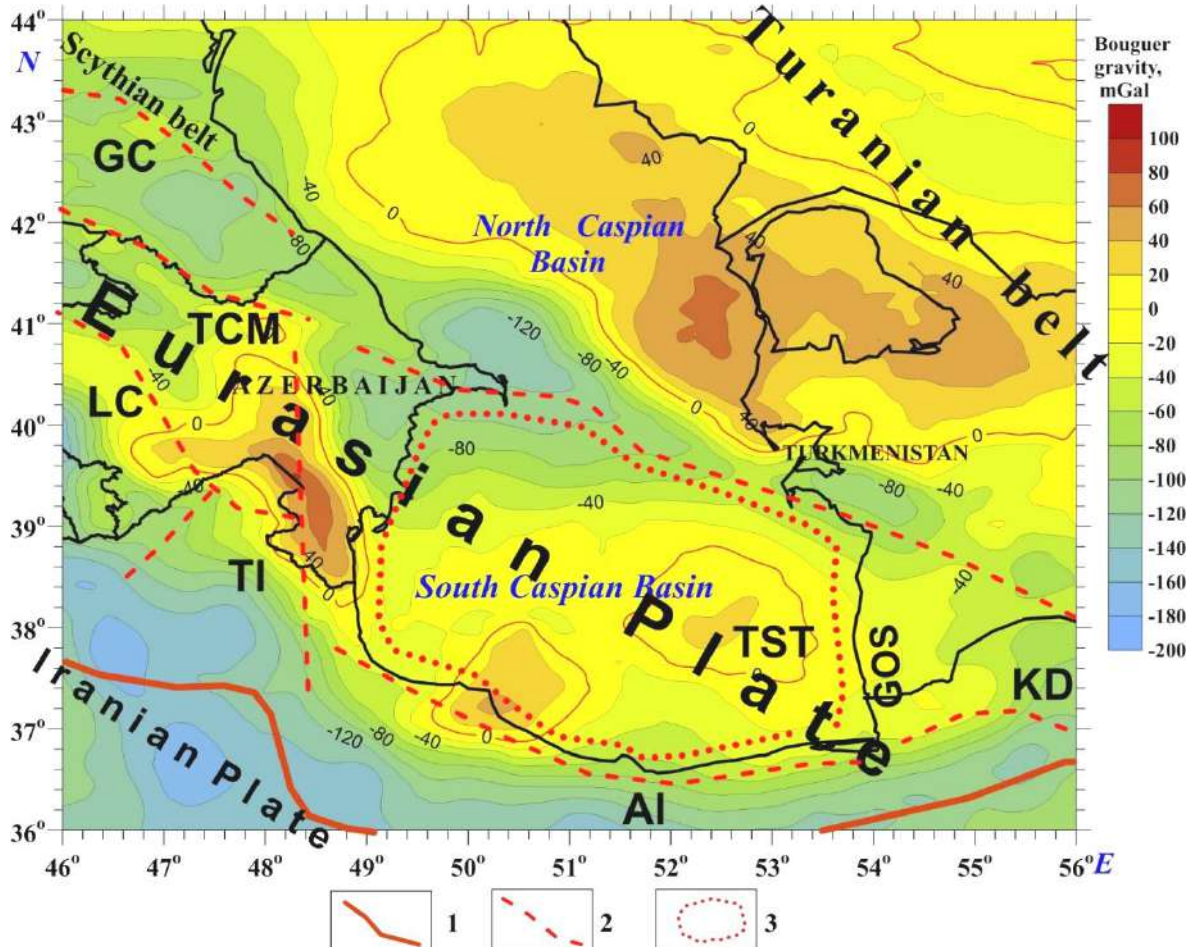


Fig. 10. A generalized Bouguer gravity map for the SCB and surrounding regions with the tectonic features (supplemented after Кадиров, 2000; Kadirov et al., 2023). (1) interplate faults, (2) intraplate faults, (3) SCB contour. Al, Alborz Mts, GC, Greater Caucasian belt, GOS, Gorgan'dag – Okerem Step, KD, Kopet-Dagh Mts, LC, Lesser Caucasus, TCM, Transcaucasian Massif, TI, Talysh zone, TST, Turkmenian Structural Terrace. The black lines show the boundaries between the land and sea

The SCB differs from the adjacent Alpines by transitional values of the Bouguer anomalies, about -50 to +20 mGal. At the same time, the eastern section with reduced thicknesses of the sedimentary layer – TST (Turkmenian Structural Terrace) – is generally characterized by the most stable regime of Bouguer anomalies with values near the zero line. To the east of the transition of the Caspian Sea to the Kopet-Dag Alpine system, the Bouguer anomalies record the GOS tectonic scarp (Figure 10).

The calculated ΔZ magnetic map on 2.5 km above the sea level implies an expressed correlation between the significant negative magnetic anomaly and the location of most mud volcanoes in the South Caspian Basin (Eppelbaum, 2024). A preliminary analysis of this anomaly reveals its profound nature (extending dozens of kilometers). This indicates that mud volcanism is associated with the deep processes in the Earth's crust and lithosphere (possibly with the Iranian Plate pressure).

Notably, the geodynamic clockwise rotation of the SCB can be detected in the bathymetry map (Figure 11) and the map of the strike angles (Figure 12) calculated from the satellite-derived gravity data using the methodology presented in Klokočník et al. (2014).

3.4. Geodynamic aspects of the ancient hominin dispersal from Eastern Africa to the Levant and South Caspian Basin boundaries

The modern geodynamics of the Middle East and the Caucasus (within the region under study) is significantly influenced by various processes from past geological periods. In the late Cenozoic era, they determined the settlement process of the most ancient hominids (Figure 13). The presence of the Caucasian and Levant areas isolated from each other, along with the remote East African region, clearly links the confinement of the habitats of the most ancient hominids with the basin factor and with active geodynamics, which influenced the de-

velopment of optimal landscapes and ecosystems in these areas (Eppelbaum and Katz, 2021). The paleogeographic map indicates that the Levant and Caucasian regions, where the most ancient hominids are found, are closely associated with the vast Neotethys-Mediterranean and Paratethys basins.

The advance of ancient hominids from the distant East African range mostly coincided with the completion of the Akchagylian hydrodynamic maximum (Eppelbaum and Katz, 2021, 2024), which manifested itself to the greatest extent in both the Levant and Caspian basins.

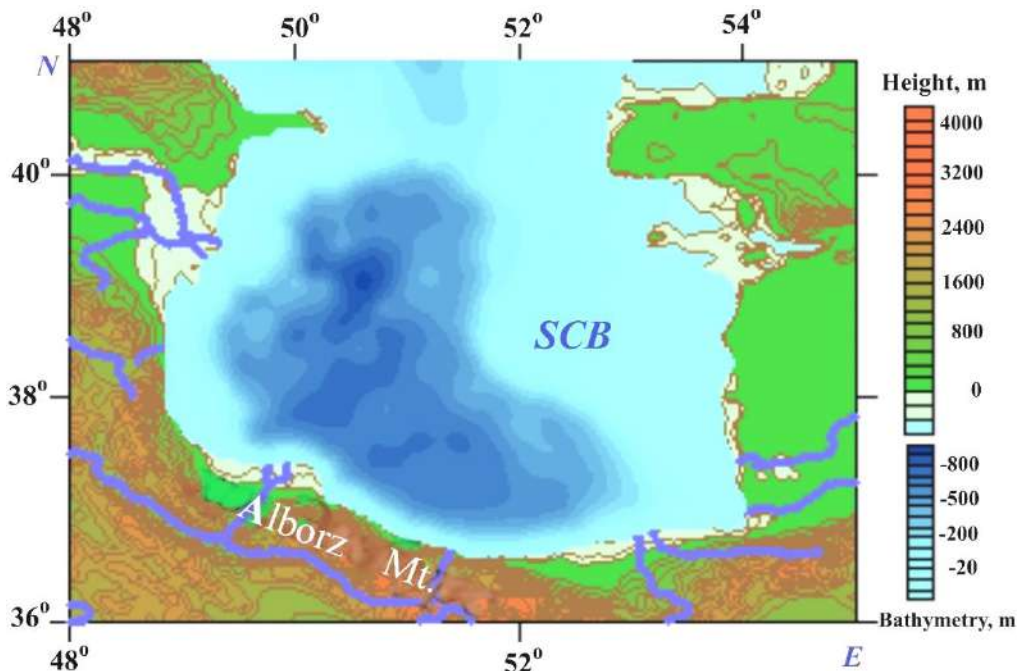


Fig. 11. Bathymetric map of the South Caspian Basin (SCB) (modified after the Caucasian Database)

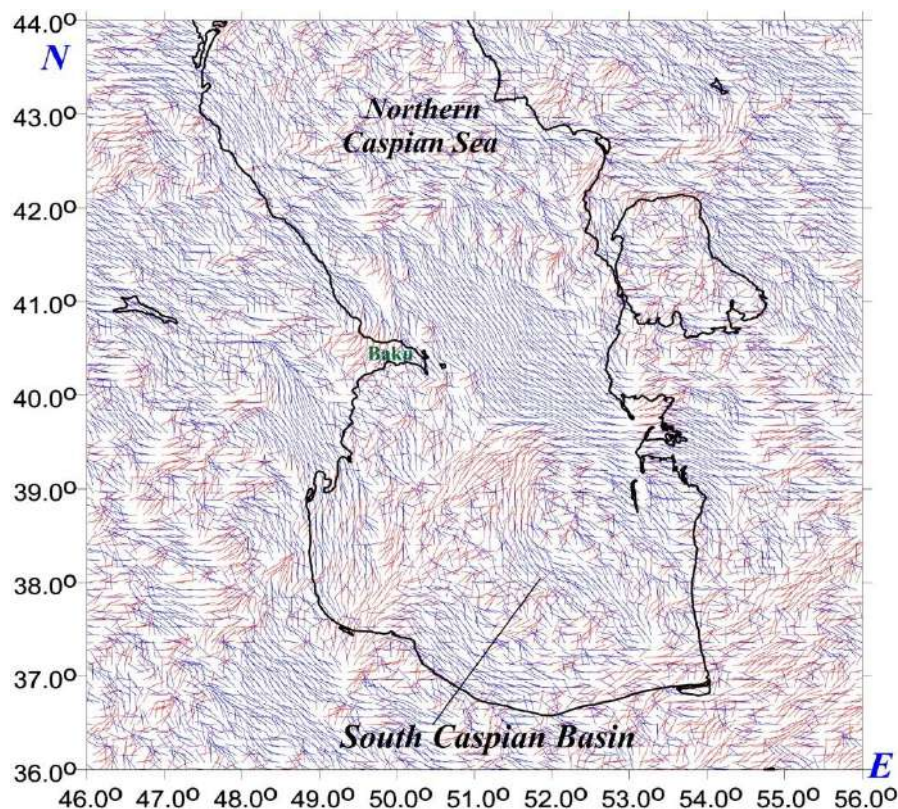


Fig. 12. Map of the strike angles (the main direction of the tensor Γ (Klokočník et al., 2014)) (revised after Kadirov et al., 2023)

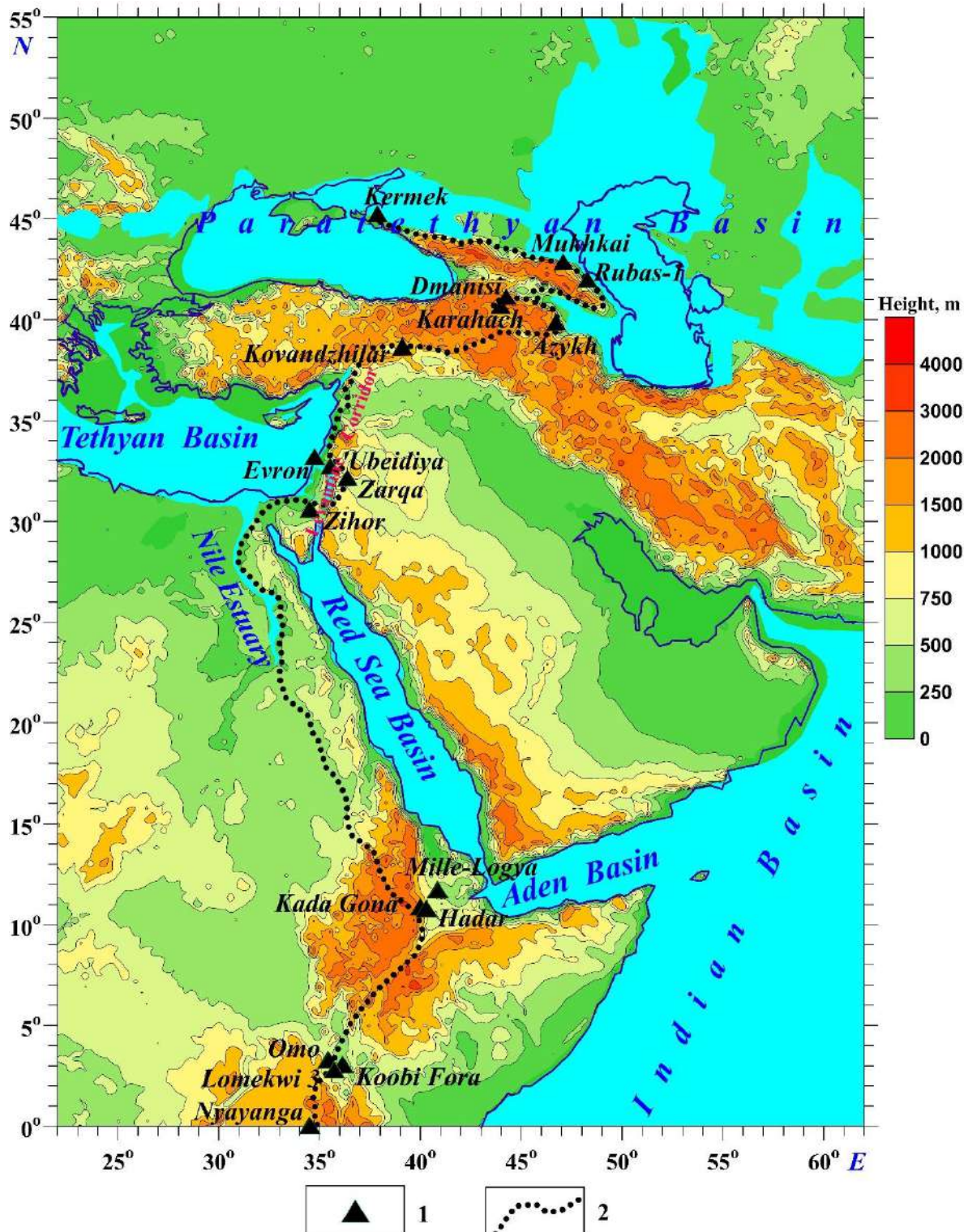


Fig. 13. Paleogeographic-anthropological map of the ancient man dispersal (based on the modern topography map) from Eastern Africa to the Levantine Corridor and the South Caspian Basin and Caucasus.

(1) ancient hominin sites of 3.3 – 1.85 Ma, (2) reconstructed ancient hominin's way from Africa to Eurasia (revised and supplemented after Eppelbaum and Katz, 2024).

The age (in Ma) of anthropological sites is taken from: Nyayanga (3.03-2.58, Plummer et al., 2023), Lomekwi (3.3, Harmand et al., 2015), Koobi Fora (2.1-1.6, Grine et al., 2019), Omo (2.4-2.3, McDougall et al., 2008), Hadar (2.4-2.3, Johanson, 2017), Kada Gona (2.6-2.0, Semaw et al., 2005), Mille-Logia (2.42-2.1, Alemseged et al., 2020), Zihor (1.95-1.78, Larrasoña et al., 2020), Zarqa (2.5-1.95, Scardia et al., 2019), 'Ubeidiya (1.6-2.6, Eppelbaum and Katz, 2024), Kovandzhilar (2.0-1.7, Ожерельев и др., 2020), Azykh (2.1-1.9, Veliyev et al., 2010), Karahach (1.85-1.78, Беляева, 2020), Dmanisi (1.85-1.77, Lordkipanidze et al., 2007), Rubas-1 (2.2-2.3, Деревянко и др., 2015), Mukhkhai (2.1-1.77, Амирханов, 2020), Kermek (2.1-1.95, Щелинский, 2021).

The hydrodynamic phenomena of these two basins were associated with their location near the Earth's critical latitude of 35° , which separated the zones of conjugate deformation of the ellipsoid of rotation and the development of the extended estuaries of the Volga and Nile rivers. On the other hand, the South Caspian and Levant basins (as shown in Figure 1) were located near different zones of the deep mantle rotating structure, whose active geodynamics influenced the troughs of the South Caspian, Levant, and related structures.

4. Discussion

The simplified geodynamic scheme (Figure 14) indicates the complex interaction of the MRCS, Iranian Plate, and SCB. The essence of this scheme is to display that the counterclockwise MRCS rotation

caused a northward displacement of the complex-constructed western part of the Iranian Plate, which, in turn, caused the SCB clockwise rotation. An essential factor is the decrease of the corresponding rotation and displacement velocities. In the MRCS contour and its interaction with the Iranian Plate, the GPS velocity consists of 10-20 mm/year (Figure 1), in the western part of the Iranian Plate, this northward velocity consists of 8-14 mm/year, and finally, SCB clockwise rotation is about 3-5 mm/year (Figure 1). It can be explained by the simple physical law of decreasing movement impulse by transferring from one target to another. This ensemble interaction includes an influence of the Earth's critical northern latitude of 35° and the Ural-African tectonic step (zone between the positive and negative geoid anomalies) (Figure 3).

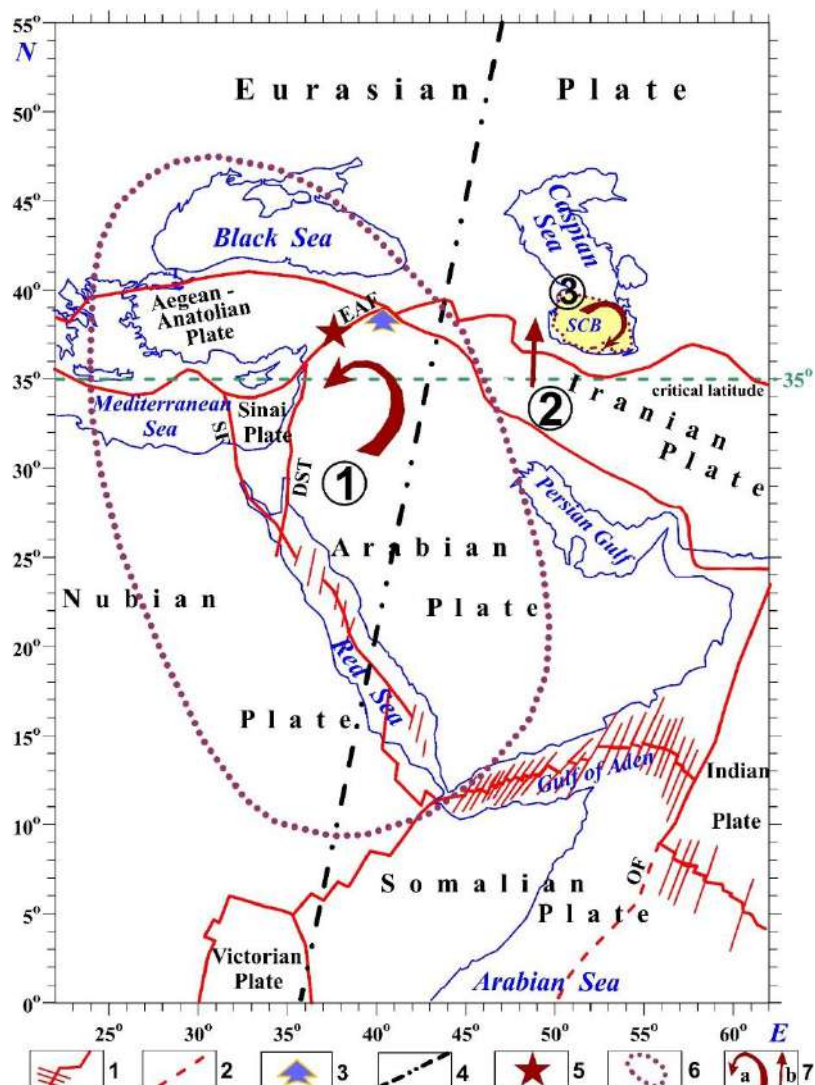


Fig. 14. Simplified geodynamic scheme of the area under study.

- (1) main interplate faults, (2) main intraplate faults, (3) a distal part of the Mesozoic Terrane Belt, (4) averaged position of the Ural-African tectonic step, (5) high-magnitude seismogenic zone in Eastern Turkey (February 06, 2023), (6) average projection of the mantle rotating counterclockwise structure, (7) tectonic movements: (a) rotation, (b) north and north-northeast displacement. Numbers in circles: 1 – mantle rotating counterclockwise structure, 2 – Iranian Plate, 3 – South Caspian Basin. SCB, South Caspian Basin, SF, Sinai Fault; DST, Dead Sea Transform; OF, Owen Fault

The geophysical evidence to discover the oceanic crust in the Easternmost Mediterranean is based on a comprehensive analysis of seismic, gravitational, magnetic, and thermal data (Ben-Avraham et al., 2002). The most significant evidence was the absence of a granite crustal layer in the Easternmost Mediterranean (approximately 40–80 km from the Israeli coast), a very low thermal regime ($15\text{--}30 \text{ mW/m}^2$), and crustal (basaltic) blocks with reverse magnetization. It should be noted that seismic, magnetic, and gravity data analysis and advanced 3D magnetic-gravity modeling were carried out simultaneously on three intersecting profiles. This work laid the foundations for the later discovery of the oldest block of oceanic crust (see Kiama block location in Figures 1 and 2).

From the conventional point of view, the age of oceanic crust blocks should not exceed 160–180 million years (Wilson, 1966). Constant subduction explained this regularity, lowering oceanic crust blocks into the upper mantle with subsequent absorption of these blocks by the hot mantle. However, this general pattern, given the complexity of the structure of the Earth's crust, is not always observed. Several authors (e.g., Stampfli and Borel, 2002; Le Pichon et al., 2019; Tugend et al., 2019) earlier postulated the Permian age of the Eastern Mediterranean oceanic crust (one of the most significant factors is the very low heat flow in the region under study). A comprehensive geological-geophysical analysis conducted by Eppelbaum et al. (2014); Eppelbaum and Katz, 2015) showed that the identified block of oceanic crust (Figure 1) corresponds to the Kiama paleomagnetic hyperzone (~255–308 Ma, Upper-Lower Permian and Upper Carboniferous). We believe this oceanic block formed no more than 285 million years ago (Permian) north of the modern Persian Gulf. The depth of this block is 10–11 km, and its total volume is about 120,000 km³ (Eppelbaum et al., 2023). It was then displaced along the transform faults to its current position, which has remained in place for more than 120 million years. Even the geometric location of this block within the Easternmost Mediterranean indicates its discordant position with the surrounding structures – the Anatolian Plate and the Mesozoic Terrane Belt. However, why was this block of oceanic crust not subducted? We proposed that the subduction is disallowed by the MRCS influence, whose counterclockwise rotation prevented this block from sinking into the upper mantle and preserved it until today.

Special attention is drawn to the anomalous biogeographic indicators (e.g., Arkell, 1956; James and Wynd, 1965; Макридин и др., 1968; Ализаде, 1972; Ализаде и др., 1983; Feldman, 1987; Hirsch, 1988; Cooper, 1989; Kazmer, 1993; Hall et al.,

2005); particularly shell remains of giant brachiopods **Septirhynchia–Somalirhynchia** (see review in Eppelbaum et al., 2021) and Mediterranean brachiopods *Pygope* (see review in Eppelbaum et al., 2024b). Based on the analysis of numerous sources, three paleobiogeographical provinces were selected (Figure 4): (1) Boreal (Eurasian shelf), (2) Mediterranean (Mediterranean Basin), and (3) Ethiopian (Eastern Africa and Southern Arabia). The constructed paleobiogeographical map (Figure 4) shows the phenomenon (indicated by the red arrow rotating counterclockwise) of the geodynamic transfer of tectonic blocks with the remains of the Ethiopian fauna from the present position of the Persian Gulf to the Levant up to the Egyptian Eastern Desert. This fact demonstrates the counterclockwise movement of the eastern and central parts of near-surface projections of the anomalous deep structure in the Jurassic and Early Cretaceous periods.

Thus, the foreland sediments of Northern Arabia and Eastern Nubia are tectonically discordantly connected to the allochthonous Mesozoic Terrane Belt, which rotated counterclockwise in the direction of the paleocontinent Gondwana. This geodynamic feature makes it possible for the first time to explain the uniqueness of the biogeographically anomalous zone of terrane block attachment to the Gondwana paleocontinent in the Levantine phase of tectonic activity (Eppelbaum and Katz, 2015). To the north of this belt, within the marginal oceanic zone (along transform arc faults), an allochthonous block with the Kiama paleomagnetic hyperzone moved west to the current Levantine basin (Figure 4).

The multistatistical map transformed from the satellite-derived gravity field (Figure 2) highlights the critical role of the applied methodology for identifying the critical properties of deep regional geodynamics. The marginal plates of the northern part of Central Gondwana – Iranian, Sinai, and Aegean-Anatolian – are associated with collisional geodynamics. Here, a thick eastern (Arabian-Iranian) sector is developed with a complete absorption of the Neotethys oceanic crust with thickening of the crust and mantle lithosphere in the subduction zone (Ver-gés et al., 2011; Teknik et al., 2019; Corcete, 2025). In the western (Aegean-Anatolian-Sinai) sector, there is a zone of incomplete subduction with anomalously low values of the crustal and mantle lithosphere thicknesses, which is demonstrated both by the drop in the values in Figure 2 and by seismic data (e.g., Ben Avraham et al., 2002; Jimenes-Munt et al., 2006). Between these two zones, there is a protrusion of the Mesozoic Terrane Belt, penetrating the zone of wedging out of the Alpine associations of the Anatolian-Aegean and Iranian plates and manifesting itself in anomalously high seismicity caused

by the rotational geodynamics of the MRCS (Eppelbaum et al., 2024a). A completely different type of geodynamics is developed within Central Gondwana and its eastern segment on the boundary with the Indian Plate. Here, according to the multistatistical analysis (Figure 2), the classical structures of spreading geodynamics are recorded – a triple junction with the formation of the Arabian, Nubian, and Somalian plates with an increase in the thickness of the mantle lithosphere (Eppelbaum and Katz, 2017; Eppelbaum et al., 2018, 2021) in the zones of ascending deep thermal inflow. The rift zones of the Red Sea and the Gulf of Aden themselves are characterized by reduced values of both the scale indicators in Figure 2 and the thickness of the crust and mantle lithosphere, which is due to the rotational processes of deep geodynamics (Eppelbaum et al., 2021).

Geophysical and hypsometric data (Figures 6-8) supported the analysis of tectonic-structural features of the studied region (see tectonic map in Figure 5). First, it is necessary to consider the satellite-derived gravity map recalculated to the Earth's surface (Figure 6). According to the presented data, we have revealed that the Iranian lithospheric plate manifests itself as an independent, geodynamically most stressed structure. This fact is prominently visible along the southern and northern borders of this plate.

The developed maps (Figures 6-8) are structurally consistent with the data of regional-tectonic zoning (Zakariadze et al., 2007; Trifonov et al., 2020; Malekzade, 2018; Eppelbaum et al., 2018) and elements of geodynamics (Eppelbaum and Katz, 2017; Rashidi et al., 2022), partially shown in Figures 1-3. The last-mentioned figures are compared with the satellite-derived gravity map (Figure 6), indicating that between the continental platforms of Eurasia and Gondwana, there is a tectonically unstable younger Alpine-Himalayan belt with increased values of the gravity field indicators. At the same time, each of the three lithospheric plates typologically differs in the gravity-structural characteristics of the latitudinal belts. On the other hand, within the lithospheric plates, the latitudinal indicators of gravity field changes are accompanied by the presence of submeridional heterogeneities. They are manifested in the meridian area of 50° eastern longitude, passing through the Caspian and Persian Gulf basins. Here, troughs are developed, marked by the reduced gravitational anomaly values. Earlier, Eppelbaum and Katz (2017) discovered this phenomenon in the satellite-derived gravity field of larger areas (long-pass Gaussian-filtered gravity map). In subsequent work (Eppelbaum et al., 2018), this zone with lowered gravity field anomalies was compared with the geoid map of the African-Arabian region (the geoid map with the central tectonic units is shown in Figure 3).

It should be noted that the Ural-African geoid step (Figures 1 and 3) is tectonically very active, and systems of deep faults are associated with it, producing numerous graben-like structures (Eppelbaum et al., 2024b) with the largest hydrocarbon deposits.

Regional geodynamic analysis, based on Figures 1-4 and examination of Alavi (1994), Ben-Avraham et al. (2002), Zakariadze et al. (2007), Moghadam and Stern (2014), Motagh et al. (2015), Eppelbaum et al. (2018), Khorrami et al. (2019), Eppelbaum et al. (2021, 2024b), Mattei et al. (2017), Malekzade (2018), Bagheri and Gol (2020), Trifonov et al. (2020), indicates the intricate interaction of the lithospheric slabs in the region. The MRCS' eastern branch slab rotation initiates a northward movement of the Iranian Plate. On the other hand, the north (north-north-east) displacement of the Iranian Plate caused a clockwise rotation of the South Caspian Basin (Eppelbaum et al., 2025). The rotation and displacement of the lithospheric blocks caused by the above factors are (along with other geodynamic causes) sources of the seismological hazard in the region under consideration. Particularly illustrative are the two recent catastrophic earthquakes in eastern Turkey on 06.02.2023, where the long-term accumulated stress (e.g., Tselentis and Drakopoulos, 1990; Nalbant et al., 2002; Şengör et al., 2005) from a rotating deep structure (Eppelbaum et al., 2024a), along with other tectonic factors, resulted in a strong seismological shock.

The Iranian lithospheric plate is discordantly attached to the Eurasian Plate. Its narrowed western part is composed of the Sanandaj-Sirjan magmatic belt, marking a collisional suture in the absorption zone of the once-vast Neotethys Ocean. The extended eastern part of the Iranian Plate is characterized by significantly lower values of the gravity field indicators since vast massifs and blocks of continental crust dominate it.

The Arabian lithospheric plate is quite sharply delimited from the Iranian Plate, since elevated gravity field values characterize the Mesozoic Terrane Belt. To the south of this belt is a zone of decreasing gravity field marks (Figure 6). To the southwest, there is a stable zone of the Arabian Craton and Neoproterozoic Belt characterized by gravity field anomalies with average values. The increase in gravity field values in the extreme southwestern outskirts of the region is due to its proximity to the tectonically active rift zone of the Red Sea. The gravity map (Figure 6) coincides with the gravity transformation anomaly (Figure 2) and the recent publication of Teknik (2024), where the Iranian Plate is distinguished by thickening of the Earth's crust and lithosphere.

Analysis of the magnetic field (ΔZ) indicators (Figure 7) shows a less contrasting but distinct picture of the differences between the identified litho-

spheric plates. At the same time, the most significant structural contrast is manifested with the Eurasian lithospheric plate.

The topography data (Figure 8) and the gravity field (Figure 6) contrast the structures of the Iranian and Eurasian lithospheric plates. The topography map (reflecting important geodynamic features) is unique to study the relationships between the Arabian and Indian plates. It demonstrates a significant geodynamic contrast in the Gulf of Oman zone (Figure 8). Above and beyond, an analysis of numerous publications indicated an increase in the Earth's crust thickness (e.g., Teknik et al., 2019; Mousavi and Fullea, 2020; Teknik, 2024), and heightened thermal flow data (e.g., Gotorbe et al., 2011; Mousavi and Fullea, 2020; Mousavi and Ardestani, 2023) within the Iranian Plate.

Our previous investigations (Eppelbaum and Katz, 2017) indicate that in the post-Carboniferous, an uplift of the Zagros zone as an isolated tectonic feature of the Neotethys Ocean began to form. Geodynamic indicators reflect the isolation of the Zagros zone and suggest that it may have been a fragment of the MTB in the southern segment of the Neotethys Ocean (Vergés et al., 2011; Koshnaw et al., 2024).

The paper presents a historical-geodynamic analysis of Gondwana, demonstrating that its differentiation is linked to a submeridional fault system. Thus, the disintegration of the supercontinent was accompanied in parallel by an uneven process of closure (collision) of the Neotethys Ocean. We distinguish the Western Gondwana, where the remains of the oceanic crust – the Mediterranean – have been preserved (partially

shown in Eppelbaum et al. (2014), Eppelbaum and Katz (2017), and Eppelbaum et al. (2024a). To the east, in Central Gondwana, on the boundary of the Arabian and Iranian lithospheric plates, the oceanic crust of the Neotethys was subducted. A narrow linear zone of the South Iranian Plateau, a belt of magmatic and metamorphic rocks of the marginal subduction zone, has remained from this process.

It was revealed that the bending arc of the Mesozoic Terrane Belt, which deviates sharply after the distal western end of the Iranian Plate to the southwest up to the south of the Sinai Plate, is associated with more ancient rotational movements along the forming deep mantle structure (Eppelbaum et al., 2021; 2024a). The collision of the Neotethys Ocean in Central Gondwana occurred later, in the middle of the Cenozoic, near the eastern branch of the deep mantle structure projection, outside the zone of influence of its rotational movements.

A general distribution of paleomagnetic vectors within the MRCS contour (mainly counterclockwise rotation) and without it (clockwise and alternating rotation) is shown in Eppelbaum et al. (2021, 2024a). A paleomagnetic direction map compiled for Azerbaijan and some surrounding areas (Figure 15) clearly shows the role of the MRCS, the Ural-African step, and the western part of the Iranian Plate in a complex form. The MRCS influence declines paleomagnetic directions counterclockwise, the African-Arabian step is an average boundary line, and the Iranian Plate impact declines paleomagnetic vector clockwise.

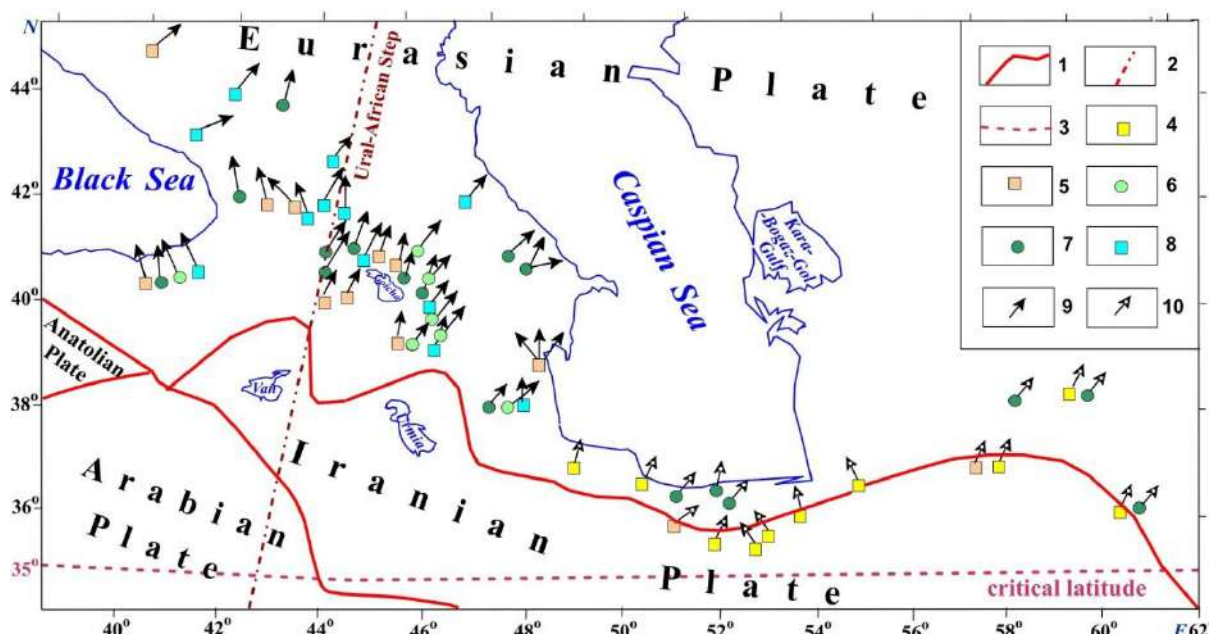


Fig. 15. Paleomagnetic-geodynamic scheme of the region at the boundary of the Iranian Plate and South Caspian Basin. (1) lithospheric plate boundaries, (2) Ural-African step, (3) Earth's critical latitude 35° , (4-10) paleomagnetic-geodynamical data: (4) for Neogene, (5) for Paleogene, (6) for Upper Cretaceous, (7) for Lower Cretaceous, (8) for Jurassic, (9) supplemented after Issayeva and Khalafli (2006), (10) modified after Mattei et al. (2019)

The geodynamic clockwise rotation over a long time must be reflected in the development of the SCB's bottom relief (see, for instance, Figure 11). This map displays the SCB's bottom relief rotation clockwise. Interestingly, the map of strike angles calculated by a complex transformation of the satellite-derived gravity data also demonstrates a circular vortex in the central part of the SCB (Figure 12). We must note that the present rapid decrease of the Caspian Sea's level can be associated not only with global warming and the diminution in the volume of the Volga runoff but also with the active near-surface tectonics in the sea caused by the instability of the regional geodynamic interaction.

The region under study (the eastern part of Central Gondwana and Eurasia) played an essential role in ancient hominin dispersal (e.g., Lordkipanidze et al., 2007; Veliyev et al., 2010; Scardia et al., 2019; Plummer et al., 2023). The examination of the recent geodynamics in the region indicates that the dissection of the coastal high plateau of the Eastern Mediterranean with the formation of optimal land landscapes for the habitation of ancient hominins began after regression at the end of the Middle Gelasian when the sea level dropped by more than 150 m (Eppelbaum and Katz, 2024). This paleogeographic effect had not previously been considered, which prevented its use in developing an archaeological research strategy. However, considering the diverse and complex aspects of hominin dispersal from Africa to Eurasia in this multifaceted region, the range must be broader. The comprehensive study of the Carmel area (northern coastal plain of Israel), displaced in the main direction of the Levantine Corridor (Figure 13) during the Pleistocene time, showed that this area was flooded during the early dispersal of hominins from Africa (Eppelbaum and Katz, 2021). We propose that the Levantine Corridor emerged after the end of the Akchagylian transgres-

sion and landscape forming in the Eastern Mediterranean. At the same time, it was evident from Figure 13 that the primary ancient hominin dispersal skirted the Iranian Plate due to its complex topography and tectonics.

Conclusions

The main results of the investigation performed are the following:

(1) The MRCS, Iranian Plate, and South Caspian Basin compose a single geodynamic ensemble in the eastern part of Central Gondwana and Eurasia,

(2) The MRSC leads in this ensemble since its eastern counterclockwise rotating branch pushes the Iranian Plate to move north. The MRCS influence is also affected by the Earth's critical latitude of 35° and the Ural-African tectonic step.

(3) The complex configuration of the western part of the Iranian Plate, moving north and north-northeast, forces the South Caspian Basin to rotate clockwise,

(4) The western-central boundaries of the Iranian Plate were contoured by a combined analysis of gravity, magnetic, topographic, tectonic-structural, and some other features,

(5) The Iranian Plate comprises an intermediate zone between the Arabian and Eurasian plates,

(6) The recent geodynamic factors (together with the climatic, habitat, and food conditions) played a significant role in the dispersal of ancient hominins from Eastern Africa to the Levantine Corridor and further to the Caucasian region 2.5-2.0 million years ago.

Acknowledgment

The authors thank an anonymous reviewer for his valuable comments that allowed us to improve the final version of our paper.

REFERENCES

- Abdullayev N.R., Guliyev I.S., Kadirov F.A., Huseynova Sh.M., Javadova A.S., Maharramov B.I., Mukhtarov A.Sh. Novel interpretation of the crustal structure and hydrocarbon evolution within the South Caspian and Kura sedimentary basins, Azerbaijan. *Geophysical Journal*, Vol. 46, No. 3, 2024, pp. 146-161, <https://doi.org/10.24028/gj.v46i3.306357>.
- Abdullayev N.R., Kadirov F.A., Guliyev I.S. Subsidence history and basin-fill evolution in the South Caspian Basin from geophysical mapping, flexural backstripping, forward lithospheric modelling and gravity modeling. In: (Brunet M.-F., McCann T. and Sobel E.R. eds.) Geological evolution of Central Asian Basins and the Western Tien Shan Range, *Geol. Soc. Lond., Spec. Publ.*, Vol. 427, No. 1, 2017, pp. 175-196, <https://doi.org/10.1144/SP427>.
- Alavi M. Tectonics of the Zagros orogenic belt of Iran: new data and interpretation. *Tectonophysics*, Vol. 229, No. 3-4, 1994, pp. 211-238, [https://doi.org/10.1016/0040-1951\(94\)90030-2](https://doi.org/10.1016/0040-1951(94)90030-2).

ЛИТЕРАТУРА

- Abdullayev N.R., Guliyev I.S., Kadirov F.A., Huseynova Sh.M., Javadova A.S., Maharramov B.I., Mukhtarov A.Sh. Novel interpretation of the crustal structure and hydrocarbon evolution within the South Caspian and Kura sedimentary basins, Azerbaijan. *Geophysical Journal*, Vol. 46, No. 3, 2024, pp. 146-161, <https://doi.org/10.24028/gj.v46i3.306357>.
- Abdullayev N.R., Kadirov F.A., Guliyev I.S. Subsidence history and basin-fill evolution in the South Caspian Basin from geophysical mapping, flexural backstripping, forward lithospheric modelling and gravity modeling. In: (Brunet M.-F., McCann T. and Sobel E.R. eds.) Geological evolution of Central Asian Basins and the Western Tien Shan Range, *Geol. Soc. Lond., Spec. Publ.*, Vol. 427, No. 1, 2017, pp. 175-196, <https://doi.org/10.1144/SP427>.
- Alavi M. Tectonics of the Zagros orogenic belt of Iran: new data and interpretation. *Tectonophysics*, Vol. 229, No. 3-4, 1994, pp. 211-238, [https://doi.org/10.1016/0040-1951\(94\)90030-2](https://doi.org/10.1016/0040-1951(94)90030-2).

- Alemseged Z., Wynn J.G., Geraads D., Reed D., Barr W.A., Bobe R, McPherron, Sh.P., Deino A., Alene M., Sier M.J., Roman D., Mohan J. Fossils from Mille-Logya, Afar, Ethiopia, elucidate the link between Pliocene environmental changes and Homo origins. *Nature Communications*, Vol. 11 (2480), 2020, pp. 1-12, <https://doi.org/10.1038/s41467-020-16060-8>.
- Alizadeh A.A. Cretaceous Belemnites of Azerbaijan. Nedra. Moscow, 1972, 280 p. (in Russian).
- Alizadeh A.A., Aliyev S.A., Katz Y.I., Gamzayev G.A., Mamedzade A.M. New data on the presence of the Danian stage between the Khacinchai and Terterchay rivers (Lesser Caucasus). *Reports of Acad. Sci. Azerb.*, Vol. 39, No. 1, 1983, pp. 49-51 (in Russian).
- Alizadeh A.A., Guliyev I.S., Kadirov F.A., Eppelbaum L.V. Geosciences in Azerbaijan, Vol. II: Geology. Springer. Heidelberg–N.Y., 2016, 239 p., <https://doi.org/10.1007/978-3-319-27395-2>.
- Alizadeh A.A., Guliyev I.S., Mamedov P.Z., Aliyeva E.G.-M., Feyzullayev A.A., Huseynov D.A., Eppelbaum L.V. Pliocene Hydrocarbon Sedimentary Series of Azerbaijan. Springer. Heidelberg – N.Y., 2024, 514 p.
- Amirkhanov H.A. Paleolithic culture of the Caucasus at the end of the Eopleistocene: Oldovan, Early Acheulean, transitional stage? *Russian Archaeology*, Vol. 2, 2020, pp. 7-21, <https://doi.org/10.31857/S086960630008862-7> (in Russian).
- Arkell W.J. Jurassic geology of the world. Olivier and Boyd. London, 1956, 808 p.
- Artyushkov E.V. Formation of the South Caspian Basin as a result of phase transitions in the lower continental crust. *Doklady Earth Sciences* (Springer), Vol. 417, No. 8, 2007, pp. 1141-1146, <https://doi.org/10.1134/S1028334X07080016>.
- Bagheri S., Gol S.D. The eastern Iranian orocline. *Earth-Science Reviews*, Vol. 210, 103322, 2020, pp. 1-43, <https://doi.org/10.1016/j.earscirev.2020.103322>.
- Ben-Avraham Z. and Ginzburg A. Displaced terranes and crustal evolution of the Levant and the Eastern Mediterranean. *Tectonics*, Vol. 9 (4), 1990, pp. 613-622, <https://doi.org/10.1029/TC009i004p00613>.
- Ben-Avraham Z., Ginzburg A., Makris J., Eppelbaum L. Crustal structure of the Levant basin, Eastern Mediterranean. *Tectonophysics*, Vol. 346, 2002, pp. 23-43, [https://doi.org/10.1016/S0040-1951\(01\)00226-8](https://doi.org/10.1016/S0040-1951(01)00226-8).
- Brunet M.-F., Korotaev M.V., Ershov A.V., Nikishin A.M. The South Caspian Basin: a review of its evolution from subsidence modelling. *Sedimentary Geology*, Vol. 156, Nos. 1-4, 2003, pp. 119-148, [https://doi.org/10.1016/S0037-0738\(02\)00285-3](https://doi.org/10.1016/S0037-0738(02)00285-3).
- Cooper G.A. Jurassic brachiopods of Saudi Arabia. *Smithsonian Contributions to Paleobiology*, Vol. 65, 1989, 213 p.
- Corchete V. A new 3D S-velocity model for the lithosphere-asthenosphere system of the Arabian Peninsula and the Iranian plateau. *Jour. of Seismology*, Vol. 29, 2025, pp. 21-30, <https://doi.org/10.1007/s10950-024-10253-0>.
- Derevianko A.P., Anoykin A.A., Kazansky A.Yu., Matasova G.G. New Data to Justify the Age of Early Paleolithic Artifacts of Rubas-1 Site (Seaside Dagestan). *Historical Sciences and Archaeology*, No. 1, 2015, pp. 78-83, [https://doi.org/10.14258/izvasu\(2015\)3.2-11](https://doi.org/10.14258/izvasu(2015)3.2-11) (in Russian).
- Eppelbaum L.V. Processing and interpreting magnetic data in the Caucasus Mountains and the Caspian Sea: A review. *AIMS Geosciences*, Vol. 10, No. 2, 2024, pp. 333-370, <https://doi.org/10.3934/geosci.2024019>.
- Alemseged Z., Wynn J.G., Geraads D., Reed D., Barr W.A., Bobe R, McPherron, Sh.P., Deino A., Alene M., Sier M.J., Roman D., Mohan J. Fossils from Mille-Logya, Afar, Ethiopia, elucidate the link between Pliocene environmental changes and Homo origins. *Nature Communications*, Vol. 11 (2480), 2020, pp. 1-12, <https://doi.org/10.1038/s41467-020-16060-8>.
- Alizadeh A.A., Guliyev I.S., Kadirov F.A., Eppelbaum L.V. Geosciences in Azerbaijan, Vol. II: Geology. Springer. Heidelberg–N.Y., 2016, 239 p., <https://doi.org/10.1007/978-3-319-27395-2>.
- Alizadeh A.A., Guliyev I.S., Mamedov P.Z., Aliyeva E.G.-M., Feyzullayev A.A., Huseynov D.A., Eppelbaum L.V. Pliocene Hydrocarbon Sedimentary Series of Azerbaijan. Springer. Heidelberg – N.Y., 2024, 514 p.
- Arkell W.J. Jurassic geology of the world. Olivier and Boyd. London, 1956, 808 p.
- Artyushkov E.V. Formation of the South Caspian Basin as a result of phase transitions in the lower continental crust. *Doklady Earth Sciences* (Springer), Vol. 417, No. 8, 2007, pp. 1141-1146, <https://doi.org/10.1134/S1028334X07080016>.
- Bagheri S., Gol S.D. The eastern Iranian orocline. *Earth-Science Reviews*, Vol. 210, 103322, 2020, pp. 1-43, <https://doi.org/10.1016/j.earscirev.2020.103322>.
- Ben-Avraham Z. and Ginzburg A. Displaced terranes and crustal evolution of the Levant and the Eastern Mediterranean. *Tectonics*, Vol. 9 (4), 1990, pp. 613-622, <https://doi.org/10.1029/TC009i004p00613>.
- Ben-Avraham Z., Ginzburg A., Makris J., Eppelbaum L. Crustal structure of the Levant basin, Eastern Mediterranean. *Tectonophysics*, Vol. 346, 2002, pp. 23-43, [https://doi.org/10.1016/S0040-1951\(01\)00226-8](https://doi.org/10.1016/S0040-1951(01)00226-8).
- Brunet M.-F., Korotaev M.V., Ershov A.V., Nikishin A.M. The South Caspian Basin: a review of its evolution from subsidence modelling. *Sedimentary Geology*, Vol. 156, Nos. 1-4, 2003, pp. 119-148, [https://doi.org/10.1016/S0037-0738\(02\)00285-3](https://doi.org/10.1016/S0037-0738(02)00285-3).
- Cooper G.A. Jurassic brachiopods of Saudi Arabia. *Smithsonian Contributions to Paleobiology*, Vol. 65, 1989, 213 p.
- Corchete V. A new 3D S-velocity model for the lithosphere-asthenosphere system of the Arabian Peninsula and the Iranian plateau. *Jour. of Seismology*, Vol. 29, 2025, pp. 21-30, <https://doi.org/10.1007/s10950-024-10253-0>.
- Eppelbaum L.V., Ben-Avraham Z., Katz Y., Cloetingh S., Kaban M. Giant quasi-ring mantle structure in the African-Arabian junction: Results derived from the geological-geophysical data integration. *Geotectonics* (Springer), Vol. 55, No. 1, 2021, pp. 67-93, <https://doi.org/10.1134/S0016852121010052>.
- Eppelbaum L.V., Katz Y.I. Key Features of Seismo-Neotectonic Pattern of the Eastern Mediterranean. *Izv. Acad. Sci. Azerb. Rep., Ser.: Earth Sciences*, No. 3, 2012, pp. 29-40.
- Eppelbaum L.V. and Katz Yu.I. Eastern Mediterranean: Combined geological-geophysical zonation and paleogeodynamics of the Mesozoic and Cenozoic structural-sedimentation stages. *Marine and Petroleum Geology*, Vol. 65, 2015, pp. 198-216, <https://doi.org/10.1016/j.marpetgeo.2015.04.008>.
- Eppelbaum L.V., Katz Yu.I. A New regard on the tectonic map of the Arabian-African Region inferred from the satellite gravity analysis. *Acta Geophysica*, Vol. 65, 2017, pp. 607-626, <https://doi.org/10.1007/s11600-017-0057-2>.
- Eppelbaum L., Katz Yu. Akchagylian hydrodynamic phenomenon in aspects of deep geodynamics. *Stratigraphy and Sedimentation of Oil-Gas Basins*, No. 2, 2021, pp. 8-26.

- Eppelbaum L.V., Ben-Avraham Z., Katz Y., Cloetingh S., Kaban M. Giant quasi-ring mantle structure in the African-Arabian junction: Results derived from the geological-geophysical data integration. *Geotectonics* (Springer), Vol. 55, No. 1, 2021, pp. 67-93, <https://doi.org/10.1134/S0016852121010052>.
- Eppelbaum L.V., Katz Y.I. Key Features of Seismo-Neotectonic Pattern of the Eastern Mediterranean. *Izv. Acad. Sci. Azerb. Rep.*, Ser.: Earth Sciences, No. 3, 2012, pp. 29-40.
- Eppelbaum L.V. and Katz Yu.I. Eastern Mediterranean: Combined geological-geophysical zonation and paleogeodynamics of the Mesozoic and Cenozoic structural-sedimentation stages. *Marine and Petroleum Geology*, Vol. 65, 2015, pp. 198-216. <https://doi.org/10.1016/j.marpetgeo.2015.04.008>.
- Eppelbaum L.V., Katz Yu.I. A New regard on the tectonic map of the Arabian-African Region inferred from the satellite gravity analysis. *Acta Geophysica*, Vol. 65, 2017, pp. 607-626, <https://doi.org/10.1007/s11600-017-0057-2>.
- Eppelbaum L., Katz Yu. Akchagylian hydrodynamic phenomenon in aspects of deep geodynamics. *Stratigraphy and Sedimentation of Oil-Gas Basins*, No. 2, 2021, pp. 8-26.
- Eppelbaum L.V., Katz Yu.I. African-Levantine areal of ancient hominin dispersal: A new look derived from comprehensive geological-geophysical integration. In: (A.F. Yousef ed.), Emerging issues in environment, Geography and Earth Science, Vol. 7, BP International, London, 2024, pp. 151-222, <https://doi.org/10.9734/bpi/eiges/v7/1184G>.
- Eppelbaum L.V., Katz Y.I., Ben-Avraham Z. A review of geo-dynamic aspects of magnetic data analysis and tectonic-paleomagnetic mapping in the Easternmost Mediterranean. Applied Sciences, Spec. Issue "Ground-Based Geomagnetic Observations: Techniques, Instruments and Scientific Outcomes", Vol. 13, No. 18, 2023, pp. 1-44, <https://doi.org/10.3390/app131810541>.
- Eppelbaum L.V., Katz Y.I., Ben-Avraham Z. The reasons for enormous accumulation of the geodynamic tension in Eastern Turkey: a multidisciplinary study. *Geology Geophysics and Earth Science*, Vol. 2, No. 2, 2024a, pp. 1-28, <https://doi.org/10.58396/gges020202>.
- Eppelbaum L.V., Katz Y.I., Kadirov F.A. The relationship between the paleobiogeography of the northern and southern sides of the Neotethys and the deep geodynamic processes. *ANAS Transactions, Earth Sciences*, No. 2, 2024b, pp. 57-76, <https://doi.org/10.33677/ggianas20240100109>.
- Eppelbaum L.V., Katz Y.I., Kadirov F.A., Guliyev I.S., Ben-Avraham Z. Why is the South Caspian Basin clockwise rotating? Trans. of the 20th EUG Meet., Geophysical Research Abstracts, Vienna, Austria, Vol. 27, 2025, pp. 1-2, <https://doi.org/10.5194/egusphere-egu25-1841>.
- Eppelbaum L., Katz Yu., Klokochnik J., Kosteletsky J., Zheludev V., Ben-Avraham Z. Tectonic Insights into the Arabian-African Region inferred from a Comprehensive Examination of Satellite Gravity Big Data. *Global and Planetary Change*, Vol. 171, 2018, pp. 65-87, <https://doi.org/10.1016/j.gloplacha.2017.10.011>.
- Eppelbaum L.V., Nikolaev A.V., Katz Y.I. Space location of the Kiama paleomagnetic hyperzone of inverse polarity in the crust of the eastern Mediterranean. *Doklady Earth Sciences* (Springer), Vol. 457, No. 6, 2014, pp. 710-714, <https://doi.org/10.1134/S1028334X14080212>.
- Eppelbaum L.V., Pilchin A.N. Methodology of Curie discontinuity map development for regions with low thermal characteristics: An example from Israel. *Earth and Planetary Sciences Letters*, Vol. 243, No. 3-4, 2006, pp. 536-551, <https://doi.org/10.1016/j.epsl.2006.01.003>.
- Feldman H.R. A new species of the Jurassic (Callovian) Brachiopod *Septirhynchia* from the Northern Sinai. *Journal of Paleontology*, Vol. 61, No. 6, 1987, pp. 1156-1172, <https://www.jstor.org/stable/1305203>.
- Goutorbe B., Poort J., Lucaleau F., Raillard S. Global heat flow trends resolved from multiple geological and geophysical proxies. *Geophys. Jour. Intern.*, Vol. 187, 2011, pp. 1405-1419, <https://doi.org/10.1111/j.1365-246X.2011.05228.x>.
- Grine F.E., Leakey M.G., Gathago P.N., Brown F.H., Monge C.S., Yang D., Jungers W.L., Leakey L.N. Complete permanent mandibular dentition of early Homo from the upper Burgi Member of the Koobi Fora Formation, Ileret, Kenya. *Jour. of Human Evolution*, Vol. 131, 2019, pp. 152-175, <https://doi.org/10.1016/j.jhevol.2019.03.017>.
- Hall J.K., Krashenninnikov V.A., Hirsch F., Benjamin C. and Flexer A. (eds.). Geological Framework of the Levant. The Levantine Basin and Israel. Jerusalem, Vol. II, 2005, 827 p.
- Harmand S., Lewis J.E., Feibel C.S., Lepre C.J., Prat S., Lenoble A., Boës X., Quinn R.L., Brenet M., Arroyo A., Taylor N., Clément S., Daver G., Brugal J.-P., Leakey L., Mortlock R.A., Wright J.D., Lokorodi S., Kirwa C., Kent D.V., Roche H. 3.3-million-year-old stone tools from Lomekwi 3, West Turkana, Kenya. *Nature*, Vol. 521, 2015, pp. 1-6, <https://doi.org/10.1038/nature14464>.

- Goutorbe B., Poort J., Lucaleau F., Raillard S. Global heat flow trends resolved from multiple geological and geophysical proxies. *Geophys. Jour. Intern.*, Vol. 187, 2011, pp. 1405-1419, <https://doi.org/10.1111/j.1365-246X.2011.05228.x>.
- Grine F.E., Leakey M.G., Gathago P.N., Brown F.H., Monge C.S., Yang D., Jungers W.L., Leakey L.N. Complete permanent mandibular dentition of early Homo from the upper Burgi Member of the Koobi Fora Formation, Ileret, Kenya. *Jour. of Human Evolution*, Vol. 131, 2019, pp. 152-175, <https://doi.org/10.1016/j.jhevol.2019.03.017>.
- Gulyev I.S., Fyodorov D.L., Kulakov S.L. Oil and gas potential of the Caspian Region. Nafta Press. Baku, 2009, 409 p. (in Russian).
- Hall J.K., Krasheninnikov V.A., Hirsch F., Benjamini C. and Flexer A. (eds.). Geological Framework of the Levant. The Levantine Basin and Israel. Jerusalem, Vol. II, 2005, 827 p.
- Harmand S., Lewis J.E., Feibel C.S., Lepre C.J., Prat S., Lenoble A., Boës X., Quinn R.L., Brenet M., Arroyo A., Taylor N., Clément S., Daver G., Brugal J.-P., Leakey L., Mortlock R.A., Wright J.D., Lokorodi S., Kirwa C., Kent D.V., Roche H. 3.3-million-year-old stone tools from Lomekwi 3, West Turkana, Kenya. *Nature*, Vol. 521, 2015, pp. 1-6, <https://doi.org/10.1038/nature14464>.
- Hirsch F. Jurassic biofacies versus sea level changes in the Middle eastern Levant (Ethiopian province). *Trans. of the 2nd Intern. Symp. of Jurassic Stratigraphy*, Lisbon, 1988, pp. 963-981.
- Hirsch F., Picard L. The Jurassic facies in the Levant. *Jour. of Petroleum Geology*, Vol. 11, No. 3, 1988, pp. 277-308, <https://doi.org/10.1111/j.1747-5457.1988.tb00819.x>.
- Ismail-Zadeh A.T. Migration of seismic activity in the Caspian Sea. *Comput. Seism. Geodyn.*, Vol. 3, 1996, pp. 125-129, <https://doi.org/10.1029/CS003p0125>.
- Issayeva M.I., Khalafli A.A. Paleomagnetic Studies of the Caucasian segment of the Alpine Fold Belt. In: Ismail-Zadeh, A. (Ed.), Proceed. of the Intern. Workshop on recent geodynamics, georisk and sustainable development in the Black Sea to Caspian Sea region (Baku, 2005), Amer. Inst. of Physics, Melville, 2006, pp. 132-135, <https://doi.org/10.1063/1.2190740>.
- James G.A. and Wynd J.G. Stratigraphic Nomenclature of Iranian Oil Consortium Agreement Area. *AAPG Bulletin*, Vol. 49, 1965, pp. 2182-2245, <https://doi.org/10.1306/A663388A-16C0-11D7-8645000102C1865D>.
- Jimenez-Munt I., Sabadini R., Gardi A. Active deformation in the Mediterranean from Gibraltar to Anatolia inferred from numerical modeling and geodetic and seismological data. *Jour. of Geophysical Research*, Vol. 108, No. B1, 2006, pp. 1-24, <https://doi.org/10.1029/2001JB001544>.
- Johanson D. The paleoanthropology of Hadar, Ethiopia. *Comptes Rendus Palevol.*, Vol. 16, 2017, pp. 140-154, <https://doi.org/10.1016/j.crpv.2016.10.005>.
- Kadirov F.A., Klokočník J., Eppelbaum L.V., Kostelecký J., Bezděk A. Integration of the Bouguer gravity data with satellite gravity transformation integration in the Caspian region: An introduction. *ANAS Transactions, Earth Sciences*, No. 1, 2023, pp. 11-16. <https://doi.org/10.33677/ggianas20230100089>.
- Kadirov F.A., Floyd M., Reilinger R., Alizadeh Ak.A., Gulyev I.S., Mammadov S.G., Safarov R.T. Active geodynamics of the Caucasus region: Implications for earthquake hazards in Azerbaijan. *ANAS Transactions, Earth Sciences*, No. 3, 2015, pp. 3-17.
- Kadirov F.A., Gadirov A.N. A gravity model of the deep structure of South Caspian Basin along submeridional profile Alborz-Absheron Sill. *Global and Planetary Change*, Vol. 114, 2014, pp. 66-74.
- Kadirov F.A., Yetirmishli G., Safarov R., Mammadov S., Kazimov I., Floyd M., Reilinger R., King R. Results from 25 years (1998-2022) of crustal deformation monitoring in Azerbaijan and adjacent territory using GPS. *ANAS Transactions, Earth Sciences*, No. 1, 2024, pp. 28-43, <https://doi.org/10.33677/ggianas20240100107>.
- Kazmer M. Pygopid brachiopods and Tethyan margins. In: (Palfy, J., Voros, A., eds.) Mesozoic brachiopods of Alpine Europe. Hungarian Geolog. Soc., Budapest, 1993, pp. 59-68.
- Kaz'min V.G., Verzhbitskii E.V. Age and origin of the South Caspian Basin. *Oceanology*, Vol. 51, No.1, 2011, pp. 131-140, <https://doi.org/10.1134/S0001437011010073>.
- Khorrami F., Philippe V., Masson F., Nilforoushan F., Mousavi Z., Nankali H., Saadat A.S., Walpersdorf A., Hosseini S., Tavakoli P., Aghamohammadi Z., Alijanzade M. An up-to-date crustal deformation map of Iran using integrated campaign-mode and permanent GPS velocities. *Geophysical Jour. International*, Vol. 217, 2019, pp. 832-843, <https://doi.org/10.1093/gji/ggz045>.
- Klokočník J., Kostelecký J., Eppelbaum L., Bezděk A. Gravity Disturbances, the Marussi Tensor, Invariants and Other Functions of the Geopotential Represented by EGM 2008. *Journal of Earth Science Research*, Vol. 2, No. 3, 2014, pp. 88-101, <https://doi.org/10.18005/JESR0203003>.

- (1998-2022) of crustal deformation monitoring in Azerbaijan and adjacent territory using GPS. *ANAS Transactions, Earth Sciences*, No. 1, 2024, pp. 28-43, <https://doi.org/10.33677/ggianas20240100107>.
- Kazmer M. Pygopid brachiopods and Tethyan margins. In: (Palfy, J., Voros, A., eds.) *Mesozoic brachiopods of Alpine Europe*. Hungarian Geolog. Soc., Budapest, 1993, pp. 59-68.
- Kaz'min V.G., Verzhbitskii E.V. Age and origin of the South Caspian Basin. *Oceanology*, Vol. 51, No.1, 2011, pp. 131-140, <https://doi.org/10.1134/S0001437011010073>.
- Khain V.E. The problem of the origin and the age of the South Caspian Basin and its possible solutions. *Geotectonics*, Vol. 39, No. 1, 2005, pp. 34-38 (in Russian).
- Khorrami F., Philippe V., Masson F., Nilfouroushan F., Mousavi Z., Nankali H., Saadat A.S., Walpersdorf A., Hosseini S., Tavakoli P., Aghamohammadi Z., Alijanzade M. An up-to-date crustal deformation map of Iran using integrated campaign-mode and permanent GPS velocities. *Geophysical Jour. International*, Vol. 217, 2019, pp. 832-843, <https://doi.org/10.1093/gji/ggz045>.
- Klokočník J., Kostecký J., Eppelbaum L., Bezděk A. Gravity Disturbances, the Marussi Tensor, Invariants and Other Functions of the Geopotential Represented by EGM 2008. *Journal of Earth Science Research*, Vol. 2, No. 3, 2014, pp. 88-101, <https://doi.org/10.18005/JESR0203003>.
- Koshnaw R.I., Kley J., Schlunegger F. The Miocene subsidence pattern of the NW Zagros foreland basin reflects the south-eastward propagating tear of the Neotethys slab. *Solid Earth*, Vol. 15, 2024, pp. 1365-1383, <https://doi.org/10.5194/se-15-1365-2024>.
- Larrasoña J.C., Waldmann N., Mischke S., Avni J., Ginat H. Magnetostratigraphy and Paleoenvironments of the Kuntila Lake Sediments, Southern Israel: Implications for Late Cenozoic Climate Variability at the Northern Fringe of the Saharo-Arabian Desert Belt. *Frontiers in Earth Sci., Sec. Geomagnetism and Paleomagnetism*, Vol. 8, 2020, pp. 1-12, <https://doi.org/10.3389/feart.2020.00173>.
- Leonov Yu.G., Volozh Yu.A., Antipov M.P., Bykadorov V.A., Kheraskova T.N. The consolidated crust of the Caspian region: Experience of zonation. GEOS. Moscow, 2010, 64 p. (in Russian).
- Le Pichon X., Gauier J.-M. The rotation of Arabia and the Levant fault system. *Tectonophysics*, Vol. 153, 1988, pp. 271-294, [https://doi.org/10.1016/0040-1951\(88\)90020-0](https://doi.org/10.1016/0040-1951(88)90020-0).
- Le Pichon X., Şengör A.M.C., İmren C. A new approach to the opening of the Eastern Mediterranean Sea and the origin of the Hellenic Subduction Zone. Part 1: the Eastern Mediterranean Sea. *Canadian Jour. Earth Sci.*, Vol. 56 (8), 2019, pp. 1190-1204, <https://doi.org/10.1139/cjes-2018-0128>.
- Lordkipanidze D., Jashashvili T., Vekua A., de León M.S.P., Zollikofer C.P.E., Pontzer H., Ferring R., Oms, O., Tappen M., Bukhsianidze M., Agusti J., Kahlke R., Kiladze G., Martinez-Navarro B., Mouskhelishvili A., Nioradze M., Rook L. Postcranial evidence from early Homo from Dmanisi, Georgia. *Nature*, Vol. 449, 2007, pp. 305-310, <https://doi.org/10.1038/nature06134>.
- Malekzade Z. Block rotation induced by the change from the collision to subduction: Implications for active deformations within the areas surrounding South Caspian Basin. *Marine Geology*, Vol. 404, 2018, pp. 111-129, <https://doi.org/10.1016/j.margeo.2018.07.002>.
- Mangino S., Priestley K. The crustal structure of the southern Caspian region. *Geophysical Jour. Intern.*, Vol. 133, 1998, pp. 630-648, <https://doi.org/10.1046/j.1365-246X.1998.00520.x>.
- Mattei M., Cifelli F., Alimohammadian H., Rashid H., Winkler A., Sagnotti L. Oroclinal bending in the Alborz Mountains (Northern Iran): New constraints on the age of South Caspian subduction and extrusion tectonics. *Gondwana Research*, Vol. 42, 2017, pp. 13-28, <https://doi.org/10.1016/j.gr.2016.10.003>.
- Mattei M., Visconti A.L., Cifelli F., Nozaem R., Winkler A., Sagnotti L. Clockwise paleomagnetic rotations in northeastern Iran: Major implications on recent geodynamic evolution of outer sectors of the Arabia-Eurasia collision zone. *Gondwana Research*, Vol. 71, 2019, pp. 194-209, <https://doi.org/10.1016/j.gr.2019.01.018>.
- McDougall I., Brown F.H., Fleagle J.G. Sapropels and the age of hominins Omo I and II, Kibish, Ethiopia. *Jour. of Human Evolution*, Vol. 55(3), 2008, pp. 409-420, <https://doi.org/10.1016/j.jhevol.2008.05.012>.
- Moghadam H.S., Stern R.J. Ophiolites of Iran: Keys to understanding the tectonic evolution of SW Asia: (I) Paleozoic ophiolites. *Jour. of Asian Earth Sciences*, Vol. 91, 2014, pp. 19-38, <https://doi.org/10.1016/j.jseas.2014.04.008>.
- Motaghi K., Tatar M., Priestley K., Romanelli F., Doglioni C., Panza G.F. The deep structure of the Iranian Plateau. *Gondwana*, Vol. 28, 2015, pp. 407-418, <https://doi.org/10.1016/j.gr.2014.04.009>.
- Mousavi N., Ardestani V.E. 3D map of surface heat flow, low-temperature basins and Curie point depth of the Iranian plateau: Hydrocarbon reservoirs and iron deposits. *Jour. Earth Space Phys.*, Vol. 48(4), 2023, pp. 137-150, <https://doi.org/10.22059/jesphys.2023.348000.1007453>.
- Mousavi N., Fullea J. 3D thermochemical structure of lithospheric mantle beneath the Iranian plateau and surrounding areas from geophysical-petrological modeling. *Geophys. J. Intern.*, Vol. 222(2), 2020, pp. 1295-1315, <https://doi.org/10.1093/gji/gga262>.

- Mangino S., Priestley K. The crustal structure of the southern Caspian region. *Geophysical Jour. Intern.*, Vol. 133, 1998, pp. 630-648, <https://doi.org/10.1046/j.1365-246X.1998.00520.x>.
- Mattei M., Cifelli F., Alimohammadian H., Rashid H., Winkler A., Sagnotti L. Oroclinal bending in the Alborz Mountains (Northern Iran): New constraints on the age of South Caspian subduction and extrusion tectonics. *Gondwana Research*, Vol. 42, 2017, pp. 13-28, <https://doi.org/10.1016/j.gr.2016.10.003>.
- Mattei M., Visconti A.L., Cifelli F., Nozaem R., Winkler A., Sagnotti L. Clockwise paleomagnetic rotations in northeastern Iran: Major implications on recent geodynamic evolution of outer sectors of the Arabia-Eurasia collision zone. *Gondwana Research*, Vol. 71, 2019, pp. 194-209, <https://doi.org/10.1016/j.gr.2019.01.018>.
- McDougall I., Brown F.H., Fleagle J.G. Sapropels and the age of hominins Omo I and II, Kibish, Ethiopia. *Jour. of Human Evolution*, Vol. 55(3), 2008, pp. 409-420, <https://doi.org/10.1016/j.jhevol.2008.05.012>.
- Moghadam H.S., Stern R.J. Ophiolites of Iran: Keys to understanding the tectonic evolution of SW Asia: (I) Paleozoic ophiolites. *Jour. of Asian Earth Sciences*, Vol. 91, 2014, pp. 19-38, <https://doi.org/10.1016/j.jseas.2014.04.008>.
- Motaghi K., Tatar M., Priestley K., Romanelli F., Doglioni C., Panza G.F. The deep structure of the Iranian Plateau. *Gondwana*, Vol. 28, 2015, pp. 407-418, <https://doi.org/10.1016/j.gr.2014.04.009>.
- Mousavi N., Ardestani V.E. 3D map of surface heat flow, low-temperature basins and Curie point depth of the Iranian plateau: Hydrocarbon reservoirs and iron deposits. *Jour. Earth Space Phys.*, Vol. 48(4), 2023, pp. 137-150, <https://doi.org/10.22059/jesphys.2023.348000.1007453>.
- Mousavi N., Fullea J. 3D thermochemical structure of lithospheric mantle beneath the Iranian plateau and surrounding areas from geophysical-petrological modeling. *Geophys. J. Intern.*, Vol. 222(2), 2020, pp. 1295-1315, <https://doi.org/10.1093/gji/ggaa262>.
- Mukhtarov A.S. Shallow and deep temperatures in the South-Caspian Basin. *International Journal of Terrestrial Heat Flow and Applications*, Vol. 1, No. 1, 2018, pp. 23-29, <https://doi.org/10.31214/ijthfa.v1i1.13>.
- Nalbant S., McCloskey J., Steacy S., Barka A.A. Stress accumulation and increased seismic risk in eastern Turkey. *Earth and Planet Sci. Lett.*, Vol. 195, 2002, pp. 291-298, [https://doi.org/10.1016/S0012-821X\(01\)00592-1](https://doi.org/10.1016/S0012-821X(01)00592-1).
- Nouri A., Rahimi B., Vavryčuk V., Ghaemi F. Tectonic stress around the South Caspian basin deduced from earthquake focal mechanisms. *International Geology Review*, Vol. 66 (17), 2024, pp. 3075-3092, <https://doi.org/10.1080/00206814.2024.2315556>.
- Ozherel'yev D.V., Trifonov V.G., Chekik H., Trihunkov Ya.I. New evidence of the Early Paleolithic in the Mountain Systems of Eastern Anatolia and the Lesser Caucasus. In: (Lapshin, V.A., Chief Ed.) The Earliest Occupation of the Caucasian Region. *Transactions of the Institute for the History of Material Culture of the Russ. Acad. of Sci.*, Sankt-Petersburg, 2020, pp. 99-127 (in Russian).
- Plummer T.W., Oliver J.S., Finestone E.M., Ditchfield P.W., Bishop L.C., Blumenthal S.A., Lemorini C., Caricola I., Bailey S.E., Herries A.I.R. et al. Expanded geographic distribution and dietary strategies of the earliest Oldowan hominins and Paranthropus. *Nature*, Vol. 379, 2023, pp. 561-566, <https://doi.org/10.1126/science.abo7452>.
- Rashidi A., Kianimehr H., Yamini-Fard F. et al. Present Stress Map and deformation distribution in the NE Lut Block, Eastern Iran: Insights from Seismic and geodetic strain and moment rates. *Pure and Applied Geophysics*, Vol. 179, 2022, pp. 1887-1917, <https://doi.org/10.1007/s00024-022-03015-x>.
- Reilinger R.E., McClusky S., Vernant P., Lawrence S., Ergintav S., Cakmak R., Ozener H., Kadirov F., Guliyev I. et al. GPS constraints on continental deformation in the Africa-Arabia-Eurasia continental collision zone and implications for the dynamics of plate interactions. *Jour. of Geophysical Research*, Vol. 111(BO5411), 2006, pp. 1-26, <https://doi.org/10.1029/2005JB004051>.
- Sandwell D.T., Smith W.H.F. Global marine gravity from retracked Geosat and ERS-1 altimetry: ridge segmentation versus spreading rate. *Jour. of Geophysical Research*, Vol. 114(B01411), pp. 1-18, <https://doi.org/10.1029/2008JB006008>.
- Scardia G., Parenti F., Miggins D.P. et al. Chronologic constraints on hominin dispersal outside Africa since 2.48 Ma from the Zarqa Valley, Jordan. *Quaternary Sci. Reviews*, Vol. 219, 2019, pp. 1-19, <https://doi.org/10.1016/j.quascirev.2019.06.007>.
- Scotese C.R. Jurassic and Cretaceous plate tectonic reconstructions. *Palaeogeography, Palaeoclimatology, Palaeoecology*, Vol. 87, 1991, pp. 493-501, [https://doi.org/10.1016/0031-0182\(91\)90145-H](https://doi.org/10.1016/0031-0182(91)90145-H).
- Semaw S., Simpson S.W., Quade J., Renne P.R., Butler R.F., McIntosh W.C., Levin N., Dominguez-Rodrigo M., Rogers M.J. Early Pliocene hominids from Gona, Ethiopia. *Nature*, Vol. 433(7023), 2005, pp. 301-305, <https://doi.org/10.1038/nature03177>.
- Sengör A.M.C., Tüysüz O., İmren C., Sakınç M., Eyidoğan H., Görür N., Le Pichon X. and Rangin C. The North Anatolian Fault: A new look. *Annu. Rev. Earth Planet. Sci.*, Vol. 33, 2005, pp. 37-112, <https://doi.org/10.1146/annurev.earth.32.101802.120415>.
- Stampfli G.M. and Borel G.D. A plate tectonic model for the Paleozoic and Mesozoic constrained by dynamic plate boundaries and restored synthetic oceanic isochrons. *Earth and Planetary Science Letters*, Vol. 196(1-2), 2002, pp. 17-33, [https://doi.org/10.1016/S0012-821X\(01\)00588](https://doi.org/10.1016/S0012-821X(01)00588).
- Stampfli G.M., Kozur H.W. Europe from the Variscan to the Alpine cycles. *Geological Society, London, Memoirs*, Vol. 32, 2006, pp. 57-82, <https://doi.org/10.1144/GSL.MEM.2006.032.01.04>.
- Teknik V. The improved Moho depth imaging in the Arabia-Eurasia collision zone: A machine learning approach integrating seismic observations and satellite gravity data. *Tectonophysics*, Vol. 893, 230553, 2024, pp. 1-21, <https://doi.org/10.1016/j.tecto.2024.230553>.

- Reilinger R.E., McClusky S., Vernant P., Lawrence S., Ergintav S., Cakmak R., Ozener H., Kadirov F., Guliyev I. et al. GPS constraints on continental deformation in the Africa-Arabia-Eurasia continental collision zone and implications for the dynamics of plate interactions. *Jour. of Geophysical Research*, Vol. 111(BO5411), 2006, pp. 1-26, <https://doi.org/10.1029/2005JB004051>.
- Sandwell D.T., Smith W.H.F. Global marine gravity from retracked Geosat and ERS-1 altimetry: ridge segmentation versus spreading rate. *Jour. of Geophysical Research*, Vol. 114(B01411), pp. 1-18, <https://doi.org/10.1029/2008JB006008>.
- Scardia G., Parenti F., Miggins D.P. et al. Chronologic constraints on hominin dispersal outside Africa since 2.48 Ma from the Zarqa Valley, Jordan. *Quaternary Sci. Reviews*, Vol. 219, 2019, pp. 1-19, <https://doi.org/10.1016/j.quascirev.2019.06.007>.
- Scotese C.R. Jurassic and Cretaceous plate tectonic reconstructions. *Palaeogeography, Palaeoclimatology, Palaeoecology*, Vol. 87, 1991, pp. 493-501, [https://doi.org/10.1016/0031-0182\(91\)90145-H](https://doi.org/10.1016/0031-0182(91)90145-H).
- Schelinsky B.E. The Early Acheulean of Western Ciscaucasia. *The Inst. of the Material Culture History, Russian Acad. of Sci.*, Sankt-Petersburg, 2021, 132-140 (in Russian).
- Semaw S., Simpson S.W., Quade J., Renne P.R., Butler R.F., McIntosh W.C., Levin N., Dominguez-Rodrigo M., Rogers M.J. Early Pliocene hominids from Gona, Ethiopia. *Nature*, Vol. 433(7023), 2005, pp. 301-305, <https://doi.org/10.1038/nature03177>.
- Şengör A.M.C., Tüysüz O., İmren C., Sakınç M., Eyidoğan H., Görür N., Le Pichon X. and Rangin C. The North Anatolian Fault: A new look. *Annu. Rev. Earth Planet. Sci.*, Vol. 33, 2005, pp. 37-112, <https://doi.org/10.1146/annurev.earth.32.101802.120415>.
- Stampfli G.M. and Borel G.D. A plate tectonic model for the Paleozoic and Mesozoic constrained by dynamic plate boundaries and restored synthetic oceanic isochrons. *Earth and Planetary Science Letters*, Vol. 196(1-2), 2002, pp. 17-33, [https://doi.org/10.1016/S0012-821X\(01\)00588](https://doi.org/10.1016/S0012-821X(01)00588).
- Stampfli G.M., Kozur H.W. Europe from the Variscan to the Alpine cycles. *Geological Society, London, Memoirs*, Vol. 32, 2006, pp. 57-82, <https://doi.org/10.1144/GSL.MEM.2006.032.01.04>.
- Teknik V. The improved Moho depth imaging in the Arabia-Eurasia collision zone: A machine learning approach integrating seismic observations and satellite gravity data. *Tectonophysics*, Vol. 893, 230553, 2014, pp. 1-21, <https://doi.org/10.1016/j.tecto.2024.230553>.
- Teknik V., Ghods A., Thybo H., Artemieva I.M. Crustal density structure of northwestern Iranian Plateau. *Canadian Journal of Earth Sciences*, Vol. 56, 2019, pp. 1347-1365, <https://doi.org/10.1139/cjes-2018-0232>.
- Trifonov V.G. Sokolov S.Yu., Sokolov S.A., Hessami K. Mesozoic-Cenozoic structure of the Black Sea-Caucasus-Caspian Region and its relationships with the Upper mantle structure. *Tectonics*, Vol. 54, No. 3, 2020, pp. 331-355, <https://doi.org/10.1134/S0016852120030103>.
- Tselentis G.-A. and Drakopoulos J. Stress transfer and nonlinear stress accumulation at the North Anatolian Fault, Turkey. *PAGEOPH*, Vol. 132, No. 4, 1990, pp. 699-710, <https://doi.org/10.1007/BF00876814>.
- Tugend J., Chamot-Rooke N., Arsenikos S., Blanpied C., Frizon de Lamotte D. Geology of the Ionian Basin and Margins: A key to the East Mediterranean Geodynamics. *Tectonics*, Vol. 38, 2019, pp. 2668-2702, <https://doi.org/10.1029/2018TC005472>.
- Veliyev C.C., Aleskerov B.D., Tagiyeva E.N. The age of the Azykh site and climatic factors of migration to the Caucasus of the most ancient people. Karabakh in the Stone Age. Proceed. of the Intern. Scientific Conf. dedicated to the 50th anniversary of discovering the Paleolithic cave site of Azykh in Azerbaijan. *Tek Nur.* Baku, 2010, pp. 46-62.
- Vergés J., Saura E., Casciello E., Fernández M., Villaseñor A., Jiménez-Munt I., García-Castellanos D. Crustal-scale cross-sections across the NW Zagros belt: implications for the Arabian margin reconstruction. *Geological Magazine*, Vol. 148 (5-6), 2011, pp. 739-761, <https://doi.org/10.1017/S0016756811000331>.
- Wilson J.T. Did the atlantic close and then re-open? *Nature*, Vol. 211 (5050), 1966, pp. 676-681, <https://doi.org/10.1038/211676a0>.
- Zakariadze G.S., Dilek Y., Adamia S.A., Oberhänsli R.E., Karpenko S.F., Bazylev B.A., Solov'eva N. Geochemistry and geochronology of the Neoproterozoic Pan-African Transcaucasian Massif (Republic of Georgia) and implications for island arc evolution of the Late Precambrian Arabian-Nubian Shield. *Gondwana Research*, Vol. 11, 2007, pp. 92-108, <https://doi.org/10.1016/j.gr.2006.05.012>.
- Ализаде А.А. Меловые белемниты Азербайджана. Недра. Москва, 1972, 280 с.
- Амирханов Х.А. Палеолитическая культура Кавказа конца эоплейстоцена: олдован, ранний ашель, переходная стадия? *Российская археология*, No. 2, 2020, с. 7-21.
- Беляева Е.В. История изучения ахейцев в Армении и вклад В.П.Любина. В: (Лапшин В.А. отв. ред.), *Записки Института истории материальной культуры Рос. Акад. Санкт-Петербург*, 2020, с. 55-69.
- Гулиев И.С., Федоров Д.Л., Кулаков С.Л. Нефтегазовый потенциал Каспийского региона. Нафта Пресс. Баку, 2009, 409 с.
- Деревянко А.П., Аноин А.А., Казанский А.Ю., Матасова Г.Г. Новые данные по обоснованию возраста раннепалеолитического комплекса артефактов местонахождения Рубас-1 (Приморский Дагестан). *Известия Алтайского государственного университета*, № 3/2(87), 2015, [https://doi.org/10.14258/izvasu\(2015\)3.2-11](https://doi.org/10.14258/izvasu(2015)3.2-11)
- Кадиров Ф.А. Гравитационное поле и модели глубинного строения Азербайджана. *Нафта Пресс*, Баку. 2000, 126 с.
- Леонов Ю.Г., Волож Ю.А., Антипов М.П., Быкадоров В.А., Хераскова Т.Н. Консолидированная кора Прикаспийского региона: Опыт районирования. ГЕОС. Москва, 2010, 64 с.
- Макридин В.П., Кац Ю.И., Кузьмичева Е.И. Принципы, методика и значение фауны коралловых построек для зоогеографического районирования юрских и меловых морей Европы, Средней Азии и сопредельных стран. Исследование рифов и методика их изучения. Свердловск, 1968, с. 184-195.

- cross-sections across the NW Zagros belt: implications for the Arabian margin reconstruction. Geological Magazine, Vol. 148 (5-6), 2011, pp. 739-761, <https://doi.org/10.1017/S0016756811000331>.
- Wilson J.T. Did the atlantic close and then re-open? Nature, Vol. 211 (5050), 1966, pp. 676-681, <https://doi.org/10.1038/211676a0>.
- Zakariadze G.S., Dilek Y., Adamia S.A., Oberhänsli R.E., Karpenko S.F., Bazylev B.A., Solov'eva N. Geochemistry and geochronology of the Neoproterozoic Pan-African Transcaucasian Massif (Republic of Georgia) and implications for island arc evolution of the Late Precambrian Arabian-Nubian Shield. Gondwana Research, Vol. 11, 2007, pp. 92-108, <https://doi.org/10.1016/j.gr.2006.05.012>.
- Ожерельев Д.В., Трифонов В.Г., Чекик Х., Трихунков Я.И. Новые свидетельства раннего палеолита в горных системах Восточной Анатолии и Малого Кавказа. В книге: (Лапшин В.А., гл. ред.) Древнейшее заселение Кавказского региона. Труды Института истории материальной культуры РОС. Акад. наук, Санкт-Петербург, 2020, с. 99-127.
- Хайн В.Е. Проблема происхождения и возраста Южно-Каспийской впадины и ее возможные решения. Геотектоника, Том 39, №. 1, 2005, с. 34-38.
- Щелинский Б.Е. Ранний ашель Западного Предкавказья. Записки Инст. истории материальной культуры Российской акад. наук, Санкт-Петербург, 2021, 132-140.

АНАЛИЗ СЛОЖНЫХ ГЕОДИНАМИЧЕСКИХ ВЗАИМОДЕЙСТВИЙ В ВОСТОЧНОЙ ЧАСТИ ЦЕНТРАЛЬНОЙ ГОНДВАНЫ И ЕВРАЗИИ

Эппельбаум Л.^{1,2}, Кац Ю.³, Кадиров Ф^{4,5}, Гулиев И.⁶, Бен-Аврахам Ц.¹

¹Кафедра геофизики, факультет точных наук, Тель-Авивский Университет, Израиль

Рамат Авив 6997801:levap@tauex.tau.ac.il

²Азербайджанский государственный университет нефти и промышленности, Азербайджан AZ1010, Баку, просп. Азадлыг, 20

³Музей естественной истории им. Штейнгарда и Национальный исследовательский центр, Факультет естественных наук, Тель-Авивский Университет, Израиль

Тель-Авив, 6997801

⁴Министерство науки и образования Республики Азербайджан, Институт нефти и газа, Азербайджан AZ1000, Баку, пр. Ф.Амирова, 9

⁵Министерство науки и образования Азербайджанской Республики, Институт геологии и геофизики Азербайджан AZ1073, Баку, просп. Г.Джавида, 119

⁶Президиум Национальной академии наук Азербайджана, Азербайджан Ул. Истиглалият, 30, Баку, AZ1001

Резюме. Восточная часть Центральной Гондваны и Евразии представляет собой тектонически сложный регион, где взаимодействует несколько крупных тектонических плит — Евразийская, Африканская, Аравийская, Эгейско-Анатолийская, Иранская и Синайская. Однако недостаточно изучения эффектов взаимодействий только этих плит. В дополнение к этому интерфейсу здесь воздействуют также следующие региональные геодинамические факторы: мантийная структура, вращающаяся против часовой стрелки, Урало-Африканская аномалия геоида и критическая широта Земли 35°. Граница Евразия-Гондвана разделяет западную часть — Эгейско-Анатолийскую плиту и Мезозойский Террейновый Пояс (МТП), связанный со сравнительно молодым Неопротерозойским Поясом, — и восточную часть — Иранскую плиту, террейны которой являются фрагментами архейско-раннепротерозойского Аравийского кратона. Иранская литосферная плита, ключевая структура на границе между Евразией и Гондваной, имеет существенное тектоно-геодинамическое воздействие на Южно-Каспийский бассейн (ЮКБ) и на восточную часть МТП. Разработаны новые тектоническая, магнитная, спутниковая гравитационная карты Иранской плиты. В геодинамическом отношении рассматриваемые тектонические объекты расположены над центральной и восточной частями вращающейся эллиптической мантийной структуры. Иранская плита находится над восточной погранично-краевой зоной вращающейся мантийной структуры и под ее влиянием перемещается на север. Это движение и сложная форма западной части Иранской плиты обуславливают вращение ЮКБ по часовой стрелке. Представлен комплексный геодинамико-геофизический анализ основных тектонических структур региона и их взаимодействие между собой. Отдельно показано влияние недавнего геодинамического события — Акчагыльского гидросферного максимума — на миграцию древних людей. Проведенный анализ имеет важное значение для понимания роли сложного геодинамического взаимодействия в переходной зоне между Евразией и Гондваной.

Ключевые слова: мантийная структура Восточного Средиземноморья, Иранская литосферная плита, Южно-Каспийский бассейн, граница Евразии и Гондваны, геодинамические вращение и смещение

**MƏRKƏZİ QONDVANANIN ŞƏRQİNDƏ VƏ AVRASIYADA
MÜRƏKKƏB GEODİNAMİK QARŞILIQLI TƏSİRLƏRİN TƏHLİLİ**

Eppelbaum L.^{1,2*}, Katz Y.³, Qədirov F.^{4,5}, Quliyev İ.⁶, Zvi Ben-Avraham¹

¹Təl-Əvviv Universiteti, Dəqiq Elmlər Fakültəsi, Geofizika Departamenti, Təl-Əvviv, İsrail
Ramat Əvviv, 6997801: levap@tauex.tau.ac.il

²Azərbaycan Dövlət Neft və Sənaye Universiteti, Bakı, Azərbaycan
AZ1010, Bakı, Azadlıq pros., 20

³Steinhardt adına Təbiət Tarixi Muzeyi və Milli Tədqiqat Mərkəzi,
Təbiət Elmləri Fakültəsi, Təl-Əvviv Universiteti, Təl-Əvviv, İsrail
6997801, Təl Əvviv

⁴Azərbaycan Elm və Təhsil Nazirliyinin Neft və Qaz İnstitutu, Bakı, Azərbaycan
AZ1000, Bakı, Fikrat Əmirov pros. 119

⁵Azərbaycan Respublikasının Elm və Təhsil Nazirliyi, Geologiya və geofizika İnstitutu, Azərbaycan
AZ1073, Bakı şəh., H.Cavid pr., 119

⁶Azərbaycan Milli Elmlər Akademiyasının Rəyasət Heyəti, Azərbaycan
İstiqlaliyyət küç., 30, Bakı, AZ1001

Xülasə. Mərkəzi Qondvana və Avrasiyanın şərqi hissəsi bir neçə böyük tektonik plitələrin - Avrasiya, Afrika, Ərəbistan, Egey-Anadolu, İran və Sinay plitələrinin qarşılıqlı əlaqədə olduğu, tektonik cəhətdən mürəkkəb bir bölgədir. Qeyd edək ki, yalnız bu plitələr arasındaki qarşılıqlı təsirlərin effektini öyrənmək kifayət deyil. Bu interfeysə əlavə olaraq, aşağıdakı regional geodinamik amillər də mövcuddur: saat əqrəbinin əksi istiqamətində fırlanan mantiya strukturu, Ural-Afrika geoid anomaliyası və Yerin 35° kritik eni dairəsi. Avrasiya-Qondvana sərhədi, Egey-Anadolu plitəsinin qərb hissəsini, nisbətən gənc Neoproterozoy qurşağı ilə əlaqəli Mezozoy Terreyn qurşağını (MTB) və terreynləri, Arxey-Erkən Proterozoya aid olan Ərəb kratonunun fragmentini ehtiva edən İran plitəsinin şərqi hissəsindən ayırır. Avrasiya ilə Qondvana arasındaki sərhəddə əsas struktur olan İran litosfer plitosi Cənubi Xəzər hövzəsi (SCB) və Mezozoy Terreyn qurşağının (MTB) şərqi hissəsinə əhəmiyyətli tektonik-geodinamik təsir göstərir. İran plitəsinin yeni tektonik, maqnit və peyk gravitasiya xəritələri hazırlanmışdır. Geodinamik baxımdan nəzərdən keçirilən tektonik obyektlər mantiya strukturunun mərkəzi və şərqi hissəsindən yuxarıda yerləşir. İran plitəsi fırlanan mantiya strukturunun şərqi sərhəd-marjinal zonasından yuxarıda yerləşir və onun təsiri altında şimala doğru hərəkət edir. Bu hərəkət və İran plitəsinin qərb hissəsinin mürəkkəb forması Cənubi Xəzər hövzəsinin (SCB-nin) saat əqrəbi istiqamətində dönməsinə səbəb olur. Məqalədə bölgənin əsas tektonik strukturları və onların qarşılıqlı əlaqələrinin hərtərəfli geodinamik-geofiziki təhlili təqdim olunur. Xüsusilə, son geodinamik hadisələrdən biri olan Ağçaqıl hidrosferik maksimumunun qədim insan müraciyalarına təsiri ayrıca aşadır. Aparılmış təhlillər, Avrasiya ilə Qondvana arasında yerləşən keçid zonasında baş verən mürəkkəb geodinamik qarşılıqlı təsirləri anlamaq baxımından mühüm əhəmiyyət daşıyır.

Açar sözlər: Şərqi Aralıq dənizinin mantiya quruluşu, İran litosfer plitosi, Cənubi Xəzər hövzəsi, Avrasiya-Qondvana sərhədi, geodinamik fırlanma və yerdəyişmə

CALCULATION ALGORITHM AND DIGITAL MODELING OF THE FULL NORMALIZED GRAVITY GRADIENT

Isgandarov E.H.

Azerbaijan State Oil and Industrial University Azerbaijan
34, Azadlig ave., Baku AZ1010: elton_iskender@mail.ru

Keywords: algorithm, block-diagram, gravity anomaly, full normalized gradient, gravity model, digital modeling, reservoir type anomaly

Summary. The paper is devoted to the problem of constructing an algorithm for computing and digital modeling of the full normalized gradient of the gravity anomaly, the solution of which plays an important role in gravity exploration for the geological interpretation of the observed anomalies. To identify density inhomogeneities of rocks, which may be associated with structural features as well as hydrocarbon deposits in the section, methods for calculating gradients and higher derivatives of gravity anomalies are widely used. The paper describes an algorithm developed at the Department of Geophysics of Azerbaijan State Oil and Industry University (ASOIU) for calculating the full normalized gradient of gravity anomalies, used to identify and localize areas of density heterogeneities along the studied section. This algorithm and the corresponding FORSE-FORTRAN program allow the calculation of the values of the full normalized gradient of the gravity anomaly by analytical continuation into the lower half-space. Muradkhanli field was selected as the studied model, in the context of which volcanic-sedimentary sediments of the Mesozoic take part, that are well displayed in the gravitational field. Using modern graphical programs and developed applied algorithms, the profile values of the full normalized gradient of the gravity anomaly of the gravitational field of the Muradkhanli rising are calculated. Using the SURFER program, digital modeling of the full normalized gradient of the gravity anomaly is performed, which gives the most complete and a visual representation of the location of anomalous geological objects and oil and gas fields.

© 2025 Earth Science Division, Azerbaijan National Academy of Sciences. All rights reserved.

Introduction

In the search, exploration and study of the geological structure of promising oil, gas and ore bearing areas, the gravimetric exploration method is of great importance, which is based on studying the distribution pattern of gravitational fields created by individual structural uplifts that have an excess density of rocks composing it. At the stage of quantitative interpretation of gravimetric data, a very important problem is also solved – modeling of gravitational anomalies, which is of great significance in the geological interpretation. Currently, this problem is being solved in the form of digital modeling using modern graphic programs in two-dimensional and three-dimensional versions based on the results of computer calculations of the observed and theoretical gravitational fields using developed algorithms and programs, which provides the most complete picture of the shape, depth and size of the desired geological objects and oil and gas fields.

A direct search for oil and gas deposits in Azerbaijan is currently becoming particularly relevant in connection with the use of Canadian-made CG5 high-precision digital gravimeters in gravity practice, the

accuracy of which reaches 0.001 mGal, which fully provides the possibility of identifying weak local anomalies associated with oil and gas deposits. In the literature, these anomalies are also called “Reservoir Type Anomalies” (RTA). Quite a few studies have been devoted to the study of weak local gravitational anomalies associated with hydrocarbon deposits (Цимельзон и др., 1984). Various methods have been developed for transforming high-precision gravity data, among which the Berezkin method of full normalized gradient of gravity is especially popular (Березкин, 1988). The full normalized gradient method and its modifications are currently widely used (Aydin, 2007; Aydin and Kadirov, 2023). Of great interest are the works of Fedi and Florio (2001), devoted to identifying source boundaries using horizontal gradients, Sarsar Naouali et al. (2011), devoted to searching for diapiric structures based on gravity survey data and Kadirov et al. (2023), which proposes the idea of using the gravity gradient tensor based on satellite gravimetric survey data together with ground-based data in solving geodynamic problems and detecting oil and gas deposits. This explains the relevance of scientific research conducted in this direction.

The purpose of this research is to describe an algorithm for calculating the full normalized gradient of the gravity anomaly and digital modeling of the profile values of the full normalized gradient of the gravity anomaly of the gravitational field of the Muradkhanli rising in the eastern part of the Middle Kura depression known in Azerbaijan in the oil and gas ratio.

Means and methods: For many years, the Department of Geophysics has been developing algorithms, programs and the corresponding methodology for processing profile and areal data of high-precision gravimetric prospecting in order to isolate RTA (Isgandarov, 2023a,b; Искендеров, 2005, 2011, 2018, 2019). We propose a graph for processing both analog and digital gravimetric data using developed algorithms and programs. The basis of these algorithms includes various methods for transforming gravimetric data with increased sensitivity: methods of higher derivatives of the potential of gravity, calculation of dispersion, and the full normalized gradient of gravity of Berezkin. The results of processing model and actual gravimetric data are presented in a modern graphical interface. Below there is the block diagram of an

algorithm for calculating the full normalized gradient of the gravity anomaly developed at the department (Fig. 1). According to this algorithm, the following data is first entered:

NP, M are the profile number and the number of nodal points; DX, DDX are the step between points along the profile and the step of outputting values to the printing device, in km;

XN, XZL are the beginning and end of the integration base on the profile, in km;

ZH, ZMAX, DZ are the initial, maximum depth of the analytic continuation and their step.

FOR is the format ratio;

NH, NMAX, ND are the initial, maximum number of harmonics and their step of change.

After entering the data, the base is calculated and a linear regional background is removed. Then, in three cycles, according to the change in the number of harmonics, the integration base, and the depth of the analytic continuation, the values of the full normalized gradient of gravity into the lower half-space are calculated by the Berezkin method. The results are printed out as node points of the map along the section.

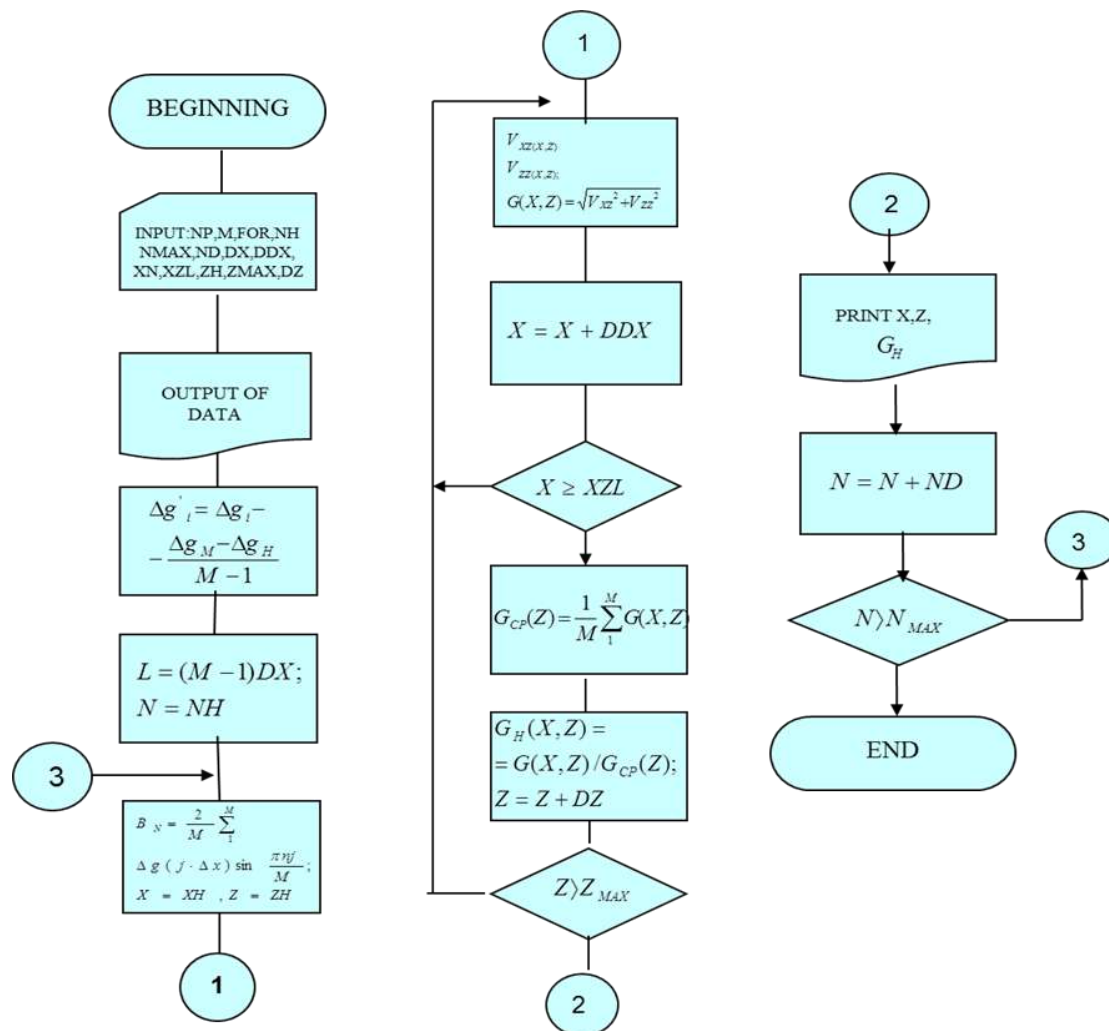


Fig. 1. Block-diagram of the algorithm GNORM

The Muradkhanli rising in the eastern part of the Middle Kura Depression (Fig. 2.), which is associated with an industrial oil and gas field, was chosen as a model. The structure itself is distinguished by its large size ($6.5 \times 8.7 \text{ km}$) and is tectonically represented by a dome-shaped fold along the Upper Cretaceous, the structure of which is complicated by discontinuous disturbances of various lengths and amplitudes (Салманов, Юсифов, 2013). In the section of the Muradkhanli rising, Mesozoic volcanogenic sedimentary deposits are involved, which have an excess density of about 0.2 g/cm^3 . It should be noted that the rise of Muradkhanli was first noted on maps of local gravity anomalies, constructed according to the data of gravity exploration.

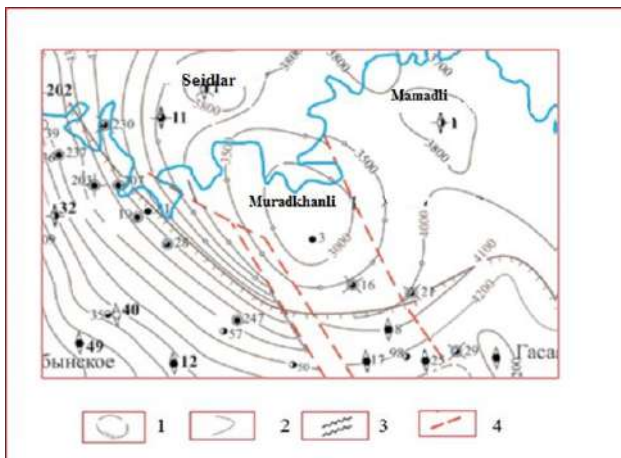


Fig. 2. The rise of Muradkhanli

Conv. Designator: 1 – structures prepared by seismic exploration; 2 – contours along the surface of the Upper Cretaceous; 3 – zone complex seismic information, associated with violations according to drilling; 4 – violations according to drilling

Results

Based on seismic data, we first performed a digital simulation of the Muradkhanli structure and compiled a structural model of the Muradkhanli rising in simplified form using the SURFER graphics program (Fig. 3). Then, according to detailed field gravimetric work data at the Geophysics Department, various transformations of the gravitational field were performed using a computer, including the method of averaging with a radius of 20 km (Δg_{20} local gravity anomalies, Искендеров, 2018). As you can see, the rise of Muradkhanli is displayed by the local maximum of gravity with the amplitude of about 4.5 mGal (Fig. 4). Based on the profile data of gravity exploration (the values of the gravity anomaly in the Bouguer reduction), we prepared the initial data in accordance with the algorithm, and then these data were processed using the appropriate GNORM program to calculate the values of the full

normalized gradient of the gravity anomaly (G_{fng} , dimensionless quantity). Then, using the SURFER program (Силкин, 2008), G_{fng} values were digitized according to the profile section and a map of the full normalized gradient of the gravity anomaly was constructed using the resulting grid file. In the beginning, it was necessary to calculate the optimal number of harmonics in the Fourier expansion. For this purpose, a priori drilling data on the location of a known oil reservoir were used. The results of calculation and digital modeling of the values of the full normalized gradient of the gravity anomaly for selection of the optimal number of harmonics are shown below (Fig. 5). The optimal number of harmonics in accordance with the drilling data turned out to be 17. After that, the values of the full normalized gradient of the gravity anomaly with the optimal number of harmonics were calculated and digital modeling of the G_{fng} section was performed. The section map of the full normalized gradient and the model of gravity anomaly curve are shown below (Fig. 6-7). As you can see, the deposit of oil lying at a depth of about 3 km (horizontal coordinate about 7.5 km) is characterized by a minimum of the full normalized gradient of gravity (Березкин, 1988), outlined by two maxima on the left and right (horizontal coordinate about 6.5 and 8.5 km). To the left of this minimum (horizontal coordinate about 5.5 km) is clearly fixed another minimum gravity that may be associated with another oil and gas field.

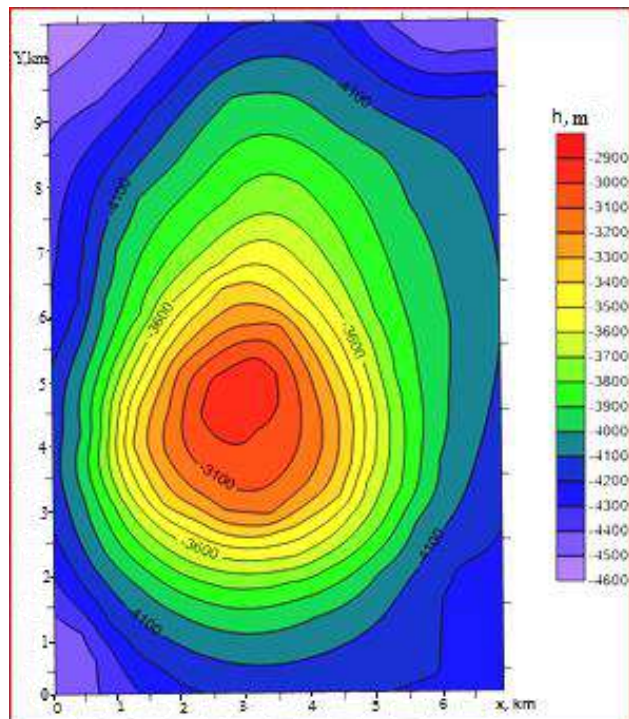


Fig. 3. Digital model of Muradkhanli structure (in the contours of depths on the surface of the Cretaceous deposits)

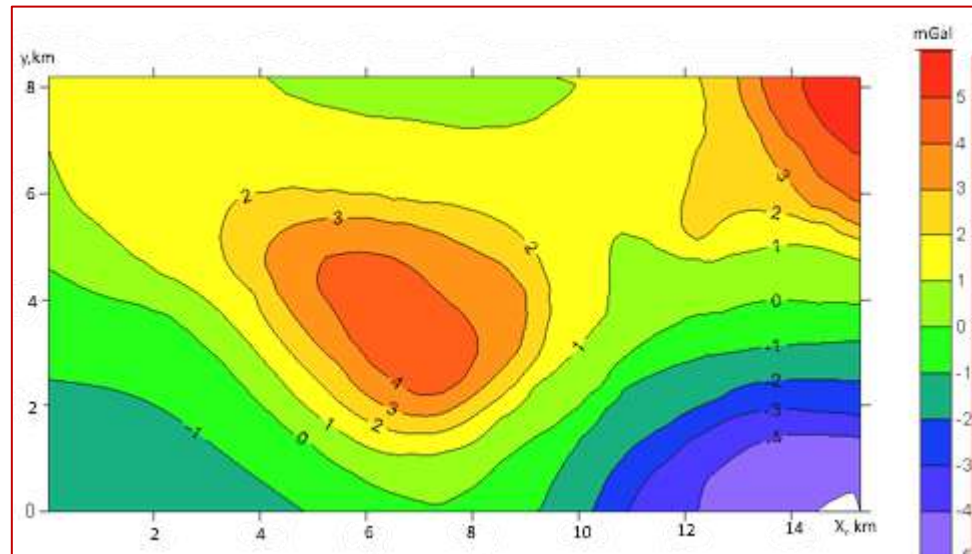


Fig. 4. Δg_{20} local gravity anomalies map of Muradkhanli area (in units mGal)

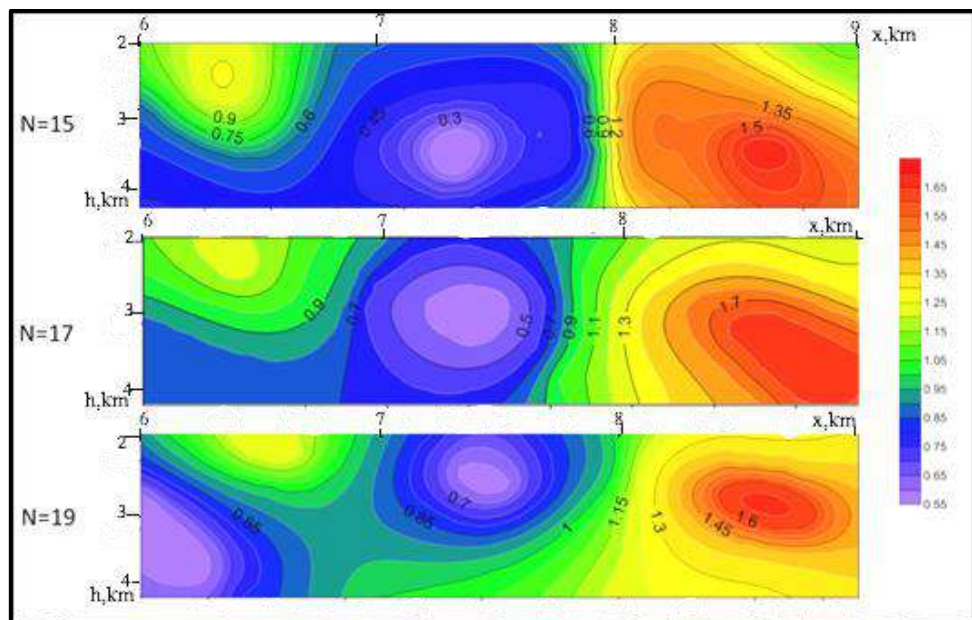


Fig. 5. Selection of the optimal number of harmonics

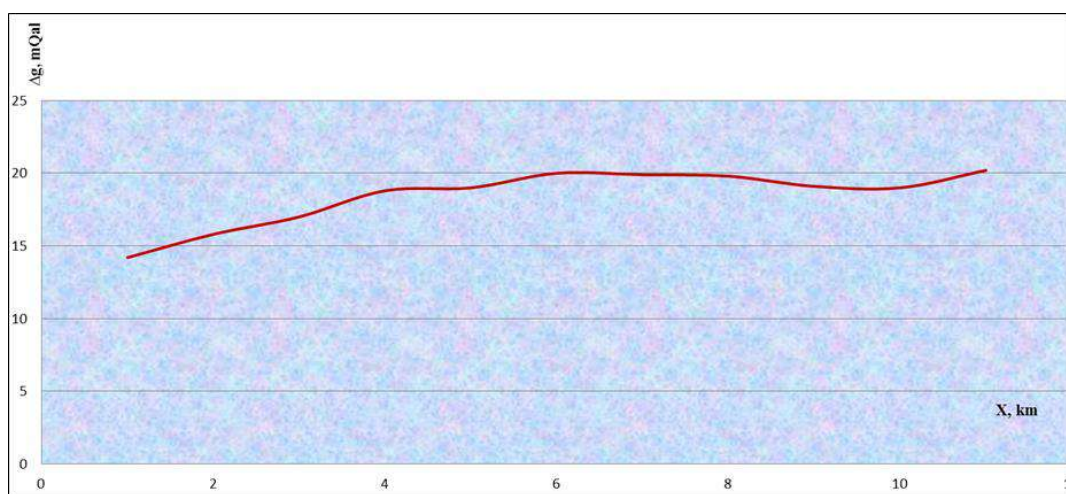


Fig. 6. The model curve of Bouguer gravity anomaly (Muradhanli maximum)

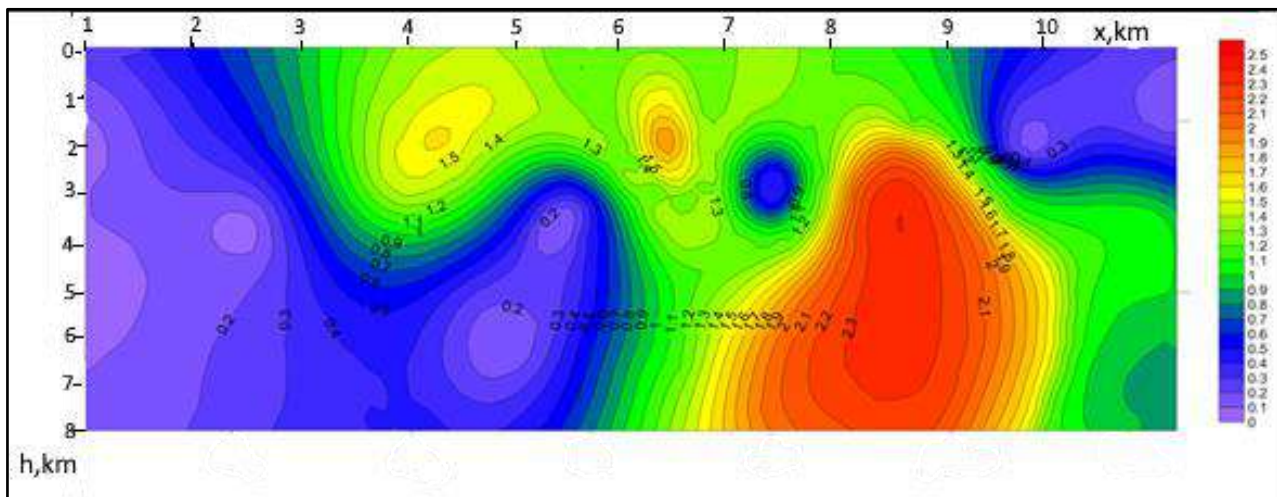


Fig. 7. Digital model of the map of the full normalized gradient of gravity field (Muradhanli maximum)

Conclusions

1. The block diagram of GNORM algorithm for calculating the full normalized gradient of the gravity anomaly in the profile version is presented. The GNORM program is implemented in the WINDOWS system using the FORCE FORTRAN compiler.

2. In the light of new geological and geophysical data, seismic, drilling, and gravity exploration data on the structure of the Mesozoic deposits of the Muradkhanli deposit are analyzed. According to the GNORM program software, the gravitational field was transformed by the method of the full normalized gradient of gravity along the profile crossing the Muradkhanli rise.

REFERENCES

- Aydin A. Interpretation of gravity anomalies with the normalized full gradient (NFG) method and an example. Pure and Applied Geophysics, Vol. 164, 2007, pp. 2329-2344.
- Aydin A., Kadirov F. Using the NFG method to gravity data of the Hasankale-Horasan petroleum exploration province. ANAS Transactions, Earth Sciences, Special Issue, 2023, pp. 57-59; DOI: 10.33677/ggianasconf20230300014.
- Berezkin V.M. The method of full normalized gradient in geophysical exploration. Nedra. Moscow, 1988, 188 p. (in Russian).
- Fedi M., Florio G. Detection of potential fields source boundaries by enhanced horizontal derivative method. Geophysical Prospecting, Vol. 49, No. 1, 2001, pp. 40-58.
- Isgandarov E.H. Digital modeling of gravity gradients for solving structural problems and direct hydrocarbons search. XII Azerbaijan International Geophysics Conference "The role of geophysical research in the exploitation of hydrocarbon resources in the caspian region and similar geological provinces" Dedicated to the 100th Anniversary of the birth of National Leader Heydar Aliyev, April 26-28, 2023a, p. 2.
- Isgandarov E.H. Digital estimation of the gravitational effect of the crystalline basement of the Yevlakh-Agjabadi Basin (Middle-Kur Depression). ANAS Transactions, Earth Sciences, No. 1, 2023b, pp. 17-24.
- Iskandarov E.H. Estimation of the gravitational influence of oil deposits at various depths. Journal "Geologist of Azerbaijan",

3. A digital simulation of the gravitational field of the Muradkhanli area in the profile version using the SURFER program has been performed, which gives the most complete two-dimensional representation of the studied geological section. On the section of the map of the full normalized gradient, the minimum of the full normalized gradient is noted, which can be associated with an oil and gas deposit.

4. The proposed algorithm for calculating the full normalized gradient of the gravity anomaly and the results of digital modeling are recommended for practical use in order to identify weak local anomalies associated with oil and gas deposits.

ЛИТЕРАТУРА

- Aydin A. Interpretation of gravity anomalies with the normalized full gradient (NFG) method and an example. Pure and Applied Geophysics, Vol. 164, 2007, pp. 2329-2344.
- Aydin A., Kadirov F. Using the NFG method to gravity data of the Hasankale-Horasan petroleum exploration province. ANAS Transactions, Earth Sciences, Special Issue, 2023, pp. 57-59; DOI: 10.33677/ggianasconf20230300014.
- Fedi M., Florio G. Detection of potential fields source boundaries by enhanced horizontal derivative method. Geophysical Prospecting, Vol. 49, No. 1, 2001, pp. 40-58.
- Isgandarov E.H. Digital modeling of gravity gradients for solving structural problems and direct hydrocarbons search. XII Azerbaijan International Geophysics Conference "The role of geophysical research in the exploitation of hydrocarbon resources in the caspian region and similar geological provinces" Dedicated to the 100th Anniversary of the birth of National Leader Heydar Aliyev, April 26-28, 2023a, p. 2.
- Isgandarov E.H. Digital estimation of the gravitational effect of the crystalline basement of the Yevlakh-Agjabadi Basin (Middle-Kur Depression). ANAS Transactions, Earth Sciences, No. 1, 2023b, pp. 17-24.
- Kadirov F.A., Klokočník J.3, Eppelbaum L.V., Kostelecký J., Bezděk A. Bouguer gravity data and satellite gravity transformation integration in the Caspian region: an introduction. ANAS Transactions, Earth Sciences, No.1, 2023, pp.11-16,

- Scientific Bulletin of the Society of Petroleum Geologists of Azerbaijan, No. 10, Baku, 2005, pp. 85-88 (in Russian).
- Iskandarov E.H. Estimation of RTA (reservoir type anomalies) associated with the zones of decompression of rocks. Journal "Geologist of Azerbaijan", Scientific Bulletin of the Society of Petroleum Geologists of Azerbaijan, No. 15, Baku, 2011, pp. 96-101 (in Russian).
- Iskandarov E.H. Digital modeling gravity field of Raising Murad-khanli. Australian Journal of Education and Science. The University of Sydney, No. 1(21), 2018, pp. 275-283 (in Russian).
- Iskandarov E.H., Yunlong You Liguo. Transformation of gravitational anomalies by methods derivatives and gradients. Danish Scientific Jurnal, No. 21, 2019, pp.13-16 (in Russian).
- Kadirov F.A., Klokočník J.3, Eppelbaum L.V., Kostelecký J., Bezděk A. Bouguer gravity data and satellite gravity transformation integration in the Caspian region: an introduction. ANAS Transactions, Earth Sciences, No. 1, 2023, pp. 11-16, DOI: 10.33677/ggianas20230100089.
- Salmanov A.M., Yusifov K.M. To petroleum prospects of a northeast board of Yevlakh-Agdzhabedy depression. SOCAR Proceedings "OilGasScientificResearchProject" Institute journal, No. 2, Baku, 2013, pp. 6-12 (in Russian).
- Sarsar Naouali B., Inoubli M.H., Amiri A., Chaqui A., Hamdi I. Subsurface geology of the Ariana region (Diapir Zone, northern Tunisia) by means of gravity analysis. Geophys. Prospect., Vol. 59, 2011, pp. 983-997.
- Silkin K.Y. Geographic information system Golden Software Surfer 8. Educational and methodological manual for higher educational institutions. Publishing and printing center of Voronezh state University. Voronezh, 2008, 66 p. (in Russian).
- Tsimilzon I.O., Amiraslanov T.S., Iskandarov E.H. et al. Prediction of the presence of hydrocarbon deposits in deep-lying volcanic-sedimentary formations of the Mesozoic according to high-precision gravity exploration. Materials of the scientific and technical geological and geophysical conference: Methods of prospecting and exploration of oil and gas deposits at great depths, Baku, 1984, pp. 57-59 (in Russian).
- DOI: 10.33677/ggianas20230100089.
- Sarsar Naouali B., Inoubli M.H., Amiri A., Chaqui A., Hamdi I. Subsurface geology of the Ariana region (Diapir Zone, northern Tunisia) by means of gravity analysis. Geophys. Prospect., Vol. 59, 2011, pp. 983-997.
- Березкин В.М. Метод полного нормированного градиента в геофизических исследованиях. Недра. Moscow, 1988, 188 с.
- Искендеров Э.Г. Оценка гравитационного влияния нефтяных залежей на различных глубинах. Журнал «Геолог Азербайджана», Научный вестник Общества геологов-нефтяников Азербайджана, No. 10, Баку, 2005, с. 85-88.
- Искендеров Э.Г. Оценка АТЗ (Аномалий типа залежи), связанных с зонами разуплотнения горных пород. Журнал «Геолог Азербайджана», Научный вестник Общества геологов-нефтяников Азербайджана, No. 15, Баку, 2011, с. 96-101.
- Искендеров Э.Г. Цифровое моделирование гравитационного поля поднятия Мурадханлы. Australian Journal of Education and Science. The University of Sydney, No. 1(21), 2018, pp. 275-283.
- Искендеров Э.Г., Юньлонг Ю Лиго. Трансформация гравитационных аномалий методами производных и градиентов. Danish Scientific Jurnal, No. 21, 2019, pp. 13-16.
- Салманов А.М., Юсифов К.М. К перспективам нефтегазоносности северо-восточного борта Евлах-Агджабединского прогиба. Журнал «Научные труды» НИПИ «Нефтегаз», No. 2, Баку, 2013, с. 6-12.
- Силкин К.Ю. Геоинформационная система Golden Software Surfer 8. Учебно-методическое пособие для вузов. Издательско-полиграфический центр Воронежского государственного университета. Воронеж, 2008, 66 с.
- Цимельзон И.О., Амирасланов Т.С., Искендеров Э.Г. и др. Прогноз наличия залежей углеводородов в глубокозалегающих вулканогенно-осадочных образованиях мезозоя по данным высокоточной гравиразведки. Материалы научно-технической геолого-геофизической конференции: Методы поиска и разведки залежей нефти и газа на больших глубинах, Баку, 1984, с. 57-59.

АЛГОРИТМ ВЫЧИСЛЕНИЯ И ЦИФРОВОЕ МОДЕЛИРОВАНИЕ ПОЛНОГО НОРМИРОВАННОГО ГРАДИЕНТА СИЛЫ ТЯЖЕСТИ

Искандаров Э.Г.

Азербайджанский государственный университет нефти и промышленности, Азербайджан
AZ1010 Баку, просп. Азадлыг, 34: elton_iskender@mail.ru

Резюме. Статья посвящена проблеме построения алгоритма вычисления и цифрового моделирования полного нормированного градиента аномалии силы тяжести, решение которой играет важную роль в гравиразведке для геологической интерпретации наблюдаемых аномалий. В настоящее время для выявления плотностных неоднородностей горных пород, которые могут быть связаны со структурными неоднородностями, а также с залежами углеводородов в разрезе, широко используются методы расчета градиентов и высших производных гравитационных аномалий. В статье описан разработанный на кафедре геофизики АГУНП алгоритм расчета полного нормированного градиента силы тяжести, который используется для выявления и локализации областей плотностных неоднородностей по изучаемому разрезу. Этот алгоритм и соответствующая FORSE-FORTRAN программа позволяют путем аналитического продолжения в нижнее полупространство расчитывать значения полного нормированного градиента. В качестве изучаемой модели было выбрано месторождение Мурадханлы, в разрезе которого принимают участие вулканогенно-осадочные отложения мезозоя, хорошо отображаемые в гравитационном поле. С использованием современных графических программ и прикладных алгоритмов, разработанных на кафедре геофизики, рассчитаны значения полного нормированного градиента вдоль профиля поднятия Мурадханлы. Также с помощью программы SURFER выполнено цифровое моделирование полного нормированного градиента силы тяжести, что дает наиболее полное и наглядное представление о местоположении аномальных геологических объектов и месторождений нефти и газа. Представленные алгоритмы и программы могут быть использованы для обработки и интерпретации высокоточных профильных гравиметрических наблюдений для локализации местоположения структурных неоднородностей, а также скоплений нефти и газа в разрезе изучаемой площади исследования.

Ключевые слова: алгоритм, блок-схема, аномалия силы тяжести, полный нормированный градиент, гравитационная модель, цифровое моделирование, аномалия типа залежи

AĞIRLIQ QÜVVƏSİNİN TAM NORMALLAŞDIRILMIŞ QRADİENTİNİN HESABLAMASI ALQORİTMİ VƏ RƏQƏMSAL MODELLƏŞDİRİLMƏSİ

İsgəndərov E.H.

Azərbaycan Dövlət Neft və Sənaye Universiteti (ADNSU), Azərbaycan
AZ1010, Bakı, Azadlıq pros., 34: elton_iskender@mail.ru

Xülasə. Məqalə ağırlik qüvvəsinin müşahidə olunan anomaliyaların geoloji şərhi üçün qravikəşfiyyatda həlli mühüm rol oynayan gravitasiya anomaliyasının tam normallaşdırılmış qradientinin hesablanması və rəqəmsal modelləşdirilməsi alqoritminin qurulması probleminə həsr edilmişdir. Hal-hazırda, strukturların qeyribircinsliyi ilə, eləcə də kəsilişdəki karbohidrogen yataqları ilə əlaqəli ola sűxurların sıxlıq qeyribircinsliyini müəyyən etmək üçün qradiyentin və ağırlik qüvvəsinin anomaliyalarının daha yüksək törəmələrinin hesablanması üsullarından geniş istifadə olunur. Məqalədə ADNSU-nun Geofizika kafedrasında işlənmiş tam normallaşdırılmış ağırlik qüvvəsinin qradientinin hesablanması alqoritm təsvir olunur ki, bu alqoritm tədqiq olunan kəsiliş boyunca sıxlıq qeyribircinslik sahələrini müəyyən etmək və lokallaşdırmaq üçün istifadə olunur. Bu alqoritm və müvafiq FORSE-FORTRAN programı aşağı yarım fəzaya analitik davam etdirərək tam normallaşdırılmış qradientin qiymətlərini hesablamaya imkan verir. Tədqiq olunan model kimi Muradxanlı yatağı seçilmişdir ki, onun kəsilişində gravitasiya sahəsində yaxşı əks olunan mezozoy vulkanogen-çökəmə çöküntülləri iştirak edir. Geofizika kafedrasında hazırlanmış müasir qrafik proqramlar və tətbiqi alqoritmlərdən istifadə etməklə Muradxanlı qalxımının profili üzrə tam normallaşdırılmış qradientin qiymətləri hesablanmışdır. Həmçinin, SURFER programından istifadə etməklə, anomal geoloji obyektlərin və neft-qaz yataqlarının yerləşməsi haqqında ən dolğun və aydın mənzərəni verən tam normallaşdırılmış qradientinin rəqəmsal modelləşdirilməsi aparılmışdır. Təqdim olunan alqoritmlər və proqramlar tədqiqat sahəsinin kəsilişində struktur sıxlıq qeyribircinsliklərin, eləcə də neft və qaz yiğilmalarının yerini lokallaşdırmaq üçün profil boyunca yüksək dəqiqlikli qravimetrik müşahidələrini emal və interpretasiya etmək üçün istifadə edilə bilər.

Açar sözlər: alqoritm, blok-sxem, ağırlik qüvvəsinin anomaliyası, tam normallaşdırılmış qradient, gravitasiya modeli, rəqəmsal modelləşdirmə, yataq tipi anomaliyası

ОСОБЕННОСТИ РАСПРЕДЕЛЕНИЯ ЗОЛОТОНОСНЫХ РОССЫПЕЙ И ИХ КОРЕННЫХ ИСТОЧНИКОВ НА ТЕРРИТОРИИ НАХЧИВАНСКОЙ АР

Тахмазова Т.Г.

Бакинский государственный университет, Азербайджан
AZ1148, Баку, ул. З.Халилова, 23: ttahmazova@yahoo.com

FEATURES OF THE DISTRIBUTION OF GOLD PLACERS AND THEIR PRIMARY SOURCES IN THE TERRITORY OF THE NAKHCHIVAN AR

Tahmazova T.H.

Baku State University, Azerbaijan
23, Z.Khalilov str., Baku, AZ1148: ttahmazova@yahoo.com

Keywords: placer gold content, river basins, primary sources, alluvial deposits, volcano-dome structures

Summary. Numerous research works have been carried out in the study area for decades. The article is devoted to a detailed analysis and assessment of placer gold content in the main river basins of the Nakhchivan Autonomous Republic, their primary sources, typomorphic features of placers, etc. This investigated the relationship of gold placers with their primary sources. The Bashkendchay and Alidzhachay river basins with tributaries for placer gold have been explored, promising areas have been identified. As a result of the research, it has been shown that these zones are highly promising. In the course of the studies, the typomorphic features of placer gold were revealed: detrital, oblate-detrital, porous, isometric, dendritic, elongated dendritic, etc., the chemical composition of gold was determined by local micro-X-ray spectral analysis. According to the results of spectral analysis, copper, mercury, lead, antimony, etc. were identified as impurity elements in the composition of gold. Bi, Cu, Fe, Hg, Mn, Rb, Sb, Te are the impurity elements in the composition of gold according to quantitative spectral analysis. The studies led to the conclusion that the location of primary deposits and manifestations of the study area close to each other determines the close location of placer gold accumulations. The considered typomorphic features, size classes, high fineness, limited fineness, a small amount of impurity elements, monograngular internal structure of alluvial gold also indicate a connection with nearby primary sources. Placer gold with high prospects is concentrated mainly in alluvial, alluvial-proluvial deposits.

© 2025 Earth Science Division, Azerbaijan National Academy of Sciences. All rights reserved.

Введение

Речная система Азербайджана очень густая и имеет огромное значение в отношении россыпной золотоносности. Основная часть этих рек относится к рр. Кура и Араз. Некоторые реки, входящие в Кура-Аразскую речную систему, берут свое начало с горных систем Большого и Малого Кавказа, Восточной Анатолии в направлении Каспийского моря, с гор Савалан, Гарадаг, Мишудаг, Готурдаг (территория Ирана). Эти горные системы являются водоразделами между Каспийским и Черным морями, озерами Урмия, Ван. Реки Азербайджана в большинстве принадлежат к типу горных рек (Балакенчай, Гарачай, Кишчай, Шинчай, Дамирапаранчай, Товузчай, Зиямчай, Шамкирчай, Кошкарчай, Асрикчай, Ахынджачай, Гянджачай, Хачынчай, Арпачай,

Алинджачай, Виляшчай и т.д.). Все они берут начало в высокогорных зонах на высоте 2500 м и более и прорезают глубокие ущелья. В наиболее поднятых частях горных хребтов отмечается нивально-ледниковый пояс, состоящий из снежников, а также фирнов и ледников, которые являются одним из источников питания рек.

Нахчivanская металлогеническая зона имеет особое значение среди выделенных в Азербайджане металлогенических провинций со своеобразным геологическим строением, магматическими и металлогеническими особенностями, полезными ископаемыми, речной сетью, в т.ч. и россыпной золотоносностью (Минерально-сырьевые ресурсы Азербайджана, 2005; Азадалиев, Керимов, 2006; Nağıyev, Məmmədov, 2010; Азадалиев и др., 2012) (рис.1).

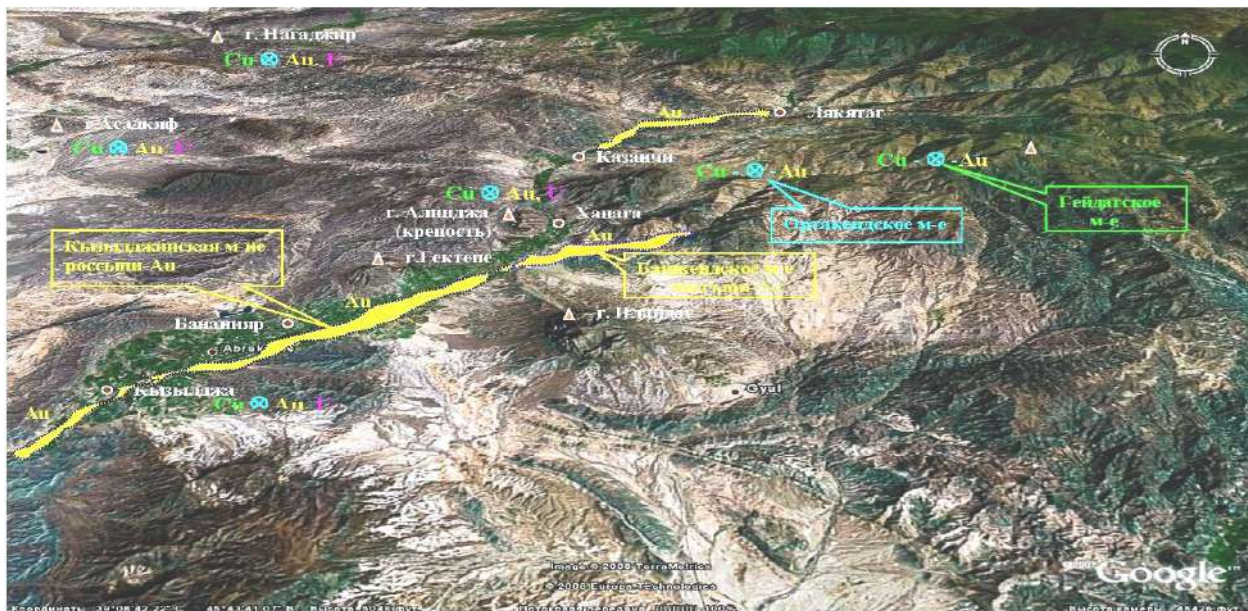


Рис. 1. Карта перспективных участков на изучаемой территории (на основе базы карт GoogleMap)

Здесь известны многочисленные коренные и россыпные месторождения промышленного значения. Они выделены на Ордубадском, Шарурском, Гейдагском, Джулфинском рудных районах – это месторождения и проявления Пъязбази, Мнундара, Шакардара, Агюрт-Мисдаг, Гейдаг, Агдара, Лякятаq, Сапдара, Гюмушлуг, Неграм, Армудлу золото-сульфидной, золото-медно-колчеданной, золото-медно-порфировой, золото-медно-полиметаллической формаций и субформаций, а также россыпные месторождения Гиланчай-Кетамчай, Кензачай, Килитчай, Арпачай, Садарак-Неграмский отрезок Араза, Джулфачай, Венандчай, Дюхлунчай, Ордубадчай, Алинджачай и др. (таблица 1).

С медно-молибденовыми и полиметаллическими месторождениями района связаны редкие концентрации рассеянных элементов, таких как Se, Te, Tl, In, Ga. Отметим, что речные системы Нахчывана берут свое начало с Конгур-Алагезского хребта Мегри-Ордубадского гранитоидного интрузива (Азадалиев и др., 2002; Геология Азербайджана, 2003; Патык-Кара, 1997; Патык-Кара, 2008; Becker, Batt, 2016; Баба-заде и др., 2003; Babazadeh et al., 2024 a,b).

Ордубадская зона разломов северо-западного простирания, как крупнейшая тектоническая структура региона, контролирует размещение коренных месторождений и проявлений рудных элементов, включая Cu, Mo, Au, W и др.

Оруденение Пъязбазинского месторождения представлено граносиенитовым интрузивом, где преобладают медь и молибден при подчиненной роли свинца, цинка, золота, серебра и др. Эндоконтакт граносиенитового интрузива является зоной формирования штокверковых и жильных медно-

молибден-порфировых месторождений (Парагачай, Гекгюндур, Агюрт, Каджаран, Агарак, Дастакерт и др.), в то время как в экзоконтактной зоне развиты золото-кварц-сульфидные жильные образования (Пъязбази, Шакярдара и др.). В северной части рудного поля положение золото-кварц-пиритовых жил контролируется преимущественно упомянутым разломом (Геология Азербайджана, 2003).

Гейдагское медно-порфиральное месторождение расположено на правом берегу р. Башкендчай, в геологическом строении которого присутствуют вулканогенные, вулканогенно-осадочные породы среднего и верхнего эоцена, интрузивы и различные дайки нижнего миоцена (рис. 2).

По Гейдагскому месторождению по отдельным блокам подсчитаны запасы меди по категориям C_2 и P_1 – 361.05 тыс. тонн, молибдена – 1.205 тонн, в отдельных пробах золото составляет от 0.2-0.6 г/т до 5.4-6 г/т, серебро – от 1.0-16 г/т до 18-20 г/т. В породах медно-молибденового рудного проявления Гылынджюрд содержание золота составляет 0.2-0.6 г/т, серебра 2.0-6.6 г/т. Точка минерализации Бейрекдаг расположена в зоне контакта пород с субвулканами эоценового возраста. На этой зоне развиты андезитодиабазы и известковые песчаники. Содержание золота составляет 0.4-2.8 г/т, серебра 1.0-7.9 г/т. На медно-порфиральном проявлении Ханага широко развиты лимонитизированные, окварцованные, хлоритизированные интрузивные породы диорит-порфирового состава. Золото-полиметаллическое проявление Ханагадаг охватывает обе стороны р.Башкендчай. Рудными минералами являются пирит, галенит, халькопирит, сфалерит (Шило, 2000; Шумилов, 1970; Aichler et al., 2008).

Таблица 1

Основные коренные источники территории, их формационная принадлежность и полезные компоненты руд

№№	Коренной источник	Рудные формации месторождений\проявлений	Полезные компоненты руд	
1.	Пъязбashi	Золото-сульфид-каврцевая	Au, Ag, Cu	
2.	Мнундара			
3.	Келаки			
4.	Шакардара	Золото-медно-порфировая	Au, Cu, Ag, , Co, Sn	
5.	Агдара	Золото-медно-полиметал-порфировая	Cu, Pb, Zn, Ag, Au, Mo, Ni (Pt)	
6.	Агюорт	Золото-медно-порфировая	Cu, Mo, Au, Ag (Pt)	
7.	Парагачай	Медно-порфировая	Cu, Mo, Au, Ag (Co, Ni, Sn, Bi, Pt)	
8.	Гапыджыг			
9.	Гейгель			
10.	Гейдаг			
11.	Диахчай			
12.	Мисдаг			
13.	Насирваз	Полиметаллическая (Zn-Pb)	Pb, Zn, Ag, Au, (Mo, Bi)	
14.	Гюмушлуг	Полиметаллическая	Pb, Zn, Ag, Au	
15.	Учурдаг	Золото	Au, Ag, Cu	
16.	Коланысу			
17.	Ашырым	Золото-медно-порфировая	Cu, Mo, Au, Ag	
18.	Айридаг			
19.	Сандара			
20.	Урмус (Урумлу)			
21.	Япраклы	Золото-полиметаллическая	Au, Ag, Pb, Zn	
22.	Хазинадара			
23.	Килит	Медно-кобальтовая	Au, Ag, Pb, Zn, Co, W (Pt)	
24.	Кетам			
25.	Фахладара	Медно-порфировая		
26.	Гейюндур			
27.	Лякятаг			
28.	Кечельдаг			
29.	Хал-хал	Медь	Cu (Au)	
30.	Говурмадара	Медно-полиметаллическая	Cu, Pb, Zn. Au, Ag	
31.	Генза			
32.	Парага			
33.	Мазра			
34.	Данзик			
35.	Гызылчынгыл	Вольфрам-молибденовая (жильная)	W, Mo, Cu, Co, Zn, Sn, (Au, Pt)	
36.	Кюю		Cu, Mo, Au, Hg	
37.	Кечелдаг			
38.	Зарнатюн			

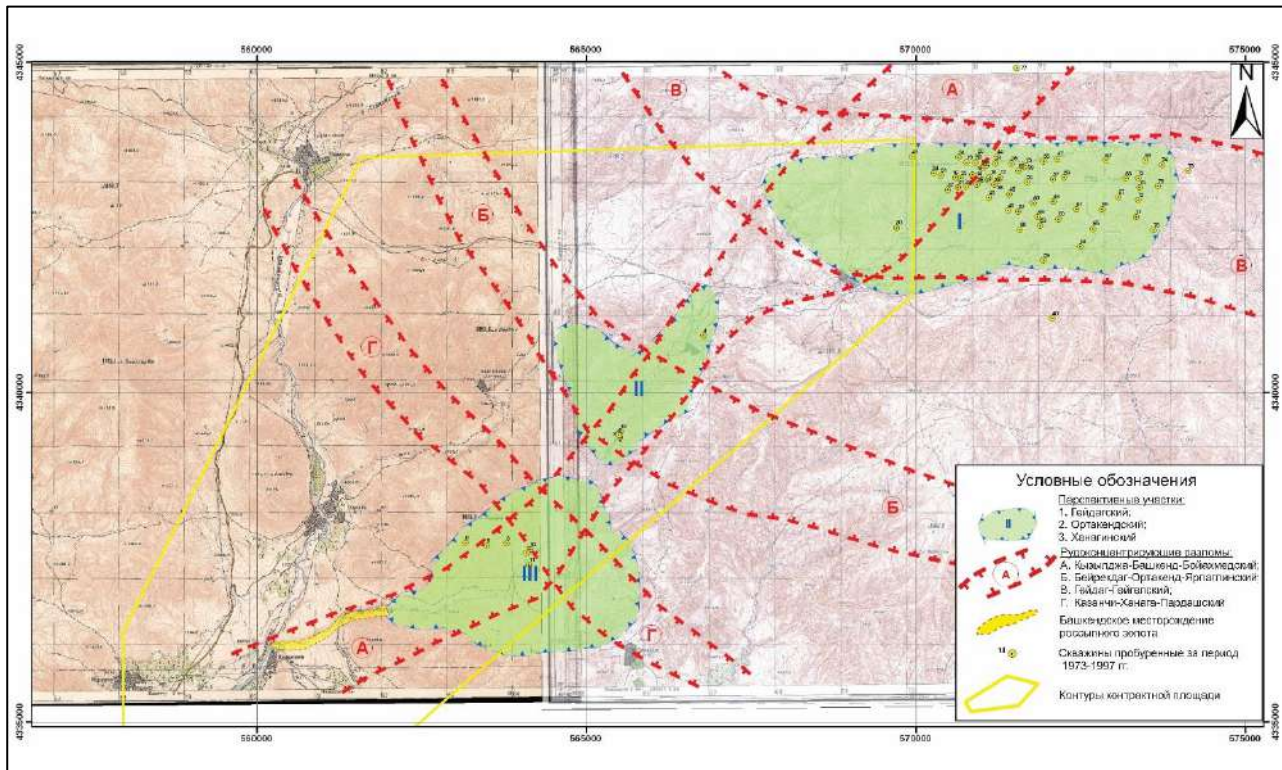


Рис. 2. Тектоническая GIS-схема Гейдагского рудного поля (масштаб 1:50 000) (Мусаев и др., 2004)

Следует рассмотреть следующую таблицу, где показаны основные речные системы с россыпной золотоносностью и связанные с ними коренные месторождения (таблица 2).

Река Алинджачай имеет длину 64 км, площадь водосбора 592 км² и начинается на склонах вершины г. Дамурлыдаг на высоте 2800 км. Ниже она прорезает Лякятагский монцонитовый интрузив, в пределах которого течет по узкой и глубокой долине с относительными превышениями водоразделов 700-800 метров. На участке от верховьев до с.Лякятаг долина приурочена к зоне параллельных разломов, ориентированных в широтном направлении (Азадалиев и др., 2012; Тәһмәзова, 2017). На нижеследующем рисунке показана рельефная карта изучаемого района (рис. 3).

Здесь аллювиальные отложения расположены на межгорной равнине и состоят из двух террас. Прогнозные ресурсы россыпного золота по категории Р₁ составляют 1576.1 кг, по категории Р₂ – 190.3 кг. Всего по бассейну р.Алинджачай геологические прогнозные запасы составляют 20 тонн золота, включая Башкендский участок, запасы которого по категории С₂+Р₁ составляют 3387.2 кг, в т.ч. по участкам, которые показаны на таблице 3.

Россыпное золото Башкендчайского бассейна отмечено с верхнего течения реки до устья. В десяти километровом интервале мощность скоплений

россыпного золота составляет 450-500 м, само месторождение охватывает 1.5 км² площади (рис. 4).

Река Башкендчай берёт начало в овражной сети, сформированной в пределах наиболее возвышенных участков одноименной вулкано-купольной структуры в районе гор Гылынджюорт и Гейдаг, и течет с северо-востока на юго-запад (рис.5). В нижнем течении реки выявлены золото-полиметаллические маломощные жилы, где в пробах содержание золота составляет 2.8 г/т, серебра – 1.27 г/т, свинца – 0.07%-12.5%. Наиболее значимые площади с промышленными концентрациями россыпного золота выделены в русловых, террасовых и пойменных аллювиальных отложениях (Carling, Breakspear, 2006; Goldfarb et al., 2015).

Долина реки характеризуется постепенным увеличением глубины от верховьев к низовьям, причем эта особенность усиливается заметным увеличением крутизны падения реки примерно на середине ее долины, вызванным наличием на этом участке эрозионно-устойчивых интрузивных пород. Именно здесь сосредоточены основные рудопроявления бассейна реки, сопровождаемые мощными зонами гидротермально измененных сульфидизированных пород. Интенсивная речная эрозия в пределах коренных источников и их притоков обусловила накопление значительных масс рыхлообломочных отложений, рудных минералов и золота в русловом аллювии.

Таблица 2

Коренные источники россыпных скоплений в реках НАР

№№	Реки, имеющие (предполагаемые) скопления россыпей золота	Источники россыпного золота и их индикаторы, морфогенетические типы
1.	Килитчай	Килитское проявление меди (Ni, Co, Cu); зона минерализации вкраплено-прожилкового типа
		Золото-травий W-Mo-(Cu); молибденит, вольфрамит, шеелитовые кварцевые жилы
2.	Кетамчай	Кетамское кобальтовое проявление (Pb-Zn-Cu) сульфидная минерализованная зона вкраплено-прожилкового типа
3.	Кензачай	Полиметаллическое проявление Кенза (Pb-Zn-Cu)
4.	Ордубадчай	Дидянчайский медно-порфировый рудник
		Рудное проявление Фахладара (медно-порфировый)
5.	Ванандчай	Рудное проявление Шалала (медно-молибден-порфировое)
		Учурдагское проявление золота
		Мисдагский медно-порфировый рудник
		Келакинский рудник золота
		Медно-порфировое проявление Данакенд
		Агюртское (Алчалых) золото-медно-порфировое проявление
6.	Дюхлунчай	Шакардаринский рудник золота (медно-порфировый)
7.	Гilanчай	Ешакмейданское золото-медно-порфировое проявление
		Айридагское медно-порфировое проявление
		Гейгельский (Газангель) медно-порфировый рудник
		Гейдагский медно-порфировый рудник
		Сапдаринское золото-медно-порфировое проявление
		Насирвазский рудно-полиметаллический рудник
		Агдаринский золото-медно-полиметаллическо-порфировый рудник
		Полиметаллическое проявление Парага
		Полиметаллическое проявление Мазра
		Золотой рудник Мнундара (Парагачай)
		Парагачайский медно-порфировый рудник
8.	Алинджачай	Урмусское (Мадандара) Au-Cu-порфировое проявление
		Говурмадаринское рудное проявление (Cu-Pb-Zn)
		Ярпаглинское (Башкенд-Ортакенд) золото-полиметаллическое проявление
		Хазинадаринское рудное проявление (золото полиметаллическое)
		Проявление золота Коланысу
		Ляятагское рудное проявление
9.	Нахчыванчай	Тазакендское мышьяково-рутунное проявление
		Даррыдагский мышьяково-сурьмяной рудник
		Халхалское проявление меди
		Проявление Сурьмалык
10.	Арпачай	Мышьяковое проявление Комюр
		Рудное проявление Кюю
10.	Арпачай	Полиметаллическое проявление Данзик
		Полиметаллический рудник Гюмушлуг



Рис. 3. Рельефная карта Алинджачайского участка (на базе карт Google Map)
Примечание: в плане высотные отметки: 1, 2 – дальние, 3,4 – близкие

Таблица 3

Параметры золотоносных участков изучаемой территории

№ №	Участки	Длина, м	Ширина, м	Мощность, м	Объем рос- сыпной золо- тоносной мас- сы, м ³	Среднее содержание Au, мг\м ³	Запасы Au по катего- рии C ₂ +P ₁ , кг
1.	Лялятагский	1200	60	15	1080000	248.4	268.3
2.	Башкендский	2000	20	2	8000	1530.0	122.4
3.	Бинанярский	7000	150	2	2100000	300.6	631.4
4.	Джамаллидинский	8000	150	2	2400000	401.3	963.1
5.	Аразский	13000	180	2	4680000	299.6	1402.1
Всего:							3387. 2

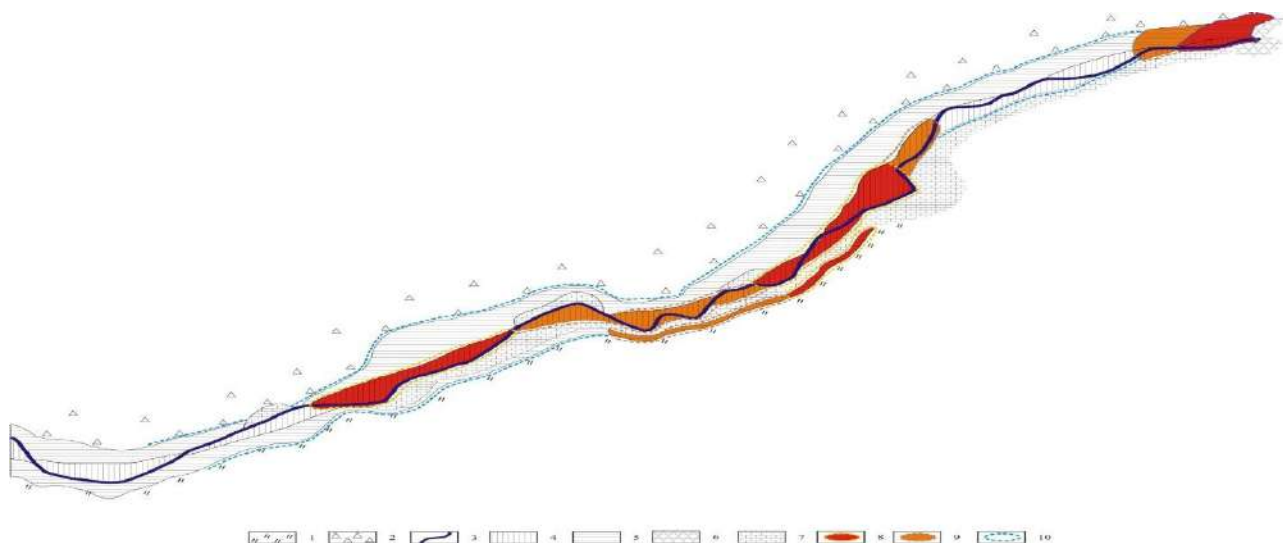


Рис. 4. Схематический план размещения золотоносных россыпей нижнего течения р.Башкендчай (Масштаб 1:2000, составлен по материалам АzeriGold)

Условные обозначения: 1-почвенно-растительный слой; 2-делювиальные отложения; 3-русло реки; 4-надрудовая терраса первого порядка; 5-надрудовая терраса второго порядка; 6-диорит-порфириты; 7-песчано-глинистые породы; зоны россыпных скоплений; 8-более 1000 м³/м³; 9-400-600 м³/м³; 100-400 м³/м³

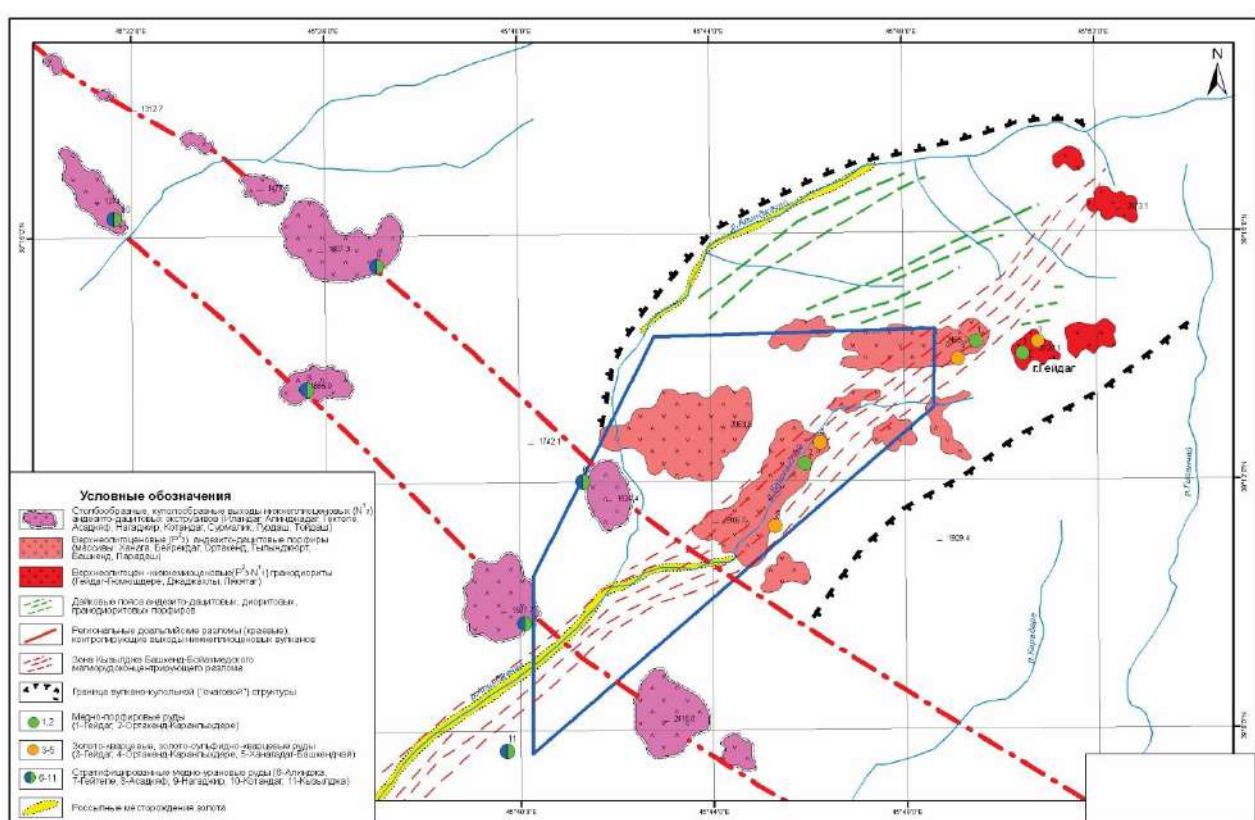


Рис. 5. Схема расположения Башкенской вулкано-купольной структуры (масштаб 1:100000) (Мусаев и др., 2004)

Установлена золотоносность аллювиальных отложений реки почти на всем ее протяжении, начиная от устья до района с.Башкенд. Центральный участок реки Башкендчай с крутым

уклоном характеризуется выносом и локальным обогащением золота на протяжённости около 1.5 км от устья у села Хошкешин до водоотводной канавы на склоне 1426.0 м. На этом участке до-

лина реки, выходя из центральной части вулкано-купольной структуры на предгорную равнину, заметно расширяется, крутые склоны сменяются более пологими. Практически этот отрезок является своеобразным конусом выноса рыхлобломочных отложений долины реки, представленным цепочкообразно расположеннымными пойменными и надпойменными террасами мощностью от 0.5 до 1.0 м, иногда 1.5-2.0 м и больше. Кроме того, выделяются еще две надпойменные террасы на высоте 3-8 м соответственно над современным руслом мощностью до 3.0-3.5 м. Содержание золота колеблется от 200 до 5000 мг\м³ и в среднем составляет 1530.0 мг\м³.

Между устьем Джаджахлинского притока и северной частью Ортакендского участка в интервале 3.5 км расположен Башкендчайский участок. Этот участок состоит в основном из песчано-глинистых коренных пород эоценового возраста. Интрузивы пластиообразные, наклонные. И аллювиальные, и деллювиально-пролювиальные отложения золотоносны. Транспортируемое золото с крутых вершин к пологим участкам аккумулируется именно на этом отрезке реки (рис. 6).

Золото в исследуемых шлихах выявлено в 26% образцов. Размер частиц варьируется в пределах от 0.2 до 0.7 мм. По форме зерна представлены преимущественно дендритовыми и обломочными типами, при этом в единичных случаях наблюдаются игловатые формы. Первая терраса более богата россыпным золотом, и это объясняется тем, что вторая терраса является дополнительным коллектором. В промытых шлихах (94%) обнаружена значительная концентрация золота. Отмечено, что по всему профилю реки количество золота в шлихах растет, но степень окатанности остается неизменной.

На следующем отрезке Башкендчайского участка выделяется участок Ханагадаг. Этот участок состоит в основном из деллювиальных отложений, и золото в шлифах встречается в количестве 62%. Далее отмечается участок Хошкешин. Этот участок охватывает конус выноса реки и продолжается до устья. Все эти участки выделены как единая Башкендская зона россыпного золота. На нижеследующей диаграмме показана связь между мощностью и длиной золотороссыпных скоплений Башкендской зоны (рис. 7).



Рис. 6. Участок россыпного золота в бассейне р.Башкендчай (на базе карт Google Map)

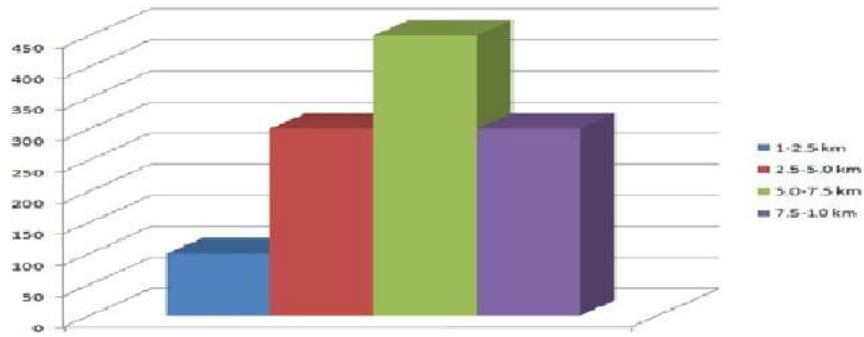


Рис.7. Параметры скоплений Башкендской зоны россыпного золота:
по вертикали мощность (м), по горизонтали длина золотороссыпных скоплений (км)

Здесь же изучены и оценены такие геологические объекты как Джаджахлы, Ортакенд, Гызылджа, Ханагадаг, Дикюрд, Мурадханлы, Гюмушдара, Гызылджаорт и т.д. В долине Джаджахлы в нижнем течении реки в полиметаллических прожилках золото составляет 0.4-2.0 г/т, серебро – 3-20 г/т. Этот факт указывает на перспективность данного участка.

Ортакендский участок реки протяженностью 3.5 км, имеет V-образную форму, наклон долины достигает 8-10⁰ (59 м/км). В промытых шлихах лишь в 16% отмечено золото. Золотины имеют обломочную форму, а размер их достигает 0.2-0.8 мм. На участках Джаджаглы, Башкенд, Ортакенд ресурсы россыпного золота оцениваются в 581 кг.

Участок Гызылджа в среднегорной области занимает 14-16 км длину и считается высокоперспективным на золото. Количества золота в 1 м³ составляет 50-1840 условных единиц. Лякяташский участок в среднегорной области занимает 15-18 км в длину и считается вторым перспективным участком на россыпное золото. Аразская зона в низкогорной области занимает 10-15 км в длину и считается третьей по перспективности на россыпное золото. В отдельных пробах количество свободного золота составляет 200-400 условных единиц на 1 м³. Коренные породы участка Ханагадаг, подвергшиеся гидротермальному изменению, располагаются в зонах пересечения разрывных нарушений, ориентированных на северо-восток и северо-запад. Аллювиальные отложения слагают лишь русло реки. Обобщенные профили Гейдаг-Ортакенд-Ханага (вдоль р.Башкендчай) показаны на рис. 8 и 9.

На участке Гызылджа в среднегорной области занимает 14-16 км длину и считается высокоперспективным на золото. Количества золота в 1 м³ составляет 50-1840 условных единиц. Лякяташский участок в среднегорной области занимает 15-18 км в длину и считается вторым перспективным участком на россыпное золото. Аразская зона в низкогорной области занимает 10-15 км в длину и считается третьей по перспективности на россыпное золото. В отдельных пробах количество свободного золота составляет 200-400 условных единиц на 1 м³. Коренные породы участка Ханагадаг, подвергшиеся гидротермальному изменению, располагаются в зонах пересечения разрывных нарушений, ориентированных на северо-восток и северо-запад. Аллювиальные отложения слагают лишь русло реки. Обобщенные профили Гейдаг-Ортакенд-Ханага (вдоль р.Башкендчай) показаны на рис. 8 и 9.

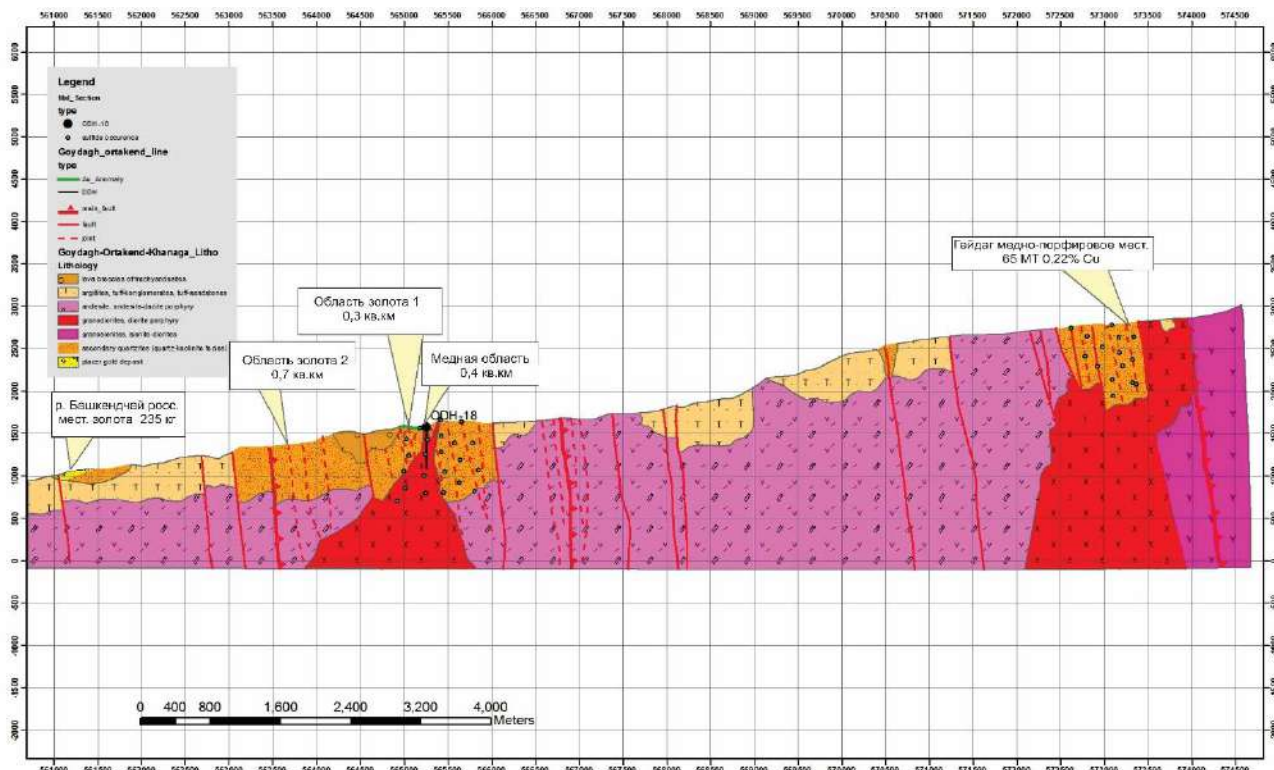


Рис.8. Продольный GIS-профиль Гейдаг-Ортакенд-Ханага (вдоль р.Башкендчай, масштаб 1:35 000) (Мусаев и др., 2004)

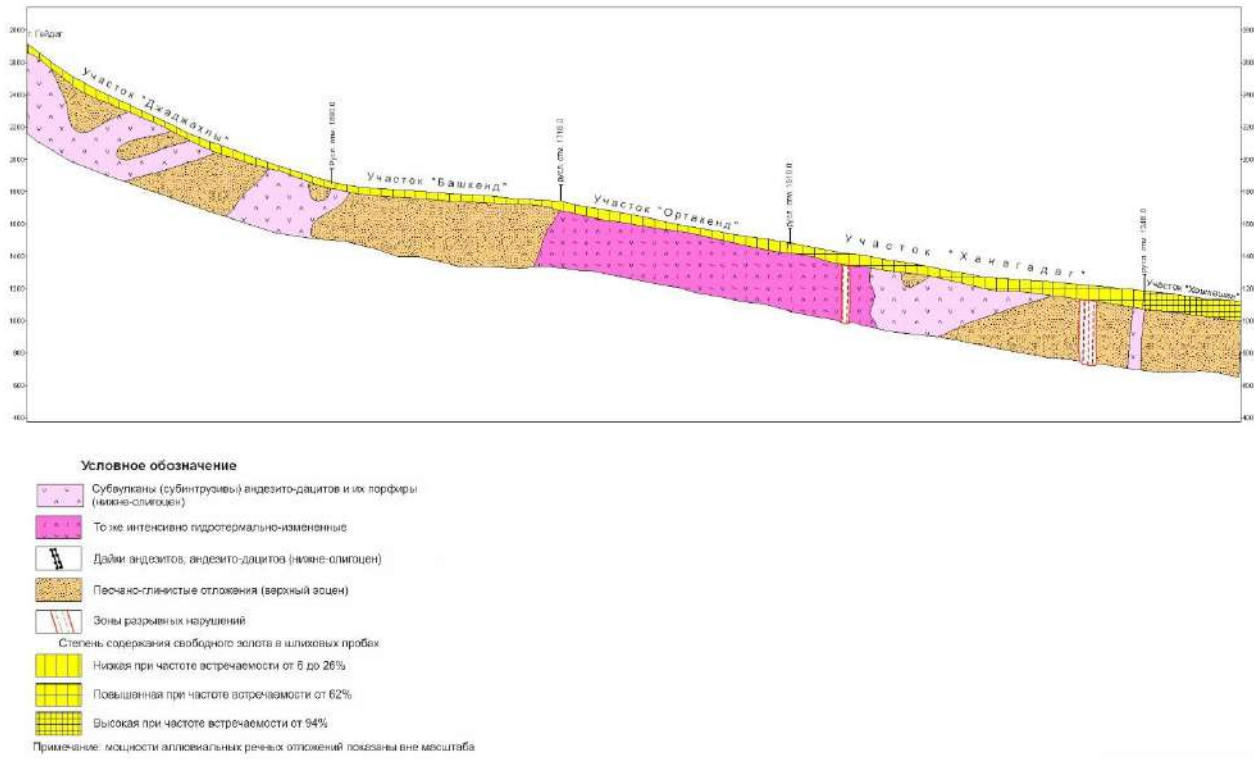


Рис. 9. GIS-профиль II по р.Башкендчай (масштабы: горизонтальный 1:50000, вертикальный 1:25000) (Мусаев и др., 2004)

В 62% шлихов обнаружено золото размерами 0.2-2.4 мм. Форма золотин обломочная, обломочно-порфировая, дендритовидная. В отдельных случаях золото покрыто гидроксидом железа красновато-серого цвета. Запасы золота подсчитаны категориями С₁, С₂. В результате проведенных анализов в 3585 шлихах в составе тяжелой фракции кроме золота выделены магнетит, гематит, пирит, лимонит, галенит, в редких случаях сфалерит, халькопирит, малахит, азурит и серебро.

Параметры блоков, выделенных по профилю II (рис.9), показаны в таблице 4.

Минеральный состав представлен магнетитом (31-49%) и гематитом (13-51%), которые являются наиболее распространенными минералами. Пирит составляет 1-26%, иногда в некоторых шлихах не выявлен. Остальные минералы обнаружены в единичных шлихах (галенит 1-6, киноварь 1-3 зерен). Состав по фракциям этих и других минералов показан на нижеследующей таблице (таблица 5).

Таблица 4
Среднее значение золота по параметрам блоков профиля II-II

Номер блока	Мощность, м	Ширина, м	Длина, м	Объем, м ³	Вес горных пород, т	Среднее значение золота по блоку
1	2.05	80.0	825	135300	1.8	110.8
2	1.85	80.0	400	54200	1.8	98.93
3	2.10	80.0	420	70560	1.8	93.9
4	2.75	80.0	445	275900	1.8	130.4
5	2.80	80.0	315	70560	1.56	80.6
6	4.3	80.0	425	146200	1.80	116.4

Таблица 5

Минералогический состав по фракциям (составлена на основании материалов
Экспедиции Оперативной Разведки Полезных Ископаемых)

Классы минералов Фракции	Самородные элементы	Оксиды и гид- рооксиды	Сульфиды	Фосфаты, карбонаты	Сульфаты
Магнитная		Магнетит	Галенит		
Тяжелая электромагнитная		Гематит Лимонит			
Тяжелая немагнитная	Золото Серебро		Пирит Сфалерит Халькопирит Киноварь	Малахит	Азурит

Несмотря на то, что широкое распространение магнетита характерно для всех речных сетей Нахчыванской Автономной Республики, на месторождении россыпного золота Башкендчай отмечается очень низкое содержание этого минерала. Известно, что в бассейне этой реки широко развиты гидротермально измененные породы, а пиритизация очень интенсивна. Кроме того, в зонах гидротермальных изменений магнетит характеризуется пониженной устойчивостью и, как правило, подвергается замещению пиритом (Aicher et al, 2008; Беркович и др., 2015). Большинство метасоматических процессов сопровождается нарушением в коренных породах магнетита и ослабеванием намагниченности пород. В связи с этим полиметаллические, медно-колчеданные, медно-порфировые месторожде-

ния, месторождения золота гидротермального происхождения характеризуются локальными аномалиями магнитного поля. В результате этих процессов в шлихах обнаруживаются кристаллы пирита размером 0.4-0.5 см.

Размеры золотин в скоплениях россыпного золота варьируют в широких диапазонах (таблица 6).

Как видно из таблицы 6, большинство зерен имеют размеры выше 1+0.5 мм. Золото в основном имеет пористую поверхность, состоит из соединений средних и крупных кристаллов в виде дендритов, друз. Зерна небольших размеров состоят из соединений изометрических кристаллов (Азадалиев, Керимов, 2005; Bogatiрев, 2009). По этим же классам крупности выявлены типоморфные особенности россыпного золота (таблица 7).

Таблица 6

Классы крупности зерен золота
(составлена по материалам Экспедиции Оперативной Разведки Полезных Ископаемых)

Общий вес шлихов	Размеры зерен, мм				
	+2	-2+1	-1+0.5	-0.5+0.25	-0.25+0.1
400 мг	мг %	мг %	мг %	мг %	мг %
	82 9.4	106 31.3	126 30.1	69 22.6	17 6.6

Примечание: анализы выполнены в Центральном Научно-Исследовательском Геолого-Разведочном Институте, г.Москва (выполняла С.В.Яблокова)

Таблица 7

Типоморфные особенности россыпного золота
(составлена по материалам Малокавказской ГРЭ)

Классы крупности	Количество зерен	Типоморфизм	Соединения на поверхности
+2	9	обломочный, сплющенно-обломочный, пористый, изометричный, дендритовидный, удлиненно дендритовидный	глинистые минералы
+1	9	Пористо-кистевидная, гемидиоморфная форма. Состоит из дендритов, овальных кристаллов	глинистые минералы
+0,5	27	массивные, друзевидные дендритоиды	желтый, мелко- зернистый
+0,25	45	удлиненные дендритоиды, неправильные сростки изометрических кристаллов, единичные тонкопористые частицы	желтый, мелко-зернистый

Золото сохраняет первичную морфологию, признаки окатывания почти не отмечаются. При анализе золотинок было установлено, что 89.5 %-поверхности состоит из золота, 10.5 % – из серебра (таблица 8).

По результатам спектрального анализа в составе золота в качестве элементов-примесей выделяются 0.02 масс % меди, 0.5 масс % ртути, 0.002 масс % свинца, 0.001 масс % сурьмы и др. (таблица 9).

Анализ поверхности золота методом Оже-спектроскопии показал, что поверхность подверглась гипергенным изменениям. В отдельных случаях встречаются серебро, имеющее пластообразную форму, и пленка ртути на поверхности золота (Рамазанов и др., 2009).

В таблице 10 представлены прогнозные параметры золотоносных россыпных скоплений по отдельным рекам изучаемой территории.

Таблица 8

Химический состав золота по локальному микрорентген-спектральному анализу

№ пробы	Химический состав (масс %)						Примечание
	Au	Ag	Hg	Sb	Cu	всего	
1.	91.2	5.55	0.16	0	0	98.91	центральный
2.	98.21	0.77	0.15	0	0	99.23	поверхность
3.	84.06	13.99	0.02	0	0	98.07	
4.	84.06	14.00	0.27	0.03	0	98.36	
5.	94.50	3.42	0.01	0	0	97.97	
6.	94.50	3.42	0.18	0	0	98.10	
7.	95.67	2.97	0.02	0.01	0	98.67	
8.	93.97	4.09	0.07	0	0	98.13	
9.	90.86	7.61	0.21	0.05	0	98.68	
10.	94.39	5.05	0.10	0	0	99.54	
11.	93.18	4.73	0.17	0	0	98.08	
12.	86.18	10.67	0.22	0	0	97.07	центральный
13.	90.51	8.16	0.25	0.25	0	98.92	

Таблица 9

Элементы-примеси в составе золота по количественному спектральному анализу

№№	Элементы	Крупные зерна	
		класс + 0.5	класс + 0.25
1.	Bi	–	0.0004
2.	Cu	0.025	0.02
3.	Fe	–	0.05
4.	Hg	0.5	0.5
5.	Mn	–	0.0003
6.	Rb	0.002	–
7.	Sb	0.001	–
8.	Te	–	–

Таблица 10

Золотносные россыпные скопления аллювиальных и аллювиально-пролювиальных отложений

№№	Реки	Название золотоносных россыпных скоплений	Прогнозные параметры россыпных скоплений		
			Объем (млн м ³)	Категория ресурсов	Ожидаемые ресурсы золота (кг)
1.	Килитчай	нижний	0.2	P ₃	40
		верхний	0.12	P ₃	30
2.	Кетамчай	Кетамчай	0.35	P ₃	105
3.	Гензачай	Гензачай	0.55	P ₂	135
4.	Ордубадчай	Ордубадчай	7.35	P ₂	700
5.	Айлисчай	верхний	21	P ₂	2100
		нижний	0.35	P ₁	105
6.	Венендчай	Венендчай-1	6	P ₂	600
		Венендчай-2	9	P ₂	900
7.	Дюхлунчай	Дюхлунчай-1	9	P ₂	900
		Дюхлунчай-2	0.42	P ₂	120
8.	Гilanчай	Гilanчай-1	2.5	P ₂	250
		Гilanчай-2	1.6	P ₂	320
		Гilanчай-3	0.3	P ₂	60
9.	Алинджачай	Алинджачай-1	3	P ₂	300
		Алинджачай-2	2.4	P ₂	240
		Алинджачай-3	0.6	P ₂	60
		Алинджачай-4	1.8	P ₁	180
10.	Нахчыванчай	Нахчыванчай-1	0.7	P ₃	700
		Нахчыванчай-2	1.35	P ₃	135
		Нахчыванчай-3	0.4	P ₃	40
11.	Арпачай	Арпачай-1	3	P ₃	300
		Арпачай-2	1.6	P ₃	160
Итого					8480

Результаты

В результате проведенных исследований установлено, что россыпная золотоносность характерна также для речных систем Килитчай, Кетамчай, Ордубадчай, Пазмарачай, Парагачай, Тивичай, Гilanчай, Нахчыванчай и др. и это дает основание на проведение более детальных геолого-разведочных работ. Золото концентрируется в основном в наиболее углубленной части русла, а на крутых склонах такие ловушки наблюдаются в относительно незначительных количествах. Но наиболее благоприятной для проникновения и улавливания золота является вертикальная трещиноватость слоистых глин и песчаников, осложненных относительно мелкими неровностями поверхности.

В целом почти все плотики золотоносных террас отличаются сложным строением, наличием многочисленных впадин, чередующихся с выступами, что имеет большое значение для концентрации золота. По мере приближения к плотикам происходит закономерное увеличение содержания золота в рыхлообломочных отложе-

ниях. Однако такая закономерность наблюдается не во всех случаях, что зависит от общей зараженности золотом террасы и элементов залегания плотика.

Золото фиксируется в рыхлообломочных отложениях всех террас, но наибольшие концентрации присутствуют в пределах пойменных и надпойменных террас первого уровня.

Выводы

Расположение вблизи друг-друга коренных месторождений и проявлений изучаемой территории обуславливает близкое расположение россыпных скоплений золота. Типоморфные особенности, крупностная классификация, высокая пробность, ограниченная дисперсность, малое количество примесных элементов и монозернистое строение золотых зерен отражают генетическую связь с коренными источниками, расположенными на расстоянии 2-3 км. Рассыпное золото с высокой перспективностью сконцентрировано в основном в аллювиальных, аллювиально-пролювиальных отложениях

ЛИТЕРАТУРА

- Азадалиев Дж.А. Установление коренных источников россыпного золота в Нахчыванской складчатой области (на примере Башкендского месторождения, Азербайджан). Отечественная геология, Москва, №.1-2, 2012, с.12-17.
- Азадалиев Дж.А., Керимов Ф.А. Некоторые вопросы изучения геолого-геоморфологических условий формирования золотоносных россыпей в бассейне реки Башкендчай (Нахчыванская Автономная Республика, Азербайджан). Доклады НАН Азербайджана, Том LXII, №. 3-4, 2006, с. 133-144.
- Азадалиев Дж.А., Керимов Ф.А. Типоморфные особенности россыпного золота в аллювиальных отложениях бассейна реки Башкендчай (Нахчыванская Автономная Республика, Азербайджан). Доклады НАН Азербайджана, Том LXI, №. 6, 2005, с. 94-101.
- Азадалиев Дж.А., Мусаев Ш.Д., Керимов Ф.А. Перспективы выявления коренных источников россыпного золота в пределах Нахчыванской Автономной Республики. Доклады НАН Азербайджана, Том LVIII, №. 5-6, 2002, с. 198-206.
- Баба-заде В.М., Мусаев Ш.Д., Насибов Т.Н., Рамазанов В.Г. Золото Азербайджана. Азербайджан Милли Энциклопедиясы. Баку, 2003, 423 с.
- Беркович К.М., Злотина Л.В., Турькин Л.А. Русловые процессы и использование природных ресурсов реки (на примере Оки). География и природные ресурсы, №. 1, 2015, с. 98-104.
- Геология Азербайджана. Том. VI – Полезные ископаемые. Рассыпное золото. Нафта-Пресс. Баку, 2003, с. 321-354.
- Минерально-сырьевые ресурсы Азербайджана. Издательство «Озан». Баку, 2005, 808 с.
- Мусаев Ш.Д., Керимов Ф.А., Исаева Н.С. Золотоносные россыпи реки Алинджачай. Физика, математика, науки о Земле, №. 2, 2004, с.76-82.
- Патык-Кара Н.Г. Рассыпные месторождения России и других стран СНГ. Научный мир. Москва, 1997, 454 с.
- Патык-Кара Н.Г. Минерагения россыпей: типы россыпных провинций. ИГЕМ РАН, Москва, 2008, 528 с.
- Рамазанов В.Г., Каландаров Б.Г., Тахмазова Т.Г., Мансуров М.И. Прогнозная оценка золотоносности территории Азербайджанской Республики. Естественные и технические науки. Серия наук о Земле. Москва, №. 4 (42), 2009, с.194-197.
- Шило Н.А. Учение о россыпях. Издательство «Академия горных наук». Москва, 2000, 632 с.
- Шумилов Ю.В. К вопросу о количественной оценке процессов россыпебразования. Проблемы геологии россыпей: Магадан, Северо-Восточный комплексный научно-исследовательский институт, 1970, с.125-132.
- Nağıyev V.N., Məmmədov I.A. Naxçıvan Muxtar Respublikasının faydalı qazıntıları. Elm. Baki, 2010, 240 s.
- Təhməzova T.H. Əlincəçay ərazisində səpinti qızıl toplularının yerləşmə xüsusiyyətləri və perspektivləri. Baki Universitetinin Xəbərləri, No. 1, 2017, s.123-131.
- Aichler J., Malec J., Vecera J., Hanzl P., Burianek D., Sidorinova T., Taborsky Z., Bolorma Kh., Byambasuren D. Prospection for gold and new occurrences of gold-bearing mineralization in the eastern Mongolian Altay. Journal of Geosciences, No. 53, 2008, pp.123-138. DOI:10.3190/jgeosci.025.
- Babazadeh V.M., Abdullayeva Sh.F., Novruzova S.R., Ibrahimov J.R. Gold-bearing volcanicogenic fields of non-ferrous metals of the Lesser Caucasus and the Eastern Pontides and their genesis. ANAS Transactions, Earth Sciences No. 2, 2024a, pp. 17-32; DOI: 10.33677/ggianas20240200123.
- Baba-zadeh V.M., Abdullayeva Sh.F., Novruzova S.R. Structural conditions for the localization of gold mineralization within the Tutkhun ore field (the central part of the Lesser Caucasus). ANAS Transactions, Earth Sciences, No. 1, 2024b, pp. 104-118, DOI: 10.33677/ggianas20240100112.
- Becker N., Batt W. Waikaia placer gold mine, Southland. Australas. Institutes Minerals Metall. Monogr., 31, 2016, pp. 387-394.
- Berkovich K.M., Zlotina L.V., Turykin L.A. Channel processes and the use of natural resources of the river (on the example of the Oka). Geography and natural resources. No. 1, 2015, pp. 98-104 (in Russian).
- Bogatyrev L.I. Typomorphic features of placer gold on Ozerninskij ore region. Freiberg Forschungsforum 60 Berg- und Hüttenmännischer Tag. TU Bergakademie Freiberg, Germany, 2009, pp. 39-42.
- Carling P.A., Breakspear M.D. Placer formation in gravel-bedded rivers. Ore Geology Reviews, Vol. 28, 2006, pp.377-401.
- Geology of Azerbaijan. Minerals. Alluvial gold. Vol. VI. Nafta-Press, Baku, 2003, pp. 321-354 (in Russian).
- Goldfarb Yu.I., Petrov A.N., Preis V.K., Skurida D.A. Geological prerequisites for differentiated approach to prospecting and exploration of alluvial gold placers: an example from the northeast of Russia. Russian Journal of Pacific Geology, Vol. 9, Issue 3, 2015, pp.166-177.
- Mineral resources of Azerbaijan. Publishing House Ozan. Baku, 2005, 808 p. (in Russian).
- Musaev Sh.D., Kerimov F.A., Isaeva N.S. Gold-bearing placers of the Alinjachay river. Physics, Mathematics, Earth Sciences, No. 2, 2004, pp. 76-82 (in Russian).
- Nagiyev V.N., Mammadov I.A. Minerals of Nakhchivan Autonomous Republic. Elm. Baku, 2010, 240 p. (in Azerbaijani).

REFERENCES

- Aichler J., Malec J., Vecera J., Hanzl P., Burianek D., Sidorinova T., Taborsky Z., Bolorma Kh., Byambasuren D. Prospection for gold and new occurrences of gold-bearing mineralization in the eastern Mongolian Altay. Journal of Geosciences, No. 53(2), 2008, pp.123-138.
- Azadaliel J.A. Establishment of primary sources of placer gold in the Nakhchivan folded region (on the example of the Bashkend deposit, Azerbaijan). Otechestvennaya Geologiya, Moscow, No. 1-2, 2012, pp. 12-17 (in Russian).
- Azadaliel J.A., Kerimov F.A. Some issues of studying the geological and geomorphological conditions for the formation of gold-bearing placers in the basin of the Bashkendchay river (Nakhchivan Autonomous Republic, Azerbaijan). Reports of National Academy of Sciences of Azerbaijan, Vol. LXII, No. 3-4, 2006, pp. 133-144 (in Russian).
- Azadaliel J.A., Kerimov F.A. Typomorphic features of placer gold in alluvial deposits of the Bashkendchay river basin (Nakhchivan Autonomous Republic, Azerbaijan). Reports of National Academy of Sciences of Azerbaijan, Vol. LXI, No. 6, 2005, pp. 94-101 (in Russian).
- Azadaliel J.A., Musaev Sh.D., Kerimov F.A. Prospects for identifying primary sources of alluvial gold within the Nakhchivan Autonomous Republic. Reports of National Academy of Sciences of Azerbaijan, Vol. LVIII, No. 5-6, 2002, pp. 198-206 (in Russian).
- Baba-zade V.M., Musaev Sh.D., Nasibov T.N., Ramazanov V.G. Gold of Azerbaijan. Azerbaijan National Encyclopedia. Baku, 2003, 423 p. (in Russian).
- Babazadeh V.M., Abdullayeva Sh.F., Novruzova S.R., Ibrahimov J.R. Gold-bearing volcanicogenic fields of non-ferrous metals of the Lesser Caucasus and the Eastern Pontides and their genesis. ANAS Transactions, Earth Sciences, No. 2, 2024a, pp. 17-32, DOI: 10.33677/ggianas20240200123.
- Baba-zadeh V.M., Abdullayeva Sh.F., Novruzova S.R. Structural conditions for the localization of gold mineralization within the Tutkhun ore field (the central part of the Lesser Caucasus). ANAS Transactions, Earth Sciences, No. 1, 2024b, pp. 104-118, DOI: 10.33677/ggianas20240100112.
- Becker N., Batt W. Waikaia placer gold mine, Southland. Australas. Institutes Minerals Metall. Monogr., 31, 2016, pp. 387-394.
- Berkovich K.M., Zlotina L.V., Turykin L.A. Channel processes and the use of natural resources of the river (on the example of the Oka). Geography and natural resources. No. 1, 2015, pp. 98-104 (in Russian).
- Bogatyrev L.I. Typomorphic features of placer gold on Ozerninskij ore region. Freiberg Forschungsforum 60 Berg- und Hüttenmännischer Tag. TU Bergakademie Freiberg, Germany, 2009, pp. 39-42.
- Carling P.A., Breakspear M.D. Placer formation in gravel-bedded rivers. Ore Geology Reviews, Vol. 28, 2006, pp.377-401.
- Geology of Azerbaijan. Minerals. Alluvial gold. Vol. VI. Nafta-Press, Baku, 2003, pp. 321-354 (in Russian).
- Goldfarb Yu.I., Petrov A.N., Preis V.K., Skurida D.A. Geological prerequisites for differentiated approach to prospecting and exploration of alluvial gold placers: an example from the northeast of Russia. Russian Journal of Pacific Geology, Vol. 9, Issue 3, 2015, pp.166-177.
- Mineral resources of Azerbaijan. Publishing House Ozan. Baku, 2005, 808 p. (in Russian).
- Musaev Sh.D., Kerimov F.A., Isaeva N.S. Gold-bearing placers of the Alinjachay river. Physics, Mathematics, Earth Sciences, No. 2, 2004, pp. 76-82 (in Russian).
- Nagiyev V.N., Mammadov I.A. Minerals of Nakhchivan Autonomous Republic. Elm. Baku, 2010, 240 p. (in Azerbaijani).

- in the Tutkhun ore field (the central part of the Lesser Caucasus). ANAS Transactions, Earth Sciences No.1, 2024b, pp. 104-118; DOI: 10.33677/ggianas20240100112
- Becker N., Batt W. Waikaia placer gold mine, Southland. Australas. Institutes Minerals Metall. Monogr., 31, 2016, pp.387-394.
- Bogatyrev L.I. Typomorphic features of placer gold on Ozerninskij ore region. Freiberg Forschungsforum 60 Berg- und Hüttenmännischer Tag. TU Bergakademie Freiberg, Germany, 2009, pp. 39-42.
- Carling P.A., Breakspeare M.D. Placer formation in gravel-bedded rivers: a review. Ore Geology Reviews, Vol. 28, 2006, pp. 377-401.
- Goldfarb Yu.I., Petrov A.N., Preis V.K., Skurida D.A. Geological prerequisites for differentiated approach to prospecting and exploration of alluvial gold placers: an example from the northeast of Russia. Russian Journal of Pacific Geology. Vol. 9, Issue 3, 2015, pp.166-177.
- Patyk-Kara N.G. Minerageny of placers: types of placer provinces. IGEM RAN, Moscow, 2008, 528 p. (in Russian).
- Patyk-Kara N.G. Placer deposits of Russia and other CIS countries. Nauchny mir. Moscow, 1997, 454 p.
- Ramazanov V.G., Kalandarov B.G., Takhmazova T.H., Mansurov M.I. Predictive assessment of the gold content of the territory of the Azerbaijan Republic. Natural and technical sciences. Series of Earth Sciences. Moscow, No. 4 (42), 2009, p.194-197 (in Russian).
- Shilo N.A. Teaching about placers. Publishing House "Academy of mining sciences". Moscow, 2000, 632 p. (in Russian).
- Shumilov Yu.V. On the issue of quantitative assessment of placer formation processes. Problems of placer geology: Magadan, Northeast Integrated Research Institute, 2000, pp.125-132 (in Russian).
- Tahmazova T.H. Spatial characteristics and potential prospects of scattered gold assemblages in the Alinjachay area. News of Baku State University, No. 1, 2017, pp. 123-131 (in Azerbaijani).

ОСОБЕННОСТИ РАСПРЕДЕЛЕНИЯ ЗОЛОТОНОСНЫХ РОССЫПЕЙ И ИХ КОРЕННЫХ ИСТОЧНИКОВ НА ТЕРРИТОРИИ НАХЧИВАНСКОЙ АР

Тахмазова Т.Г.

Бакинский государственный университет, Азербайджан
AZ1148, Баку, ул. З.Халилова, 23: ttahmazova@yahoo.com

Резюме. В течение нескольких десятилетий на изучаемой территории проводились многочисленные научно-исследовательские работы, направленные на выявление золотоносных участков. Настоящая статья посвящена детальному анализу и комплексной оценке, пространственно-генетическим факторам размещения россыпной золотоносности основных речных бассейнов Нахчыванской Автономной Республики, их взаимосвязи и корреляции с потенциальными коренными источниками золота, типоморфным особенностям россыпей, а также другим важным геологическим аспектам. В рамках исследования были подробно изучены речные бассейны Башкендчай и Алинджачай с их притоками, представляющими интерес с точки зрения россыпной золотоносности, а также выделены наиболее перспективные районы с высоким потенциалом. В ходе исследований выявлены типоморфные особенности золота, включающие обломочные, сплющенно-обломочные, пористые, изометричные, дендритовидные, удлинённо-дендритовидные, а также другие распространенные морфологические разновидности. Золото сохраняет первичную морфологию, при этом признаки окатанности практически не наблюдаются. Химический состав золота определялся с помощью локального микрорентген-спектрального анализа, который выявил наличие таких элементов-примесей, как медь, ртуть, свинец, сурьма и другие. По результатам количественного спектрального анализа в составе золота обнаружены Bi, Cu, Fe, Hg, Mn, Rb, Sb и Te. Полученные данные свидетельствуют о том, что близкое пространственное расположение коренных источников является одним из ключевых факторов, определяющих формирование и концентрацию россыпного золота в прилегающих зонах. Типоморфные особенности, классы крупности, ограниченная дисперсность, низкое содержание элементов-примесей и монозернистое строение золотых зерен подтверждают их генетическую связь с коренными источниками, расположенными в непосредственной близости. Россыпное золото высокой перспективности сосредоточено преимущественно в аллювиальных и аллювиально-пролювиальных отложениях. Результаты исследования могут быть использованы для совершенствования поисково-оценочных работ и разработки прогнозных моделей россыпного и коренного золоторудного оруднения в исследуемом регионе, а также иметь практическое значение при изучении аналогичных областей.

Ключевые слова: россыпная золотоносность, речные бассейны, коренные источники, аллювиальные отложения, вулкано-купольные структуры

NAXÇIVAN MR ƏRAZİSİNDE SƏPİNTİ QIZIL VƏ ONLARIN KÖKLÜ MƏNBƏLƏRİNİN PAYLANMA XÜSUSİYYƏTLƏRİ

Тəhməzova T.H.

Bakı Dövlət Universiteti, Azərbaycan
AZ1148, Bakı, Z. Xəlilov küç., 23: ttahmazova@yahoo.com

Xülasə. Bir neçə onillikdə tədqiq olunan ərazidə qızıl daşıyan sahələrin müəyyən edilməsi məqsədilə çoxsaylı elmi-tədqiqat işləri aparılmışdır. Məqalə Naxçıvan Muxtar Respublikasının əsas çay hövzələrində səpinti qızılın yerləşməsinin məkan-genetik amilləri, onların potensial köklü qızıl mənbələri ilə qarşılıqlı genetik əlaqəsi və korrelyasiyası, səpintilərin tipomorf xüsusiyyətləri, eləcə də digər mühüm geoloji aspektlərin ətraflı təhlili və kompleks qiymətləndirilməsinə həsr olunmuşdur. Bu tədqiqat çərçivəsində Başkəndçay və Əlincəçay çay hövzələri, o cümlədən onların səpinti qızılının yayılması və konsentrasiyası baxımından əhəmiyyətli olan qolları geniş və ətraflı şəkildə təhlil edilmişdir. Yüksək səpinti qızıl potensialına malik ən perspektivli sahələr müəyyən edilmişdir. Tədqiqat zamanı qızılın tipomorf xüsusiyyətləri – qırıntı, məsaməli, izometrik, dendrit, uzunsov dendrit və digər geniş yayılmış morfoloji növlər aşkar edilmişdir. Qızıl ilkin morfologiyasını saxlayır, yuvarlanma əlamətləri isə demək olar ki, müşahidə olunmur. Qızılın kimyəvi tərkibi lokal mikrorentgen spektral analizi vasitəsilə müəyyən edilmiş və mis, civə, qurğuşun, sürmə və s.

kimi element-qarışqlar aşkar olunmuşdur. Kəmiyyət spektral analiz nəticələrinə əsasən qızılda Bi, Cu, Fe, Hg, Mn, Rb, Sb və Te elementləri müəyyən edilmişdir. Alınan məlumatlar və aparılan analitik tədqiqatların nəticələri qəti şəkildə göstərir ki, köklü qızıl mənbələrinin məkan baxımından yaxın yerləşməsi çay hövzələrində səpinti qızılın formallaşması və sonrakı konsentrasiyásında əsas və müəyyənedici amillərdən biridir. Tipomorf xüsusiyyətlər, ölçü sinifləri, monodənəlilik, az miqdarda element-qarışqlar onların yaxınlıqda köklü mənbələrlə genetik əlaqəsini təsdiqləyir. Yüksək perspektivli səpinti qızıl əsasən alluvial və alluvial-proluvial çöküntülərdə cəmlənmişdir. Alınan nəticələr tədqiqat sahəsində səpinti və köklü qızıl yataqlarının proqnozlaşdırılması və qiymətləndirilməsi işlərinin təkmilləşdirilməsi üçün istifadə oluna və analoji geoloji şəraitdə tətbiq edilə bilər.

Açar sözlər: səpinti qızıl, çay hövzələri, köklü mənbələr, alluvial çöküntülər, vulkan-günbəz strukturları

MÜNDƏRİCAT

Moldabayeva G.J., Abbasova S.V., Zakenov S.T., Kirisenko O.G., İklasova J.U., Janturin J.K., Tuzelbayeva Ş.R., Vanq J. – Geoloji-texniki tədbirlərin effektivliyinin qiymətləndirilməsi üsullarının təhlili və onların seçilməsi üzrə qərarların qəbul edilməsi: konseptual icmal	3-11
Hümbətov F., İbrahimov G., Aslanova G., Necati Solut H., Balayev V., Kərimova N., Kərimbəyli I. – Azərbaycan Respublikasının Qubadlı rayonunda radioekoloji risklərin və su keyfiyyətinin içməli və kənd təsərrüfatı üçün yararlılığının qiymətləndirilməsi.....	12-21
Pirs İ., Quliyev İ.S., Yetirmişli Q.C., Kazımova S.E., Uolker R., Kazımov İ.E., Abdullayev N.R., Conson B., Marşal N. – 1668-ci və 1902-ci illərin Şamaxı zəlzələlərinin pleistosenesmik bölgəsində paleoseysmoloji tədqiqatlar.....	22-41
Abetov A.E., Seyidjanov A.K., Samenov E.R. – Litofasiyaların xəritələndirilməsi və kollektor xüsusiyyətlərinin qiymətləndirilməsi təpsiriqlərində maşın öyrənməsi və neyron şəbəkə metodlarının tətbiqi: metodların təhlili və seçimi	42-51
Kərimov V.Yu., Yusubov N.P., Quliyev İ.S., Qədirov F.A. – Azərbaycan ərazisinin neft-qaz sahələrinin geoloji rayonlaşdırılmasına yeni yanaşma	52-67
Munduzova M.A., Sayitov S.S., Nurhocayev A.K. – Karlin tipli yataqlara malik Almalık filiz rayonunun terrigen-karbonat çöküntülərinin qızılılığının müqayisəli səciyyəsi	68-78
Yuliyanto G., Nurwidiyanto M.İ.N., Harmoko U., Yulianto T., Fernando G.A. – Mikrotremor və geoelektrik üsullardan əldə edilən nəticələrin korrelyasiya analizi istifadə edilməklə susaxlayan horizontların ayrılması.....	79-88
Muluaem A., Demsi T., Şano L., Getahun E., Solomon H. – Veyto bəndinin tikinti sahəsində mühəndislik xüsusiyyətlərinin müəyyənləşdirilməsi üçün əks olunan dalğaların üsulu əsasında seysmik tədqiqatın tətbiqi, Cənubi Efiopiya	89-106
Eppelbaum L., Katz Y., Qədirov F., Quliyev İ., Ben-Avraham Z. – Mərkəzi Qondvananın şərqində və Avrasiyada mürəkkəb geodinamik qarşılıqlı təsirlərin təhlili.....	107-133
İsgəndərov E.H. – Ağırlıq qüvvəsinin tam normallaşdırılmış qradientinin hesablanması alqoritmi və rəqəmsal modelləşdirilməsi	134-140
Təhməzova T.H. – Naxçıvan MR ərazisində səpinti qızıl və onların köklü mənbələrinin paylanması xüsusiyyətləri.....	141-156

CONTENTS

Moldabayeva G.Zh., Abbasova S.V., Zakenov S.T., Kirisenko O.G., Iklasova J.U., Zhanturin Zh.K., Tuzelbayeva Sh.R., Wang J. – Analysis of methods for evaluating the effectiveness of geological and technical measures and decision-making for their selection: conceptual review.....	3-11
Humbatov F., Ibrahimov G., Aslanova G., Nejati Solut H., Balayev V., Karimova N., Karimbeyli I. – Assessment of radioecological risks and the suitability of water quality for drinking and agricultural use in Gubadli district of the Republic of Azerbaijan	12-21
Pierce I., Guliyev I.S., Yetirmishli G.J., Kazimova S.E., Walker R., Kazimov I.E., Abdullayev N.R., Johnson B., Marshall N. – Paleoseismological studies in the pleistoseismic area of the 1668 and 1902 Shamakhi earthquakes	22-41
Abetov A.E., Seitzhanov A.K., Samenov Ye.R. – Application of machine learning methods and neural networks in the objectives of lithofacies mapping and reservoir properties assessment: analysis and selection of methods	42-51
Kerimov V.Yu., Yusubov N.P., Guliyev I.S., Kadirov F.A. – A new approach to the oil and gas geological zoning of the territory of Azerbaijan	52-67
Munduzova M.A., Sayitov S.S., NurkhodjaevA.K. – Comparative characteristics of the gold content in terrigenous-carbonate deposits of the Almalyk Ore Region with deposits of the Karlin Type.....	68-78
Yuliyanto G., Nurwidjanto M.I.N., Harmoko U., Yulianto T., Fernando G.A. – Aquifer zone delineation using correlation between microtremor methods and geoelectricity	79-88
Mulualem A., Demsie T., Shano L., Getahun E., Solomon H. – Application of seismic refraction survey for engineering site characterizations of Weyto dam construction site, Southern Ethiopia	89-106
Eppelbaum L., Katz You., Kadirov F., Guliyev I., Ben-Avraham Z. – Analysis of complex geodynamic interactions in the eastern part of Central Gondwana and Eurasia	107-133
Isgandarov E.H. – Calculation algorithm and digital modeling of the full normalized gravity gradient	134-140
Tahmazova T.H. – Features of the distribution of gold placers and their primary sources in the territory of the Nakhchivan AR.....	141-156

ОГЛАВЛЕНИЕ

Молдабаева Г.Ж., Аббасова С.В., Закенов С.Т., Кирисенко О.Г., Икласова Ж.У., Жантурин Ж.К., Тузельбаева Ш.Р., Ванг Дж. – Анализ методов оценки эффективности геологотехнических мероприятий и принятия решений по их выбору: концептуальный обзор	3-11
Гумбатов Ф., Ибрагимов Г., Асланова Г., Неджати Солут Х., Балаев В., Каримова Н., Каримбейли И. – Оценка радиоэкологических рисков и пригодности качества воды для питьевого и сельскохозяйственного использования в Губадлинском районе Республики Азербайджан	12-21
Пирс И., Гулиев И.С., Етирмишли Г.Дж., Казимова С.Э., Уолкер Р., Казимов И.Э., Абдуллаев Н.Р., Джонсон Б., Маршалл Н. – Палеосейсмологические исследования в плейстосейсмической области Шамахинских землетрясений 1668 и 1902 гг.....	22-41
Абетов А.Е., Сейтжанов А.К., Саменов Е.Р. – Применение методов машинного обучения и нейронных сетей в задачах картирования литофаций и оценки коллекторских свойств: анализ и выбор методов.....	42-51
Керимов В.Ю., Юсубов Н.П., Гулиев И.С., Кадиров Ф.А. – Новый подход к нефтегазогеологическому районированию территории Азербайджана	52-67
Мундузова М.А., Сайитов С.С., Нуходжаев А.К. – Сравнительная характеристика золотоносности терригенно-карбонатных отложений Алмалыкского рудного района с месторождениями Карлинского типа	68-78
Юлиянто Г., Нурудянто М.И.Н., Хармоко У., Юлиантон Т., Фернандо Г.А. – Выделение зон водоносных горизонтов с использованием корреляционного анализа результатов микротреморного и геоэлектрического методов.....	79-88
Мулуалем А., Демси Т., Шано Л., Гетахун Э., Соломон Х. – Применение сейсмической съемки методом отраженных волн для определения инженерных характеристик участка строительства плотины Вейто, Южная Эфиопия.....	89-106
Эппельбаум Л., Кац Ю., Кадиров Ф., Гулиев И., Бен-Аврахам Ц. – Анализ сложных геодинамических взаимодействий в восточной части Центральной Гондваны и Евразии	107-133
Искандаров Э.Г. – Алгоритм вычисления и цифровое моделирование полного нормированного градиента силы тяжести	134-140
Тахмазова Т.Г. – Особенности распределения золотоносных россыпей и их коренных источников на территории Нахчыванской АР	141-156